Novel mechanisms of HER2-targeted therapy resistance in breast cancer

A thesis submitted for the degree of PhD by:

Neil Conlon, BSc.

January 2018

The work in this thesis was carried out under the supervision of:

Dr. Norma O' Donovan,

Dr. Denis Collins,

National Institute for Cellular Biotechnology

School of Biotechnology

Dublin City University

&

Prof. John Crown

St. Vincent's University Hospital

I hereby certify that this material, which I now submit for assessment on the programme of study leading to the award of PhD, is entirely my own work, that I have exercised reasonable care to ensure that the work is original, and does not to the best of my knowledge breach any law of copyright, and has not been taken from the work of others save and to the extent that such work has been cited and acknowledged within the text of my work.

Signed: _____

ID No.: <u>13212159</u>

 Date: _____

Acknowledgements

Table of Contents

Abbreviations

ACE	Angiotensin converting enzyme
ADCC	Antibody-dependent cell-mediated cytotoxicity
AKT	Protein kinase B
AMPK	5' adenosine monophosphate activated protein kinase
BAX	BCL-2-associated protein X
BCA	Bicinchoninic acid
Bcl-2	B cell lymphoma 2
BIM	BCL-2 interacting protein
CBR	Clinical benefit rates
CI	Combination index
CIP2A	Cancerous inhibitor of PP2A
CNS	Central nervous system
CNV	Copy number variant
DFS	Disease-free survival
DMSO	Dimethyl sulfoxide
ECD	Extracellular domain
eEF2	Eukaryotic elongation factor 2
EGF	Epidermal growth factor
EGFR	Epidermal growth factor receptor
EMT	Epithelial-mesenchymal transition
ER	Estrogen receptor
ERK 1/2	Extracellular signal-regulated kinase 1/2
FAK	Focal adhesion kinase
FBS	Foetal bovine serum
FDA	Food and drug administration
FFPE	Formalin fixed paraffin embedded
FGFR2	Fibroblast growth receptor 2
FISH	Fluorescent in situ hybridisation
GAB1	GRB2-associated binding protein 1

GRB2	Growth factor receptor-bound protein 2
GSK3β	Glycogen synthase kinase 3 beta
HB-EGF	Heparin-binding epidermal growth factor-like growth factor
HEPES	4-(2-Hydroxyethyl)piperazine-1-ethanesulfonic acid, N-(2-Hydroxyethyl)piperazine-N′-(2-ethanesulfonic acid)
HER2	Epidermal growth factor receptor 2
HER3	Epidermal growth factor receptor 3
HER4	Epidermal growth factor receptor 4
HMGB1	High mobility group protein B1
HPMC	Hydroxypropyl methylcellulose
iDFS	Invasive disease-free survival
IGF-1R	Insulin growth factor receptor-like 1
InDel	Insertion/deletion
IRS4	Insulin receptor substrate 4
ITGA9	Integrin alpha subunit 9
ITGB4	Integrin beta subunit 4
KI-67	Proliferation marker protein Ki-67
MAPK	Mitogen-activated protein kinase
MCL-1	Myeloid leukemia cell differentiation protein
MEK 1/2	Mitogen-activated protein kinase kinase
MET	Hepatocyte growth factor receptor
MRD	Minimum residual disease
MTD	Maximum tolerated dose
mTOR	Mammalian target of rapamycin
MUC4	Mucin 4
NFκB	Nuclear factor kappa B
NK	Natural killer
NR4A1	Nuclear receptor 4A
NRG	Neuregulin
NSCLC	Non-small cell lung cancer
OA	Okadaic acid
ORR	Objective response rate
OS	Overall survival

PARP	Adenosine diphosphate-ribose polymerase
PBS	Phosphate buffer saline
pCR	Pathological complete response
PFS	Progression-free survival
PI3K	Phosphoinositide 3-kinase
PKCα	Protein kinase C alpha
PMSF	Phenylmethylsulfonyl fluoride
Poly-HEMA	Poly-hydroxyethylmethacrylate
PP2A	Protein phosphatase 2A
PR	Progesterone receptor
PTEN	Phosphatase and tensin homolog
RON	Recepteur d'orgine nantais
RPPA	Reverse phase protein array
RTK	Receptor tyrosine kinase
SCID	Severe combined immunodeficiency
SDS	Sodium dodecyl sulfate
SET	Inhibitor-2 of protein phosphatase 2A
SFK	Src family kinase
SH4	Src-homolog 4
Shc	Src homology 2 domain containing transforming protein
siRNA	Small interfering RNA
SNV	Single nucleotide variant
STAT3	Signal transducer and activator of transcription 3
T-DM1	Trastuzumab emtansine
TGF-α	Transforming growth factor alpha
TKI	Tyrosine kinase inhibitor
TRAIL	TNF-related apoptosis-inducing ligand
VEGF	Vascular endothelial growth factor
VEGFR	Vascular endothelial growth factor receptor

Abstract

HER2-targeted therapies have greatly improved the outcome for patients with HER2-positive breast cancer. However, resistance to these therapies is an on-going clinical problem. Therefore, novel therapeutic strategies to overcome or prevent resistance are required. The aim of this PhD project was to investigate mechanisms of resistance to HER2-targeted therapies and to develop strategies to overcome resistance.

Two lapatinib resistant cell lines (SKBR3-L and HCC1954-L) previously generated in our lab showed increased protein phosphatase 2A (PP2A) activity. In this study, the resistant cell lines were more sensitive to PP2A inhibition by okadaic acid and the therapeutic PP2A inhibitor LB-100. PP2A inhibition also enhanced the effect of lapatinib and the combination induced apoptosis in both cell lines. Addition of LB100 to lapatinib prevented the development of lapatinib resistance in two lapatinib-naive cell lines. HCC1954-L cells produced xenograft tumours in mice. The combination of lapatinib and LB-100 did not cause systemic side effects, deeming the combination safe for efficacy testing in the HCC1954-L xenograft model.

In a panel of HER2-positive cell lines, sensitivity to PP2A inhibition with okadaic acid correlated with lapatinib resistance. PP2A catalytic subunit and structural subunit expression did not correlate with lapatinib or PP2A inhibition response. However, expression levels of the PP2A inhibitor CIP2A correlated with improved survival in HER2-positive breast cancer patients in a publicly available dataset.

An afatinib-resistant SKBR3 cell line (SKBR3-A) was analysed by reverse phase protein array. Phospho-Src (Y416) was elevated in SKBR3-A compared to SKBR3 cells. SKBR3-A cells were more sensitive to Src inhibition by dasatinib and the combination of afatinib and dasatinib was highly synergistic. The combination inhibited both HER2/EGFR and Src signalling and caused non-apoptotic cell death. Addition of dasatinib prevented the development of afatinib resistance in three of four treatment-naive HER2-positive cell lines and two of three cell lines with acquired trastuzumab resistance.

In conclusion, the drug combinations of lapatinib plus LB-100 and afatinib plus dasatinib show potential for the treatment of HER2-positive breast cancer.

1 Introduction

1.1   Introduction

Cancer is a heterogeneous disease that can be characterised by its ability to sustain proliferation, evade cell death, stimulate angiogenesis, circumvent growth suppression and invade other tissues [1, 2]. However, the term cancer does not refer to a single disease but to a spectrum of malignancies that arise through particular genetic abnormalities.

Breast cancer is the most common malignant tumour diagnosed in women in Ireland, with a 1 in 10 chance of an Irish woman developing malignant breast cancer before her 75th birthday. Although the breast cancer five-year survival rate is 82%, it is still the second most common cause of cancer death in women. From 1994 to 2013, the number of invasive breast cancer incidences increased annually by approximately 1.5%. A similar trend was observed in *in situ* breast cancer cases, with an 8.8% increased trend. In contrast, the mortality rate is declining on average by 1.9% annually [3].

1.2   Breast cancer subtypes

Breast cancer is defined by its origins in breast tissue. Most commonly, breast tumours originate from ductal tissue, termed ductal carcinoma, or in the lobules, which is called lobular carcinoma. However, in rare cases, tumours can occur from other breast tissue types [4, 5].

Breast cancer can be divided into several subtypes by morphological or molecular characteristics, each subtype with different clinical prognoses. Traditionally, the classification of a cancer was simply based on the tissue from which it originated e.g. breast cancer. However, developments in molecular biology led to breast cancer classification by the presence or absence of certain extracellular receptors, for example, the hormone receptors estrogen receptor (ER) and progesterone receptor (PR), and epidermal growth factor receptor 2 (HER2). This defined three basic breast cancer subtypes: hormone receptor-positive, HER2-positive and triple negative breast cancer. With the application of gene expression profiling, this classification was revised and five intrinsic breast cancer subtypes were proposed: HER2-enriched, luminal A, luminal B, basal-like and normal-like. Recently, three additional subtypes

have been proposed: claudin-low, molecular apocrine and luminal-like [6–10] (Table 1-1).

Luminal breast cancers are characterised by their high expression of the ER and largely originate from the luminal epithelial cells of the mammary gland. The St. Gallen International Expert Consensus divides luminal breast cancer into luminal A and luminal B. The luminal subtypes are the most heterogeneous in terms of gene expression, mutation and gene copy number profile [11]. Luminal A and B are distinguished by their Ki-67 and PR status. Luminal A tumours are both ER and PR positive and are Ki-67 negative. These cancers are highly sensitive to hormone therapy and generally respond poorly to chemotherapy. Luminal B breast cancers are either PR-negative or have high Ki-67 levels, have lower levels of ER than luminal A and can also be HER2 over-expressing [12].

HER2-enriched breast cancer is characterised by its over-expression of genes on the 17q ERBB2 amplicon, most notably HER2 and other associated genes such as GRB7 and STARD3 [8]. The 17q ERBB2 amplicon, a region of DNA on chromosome 17q, is amplified in roughly 20% of breast cancers and this amplification is the most commonly occuring mechanism of HER2 activation [13]. Tumours of this subtype are highly proliferative and, prior to the advent of HER2-targeted therapies, had an exceptionally poor prognosis [14]. The basal-like subtype cancers are generally triple negative and are categorised by expression of genes characteristic of basal myoepithelial cells; cytokeratin 5 and/or cytokeratin 17. The normal-like subtype expresses genes typical of adipose tissue. The claudin-low subtype has low expression of claudins 3, 4 and 7, E-cadherin and CD24 [15]. Molecular apocrine subtype tumours over-express the androgen receptor and lack ER [16].

Table 1-1: Breast cancer subtypes and their molecular features [6–10].

Breast cancer subtype	Features
HER2-enriched	Overexpression of genes on the 17q ERBB2 amplicon; such as HER2, GRB7 and STARD3
Luminal A	ER- and PR-positive, Ki67-negtive
Luminal B	ER-positive, either PR-negative or high Ki67 levels, can also have HER2 overexpression
Basal-like	Mostly HER2-, ER- and PR-negative, overexpression of cytokeratin 5 and/or cytokeratin 17
Normal-like	Overexpression of adipose tissue-associated genes
Claudin-low	Low expression of claudins 3, 4 and 7, E-cadherin and CD24
Molecular apocrine	Overexpression of androgen receptor and ER-negative

1.3 HER2-positive breast cancer

1.3.1 HER family structure and function

HER2 is a 185 kDa receptor tyrosine kinase (RTK) encoded by the *HER2-neu* proto-oncogene on chromosome 17q21 and, along with EGFR (HER1 or ErbB1), HER3 (ErbB3) and HER4 (ErbB4), is a member of the ERBB/HER family of RTKs (Figure 1-1). These membrane receptors are composed of a glycosylated extracellular domain, a transmembrane region and, an intracellular tyrosine kinase domain [17–19]. The extracellular domain is composed of approximately 630 amino acids and can be divided into four sub-domains. Sub-domain I contains the ligand binding site that, when activated binds to sub-domain III. This triggers a conformational change that exposes sub-domain II, the dimerization domain. The four HER family members originate from a gene duplication event, resulting in an EGFR/HER2 precursor and HER3/HER4 precursor, and subsequent gene duplications then produced the four receptors [20]. These receptors are ubiquitously expressed and are critical for normal development.
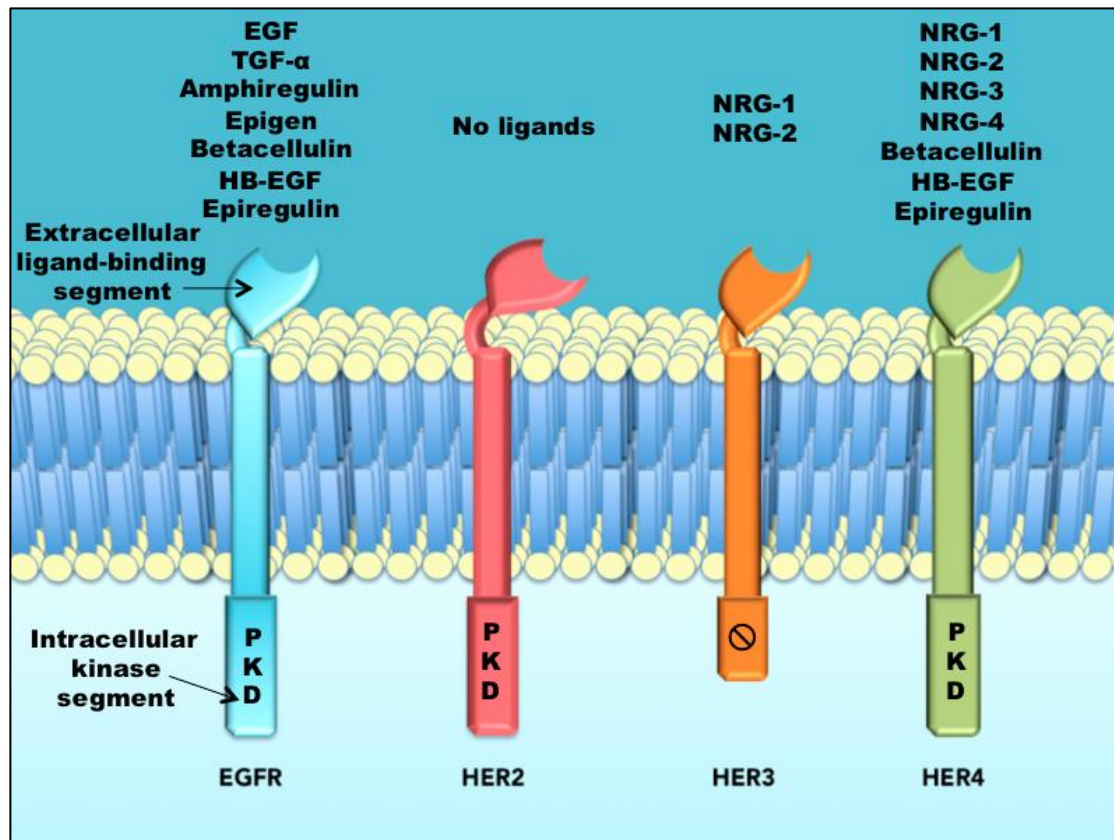
Figure 1-1: HER family members of receptor tyrosine kinase receptors. The extracellular domains of EGFR, HER3 and HER4 contain ligand binding domains for HER family ligands. EGF = epidermal growth factor, TGF-α = transforming growth factor alpha, HB-EGF = heparin-binding epidermal growth factor-like growth factor, NRG = neuregulin, PKD = protein kinase domain. HER3 has a truncated intracellular segment and does not have an active PKD (adapted from [19]).

There are 12 known ligands that can activate members of the HER family of receptors [21]. These ligands can act in either a receptor-specific manner, such as EGF, TGF-α and epigen for EGFR, or a non-specific fashion, for example, neuregulins for HER3 and HER4 and epiregulin for EGFR and HER4. They are approximately 55 amino acids in size and share a conserved EGF-like pattern of three disulphide bonds and loop-rich structure [20, 22]. In contrast to the other members of the HER family, HER2 does not require a ligand for activation. Instead, HER2 resides in a permanent, ligand-independent open conformation as sub-domain I of the extracellular domain is in constant contact with sub-domain III, which allows it to homo- or heterodimerise

[23]. In comparison, the EGFR subdomains II and IV are bound together by a β-hairpin loop projecting from subdomain II. This can only be released through ligand binding, inducing an allosteric conformational change resulting in exposure of subdomain II similar to HER2 [24]. It must be noted though, that in order for HER2 to heterodimerise, its binding partner must be ligand activated. Therefore, although HER2 is not reliant on specific ligands for activation, its level of dimerisation is governed by ligand binding to other HER receptors.

There are ten possible HER family dimer combinations. However, HER2 is the preferred dimerisation partner of all other members of the HER family [22]. These HER2-containing dimers have a decreased dissociation rate and a greater transduction of the signal compared to the other possible dimers [25]. Dimerisation results in the trans-phosphorylation of the tyrosine kinase domain. This provides docking sites for signalling proteins that possess Src homology 2 (SH2) and phosphotyrosine binding domains. The number of tyrosine phosphorylation sites varies between HER receptors, HER2 having 19 different sites. This phosphorylation allows for activation of a number of signal transduction pathways, most notably the mitogen-activated protein kinase (MAPK) and phosphoinositide 3-kinase (PI3K) pathways [26]. Through the activation of these pathways, HER signalling stimulates cell proliferation, migration invasion and regulation of apoptosis.

1.3.2 HER2 in normal development

The HER family receptors play a paramount role in normal mammalian development and HER2 is of particular significance in central nervous system and cardiac development [27, 28]. Gene mutation studies have shown that HER2-mutant mice develop nervous system defects and cannot survive gestation [29]. HER2, along with HER4 and neuregulin, are required for ventricular development. Mutations of HER2 in ventricular cardiomyocytes results in dilated cardiomyopathy [30]. HER2 is expressed in epithelial cells in stomach, skin, heart, breast and kidney tissues [30–32]. This must be taken into consideration when assessing the clinical implications of HER2-targeted therapies.

1.3.3 HER2-positive breast cancer occurrence

The incidence of HER2-positive breast cancer is reported as between 15% and 30% of all breast cancers [3, 33]. In Ireland, the average reported occurrence of HER2-positive breast cancer from 2004 to 2013 was 15.4%, equalling approximately 448 patients per year. Of those patients with HER2-positive status, 68% received trastuzumab within one year of diagnosis [3].

1.4 HER2-targeted therapies

1.4.1 Overview of approved HER2-targeted therapies

There are currently five FDA-approved HER2-targeted therapies for the treatment of HER2-positive breast cancer: trastuzumab, pertuzumab, trastuzumab emtansine (T-DM1), lapatinib and neratinib (Figure 1-2). These molecules can be divided into three main categories: anti-HER2 monoclonal antibodies, antibody-drug conjugate, and small molecule HER family tyrosine kinase inhibitors.

Trastuzumab was the first HER2-targeted therapy approved and is approved for the treatment of both early-stage and metastatic HER2-positive breast cancer [34]. Lapatinib was next approved in combination with capecitabine as second-line therapy for metastatic HER2-positive breast cancer that has become refractory to trastuzumab [35]. The second anti-HER2 monoclonal antibody, pertuzumab, was approved in dual HER2-targeted therapy with trastuzumab for the treatment of both metastatic and early-stage HER2-positive breast cancer [36, 37]. T-DM1 then showed improved efficacy as a second-line therapy compared to lapatinib plus capecitabine and was therefore approved for second-line treatment after relapse following trastuzumab treatment for metastatic disease [38]. More recently, neratinib was approved for the treatment of early-stage HER2-positive breast cancer following adjuvant trastuzumab treatment [39]. Several additional clinical trials are on-going to determine the optimal combinations and order of treatment in HER2-positive breast cancer.
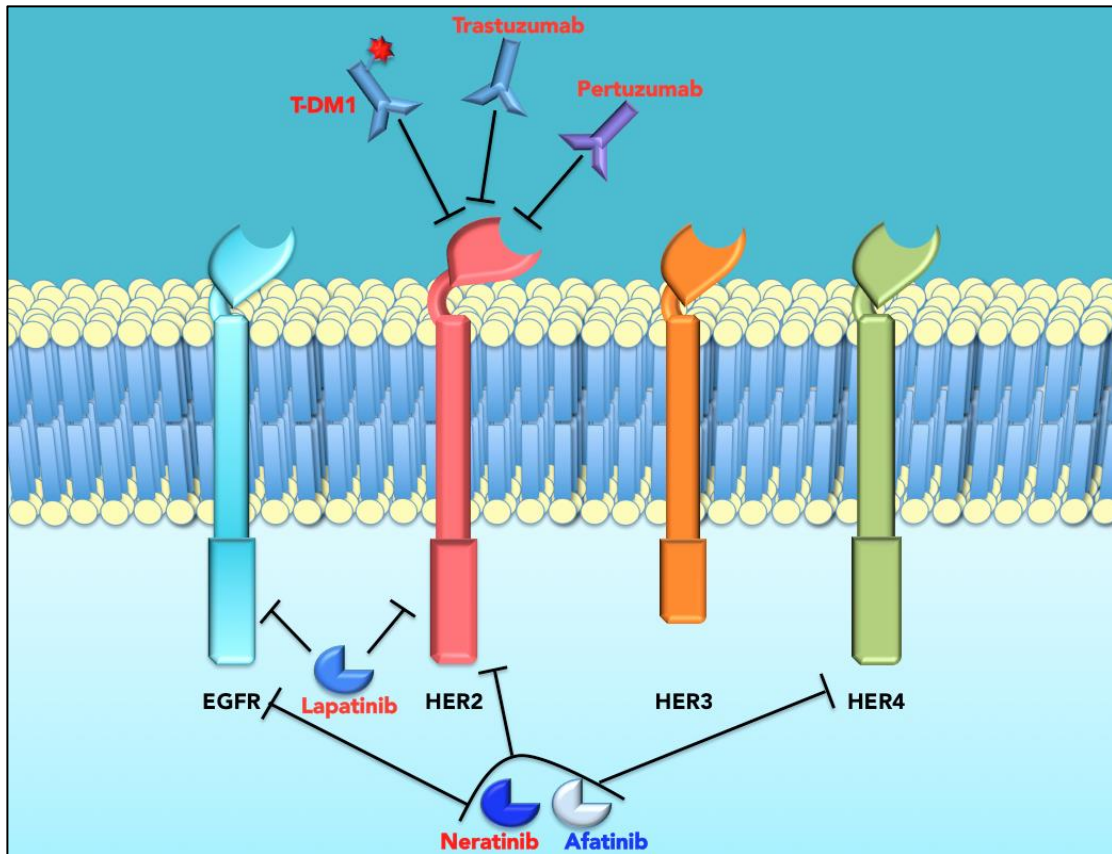
Figure 1-2: HER2-targeted therapies approved (red) and currently in clinical trials (blue) for HER2-positive breast cancer.

1.4.2 Anti-HER2 monoclonal antibodies

1.4.2.1 Trastuzumab

1.4.2.1.1 Pre-clinical investigation of trastuzumab

Trastuzumab (Herceptin^{TM}, Genentech) is a humanised IgG$_1$ monoclonal antibody that binds to the C-terminal region of domain IV of the extracellular domain [18] of HER2 causing suppression of HER2 signalling [40], antibody dependent cell-mediated cytotoxicity (ADCC) through the recruitment of natural killer cells [41, 42], induction of HER2 internalisation [43], reduction in angiogenesis [44], and G1 cell cycle arrest [45].

The development of trastuzumab stemmed from academic and industry research groups producing murine monoclonal antibodies against the extracellular domain of

HER2, p185^{HER2} [46, 47]. One of these antibodies, muMAb 4D5 showed pre-clinical efficacy in HER2-positive cancer cell lines [48]. The 4D5 murine antibody was humanised to avoid immune response against the antibody. The resulting monoclonal antibody actually bound to HER2 more effectively than the murine antibody and also elicited ADCC *in vivo*, which was not seen with the murine 4D5 [49].

1.4.2.1.2 Clinical investigation of trastuzumab

The first clinical trials for the use of trastuzumab showed the potential of trastuzumab even in heavily-pre-treated HER2-positive metastatic patients [50, 51]. Single agent trastuzumab displayed an objective response rate (ORR) of 15% with a median overall survival (OS) of 13 months [50]. Trastuzumab also showed a clinical improvement in combination with chemotherapy versus chemotherapy alone. The addition of trastuzumab increased ORR from 32 months to 50 months, with OS after one year 78% versus 67% [51]. In 1998, trastuzumab was FDA approved for the treatment of metastatic HER2-positive breast cancer and was the first HER2-targeted therapy used clinically [34]. A recent study of response to trastuzumab in patients with metastatic breast cancer showed that 9.5% of patients achieved a durable complete response [52].

Meta-analysis of five clinical trials assessing trastuzumab treatment in the adjuvant setting showed that trastuzumab-containing therapy improves survival rates and lowers the rate of recurrence and metastasis compared to adjuvant therapy without trastuzumab [53]. Patients treated with a trastuzumab-based regimen had a reduced recurrence by approximately 50%. This also extends to small localised disease, tumours $\leq$ 2 cm, as adjuvant trastuzumab treatment improves both disease-free survival (DFS) and OS [54]. Based on the adjuvant clinical trials, trastuzumab approval was expanded to include early-stage HER2-positive breast cancer in 2006 [55].

The optimal duration of adjuvant trastuzumab treatment has been a controversial topic. The PHARE clinical trial of six-months versus 12-months trastuzumab treatment could not provide evidence of inferiority of the shorter treatment and shorter treatment had decreased occurrence of cardiotoxicity [56]. However, in a meta-analysis of four clinical trials, one year of trastuzumab treatment was shown to

improve overall survival and disease free survival compared to shorter treatment regimens [57]. This suggests 12-months of trastuzumab treatment should remain the standard of care. In addition, the HERA trial showed that two-years of trastuzumab treatment did not further improve response compared to one year of treatment [58].

Trastuzumab has shown considerable efficacy against HER2-positive breast cancer in the neo-adjuvant setting. In the Phase III NOAH trial, neo-adjuvant trastuzumab plus chemotherapy produced increased event-free survival (58% versus 43%) and pathological complete response (pCR) (38% versus 19%) compared to chemotherapy alone in locally advanced HER2-positive breast cancer [59].

The most commonly occurring adverse effect of trastuzumab is fatigue. However, the most clinically significant effect observed is cardiotoxicitiy. Trastuzumab was found to cause cardiotoxicity in 4.7% of 221 patients treated [50]. Other anti-neoplastic drugs such as anthracyclines can cause cardiomyopathy and congestive heart failure. This effect is increased by the addition of trastuzumab, but can be improved with angiotensin-converting enzyme (ACE) inhibitor and beta-blocker treatment [60, 61]. Therefore, anthracycline-containing chemotherapy regimens are not given concomitantly with trastuzumab [62].

1.4.2.2   <u>Pertuzumab</u>

1.4.2.2.1   <u>Pre-clinical investigation of pertuzumab</u>

Pertuzumab (Perjeta^{TM}, Genentech) is a second-generation HER2-targeted humanised monoclonal antibody. Pertuzumab received FDA approval in 2012 for the treatment of metastatic breast cancer and in 2013 also gained accelerated approval for neo-adjuvant treatment of early-stage breast cancer. Unlike trastuzumab that targets subdomain IV of the extracellular domain of HER2, the epitope targeted by pertuzumab is subdomain II of HER2, which prevents HER2 homo- and hetero-dimerisation [63]. This dimerisation inhibition is more effective than that of trastuzumab [64]. Aside from inhibiting dimerisation, pertuzumab has also been shown, *in vitro*, to inhibit PI3K and MAPK signalling and to mediate ADCC [65]. Pre-clinical data showed that pertuzumab plus trastuzumab caused increased induction of apoptosis, enhanced Akt signalling suppression, and reduced hetero- and homo-dimerisation in the HER2-positive breast cancer cell line BT474 [66].

1.4.2.2.2   Clinical investigation of pertuzumab

Dual blockade of HER2 with the combination of both monoclonal anti-HER2 antibodies was assessed in the phase III CLEOPATRA clinical trial (n = 808). This trial evaluated the efficacy of docetaxel plus trastuzumab and a placebo versus docetaxel plus trastuzumab and pertuzumab in HER2-positive metastatic breast cancer. Pertuzumab significantly enhanced trastuzumab and docetaxel response compared to the placebo addition. OS of the triple combination was 15.6 months longer (56.5 months versus 40.8 months) and PFS was 18.7 months compared to 12.4 months [67]. Importantly, the addition of pertuzumab caused similar levels of adverse effects, with only febrile neutropenia and grade $\geq$ 3 diarrhoea increased in the pertuzumab-treated group [68]. The results of this trial led to the approval of pertuzumab in combination with trastuzumab and docetaxel as a first-line therapy for metastatic or locally recurrent disease [69].

With pertuzumab showing enhancement in combination with trastuzumab and docetaxel in the metastatic setting, its possible role in neo-adjuvant treatment was examined. The NeoSphere trial (n = 417) compared the efficacy of trastuzumab plus pertuzumab, trastuzumab plus docetaxel, pertuzumab plus docetaxel, or the triple combination, using locoregional total pCR as the primary endpoint. The dual HER2 blockade significantly increased total pCR rates, which was further improved by the addition of docetaxel . Of the patients on the triple combination 45.8% achieved pCR compared to 16.8% in the dual antibody combination, 29% of the trastuzumab plus docetaxel group and 24% of the pertuzumab plus docetaxel group [70, 71]. The triple combination marginally improved PFS and DFS compared to trastuzumab plus docetaxel, the group with the second best response (Table 1-2). This also then led to the approval of the triple combination in the neo-adjuvant setting for patients with locally advanced or early-stage HER2-positive breast cancer [37].

Table 1-2: Percentage 5-year disease-free survival and progression-free survival per treatment group in the CLEOPATRA clinical trial [67]. T = trastuzumab, P = pertuzumab, D = docetaxel.

Treatment group	Disease-free survival (%)	Progression-free survival (%)
T+D	81	81
P+T+D	86	84
T+P	73	80
P+D	73	75

1.4.3   Antibody-drug conjugate

1.4.3.1   Trastuzumab emtansine (T-DM1)

1.4.3.1.1   Pre-clinical investigation of T-DM1

Trastuzumab-emtansine (T-DM1) (Kadcyla™, Genentech) is an antibody-drug conjugate of trastuzumab and DM1 (emtansine, a derivative of maytansine), linked by a non-reducible thioester linker. Antibody-drug conjugates provide a targeted delivery system of highly cytotoxic agents to cancer cells. T-DM1 carries approximately 3.5 DM1 molecules per trastuzumab antibody. T-DM1 has shown significant anti-proliferative effect *in vitro* and *in vivo* against HER2-positive breast cancer cell lines, including cell lines with innate or acquired trastuzumab and lapatinib resistance [72, 73]. In a pre-clinical study of T-DM1 in a panel of HER2-positive breast cancer cell lines, including three cell lines that are innately resistant to trastuzumab and lapatinib, T-DM1 caused mitotic catastrophe and apoptosis and elicited ADCC similar to trastuzumab [74].

T-DM1 binds to the extracellular domain of HER2 and is internalised by endocytosis. Cleavage of the linker molecule and release of DM1 occurs in lysosomal processing. Released DM1 can then inhibit microtubule assembly. Due to the anti-HER2 activity of the trastuzumab molecule and the cytotoxicity of DM1, T-DM1 as a single agent

can cause cell death by several mechanisms, including apoptosis, mitotic catastrophe and ADCC [73, 75].

1.4.3.1.2   Clinical investigation of T-DM1

T-DM1 was safely tolerated and showed some clinical efficacy in heavily pre-treated patients in phase I clinical trials [76]. The dose limiting toxicity was thrombocytopenia, due to T-DM1 affecting platelet production. Cardiac toxicity requiring dose modification was not observed [76, 77]. The phase III EMILA trial assessed T-DM1 in metastatic HER2-positive breast cancer as a second line therapy against the approved combination of lapatinib and capecitabine. In this trial, T-DM1 was superior in PFS (9.6 months versus 6.4 months) and OS (30.9 versus 25.1 months) [78, 79]. On the basis of the EMILA trial, T-DM1 was approved for second-line treatment of metastatic HER2-positive breast cancer [38, 80]. The combination of T-DM1 with pertuzumab is now under investigation, with a phase IIa trial showing clinical activity (ORR = 41%, 33% in metastatic disease, 57% in first-line therapy) [81]. T-DM1 is now being tested in neo-adjuvant and adjuvant treatment of HER2-positive breast cancer. These trials include T-DM1 as a single agent and in combination with various chemotherapies, HER2-targeted therapies, immunotherapy and other targeted therapy agents, including neratinib, ONT-380, palbociclib and pembrolizimab.

1.4.4   Small molecule tyrosine kinase inhibitors

1.4.4.1   Lapatinib

Lapatinib (Tykerb^{TM}, Novartis) (Figure 1-3) is a reversible, tyrosine kinase inhibitor of EGFR and HER2. In 2001, it received FDA approval in combination with capecitabine for the treatment of metastatic HER2-positive breast cancer that has failed trastuzumab therapy [82]. It was subsequently also approved for the treatment of HER2-positive, ER-positive breast cancer in combination with letrozole [83].
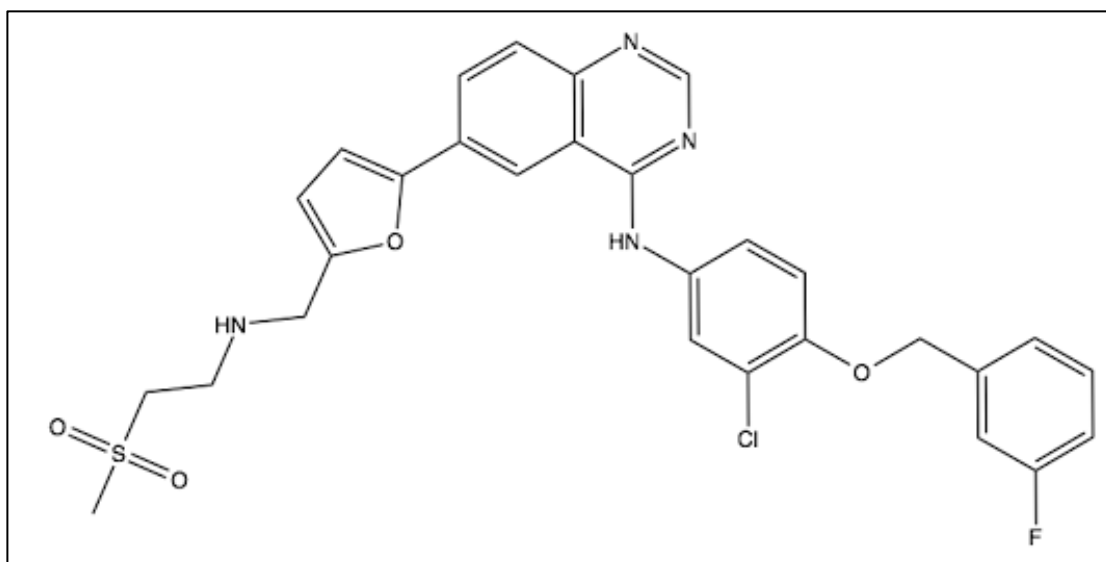
Figure 1-3: Chemical structure of lapatinib (reproduced from PubChem; CID no. = 208908 [84])

The predominant mechanism of action of lapatinib in HER2-positive breast cancer is inhibition of HER2 signalling (IC_{50} value = 9.2 nM). Downstream of HER2 signalling lapatinib can induce apoptosis, cause cell cycle arrest, senescence and has been indicated to induce autophagy [85–87]. Although lapatinib is also an EGFR inhibitor (IC_{50} value = 10.8 nM), its efficacy is independent of EGFR expression in HER2-overexpressing breast cancer cell lines and patient tumours [88–90]. When bound to HER2, lapatinib inhibits both PI3K/Akt and MAPK signalling pathways [88]. This inhibition of MAPK signalling causes increased Bcl-2 interacting mediator of cell death (BIM), which results in apoptosis. Apoptosis can also be induced by lapatinib through decreased levels of survivin and increased myeloid cell leukaemia 1 (MCL-1) [91–94]. The intracellular binding site of lapatinib is advantageous as, unlike trastuzumab, lapatinib can also bind to and inhibit p95, the cleaved constitutively active form of HER2 [95]. Lapatinib also induces stabilisation and accumulation of HER2 on the cell surface which may allow for greater trastuzumab-mediated ADCC alone [42, 96]. Lapatinib in combination with trastuzumab increases growth inhibition in HER2-positive breast cancer cell lines compared to either single agent [88]. This effect was seen in cell lines sensitive to both single agents, resistant to trastuzumab, and innately resistant to both agents.

Lapatinib monotherapy was found to be ineffective in HER2-positive breast cancer compared to trastuzumab [97]. However, lapatinib combined with capecitabine showed a greater clinical benefit than capecitabine alone (PFS of 8.4 months vs. 4.4 months) for patients with trastuzumab-refractory metastatic breast cancer [35, 98]. Capecitabine (Xeloda, Roche) is a chemotherapy pre-drug that is converted to 5-fluorouracil in tumour cells. This combination also performed better than continued trastuzumab with capecitabine when the patient's tumour progressed after initial trastuzumab treatment (median PFS of 6 months vs. 4.5 months) [99]. The results of this trial led to the FDA approval of lapatinib in combination with capecitabine. Therefore, proceeding clinical trials focused on possible lapatinib efficacy in combination with other HER2-targeted therapies or chemotherapies.

The potential benefit of dual HER2 blockade with trastuzumab and lapatinib in HER2-positive breast cancer was examined in the metastatic setting with the EGF104900 trial and in early stage disease with the ALTTO trial. The addition of lapatinib to trastuzumab showed a 4.5 month increase in overall survival compared to lapatinib alone in trastuzumab-refractory metastatic disease [100]. In the ALTTO trial, patients with early-stage HER2-positive breast cancer received adjuvant chemotherapy combined with trastuzumab alone (T), lapatinib alone (L), trastuzumab followed by lapatinib (T->L), or trastuzumab plus lapatinib (T+L) [101]. The L arm was discontinued when inferiority to trastuzumab alone was observed. At a median follow-up of 4.5 years, there was a 16% reduction in the hazard ratio in T+L compared to T, but this was not statistically significant at the defined $p<0.025$ significance level ($p = 0.048$). There was no significant difference in OS after 4 years. However, results of trials of this combination in the neo-adjuvant setting were more promising. The NeoALTTO trial ($n = 455$) compared the efficacy of lapatinib alone versus trastuzumab alone versus trastuzumab plus lapatinib for six weeks followed by the same targeted therapy plus paclitaxel for 12 weeks prior to surgery [102]. The combination of trastuzumab and lapatinib showed significantly improved pCR compared to trastuzumab alone (46.8% versus 27.6%), and those that achieved pCR had increased event-free survival (86% versus 72%) and OS (94% versus 87%) [102, 103]. The combination of trastuzumab and lapatinib has also shown efficacy in patients with heavily trastuzumab pre-treated metastatic HER2-positive breast cancer. The combination arm showed increased PFS and clinical benefit rates (CBR) compared to lapatinib alone, with a satisfactory safety profile [104]. Preliminary

results from the EPHOS-B trial (n = 257) further highlighted the potential benefit of neoadjuvant lapatinib plus trastuzumab. In this trial, patients were given the combination of lapatinib and trastuzumab, trastuzumab alone or a placebo without any chemotherapy during an 11-day treatment window after diagnosis and prior to surgery. Remarkably, in the combination arm, 17% of patients had tumours of less than 5 mm in diameter, defined as minimum residual disease (MRD), and a further 11% had pCR. In comparison, the trastuzumab only arm produced no pCR and 3% MRD while the control group had no occurrences of pCR or MRD [105].

Clinically, HER2-positive breast cancer presents as a heterogeneous disease; incorporating HER2-enriched, luminal A, luminal B, basal-like, and normal-like cancers. In the phase II PAMELA trial, patients were characterised by PAM50 breast cancer subtype predictor and given lapatinib plus trastuzumab. Patients with hormone receptor positive disease also received endocrine therapy. Of the HER2-positive breast cancer patients 67% had HER2-enriched disease. Of these patients 41% achieved pCR compared to 10% of the non-HER2 enriched patients [106]. This result therefore indicates that PAM50 HER2 subtype classification may be a better predictor of response to lapatinib and trastuzumab than traditional HER2-positive characterisation.

In summary, the assessment of trastuzumab plus lapatinib in combination has shown mixed response. Adjuvant dual therapy did not significantly improve survival outcomes and although the combination increased pCR in the NeoALTTO trial, this did not translate into improved OS. However, trials like the EPHOS-B trial hold promise, as trastuzumab plus lapatinib without chemotherapy significantly increased pCR, but the effect on OS is not yet known. The PAMELA trial suggests that the combination may perform better against a trastuzumab alone regimen with PAM50 HER2-enriched patient selection.

1.4.4.3   Neratinib

1.4.4.3.1   Pre-clinical investigation of neratinib

Neratinib (Nerlynx™, Puma Biotechnologies) (Figure 1-4) is an anilinoquinoline derivative of pelitinib (EKB-569, Wyeth), an irreversible EGFR inhibitor [107]. It is a pan-HER family tyrosine kinase inhibitor that is approved for the treatment of early-stage HER2-positive breast cancer [39].
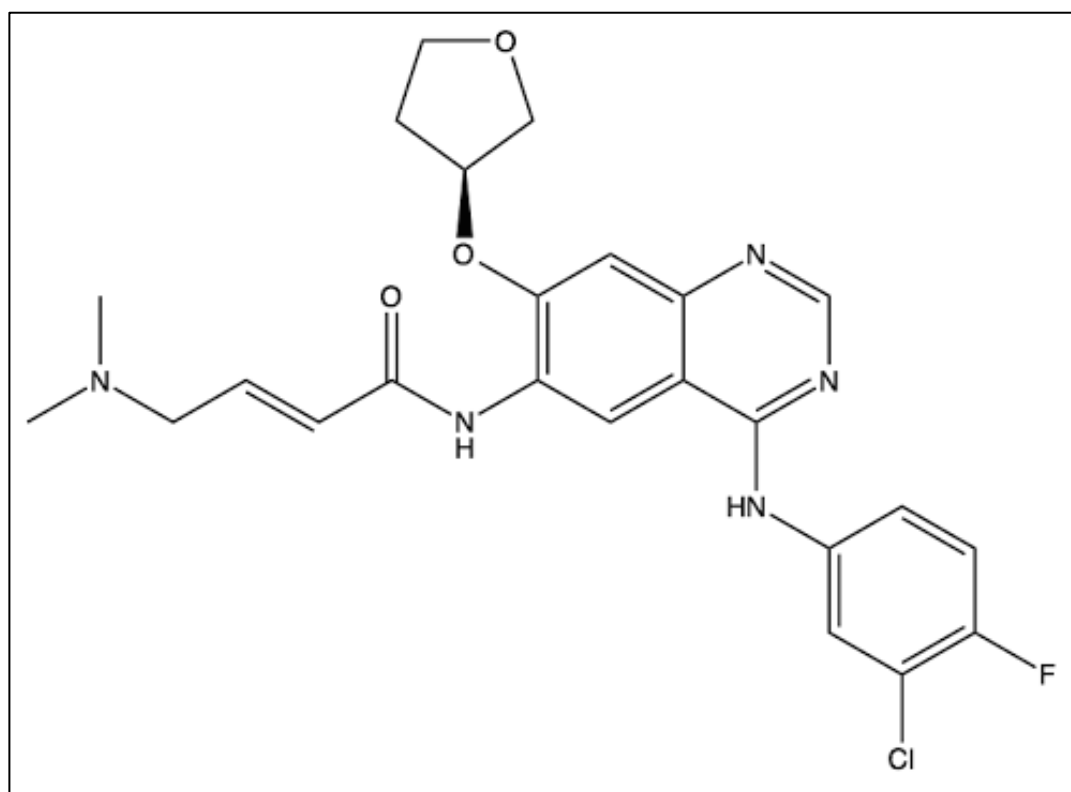
Figure 1-4: Chemical structure of neratinib (reproduced from PubChem; CID no. = 9915743 [84])

Neratinib is a potent inhibitor of HER2-amplified or HER2-driven cancers. It has shown significantly greater activity in HER2-amplified breast cancer cell lines compared to HER2-low or non-amplified cells and sensitivity to neratinib correlated with baseline and phosphorylated HER2 levels, but not EGFR levels. Neratinib suppressed HER receptor activation and decreased downstream pathway signalling, through PI3K and MAPK. However, AKT and HER3 activity was restored after drug withdrawal, which was prevented when neratinib was combined with trastuzumab

[108]. This suggests the combination of trastuzumab and neratinib may be more effective than single agent therapy. Furthermore, neratinib has demonstrated *in vitro* and *in vivo* efficacy against trastuzumab-resistant HER2-positive breast cancer. Innately trastuzumab resistant cell lines are also sensitive to neratinib. The combination of neratinib and trastuzumab enhanced the single agent effect in acquired trastuzumab resistant SKBR3 and BT474 cell lines. The addition of neratinib to trastuzumab treatment can also inhibit HER4 cleavage and nuclear translocation, which is associated with trastuzumab resistance [109].

1.4.4.3.2   Clinical investigation of neratinib

Neratinib has been investigated in several cancer types, including breast, lung, bladder, and colorectal cancer [110–112], with a focus on HER2-amplified and HER2-mutated cancers. Phase I clinical investigation showed that neratinib was well tolerated up to 320 mg daily dosage, with a therapeutic dose set at 240 mg [110]. The most common neratinib-related toxicity and the primary dose-limiting toxicity was diarrhoea, with 32% of patients experiencing grade 3 or higher diarrhoea. Neratinib showed significant efficacy in the breast cancer setting. Partial responses were observed in eight breast cancer patients, accounting for 32% of breast cancer patients enrolled in the phase I study. These 8 patients had HER2-positive breast cancer, with 7 of the 8 partial responders having HER2 immunohistochemical staining of 3 [110]. Neratinib has shown clinical activity in HER2-positive breast cancer, regardless of previous trastuzumab treatment. However, there is some reduction in efficacy in cancers previously treated with HER2-targeted therapies. In a phase II clinical trial, patients were divided into two cohorts: 63 with prior trastuzumab therapy and 64 being trastuzumab-naïve. Both cohorts received 240 mg neratinib monotherapy daily, with the primary endpoint of 16-week PFS rate. Patients with prior trastuzumab therapy had a 16-week PFS rate of 59% and ORR of 24%. For patients with no previous trastuzumab, the 16-week PFS rates were 78% and ORR 56% [113]. Neratinib has also demonstrated efficacy in lapatinib-treated breast cancer. A phase I/II clinical trial showed tolerability of neratinib in combination with capecitabine and examined this combination in patients with metastatic HER2-positive breast cancer, of which seven patients had previously received lapatinib therapy. Clinical response

was observed at the MTD in 64% of lapatinib-native patients and 57% of patients that previously received lapatinib. Median PFS was 40 weeks for patients with no prior lapatinib and 26 weeks for those who received lapatinib [114]. Neratinib was observed to significantly improve invasive disease free survival (iDFS) compared to a placebo when given after two years of trastuzumab therapy for early-stage HER2-positive breast cancer in the phase III ExteNET trial. After two years follow-up, iDFS was 94.2% for the neratinib arm compared to 91.9% for placebo. The results of this trial led to the approval of neratinib for the treatment of early-stage HER2-positive breast cancer following adjuvant trastuzumab.

A number of trials have been launched to test the efficacy of neratinib compared to lapatinib. One phase II clinical trial compared neratinib monotherapy to lapatinib plus capecitabine in patients with advanced HER2-positive breast cancer who previously received trastuzumab. Lapatinib and capecitabine showed higher ORR and median PFS than the neratinib monotherapy. However, this difference was not statistically significant [115]. This led to the phase III NALA trial which is currently examining neratinib plus capecitabine versus lapatinib plus capecitabine in metastatic HER2-positive breast cancer patients who have received two or more previous HER2-targeted therapies(excluding HER2-targeted TKIs). This clinical trial should determine if neratinib shows superiority over lapatinib in the HER2-positive metastatic setting. The primary outcomes of this study are PFS and OS and the estimated primary completion date is 2019 [116].

Several trials are underway or completed examining combinations of neratinib with other HER2-targeted therapies. The FB-8 trial showed that neratinib combined with trastuzumab and paclitaxel is safe, but suggested reducing the therapeutic dose of neratinib to 200 mg daily when in combination with trastuzumab and paclitaxel [117].

1.4.4.4   Afatinib

1.4.4.4.1   Pre-clinical investigation of afatinib

Afatinib (Gilotrif^{TM}, Boehringer Ingelheim) (Figure 1-5) is a quinazoline derivative small molecule tyrosine kinase irreversible inhibitor of EGFR, HER2 and HER4 [118]. Afatinib is FDA approved for metastatic non-small cell lung cancer (NSCLC) with either EGFR exon-29 deletions or Leu858Arg mutation [119]. *In vitro* assays

showed afatinib is a potent inhibitor of wild type EGFR (EC_{50} = 0.5 nM), HER2 (14 nM), HER4 (1 nM) and mutant EGFR variants ($EGFR^{L858R}$ = 0.4 nM and $EGFR^{L585R/T790M}$ = 10 nM) [120]. Afatinib covalently binds to Cys-773 and Cys-805 of EGFR and HER2, respectively, which are situated in the ATP binding pocket of the kinase domain.
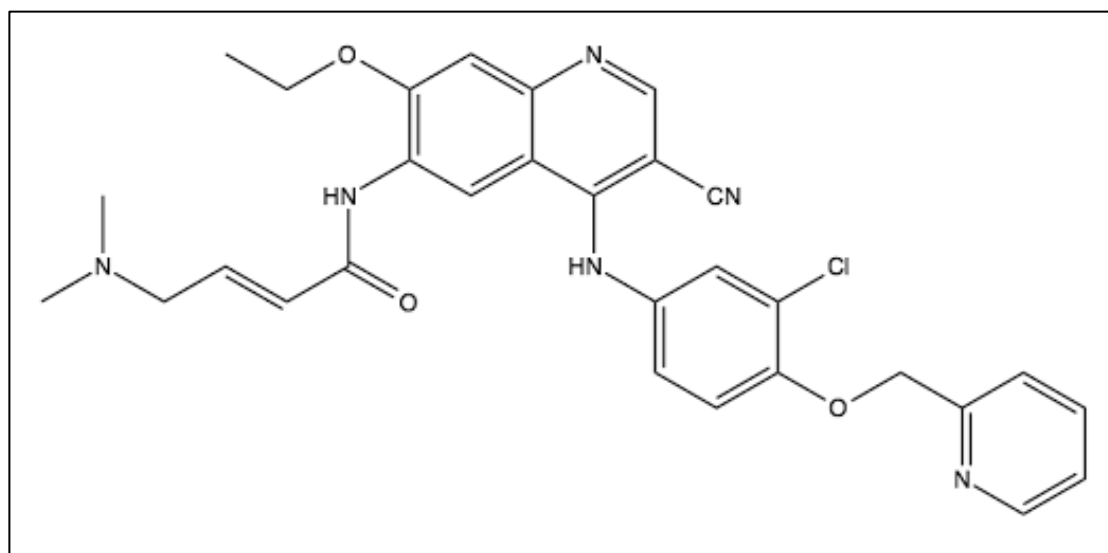
Figure 1-5: Chemical structure of afatinib (reproduced from PubChem; CID no. = 10184653 [84])

Pre-clinical assessment of afatinib demonstrated efficacy in HER2-overexpressing and/or EGFR-amplified breast, lung, pancreatic, prostate and gastric cancer cell lines [118, 121, 122]. Afatinib showed high specificity and potency to suppress phosphorylation of both wild type and mutant EGFR and HER2. In particular, HER2-positive breast cancer cell lines were highly sensitive to afatinib and an additive effect was seen with the combination of afatinib and trastuzumab in four trastuzumab sensitive cell lines and an acquired trastuzumab resistant cell line. This sensitivity was also reflected in an *in vivo* xenograft model [123].

1.4.4.4.2 <u>Clinical investigation of afatinib</u>

The described pre-clinical data led to the initiation of multiple phase I clinical trials to investigate the safety and clinical activity of afatinib, alone or in combination with chemotherapy, in advanced solid cancers.

Four afatinib monotherapy phase I clinical trials were performed to determine the safety and tolerability of afatinib in solid tumours. Two of these trials used a continuous dosing schedule, one study used a 14-days on/14-days off programme and another used a three-weeks on/one-week off schedule [124–127]. The adverse effects observed in these trials were typical of EGFR inhibitors and were most commonly gastrointestinal-related, skin rashes and fatigue. These trials demonstrated that afatinib is orally bioavailable and the maximum plasma concentration at the MTD was 25- to 700-fold higher than required to inhibit EGFR phosphorylation *in vitro* [126]. However, EGFR-associated biomarkers were unchanged but Ki-67 levels were significantly reduced on therapy. From these trials, the recommended dose for phase II trials was established as 50 mg daily [127].

Clinical investigation of afatinib in breast cancer has focused on two areas: second-line therapy after progression on trastuzumab, and as a neo-adjuvant therapy. A phase II clinical trial of afatinib as a second-line therapy examined afatinib monotherapy in a single-arm study [128]. Eleven percent of patients achieved a partial response, with 37% having stable disease. These patients had all previously been treated with trastuzumab and had also received a median of three chemotherapies. This indicated that afatinib might have efficacy in trastuzumab-refractory disease. The LUX-Breast phase III clinical trials further investigated second-line afatinib therapy. The LUX-Breast 1 trial compared afatinib plus vinorelbine to continued trastuzumab plus vinorelbine in metastatic breast cancer patients [129]. This trial was stopped early as independent benefit-risk analysis showed that afatinib was inferior to trastuzumab. Median PFS of the afatinib group was 5.5 months and 5.6 months for the trastuzumab group. As CNS metastasis is a common occurrence in HER2-positive disease, the LUX Breast 3 trial was carried out to determine if afatinib could improve current therapy. Afatinib alone and afatinib plus vinorelbine were compared to the investigator's choice of treatment [130]. Neither afatinib-based therapy showed a greater clinical benefit compared to investigator's choice. Clinical benefit was defined as no additional CNS tumour development or tumour-related worsening of

neurological symptoms at 12 weeks. The LUX-Breast 2 trial examined afatinib in metastatic breast cancer that progressed on trastuzumab and/or lapatinib. This trial compared three treatment arms: afatinib alone, afatinib followed by paclitaxel after progression on afatinib, and afatinib followed by vinorelbine. Results of this trial are so far unpublished [131].

In the neo-adjuvant setting, a phase II clinical trial examined the potential of afatinib in the treatment of locally advanced HER2-positive breast cancer [132]. Patients on this trial received afatinib, trastuzumab, or lapatinib for six weeks prior to surgery. This trial was terminated early due to low accrual rate. However, 28 patients were enrolled in the trial. Objective responses were observed in 8 of 10 afatinib treated patients, 4 of 11 that received trastuzumab, and 6 of 8 of the lapatinib group. Afatinib was associated with a much higher rate of adverse events compared to trastuzumab or lapatinib. The DAFNE phase II clinical trial was a single arm study of neo-adjuvant afatinib plus trastuzumab, followed by afatinib, trastuzumab and paclitaxel, then epirubuicin, cyclophosphamide and trastuzumab prior to surgery [133]. This regimen showed a tolerable safety profile and similar pCR (49.2%) to other HER2-targeted neo-adjuvant treatment. However, pCR achieved was still below desired the significant pCR of 55%.

1.5   HER2-targeted therapy resistance

HER2-targeted therapies have significantly improved clinical outcome for HER2-positive breast cancer patients; especially in early stage disease. However, *de novo* and acquired resistance to HER2-targeted therapies is a pertinent clinical problem. Therefore, there is a need to investigate the mechanisms of HER2-targeted therapy resistance. This can be achieved by examining primary tumour samples of HER2-positive breast cancer patients treated with HER2-targeted therapies or by establishing *in vitro* cell line models of drug resistance. Cell lines are the most commonly used models of drug resistance. Cancer cell lines provide a sustainable, indefinite supply of highly homogeneous cells that are largely representative of the tumours from which they are derived [134]. Nonetheless, there are several limitations to cancer cell lines. Cell lines lack the supporting stromal cells, which interacts with the cancer cells and can alter response. In addition, most breast cancer cell lines are derived from pleural

effusions of metastatic cancers. This limits the representation of the different stages of breast cancer [135].

1.5.1 Trastuzumab resistance

Several mechanisms of resistance have been discovered using both *in vitro* resistance models and patient samples [Reviewed in 132–135]. With inhibition of HER2 by trastuzumab, other RTKs can become over-expressed or up-regulated. For example, HER3 has been shown to be increased in trastuzumab resistant cells, which causes increased HER2-HER3 dimerisation and maintenance of PI3K activation [140]. The RTK Met can also be increased in trastuzumab resistance and correlates with poor survival in trastuzumab-treated patients [141, 142]. Previous work from our lab implicated IGF-1R in trastuzumab resistance [143]. In this study, trastuzumab-resistant SKBR3 and BT474 cells displayed increased levels of IGF-1R and IGF-1R inhibition enhanced trastuzumab response in these cell lines. As trastuzumab response is reliant on trastuzumab/HER2 binding, cancer cells can cleave the ECD of HER2 or sterically hinder the binding of trastuzumab. HER2 ECD shedding is associated with poor response to trastuzumab [144–146]. This can be analysed by examining levels of cleaved HER2 ECD in the blood and tumour levels of p95 HER2 [95, 147]. Mucin 4 (MUC4) can also be increased in trastuzumab-resistant breast cancer to prevent efficient binding of trastuzumab to HER2 ECD [144–146].

1.5.2 *In vitro* models of lapatinib resistance

This study focuses particularly on resistance and response to HER2-targeted tyrosine kinase inhibitors. Nine different HER2-positive breast cancer cell lines have been used to produce acquired lapatinib resistant cell lines. The majority of cell lines used were luminal adenocarcinomas that are HER2-positive and ER/PR-negative. Although, two ER-positive cell lines have been used to generate lapatinib-resistant cell lines, BT474 and MDA-MB-361 cell lines.

There are several methods to develop drug resistant cell lines [148]. Lapatinib resistant cell lines have been developed through continuous exposure to lapatinib, by dose escalation treatments and by single cell cloning techniques (Table 1-3). The

published lapatinib resistant cell lines have been produced from a variety of different HER2-positive cell lines and the concentrations used, both starting and fixed concentrations, vary between studies; lapatinib concentrations used range between 50 nM and 5 μM. Only two established cell lines were generated using concentrations in excess of the steady state concentrations achieved in patients' blood. Xia and colleagues [149] exposed the BT474 cell line to increasing concentrations of lapatinib from 250 nM to 5 μM and Liu and colleagues pooled 21 resistant BT474 clones, which had been exposed to 1, 3 or 5 μM lapatinib [150]. A number of different approaches have been used in the development of the clinically relevant models. Most resistant cell lines were exposed to a low dose of lapatinib, which was gradually increased. However, both the starting concentration and final maintaining concentration vary widely. SKBR3 cells have been exposed to 5 nM lapatinib increasing to 250 nM over six months [151], 250 nM increasing to 1 μM over six months [152], 100 nM to 1 μM for 3 to 12 months and an escalating lapatinib concentration up to 2.6 μM [153]. In our laboratory, a resistant SKBR3 cell line was developed using continuous treatment with 250 nM lapatinib for six months [154]. The variation in lapatinib concentrations used, length of exposure, and numerous parental cell lines used has resulted in the wide variety of lapatinib resistance mechanisms discovered.

1.5.3   Mechanisms of lapatinib resistance

Twenty mechanisms of lapatinib resistance have been proposed utilising acquired resistance cell line models (Table 1-3). These mechanisms can be largely divided into three categories: activation of alternative RTKs, re-activation of downstream signalling, and phenotypic switching.

Table 1-3: Mechanisms of lapatinib resistance and the methods used to generate lapatinib resistant cell lines.

Author	Parental cell lines	Method of resistant cell line development	Proposed mechanism of resistance
Azuma, et al. [155]	UACC-812	0.01 μM to 1 μM over 8 months	Switching addiction to FGFR2
Bi, et al. [156]	BT474	Continuous exposure to lapatinib up to 2 μM (cell line developed in [157])	Not stated. Biochemical composition difference observed with Raman spectroscopy
Brady, et al. [158]	BT474, UACC-893	2.1 μM lapatinib for >9 months (BT474) or increasing doses until reaching 2.1 μM for a total of >5 months (UACC893)	Enhanced PI3K p110α signalling
Chen, et al. [159]	BT474-L, AU565-L	Continuous 2 μM lapatinib exposure for 12 months	Protective autophagy
Corcoran, et al. [151]	SKBR3, HCC1954	5 nM to 250 nM over 6 months	IGF1R stimulates resistance. Increasing miR-630 reduces resistance
Formisano, et al. [160]	MDA-MB-361	Not stated	Src mediated EGFR activity
Huang, et al. [161]	BT474	Increasing concentrations 0.1 to 1 μM for 3-12 months	β-integrin mediated survival
Jegg, et al. [153]	SKBR3	Increasing lapatinib concentration up to final concentration of 2.6 μM	Constitutive activation of mTORC1 in the absent of upstream PI3K/AKT signalling
Komurov, et al. [162]	SKBR3	Increasing doses of lapatinib over one year	Glucose deprivation network alterations
Lesniak, et al. [163]	SKBR3	Selection of mesenchymal colony clusters of SKBR3 and beta-integrin transfected-SKBR3	Spontaneous EMT

Liu, et al. [150]	BT474	Continuous exposure to 1, 3 or 5 μM lapatinib. 21 L-resistant clones generated and pooled.	Activation of AXL
Ma, et al. [152]	SKBR3	Increasing lapatinib concentration from 0.25 μM up to final concentration of 1 μM for at least 6 months	Proteasome alterations. Shows synergy of lapatinib and bortezomib
McDermott, et al. [154]	SKBR3, HCC1954	Continuous exposure to 250 nM lapatinib (SKBR3) and 1 μM (HCC1954)	Increased PP2A activity
Puig, et al. [164]	AU565	3.5 μM to 7 μM lapatinib over 6 months	Fatty acid synthase activity
Rani, et al. [165]	SKBR3	Continuous exposure over 6 months	NeuromedinU causes HER2 stability
Rexer, et al. [157]	SKBR3, HCC1954, BT474, MDA-MB-361, UACC-893, SUM190PT	Continuous exposure increasing to 1μM or 2 μM lapatinib	Src family kinases maintaining PI3K/AKT signalling
Wang, et al. [166]	SKBR3, BT474	Increasing from 0.1 to 1 μM over 3-12 months	Role of ER and HER2 reactivation
Wang, et al. [167]	SKBR3	0.05 μM escalating to 2 μM over 12 months	RON activation of PI3K/AKT pathway
Xia, et al. [168]	BT474	Pool of single cell clones. Gradual increase from 0.25-5 μM over at least 2 months and then maintained in 5 μM lapatinib	Switching to ER signalling
Xia, et al. [169]	BT474, SKBR3, AU565, SUM190	Generated and maintained in 1 μM lapatinib	Heregulin-EGFR-HER3 autocrine signalling

1.5.3.1 <u>Activation of alternative RTKs</u>

Although proliferation of HER2-positive breast cancer cells is driven by HER2 signalling, there are redundant survival mechanisms that can be activated when HER2 signalling is suppressed. This can occur through up-regulation of other RTKs, including other HER family members, or MET, FGFR2 and IGF-1R.

In one study of four acquired lapatinib resistant cell lines, lapatinib was found to inhibit HER2 activity but downstream PI3K signalling persisted despite no changes in PTEN levels and a lack of PI3K mutation [169]. This was determined to be mediated by switching to EGFR-HER3 dimerisation, which was regulated by increased levels of membrane-bound heregulin. Acquisition of HER2 mutations such as T798I, L755S, and T733I can prevent effective lapatinib binding, nullifying the growth inhibitory effect of lapatinib [170, 171].

Insulin-like growth factor 1 receptor (IGF-1R) has been associated with several cancer types, including lung, colorectal and breast [172, 173]. IGF-1R is regulated by miR-630 and increased miR-630 results in degradation of IGF-1R [174]. Corcoran *et al*. investigated the role that miR-630 may have in lapatinib response and resistance. The introduction of miR-630 into acquired lapatinib resistant SKBR3 and HCC1954 cells resulted in restored lapatinib sensitivity. Likewise, inhibition of miR-630 in sensitive cell lines resulted in reduced sensitivity to HER2-targeted TKIs. The main mechanism of action of miR-630-mediated lapatinib insensitivity proposed is through regulating the expression of IGF-1R [151].

MET-related RTKs have been implicated in lapatinib resistance. A lapatinib resistant cell line was developed by escalating SKBR3 exposure to lapatinib (0.05 to 2 μM) over a 12-month period. This cell line utilised Recepteur d'Origine Nantais (RON), a member of the MET proto-oncogene family. This RON activation sustained PI3K signalling even with HER2 inhibition. RON inhibition with siRNA and the RON-selective inhibitor RON I reversed lapatinib resistance [167]. A BT474-L cell line exploited AXL to overcome lapatinib treatment. AXL activation results in stimulation of the PI3K signalling pathway and thereby induces cell survival, proliferation, migration and differentiation [175]. Overexpression of AXL has been associated with poor prognosis in breast, gastric, ovarian, glioma and lung cancer. The lapatinib resistant cell line maintained Akt activation despite decreased EGFR and HER2

levels. Inhibition of AXL with foretinib, a small molecule TKI inhibitor of AXL, MET and VEGFR, restored sensitivity to lapatinib. Lapatinib plus foretinib is currently undergoing clinical investigation. The combination was demonstrated to be safe in a phase Ib trial. The combination showed little efficacy which could be due to low levels of MET in the cohort [176].

Fibroblast growth factor receptor 2 (FGFR2) has also been implicated in lapatinib resistance [155]. FGFR2 is one of four members of the FGFR RTK family. Like HER2, FGFR2 dimerisation leads to autophosphorylation and activation of the PI3K and MAPK pathways. FGFR2 overexpression has been observed in breast and gastric cancer [177]. UACC812 cells were treated with $0.01 - 1$ µM lapatinib over 8 months until lapatinib resistance emerged. This cell line had FGFR2 amplification and over-expression and was highly sensitive to an FGFR2 inhibitor. The reliance on FGFR2 in lapatinib resistant breast cancer was also examined in tumour samples, which showed a correlation between poor survival outcome and FGFR2 levels [155]. FGFR1 and FGF3 amplification have also been correlated with poor response to HER2-targeted therapies. In a xenograft BT474 cell line model of acquired lapatinib and trastuzumab resistance, FGF3, 4 and 9 genes were amplified, which conferred increased FGFR phosphorylation and reduced lapatinib uptake. These resistant tumours were sensitised to FGFR inhibition [178].

1.5.3.2 Re-establishment of downstream signalling

HER2 signalling results in the activation of the PI3K pathway, which is inhibited by HER2-targeted therapies. Hyperactivity of PI3K may be due to mutation of the catalytic subunit 110α [179], loss of PTEN [180] or INPP4B, mutation of AKT1 [181] or amplification of AKT2 [182]. This increase in PI3K activity is found in approximately 25-30% of all breast cancers [179]. Although HER2-targeted therapies should inhibit PI3K signalling, its activation or re-activation is associated with resistance to trastuzumab and lapatinib [40, 153, 158, 183, 184], though, there is evidence of lapatinib sensitivity in some cell lines with PI3K mutations [184]. Four different mechanisms of resistance have been found that utilise activation of the PI3K signalling pathway [153, 157, 158, 183]. Six HER2-positive cell lines with acquired lapatinib resistance have maintained PI3K signalling, despite suppression of HER2

activation, indirectly through Src family kinases [157]. The up-regulation of Src family kinases was identified using global phospho-tyrosine profiling. The inhibition of the Src family kinases using sarcatinib and dasatinib repressed growth and PI3K/AKT signalling and the combination of sarcatinib with lapatinib was synergistic in xenografts. Significantly, Src family kinase expression was increased in patient tumours after lapatinib treatment [157]. Src was also implicated in another study involving an acquired lapatinib resistant MDA-MB-361 model and innately lapatinib resistant cell lines such as JIMT-1. The combination of lapatinib and the Src inhibitor saracatinib significantly decreased HER2 signalling and Akt and ERK activation compared to either single agent [160].

PI3K inhibition with copanlisib restored sensitivity to both lapatinib and trastuzumab in acquired resistant cell line models. These cell lines included SKBR3-L, SKBR3-TL, and HCC1954-L cell lines. Copanlisib plus lapatinib was also synergistic in lapatinib resistant cells and trastuzumab resistant cell lines [185].

Insulin receptor substrate 4 (IRS4) is another indirect cytoplasmic activator of PI3K signalling associated with HER2-targeted therapy resistance. IRS4 was found to be associated with innate and acquired trastuzumab and lapatinib resistance by causing hyper-activation of the PI3K pathway, independent of HER2 [186].

Lapatinib-resistant BT474 cells were found to have reactivated PI3K signalling through up-regulation of PI3K p110α mutants and possibly through the acquisition of secondary mutations such as a p100α E542K-activating mutation. An increase in p110α H1047R was also found in a lapatinib resistant UACC-893 cell line. PI3K inhibition with BYL719, a p100α-selective inhibitor, overcame lapatinib resistance *in vitro* and, in combination with lapatinib, *in vivo* [158].

HER2 signalling reactivation can also occur due to HER2 mutation. The HER2L744S mutation occurred in BT474 cells with acquired resistance to lapatinib, to trastuzumab, and to trastuzumab plus lapatinib. When this mutation was simulated in trastuzumab- and lapatinib-sensitive cell lines, sensitivity to both HER2-targeted agents was reduced [170].

1.5.3.3   ER signalling

Phenotypic switching of dependency on HER2 and ER is often observed in the clinic, especially after HER2-targeted therapy or anti-oestrogen treatment [187]. Lapatinib resistance has been shown to up-regulate ER expression in a lapatinib resistant model of the triple-positive cell line BT474. This was mediated by increased activity of FOXO3a. This increased FOXO3a activity was observed in patients tumour samples following treatment with lapatinib [168].

1.5.3.4   Epithelial-mesenchymal transition

Cancer cells treated with anti-neoplastic drugs can undergo adaptive changes such as epithelial-mesenchymal transition (EMT). EMT results in a stem cell-like phenotype that is more resistant to conventional anti-cancer therapy [188]. Random isolation and expansion of SKBR3 colony clusters resulted in spontaneous EMT. The resulting cells expressed EMT markers and had decreased HER2 expression. These basal/mesenchymal cells were resistant to both trastuzumab and lapatinib. This mesenchymal lapatinib-resistant SKBR3 cell line had high expression of N-glycosylated β1-integrin, which is involved with EMT induction and has previously been associated with breast cancer, and inhibition of β1-integrin, with the anti-integrin inhibitory antibody AIIB2, restored the epithelial phenotype [163]. β1-integrin has been implicated in lapatinib resistance in BT474 and HCC1954 lapatinib resistant cell lines. These lapatinib resistant cell lines were highly sensitive to AIIB2 [161].
Another EMT marker, SLUG/SNAIL2, has been implicated in trastuzumab resistance. Knockdown of SLUG in JIMT-1, a cell line from a trastuzumab-refractory HER2-positive breast cancer patient that is also resistant to lapatinib, resulted in increased trastuzumab sensitivity [189].

1.5.3.5   Protective autophagy

One of the proposed mechanisms of action of lapatinib as an anti-cancer therapy is induction of autophagy [87]. Interestingly, two lapatinib resistant HER2-positive breast cancer cell lines, BT474-L and AU565-L, displayed increased levels of

autophagosome formation compared to their parental cell lines. Inhibition of autophagy with lapatinib treatment resulted in reduced cell proliferation and an induction of apoptosis [159].

1.5.3.6 Protein phosphatase 2A activity

The functioning of approximately a third of all cellular proteins is governed by phosphorylation, controlling key cellular activities such as cell cycle regulation, proliferation and apoptosis. Phosphatases play a key role in this process by regulating de-phosphorylation. The serine/threonine phosphatase protein phosphatase 2A (PP2A) is involved in the modulation of several survival and proliferation pathways, such as Akt, MAPK and Wnt pathways [190–192]. Our research group found that PP2A activity was significantly increased in two lapatinib resistant cell lines [154]. Phosphorylation of PP2A has been correlated to HER2 signalling, which results in inactivation of PP2A. Heregulin-induced BT474 cells had increased phosphorylated PP2A and, upon treatment with AG825, a HER2 inhibitor, the level of PP2A phosphorylation was reduced, resulting in increased activity [193]. Potentially, PP2A could be a therapeutic target in the clinical setting as LB-100, a PP2A inhibitor, is currently in phase I/II clinical trials [194–196]. In contrast, the endogenous PP2A inhibitor protein CIP2A has been shown to be elevated in lapatinib resistant breast cancer cells [197]. This illustrates that the role of PP2A in lapatinib response and resistance is complex and is context dependent.

1.5.4 Mechanisms of afatinib resistance

Afatinib is currently in phase III clinical trials in HER2-positive breast cancer but is FDA approved for the treatment of NCSLC. Resistance to afatinib has not yet been examined in HER2-positive breast cancer. However, several mechanisms of resistance have been proposed in lung cancer.
In one study, three afatinib resistant variants of the lung cancer cell line PC-9 were developed and showed three independent mechanisms of resistance to afatinib. All three resistant cell lines had increased expression of EGFR compared to untreated cells. In one resistant cell line, wild-type KRAS was amplified and over-expressed.

Interestingly, withdrawal of afatinib treatment resulted in a loss of KRAS amplification and the cells were re-sensitised to afatinib. Another resistant variant switched its survival signalling to the IGF1R pathway to overcome the effect of afatinib. Finally, the third variant had gained a secondary EGFR mutation, EGFR T790M [198]. This mutation has been previously associated with afatinib resistance in lung cancer; 47.6% of tumour samples from afatinib-resistant lung cancers had acquired a T790M mutation [199]. Other studies have shown no survival differences between patients with tumours harbouring T790M mutations and those without [200]. Other mutations can confer reduced sensitivity to afatinib. The combination of EGFR L858R and V8431 mutations alter the protein conformation of EGFR, thereby reducing the binding potential of afatinib [201].

Kinases downstream of EGFR and HER2 have also been associated with afatinib resistance. Up-regulation of mTORC activity has previously been associated with trastuzumab and lapatinib resistance [153, 202]. In a xenograft model of acquired resistance to afatinib and the EGFR monoclonal antibody cetuximab, mTORC activity was found to be increased due to loss of the genes TSC1 and NSF2. This afatinib plus cetuximab resistant model was generated by implanting PC9 lung cancer cells with EGFR mutations in immunocompromised mice and treating for one month, followed by a one-month drug holiday, for three cycles [203].

Src has also been implicated in afatinib resistance. An afatinib resistant model was generated by treating the lung cancer cell line H1975 with afatinib *in vivo*. The resulting afatinib resistant tumours had no additional mutations but had elevated Src phosphorylation and increased MET, KIT and PDGRβ levels. Combining afatinib with dasatinib overcame resistance to afatinib by enhancing autophagy. The combination of Src inhibition and afatinib was more effective than afatinib plus the multi-kinase inhibitor sunitinib, the ALK/ROS1 inhibitor crizotinib, or the c-Kit, PDGFRα and Flt3 inhibitor amuvatinib [204]. The combination of afatinib and dasatinib has also been demonstrated to be tolerable in a phase I clinical trial in EGFR-mutant NSCLC [205]. No significant interaction was observed between the drugs and the MTD for the combination was deemed to be 30 mg afatinib with 100 mg dasatinib.

1.5.5 Mechanisms of neratinib resistance

Neratinib has been approved for the treatment of early-stage HER2-positive breast cancer after at least one year of trastuzumab treatment [39]. However, resistance has been observed in the clinic and with acquired resistance cell line models.

The innately trastuzumab resistant cell line HCC1954 and the trastuzumab-sensitive SKBR3 and EFM192A cell lines were used to generate neratinib resistant models. In this study, the neratinib resistant cell lines were cross-resistant to other HER2-targeted therapies and more aggressive than their parental cell lines. These cell lines had decreased expression of HER family members and increased CYP3A4 levels, a cytochrome P450 enzyme. It was hypothesised that this increased CYP3A4 activity increases metabolism of neratinib [206].

Neratinib is currently being investigated in non-amplified HER2-mutant breast cancer and has been shown to actively inhibit common occurring HER2 mutations *in vitro* [111, 207]. However, a HER2 mutation has also been shown to cause neratinib resistance. A patient with HER2 L869R mutant breast cancer initially responded to neratinib, until the emergence of a secondary HER2 mutation, HER2T798I. This mutation caused a conformational change which sterically hindered neratinib binding. Interestingly, this HER2 L869R/T798I-mutant breast cancer still responded to afatinib [208].

1.6 Proteins of interest

As PP2A and Src are investigated in detail in this study, the role of both proteins in cancer and their therapeutic potential are described below.

1.6.1 The role of Src in cancer

The proto-oncogene Src has been implicated in several cancer types, such as leukaemia, breast, pancreatic, lung and skin cancers [209–211]. Src is one of ten members of the Src family of non-receptor tyrosine kinases (SFKs). Each SFK member is composed of a N-terminal Src homology 4 (SH4) domain, an SH3 domain,

an SH2 domain, a linker sequence, tyrosine kinase domain, and the C-terminal tail. SFKs contain a tyrosine 416 residue that, once phosphorylated, activates the kinase and a tyrosine 527 reside that deactivates the protein when phosphorylated [212]. SFKs can be divided into three families. Src family A consists of Src, Yes, Fyn, and FGR, and are ubiquitous in all tissues. Src family B is made up of Lck, Hck, Blk, and Lyn. Frk, Fyn-related kinase, is its own subfamily.

Src has demonstrated a role in hormone-receptor-positive, HER2-positive, and triple negative breast cancers. *In vitro* testing of a Src inhibitor, dasatinib, showed triple negative breast cancer cell lines were most sensitive to Src inhibition [213]. Src/EGFR signalling can up-regulate β4-integrin-FAK interaction in triple-negative breast cancer. This increases the metastatic potential of the cell line tested [214]. In estrogen-receptor positive disease, Src activation was observed in tamoxifen resistance [215, 216]. In HER2-positive breast cancer, Src inhibition reduced mammary tumour development *in vivo* by inhibiting ERK 1/2 signalling, c-Myc translation and reducing glucose metabolism [216]. Src activation is also associated with brain metastasis, which is more common in HER2-positive breast cancer. *In vivo* Src inhibition with saracatinib in combination with lapatinib prevented brain metastasis growth and caused cancer cell cycle arrest [217]. This combination inhibited both AKT and ERK signalling in SKBR3-L cells and restored lapatinib sensitivity [218].

1.6.1.1 Src inhibitors in cancer

Dasatinib (Sprycel, Bristol-Myers Squibb) is a multi-kinase inhibitor, which targets SFK, BCR-Abl, C-Kit, PDGFR, and ephrin-A, and most potently inhibits Src kinase with an IC_{50} value of 3 nM [219]. Dasatinib was FDA approved for the treatment of chronic myeloid leukaemia and philadelipha-positive acute lymphocytic leukaemia [220]. It has also been shown to have preclinical activity against several solid tumour types [213, 219]. However, dasatinib failed to show single-agent efficacy in the clinical setting [221–223]. Therefore, clinical investigation of dasatinib has now focused on combinations of dasatinib with chemotherapy or other targeted therapies.

There are two trials of dasatinib in combination with HER family-targeted therapies currently underway. The safety of dasatinib in combination with trastuzumab plus paclitaxel is underway in HER2-positive metastatic breast cancer (NCT01306942). The safety of dasatinib plus lapatinib is being investigated in patients with solid tumours that cannot be removed by surgery (NCT01306942). In addition, a phase I trial of dasatinib plus afatinib showed that the combination was well tolerated, as discussed in Section 1.5.4.

1.6.2 PP2A

Protein phosphorylation allows cells to rapidly respond to external stimuli and is tightly regulated by a balance of kinases and phosphatases. PP2A is a ubiquitously expressed serine/threonine phosphatase that is responsible for up to 90% of serine and threonine dephosphorylation. PP2A regulates a myriad of cellular processes including cell cycle progression, migration, metabolism and proliferation. PP2A is a complex heterotrimeric holoenzyme composed of three subunits (Figure 1-6). The structural (A) subunit, which acts as a scaffold for the other subunits, exists in two isoforms (PPP2R1A and PPP2R1B). Approximately 90% of PP2A holoenzymes contain the PPP2R1A isoform and knockdown of this subunit cannot be substituted by the PPP2R1B isoform. Likewise, the catalytic (C) subunit also exists in two isoforms (PPP2CA and PPP2CB). The C subunit carries out the phosphatase activity of the holoenzyme. Although dimerisation of the A and C subunits can stably occur, the regulatory (B) subunit is required for substrate specificity and cellular localisation of the holoenzyme. There are at least 26 regulatory subunit isoforms that can form the PP2A holoenzyme, which includes splice variants and alternate transcripts of 15 different genes. The regulatory subunits can be divided into four subfamilies: the B, B', B'', and B''' families. The array of regulatory subunits allows for both substrate specificity and functional diversity. For example, PP2A-B55 holoenzyme can interact with Akt, RAF, Rb, p53 and Src. With two isoforms each for structural and catalytic subunits and 26 regulatory subunits, there are 96 possible combinations of PP2A composition. Therefore, PP2A composition differs between cell types and can respond rapidly to cell stress.
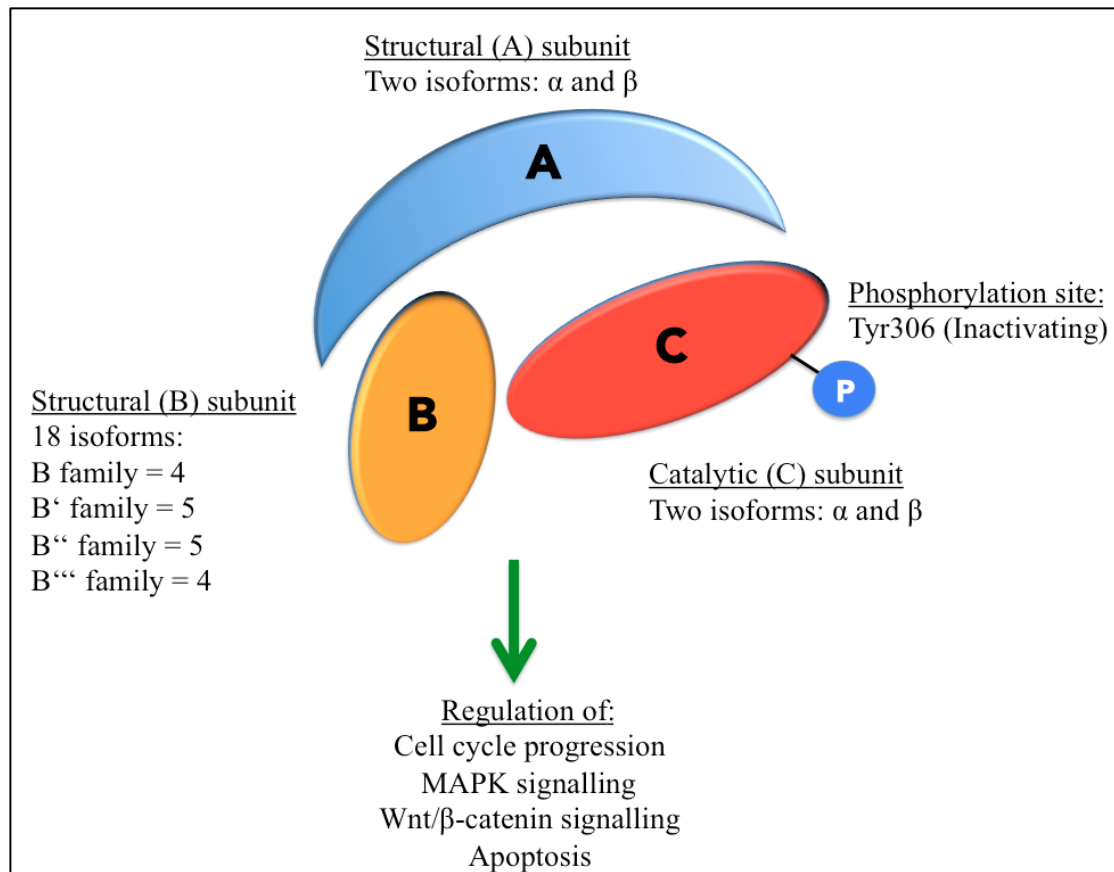
Figure 1-6: PP2A holoenzyme composition and subunit isoforms (adapted from [224]).

1.6.2.1 PP2A as a tumour suppressor

Knockdown of PPP2CA causes embryonic lethality and infertility in adults. Interestingly, PPP2CB knockdown does not cause an abnormal phenotype and these knockdown mice remain fertile [225]. PP2A is a vital negative regulator of several cellular growth pathways. PP2A dephosphorylates JAK3 and STAT5, which have a role in angiogenesis, cancer cell survival and immunosuppression [226, 227]. PP2A also deactivates the MAPK signalling molecules ERK2 and MEK 1/2 [228], and dephosphorylates c-Myc, which destabilises the protein for proteasomal degradation [229]. This indicates that some PP2A holoenzymes are tumour suppressors. In fact, some oncogenic viruses generate viral proteins that inhibit PP2A activity. One mechanism of PP2A suppression by viruses, including the simian virus small t and polyoma middle T virus, is by direct interaction with the core dimer and disruption of

regulatory subunit binding. This interaction then allows for the activation of survival pathways such as the MAPK and AKT pathways.

Cancerous inhibitor of PP2A (CIP2A) is a negative regulator of PP2A and has been shown to decrease PP2A activity, promoting c-Myc stabilisation. CIP2A expression has been shown to be over-expressed and associated with poor survival in a number of cancers [230, 231]. An array of PP2A inhibitor proteins are over-expressed and correlates with poor outcome in acute myeloid leukaemia, including SET, CIP2A and SETBP1 [232].

1.6.2.2   PP2A as an oncogene

As discussed, PP2A regulates several signalling pathways, including PI3K/AKT signalling and Wnt/β-catenin pathway. PP2A complexes with APC, GSKα and dishevelled (Dsh), which then targets β-catenin for degradation. PP2A can also stimulate Wnt signalling. In a colon cancer cell line model, aspirin caused phosphorylation of the PP2A catalytic subunit, deactivating the phosphatase. This led to suppression of Wnt signalling. Moreover, PP2A inhibition was vital for the Wnt signalling inhibition effect of aspirin and indicates that inhibition of PP2A is a mediator of the cancer preventative properties of aspirin [233].

As well as having a pro-apoptotic function, PP2A can also act as an anti-apoptosis enzyme. This anti-apoptotic activity occurs through regulation of p53 and Bcl-2 [234, 235]. PP2A inhibition can aid in the induction of apoptosis by regulating p53 in two ways: increased p53 S15 phosphorylation can decrease p53 levels, block cell cycle arrest and thereby improve chemotherapy response, or paradoxically, PP2A inhibition can activate over-expressed p53 and induce up-regulation of the pro-apoptotic Bax and p21 causing cell cycle arrest [236].

1.6.2.3   Targeting PP2A in cancer

There are several naturally occurring and synthetic compounds that alter PP2A activity, either directly or indirectly (Figure 1-7). Inhibitors of PP2A include okadaic acid, fostricien, cantharidin, and LB-100.
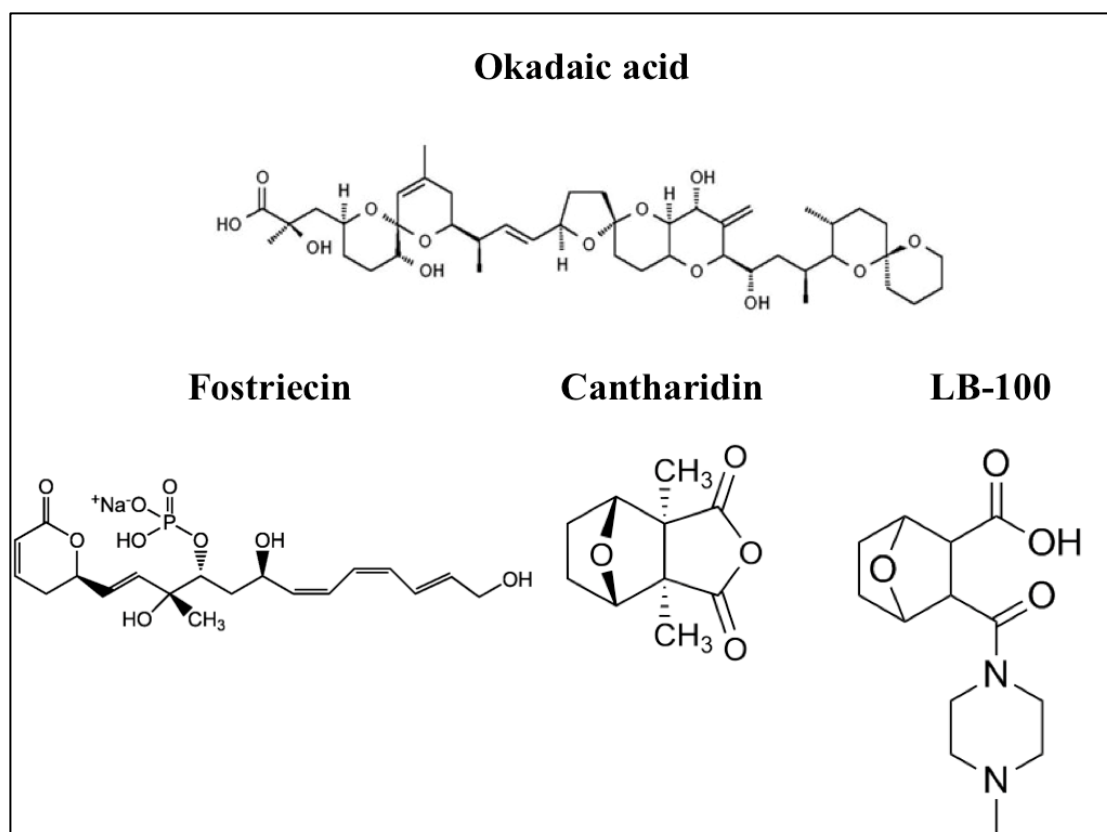
Figure 1-7: PP2A inhibitory molecules that have been used in *in vitro* testing (Structures adapted from PubChem; CID numbers: okadaic acid = 446512, fostriecin = 6913994, cantharadin = 5944, and LB-100 = 3578572, [84])

1.6.2.3.1 Okadaic acid

Okadaic acid (OA) is a toxin produced by dinoflagellates and is used as a defence mechanism by molluscs. It is a potent phosphatase inhibitor with selectivity for PP2A and PP1 (IC_{50} = 0.1 – 1 nM and 3 – 15 nM, respectively). OA was the first classified PP2A inhibitor [237]. It has been used in *in vitro* and *in vivo* testing to examine the role of PP2A. OA has been used to demonstrate the dual role of PP2A as a tumour suppressor and oncogene. Treatment of OA was shown to inhibit apoptosis induction by radiation in leukemia cells and also induce apoptosis, necrosis, cell cycle arrest and DNA damage in other cancer cell lines [238, 239].

1.6.2.3.2 Fostriecin

Fostriecin is a highly specific PP2A inhibitor (IC_{50} = 3.2 nM, PP1 IC_{50} = 131 µM) [240]. It is an antibiotic molecule, first isolated from Streptomyces pulveraceus [241]. Originally, fostriecin was classified as a topoisomerase II inhibitor, by mechanisms independent of anthracyclines such as doxorubicin. However, its complete topoisomerase II inhibitory effect occurs at high concentrations (100 µM) [242]. It is a phosphate monoester that binds covalently to Cys269 of the PP2A catalytic subunit [243]. Fostriecin has shown anti-cancer activity in several cancer types including leukemia and ovarian, breast, and lung cancers [244, 245]. A phase I clinical trial was initiated with fostriecin as a single agent. Of the 46 patients in the trial, 16 achieved stable disease with a median response time of 2.6 months [246]. An MTD could not be reached in this trial due to problems with fostriecin supply. Novel synthesis methods have been developed, which may lead to further clinical investigation of fostriecin [247, 248].

1.6.2.3.3 Cantharidin

Cantharidin is another PP2A inhibitor that is a naturally found toxin, derived from blister beetles, and has been used in traditional Chinese medicine. Cantharidin is 10-fold more specific to PP2A than PP1 [249]. Cantharidin induced apoptosis and DNA damage in leukaemia cells [250]. Some cantharidin-induced cell death seems to be p53-dependent and can be affected by Bcl-2 levels [251]. However, p53-independent cell death has also been observed in cantharidin-treated cells [252]. Cantharidin stimulated G1 cell cycle arrest and inhibited cell migration in the triple negative breast cancer cell line, MDA-MB-231 [253]. It has also shown apoptotic activity in oral squamous cell carcinoma cell lines as a single agent. Cantharidin caused increased activation of pro-Bcl-2 family member proteins and induced endoplasmic reticulum stress [254]. Efficacy of cantharidin was seen in pancreatic cancer [255]. Cantharidin inhibits the invasive behaviour of pancreatic cells by down-regulating matrix metalloproteinase 2, MMP2. Interestingly, the anti-cancer effect of cantharidin, and its de-methylated derivative noracantharidin, was enhanced in

pancreatic cancer cells with the addition of tamoxifen [256]. This effect was found to be independent of ER levels and mediated through PKC inhibition.

Cantharidin has not been tested clinically as an anti-cancer agent, but it has been evaluated in a phase I clinical trial for pediatric molluscum contagiosum, a viral dermatalogical condition. Although it showed no effect against this disease, its topical application had minimal side effects [257].

1.6.2.3.4   LB-100

LB-100 is a synthetic cantharidin derivative that does not exhibit the toxicities associated with cantharidin. LB-100 has shown *in vitro* and *in vivo* efficacy against hepatocellular carcinoma, glioblastoma, breast, pancreatic and ovarian cancers [258–264]. It has demonstrated single agent activity as well as enhancing the cytotoxic effects of chemotherapy and radiotherapy *in vitro* and *in vivo*. The radiation-enhancing effect was observed in glioblastoma, nasopharyngeal carcinoma, and pancreatic cancer cell lines [262–264]. The addition of LB-100 induced mitotic catastrophe and increased DNA damage. LB-100 can enhance the cytotoxicity of chemotherapy through a number of mechanisms. In hepatocellular carcinoma, LB-100 increased tumour levels of doxorubicin and cisplatin tumour accumulation and increased vascularity of *in vivo* tumours [265]. LB-100 also improved cisplatin response in ovarian cancer and medulloblastoma in cell lines [258, 260]. The combination of cisplatin and LB-100 induced apoptosis, inhibited migration, and increased cisplatin uptake. The enhancement of doxorubicin was also observed in pancreatic cancer. Interestingly, the increase in doxorubicin efficacy with LB-100 was found *in vivo*, but not *in vitro*. This was reported to be due to elevated vascular permeability *in vivo* [265]. There is also evidence of LB-100 improving response to targeted therapies. LB-100 enhanced sorafenib induced apoptosis in hepatocellular carcinoma cell lines [266]. LB-100 treatment increased levels of phospho-Smad3 and down-regulated Bcl-2 levels. This enhancement was hypoxia-dependent, as hypoxia elevated p38 MAPK activity, which further increases phospho-Smad3 levels. The combination effect of LB-100 was also observed in gefitinib-resistant EGFR-mutant NSCLC. LB-100 and gefitinib were synergistic *in vitro* and *in vivo* [267]. With this pre-clinical evidence, LB-100 was tested for tolerability and preliminary efficacy in

patients with solid tumours [268]. LB-100 was given by intra-veneous injection for three days in 21-day cycles. Twenty-nine patients were treated in this trial, with 20 of these patients evaluable for tumour response. Half of all patients achieved stable disease. Dose limiting toxicity was determined to be related to elevated serum creatinine, anemia, dyspnea, hyponatremia, and lymhopenia. The recommended phase II dosage was deemed to be 2.33 mg/m^2.

1.7   Summary

There are now several HER2-targeted therapies approved for the treatment of HER2-positive breast cancer. However, despite the clinical success of these therapies, *de novo* and acquired resistance is a significant challenge. Therefore, novel treatment options are essential. In this study, cell lines with acquired resistance to HER2-targeted therapies were examined for sensitivity to other HER2-targeted therapies and novel treatment strategies were tested. PP2A was previously identified as a potential target to overcome lapatinib resistance [154]. This study further investigated its role in HER2-targeted therapy response. In addition, resistance to the irreversible pan-HER TKIs and the role of Src kinase were examined.

1.8   Study aims

The main objectives of this study were:

- To determine if lapatinib-resistant HER2-positive breast cancer cell lines are cross-resistant to other HER2-targeted therapies.
- To evaluate PP2A inhibition in cell line models of resistance to HER2-targeted therapies, by examining the activity and mechanisms of action of PP2A inhibitors.
- To test the potential of the PP2A inhibitor LB-100 *in vitro* and *in vivo* against lapatinib resistant cells.
- To examine the potential of PP2A inhibition in a panel of HER2-positive breast cancer cell lines representing cell lines that are innately sensitive or resistant to lapatinib and/or trastuzumab.
- To evaluate the relationship between PP2A expression and sensitivity to HER2-targeted therapies.
- To investigate mechanisms of resistance to afatinib and neratinib in HER2-positive breast cancer and to identify novel targets to overcome resistance.

2 Methods

2.1 Cell lines and reagents

Seventeen HER2-positive cell lines were used in this project, ten established HER2-positive cell lines and seven HER2-targeted therapy resistant human breast cancer cell lines. This includes two lapatinib resistant cell lines (SKBR3-L and HCC1954-L) three trastuzumab resistant cell lines (SKBR3-T, BT474-T, EFM192A-T), a neratinib resistant cell line (HCC1954-N), an afatinib resistant cell line (SKBR3-A), and their respective parental cell lines. The cell lines EFM192A, HCC1419, HCC1569, HCC1954, JIMT-1, MDA-MB-453, SKBR3, and UACC-732 were cultured in Roswell Park Memorial Institute-1640 medium (RPMI-1640) (Sigma Aldrich) supplemented with 10% foetal bovine serum (FBS) (Gibco). MDA-MB-361 were cultured in Leibovitz's L-15 medium (ATCC) supplemented with 10% FBS and L-glutamine (Table 2-1). Dr. Brigid Browne (NICB) established the SKBR3-L cell line by continuous culturing of SKBR3 cells in RPMI-1640 supplemented with 250 nM lapatinib over six months [154]. Dr. Martina McDermott (NICB) generated the HCC1954-L cell line by six months continuous culturing in 1 μM lapatinib [148]. Dr. Alexandra Canonici (NICB) generated the afatinib resistant SKBR3 cells by continuous culture with 150 nM afatinib (Boehringer Ingelheim). Dr. Susan Breslin (TCD) produced the HCC1954-N cell line by continuous exposure of 250 nM neratinib (Sequoia) [206]. The SKBR3-T cell line was created by Dr. Brigid Browne (NICB) and the EFM192A-T and BT474-T cell lines were generated in the lab of Dr. Dennis Slamon (UCLA). All cell culture procedures were performed as per the guidelines set out in NICB standards of practice (SOP) [#001-01, #002-01 and #003-01]. All compounds used in this study and their storage conditions are listed in Table 2-3.

Table 2-1: The cell lines used in this project and the culture conditions required.

Cell line	Culture medium	Culture conditions
BT474	RPMI-1640 + 10% FBS	37ºC, 5% CO_2
EFM192A	RPMI-1640 + 10% FBS	37ºC, 5% CO_2
HCC1419	RPMI-1640 + 10% FBS	37ºC, 5% CO_2
HCC1569	RPMI-1640 + 10% FBS	37ºC, 5% CO_2
HCC1954	RPMI-1640 + 10% FBS	37ºC, 5% CO_2
JIMT-1	RPMI-1640 + 10% FBS	37ºC, 5% CO_2
MDA-MB-361	Leibovitz's L-15 medium + 10% FBS	37ºC, no CO_2
MDA-MB-453	RPMI-1640 + 10% FBS	37ºC, 5% CO_2
SKBR3	RPMI-1640 + 10% FBS	37ºC, 5% CO_2
UACC-732	MEM + 15% FBS	37ºC, 5% CO_2
HCC1954-L	RPMI-1640 + 10% FBS	37ºC, 5% CO_2
SKBR3-L	RPMI-1640 + 10% FBS	37ºC, 5% CO_2
HCC1954-N	RPMI-1640 + 10% FBS	37ºC, 5% CO_2
SKBR3-A	RPMI-1640 + 10% FBS	37ºC, 5% CO_2
BT474-A	RPMI-1640 + 10% FBS	37ºC, 5% CO_2
SKBR3-T	RPMI-1640 + 10% FBS	37ºC, 5% CO_2
BT474-T	RPMI-1640 + 10% FBS	37ºC, 5% CO_2
EFM192A-T	RPMI-1640 + 10% FBS	37ºC, 5% CO_2

Table 2-2: Description of HER2-targeted therapy resistant cell lines used in this study.

Cell line	Method of resistant cell line generation	Reference
SKBR3-L	Continuous exposure to 250 nM lapatinib for 6 months	[154]
HCC1954-L	Continuous exposure to 1 μM lapatinib for 6 months	[148]
SKBR3-T	Continuous exposure to 10 μg/mL trastuzumab for 6 months	[269]
BT474-T	Continuous exposure to 100 μg/mL trastuzumab for 6 months	[88]
EFM192A-T	Continuous exposure to 100 μg/mL trastuzumab for 6 months	
SKBR3-A	Continuous exposure to 150 nM afatinib for 6 months	[123]
HCC1954-N	Continuous exposure to 250 nM neratinib for 6 months	[206]

Table 2-3: List of compounds used in this study, stock concentrations and long- (> 3months) and short-term storage conditions.

Compound	Supplier	Stock concentration	Long-term storage (> 3 months)	Short-term storage
Lapatinib	Sequioa Research Products	10 mM in DMSO	−20 ℃	Room temperature
Afatinib	Sequioa Research Products	10 mM in DMSO	−20 ℃	Room temperature
Neratinib	Sequioa Research Products	10 mM in DMSO	−20 ℃	Room temperature
Trastuzumab	St. Vincent's University Hospital	21 mg/mL	4 ℃	4 ℃
Pertuzumab	St. Vincent's University Hospital	30 mg/mL	4 ℃	4 ℃
Okadaic acid	Cell Signalling Technologies	1 mM in DMSO	−20 ℃	−20 ℃
LB-100	Sequoia Research Products	50 mM in PBS	−80 ℃	−80 ℃
Dasatinib	Sequioa Research Products	10 mM in DMSO	−20 ℃	Room temperature
FTY720	Cell Signalling Technologies	10 mM in DMSO	−20 ℃	−20 ℃

2.3   Mycoplasma testing

All cell lines were routinely tested for mycoplasma as follows. Cell culture supernatant was collected for each cell line, a minimum of three passages after thawing and 72 hours (h) post media change. For cell lines cultured in the presence of drug, cells were grown for at least one week without drug. The presence of mycoplasma was tested by two methods: fluorescent microscopy, and MycoAlert mycoplasma detection kit.

The supernatant was added to normal rat kidney epithelial cells (NRKs) that were cultured on glass coverslips to 70% confluence in technical duplicates. The supernatant and NRKs were incubated for four days at 37ºC with 5% CO_2. Supernatant and NRK medium was removed and NRKs were fixed in Carnoy's Fixative (1:2 glacial acetic acid: methanol) for 20 minutes (mins) on ice and allowed to air dry. After fixation, NRKs were stained with Hoechst 33258 (Sigma) for 10 mins. Each coverslip was washed twice with ultra high purity water and read on a fluorescent microscope at an excitation wavelength of 400 nm.

Alternatively, conditioned medium was tested for the presence of mycoplasma using the MycoAlert kit (Lonza). Briefly, 100 µL of conditioned medium was added to a white 96-well plate. 100 µL of MycoAlert reagent was added to the medium and incubated at room temperature for 5 mins. Luminescence was determined on a plate reader (Biotech). 100 µL of MycoAlert substrate was added and the plate was incubated for a further 10 mins. Luminescence was measured again. Mycoplasma presence was determined by calculating the ratio of reading two to reading one (Table 2-4).

Table 2-4: Interpretation of luminescence ratio for the presence of mycoplasma using MycoAlert kit.

Ratio	Interpretation
< 1	Mycoplasma negative
1 – 1.2	Borderline
> 1.2	Mycoplasma positive

2.4   Immunoblotting

Cells were seeded in 100 mm petri dishes or 6 well plates and grown to 70% confluency. Cells were washed three times with phosphate buffer saline (PBS) and 300 μl/dish or 150 μl/well RIPA buffer ((Sigma) 5 mM Tris-HCl pH 7.4, 1% NP-40, 0.1% SDS, 150 mM NaCl, 1% Triton x-100) containing 1X Protease Inhibitor cocktail (Calbiochem), 2 mM PMSF (Sigma), and 1 mM sodium orthovanadate (Sigma) was added and cells were incubated on ice for 20 mins. Cells were scraped and lysis buffer was collected. Lysates were sheared with a 21 gauge needle and centrifuged at 10,000 rpm for 10 mins at 4°C. Supernatant was collected and stored at -80°C. Protein quantification was carried out using a bicinchoninic acid (BCA) quantification kit (Pierce).

Thirty μg of protein was electrophoretically resolved on 4-12% Bis-Tris polyacrylamide gels (Life Technologies). The proteins were transferred to a nitrocellulose membrane using the iBlot 2 transfer system (Invitrogen) or Power blotter system (Thermo Scientific). Ponceau S (Sigma) was used to confirm protein transfer and the membrane was blocked with 1X Odyssey PBS blocking buffer (Licor). Primary antibodies were prepared in 1:1 Odyssey buffer: PBS-Tween (0.15%) as detailed in Table 2-5 and the membrane was incubated at 4 °C overnight in primary antibody. Membranes were washed for 10 mins three times with PBS-Tween before and after 1h incubation in the appropriate secondary antibody at room temperature. Blots were visualised using the Licor Odyssey with Odyssey V2 software. Densitometry was also performed using the Odyssey V2 software.

Table 2-5: Antibody conditions, secondary antibodies, positive control, suppliers and catalogue numbers for immunoblotting.

Antibody	Post-translational modification	Dilution	Blotting conditions	Secondary antibody	Positive Control	Supplier	Cat. No.
Anti-mouse secondary	-	1:5000	1:1 Odyssey buffer: PBS-T	-	-	LiCor	
Anti-rabbit secondary	-	1:5000	1:1 Odyssey buffer: PBS-T	-	-	LiCor	
Anti-α-tubulin	-	1:1000	1:1 Odyssey buffer: PBS-T	Mouse	-	Sigma Aldrich	T6199
Anti-HER2	-	1:1000	1:1 Odyssey buffer: PBS-T	Mouse	BT474	Calbiochem	OP15
Anti-phospho-HER2	Tyr1221/1222 phosphorylation	1:1000	1:1 Odyssey buffer: PBS-T	Rabbit	BT474	CST	#2249
Anti-EGFR	-	1:1000	1:1 Odyssey buffer: PBS-T	Rabbit	A431	CST	#2232
Anti-eEF2	-	1:1000	1:1 Odyssey	Rabbit	MDA-MB-	CST	#3021

			buffer: PBS-T		453		
Anti-phospho-eEF2	Thr56 phosphorylation	1:1000	1:1 Odyssey buffer: PBS-T	Rabbit	MDA-MB-453	CST	#3022
Anti-PPP2CA	-	1:1000	1:1 Odyssey buffer: PBS-T	Mouse	A431	Millipore	05-421
Anti-phospho-PPP2CA	Tyr307 phosphorylation	1:1000	1:1 Odyssey buffer: PBS-T	Rabbit	A431	Abcam	Ab32104
Anti-methyl-PPP2CA	Leu309 methylation	1:1000	1:1 Odyssey buffer: PBS-T	Mouse	HEK293	Abcam	Ab66597
Anti-PPP2R1A	-	1:1000	1:1 Odyssey buffer: PBS-T	Rabbit	MDA-MB-231	Antibodies-online GmbH	ABIN1881682
Anti-PPP2R1B	-	1:1000	1:1 Odyssey buffer: PBS-T	Rabbit	HeLa	Antibodies-online GmbH	ABIN1530362
Anti-PPP2CB	-	1:1000	1:1 Odyssey buffer: PBS-T	Rabbit	A431	Abcam	Ab32673

Anti-Src	-	1:500	1:1 Odyssey buffer: PBS-T	MCF7	Millipore
Anti-phospho-Src	Tyr416 phosphorylation	1:1000	1:1 Odyssey buffer: PBS-T	MCF7	CST

2.5   Reverse Phase Protein Array

Cells were grown to 70% confluency, and treated for 18 h with 500 nM lapatinib, 3 nM okadaic acid or the two combined. Cells were washed twice with PBS and lysis buffer was added (1% Triton X-100, 50 mM HEPES, pH 7.4, 150 mM NaCl, 1.5 mM MgCl2, 1 mM EGTA,100 mM NaF, 10 mM sodium pyrophosphate, 1 mM Na_3VO_4, 10% glycerol, plus freshly added Roche protease (#04693116001) and phosphatase (#04906845001) inhibitors). Plates were incubated for 20 mins on ice. Cells were scraped from the plates and lysate was transferred to eppendorf tubes. Lysates were centrifuged at 14,000 rpm for 10 mins at 4 ^{o}C. Supernatant was collected and stored at -80 ^{o}C. Protein quantification was determined by bicinchoninic acid (BCA) assay and protein concentration was adjusted to 1.5 mg/mL. Cell lysates were mixed with 4X SDS buffer (40% glycerol, 8% SDS, 0.25 M Tris-HCl, pH 6.8, 10% 2-mercaptoethanol) (three parts lysate to one part 4X SDS buffer).

RPPA was carried out by Dr. Mattia Cremona in RCSI, Beaumont as described in [270]. A 2470 arrayer (Aushon) created an 850-sample array on Oncyte Avid nitrocellulose-coated slides (Grace Bio-Labs). The slides were stored at −20 °C prior to immunostaining.

Immunostaining was performed on an automated slide stainer (Dako), according to manufacturer's instructions. Each slide was incubated with a single primary antibody at room temperature for 30 mins. Secondary antibody was goat anti-rabbit IgG (1:5000) (Vector Laboratories) or rabbit anti-mouse IgG (1:10) (Dako). Secondary antibodies (Dako) were used as a starting point for amplification via horseradish peroxidase-mediated biotinyl tyramide with chromogenic detection (diaminobenzidine) according to the manufacturer's instructions (Dako).

Scanned TIFF images of slides were analysed using Microvigene software version 5.1 (VigeneTech Inc.) to generate spot signal intensities. Instead of generating multiple linear regression curves for data quantification over each series of serial dilutions, the QRPPA module of Microvigene using a 4 parameter logistic-log model ("SuperCurve" algorithm) that uses all spots within one array to form a sigmoid antigen-binding kinetic curve. Finally, the spots are normalised by protein loading using the entire panel of antibodies. Briefly, normalisation was processed as follows: the median was determined for each antibody across the sample set and each raw

linear value was divided by the median within each antibody to get the median-centred ratio. After that, the median was calculated from median-centred ratio for each sample across the entire panel of antibodies. This median functions as a correction factor (CF) for protein loading adjustment. Samples were considered an outlier if the CF was above 2.5 or below 0.25. Finally, the raw data was divided in linear value by the CF to obtain the normalised value.

2.6 Immunohistochemistry

2.6.1 Fresh frozen cell line slide preparation

HCC1954-L cells were grown in a T75 to approximately 70% confluency, trypsinised and resuspended. Cells were placed dropwise onto a SuperFrost Plus slide (ThermoFisher, 4591PLUS4) marked with a wax pen border. The slides were placed in petri-dishes with a moist lint-free wipe in a 37 °C incubator overnight. The slides were then rinsed with PBS three times and allowed to dry. The slides were formalin fixed for immediate immunohistochemistry analysis or covered in aluminium foil and stored at -80 °C.

2.6.2 Sectioning

Sectioning of *in vivo* tumour samples was carried out using a Reichert-Jung 2030 microtome. Blocks were cut into 5 μM sections, which were floated in a water bath at 40 ˚C and mounted onto SuperFrost Plus slide (ThermoFisher, 4591PLUS4) and allowed to dry at 180 ˚C for 2h.

2.6.3 Immunostaining

Automated immunohistochemistry (IHC) was performed using a DAKO autostainer Plus. An antibody against human mitochondria (1/1000) was used as a control to differentiate human and mouse cells. Antigen retrieval was performed on cell line block and *in vivo* tumour block slides using the Dako PT Link with Target Retrieval Solution pH 6 (Dako S1699). Slides was placed in the Dako PT link at 65 ˚C, heated

to 97 ˚C, and maintained at 97 ˚C for 20 mins. The slides were cooled to 65 ˚C and removed. After de-paraffinisation, the slides were placed in the DAKO Autostainer, which performed the programmed application of reagents in order as listed in Table 2-6Table 2-6. Washes were performed, with DAKO wash buffer, before and after the application of each reagent, except in the case of the Real HP Block, where a blow step was performed. Slides were subsequently dehydrated in grading alcohols 70 %, 90 %, and 100 %, cleared in xylenes (2 x 3 mins each) and mounted in di(nbutyl) phthalate in xylene (DPX) (Sigma).

Table 2-6: Steps for immunostaining on DAKO Autostainer

Reagent	Time (mins)
Real HP Block (DAKO)	10
Antibody	30
Real EnVision (DAKO)	30
Real DAB (DAKO)	5
Haematoxylin	5

2.7   Proliferation Assays

2.7.1   Acid phosphatase proliferation assay

Cell lines were seeded in 96 well plates at a cell density as detailed in Table 2-7. After 24 h, cells were treated with a drug or combination of drugs of interest in 100 μL of medium. After five days' incubation, proliferation was measured using the acid phosphatase assay. Medium was removed and cells were washed three times with PBS. 100 μL of acid phosphatase substrate (10 mM p-nitrophenol phosphate (Sigma) in 0.1 M sodium acetate (Sigma), 0.1% Triton X-100 (BDH, pH 5.5) was added to each well and the plate was then incubated at 37°C for one to 2 h. The reaction was halted with the addition of 50 μL of 0.1 M sodium hydroxide. The absorbance was then read at 405 nm and at 620 nm as a reference on a plate reader (Biotek) using Gen4 software. Percentage growth was calculated relative to an untreated control. All assays were performed in triplicate.

Table 2-7: The number of cells seeded per well in 96 well plates for proliferation assays determined by assay optimisation and previously published data.

Cell line	Cells seeded/well
BT474	5000
EFM192A	5000
HCC1419	3000
HCC1569	3000
HCC1954	2500
JIMT-1	2500
MDA-MB-361	5000
MDA-MB-453	3000

SKBR3	3000
UACC-732	3000
HCC1954-L	2500
SKBR3-L	3000
HCC1954-N	2500
SKBR3-A	3000

2.7.2 Three-dimensional growth assay

96-well plates were coated with 50 µL poly-HEMA (Sigma Aldrich, 5 mg/mL in 96% ethanol) and incubated at 50ºC for 48 h. Poly-HEMA–coated plates were stored at room temperature for up to six months. Cells were seeded in 90 µL of medium containing 10% FBS and 4% Matrigel (BD Biosciences) at the same density as for the two-dimensional (2D) acid phosphatase assay (Table 2-7). After which, the plate was incubated overnight at 37ºC. 30 µL of medium containing 10% FBS with/without drugs of interest was added to each well and incubated at 37ºC for 7 days. 12 µL of PrestoBlue cell viability reagent (Life Technologies) was added to each well and incubated for 2-4 h at 37ºC. Fluorescence was measured at 535/590 excitation/emission wavelengths on a plate reader (Biotek) using Gen4 software. Background fluorescence was calculated by using a blank consisting of medium containing 10% FBS and 4% Matrigel (BD Biosciences). Percentage viability was calculated relative to untreated controls.

2.8 Small interfering RNA (siRNA) transfection

A pool of four PPP2CA siRNA molecules targeting PPP2CA (L-003598-01, Dharmacon) and a scrambled sequence siRNA (D-00180-10) were obtained from Millipore. A validated siRNA molecule targeting kinesin was obtained from Sigma as a transfection control. All siRNAs were transfected at a final concentration of 25 nM. The siRNA was diluted in Opti-MEM reduced serum medium (Invitrogen) and Trans-IT X2 transfection reagent (Mirius) was added, as per Table 2-8Table 2-8. The transfection solution was incubated for 20 mins at room temperature. Meanwhile, 2 x 10^5 cells/well in 10% FBS RPMI-1640, for protein expression analysis, or 1 x 10^5 cells/well in 10% FBS RPMI-1640, for growth inhibition assay, were prepared for a 6-well plate. The appropriate transfection solution was added to each well, followed by the cell suspension. After 24 h, the medium in each well was replaced with fresh medium with or without DMSO or 500 nM lapatinib. Cells were either lysed after a further 48 h for Western blotting analysis or after 72 h for proliferation analysis. Proliferation was measured by harvesting cells. Ten µL of cell suspension was combined with 10 µL trypan blue. Cells were then counted using a haemocytometer.

Table 2-8: siRNA transfection reaction mixture (6-well plate).

Solution	Volume
Cell suspension	1.5 mL
Opti-MEM reduced serum medium	250 µL
Trans-IT X2	7.5 µL
siRNA	6.8 µL

2.9   Short-term drug resistance development assay

Cells were seeded in two or three 12-well plates (1-3 x 10^4 cells/well), as shown in Figure 2-1 and incubated at 37 °C overnight. After this, cells were fed or treated with drugs alone or in combination. Cells were then treated twice weekly. The first plate was fixed and stained with 0.1% crystal violet once the control cells became confluent. The second plate was fixed and stained when cells had developed resistance to one of the drugs alone. If the cells did not develop resistance to Drug A, a third plate was used, which was fixed and stained when the cells treated with Drug A only developed resistance (Figure 2-9).
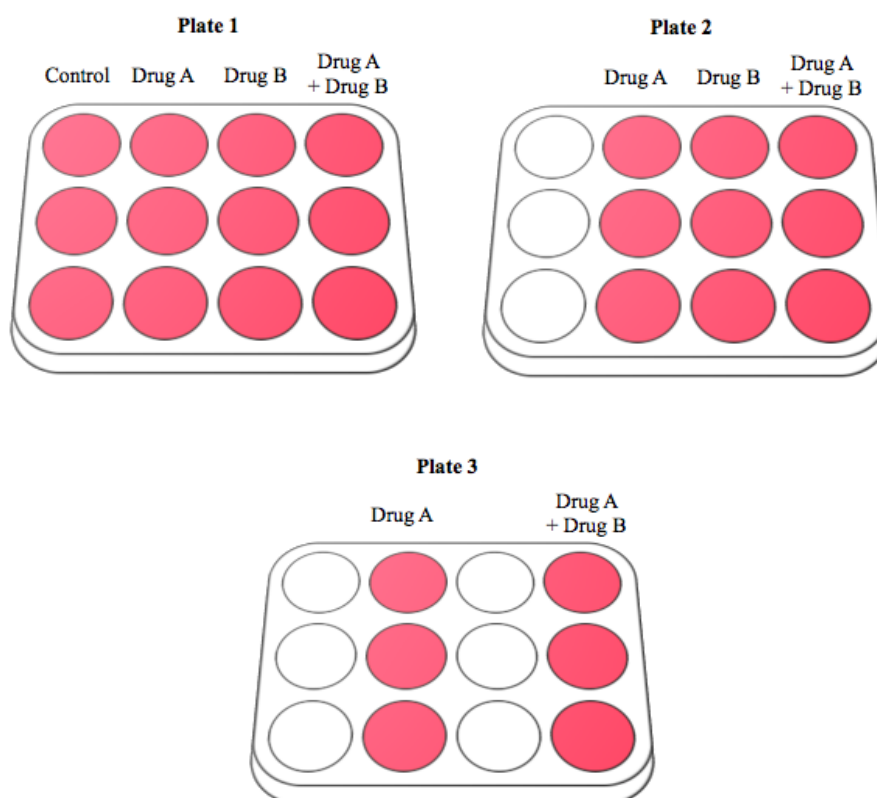
Figure 2-1: Plate layout for drug resistance development assay. If the cell line is resistant to Drug B, a third plate is required. Plate 1 is fixed and stained when control cells become confluent. Plate 2 is fixed and stained when cells that are

treated with either Drug A or Drug B become confluent. Plate 3 is stopped when cells treated with drug A developed resistance and were actively growing.

2.10 Cell cycle assay

2.5×10^4 cells were seeded per well in a 24 well plate and incubated at 37 °C. After 24 h, appropriate treatments were added to each well. Following 48 h incubation, medium was collected and the wells were rinsed with PBS. Cells were trypsinised and added to collected medium. The medium was centrifuged at 1500 rpm for 5 mins and the supernatant was aspirated. The pellet was re-suspended in 150 μL PBS and transferred to a round bottom 96-well plate. The plate was centrifuged at 1500 rpm for 5 mins and the supernatant was removed, leaving approximately 15 μL per well. The remaining volume was resuspended and 200 μL of ice cold 70% ethanol was added. The plate was stored for 2 h at -20°C. After fixing the cells, the plate was spun at 2000 rpm for 5 minute. The supernatant was removed, 200 μL of PBS was added and the plate was centrifuged again at 450 x g for 5 mins. The PBS was removed and 200 μL of Guava Cell Cycle reagent (Merck Millipore) was added to each well. The cells were resuspended and stored at room temperature in the dark for 30 mins. Cells were then analysed on the Guava EasyCyte (Merck Millipore) and the data was analysed using Modfit LT software (Verify).

2.11 Apoptosis assay

Apoptosis induction and activation of caspase 3/7 was examined using the Caspase-Glo 3/7 assay (Promega). Briefly, 9×10^3 cells were seeded per well in a white-walled 96-well plate. After 24 h, medium was removed and 100 µL of fresh medium with or without drug was added. The plate was further incubated for 48 h. Caspase-Glo 3/7 reagent was equilibrated to room temperature and 100 µL of the reagent was added to each well. After 1 h of incubation, luminescence was analysed using a plate reader (Biotek) with Gen4 software.

2.12   Autophagy assay

CYTO-ID autophagy detection kit (Enzo Bioscience) was used to determine autophagy levels. 9×10^3 cells were seeded in a white-walled, clear-bottomed, 96-well plate. After 24 h, cells were treated and incubated for 48 h. Medium was then removed and the cells were washed twice with PBS. Phenol-red free RPMI 1640 with 10% FBS with 0.1% Hoescht stain and 0.1% Autophagy marker was added to wells for quantitative analysis using fluorescence spectrophotometry. Fluorescence was analysed for autophagy marker at excitation 480 nm and emission 530 nm, and at 360 nm excitation and 480 nm emission for Hoeschst nuclear staining. Phenol-red free RPMI-1640 with 10% FBS containing 0.1% Hoeschst stain and 0.2% autophagy marker was added to wells for fluorescence microscopy. Images were taken using a Leica DFC 500 fluorescent microscope with FITC and DAPI filters.

2.13   DNA extraction

Genomic DNA was isolated using the Qiagen AllPrep DNA/RNA kit. SKBR3-Par and SKBR3-A cells were grown to 80% confluency in a T175 flask. Cells were trypsinised and resuspended in medium and counted. Cells were centrifuged at 900 rpm for four mins and washed twice with PBS. Cells were homogenised in 600 µL Buffer RLT, containing 0.1% β-mercaptoethanol. The cell lysate was mixed and sheared using a syringe with a 20 guage blunt needle. The lysate was transferred to an AllPrep DNA spin column in a 2 mL collection tube and centrifuged for 30 seconds at 14,000 rpm. 500 µL Buffer AW1 was added to the column and centrifuged for 15 seconds at 14,000 rpm. Flow through was discarded and 500 µL Buffer AW2 was added to the column. Tubes were centrifuged for 2 mins at 14,000 rpm. The column was transferred to a fresh 1.5 mL collection tube, 100 µL of 70 ºC Buffer EB was added and incubated at room temperature for 2 mins. Tubes were centrifuged for one minute at 10,000 rpm and DNA elution was collected. DNA was purified by sodium acetate precipitation. DNA was quantified using the Nanodrop V1000.

2.14   Whole exome sequencing

Whole exome sequencing was conducted by Beijing Genomic Institute using the Agilent SureSelect system (Figure 2-2). Twenty µg of genomic DNA is randomly fragmented by Covaris sonication to approximately 150 to 200 bp fragments. Adapters were then added which ligated to both ends of the fragments. Adapter-ligated fragments were purified using Agencourt AMPur SPRI beads. The DNA was then amplified by ligation-mediated PCR, purified and hybridised to the SureSelect Biotinylated RNA library for enrichment. Non-hybridised fragments were washed out after 24 h and hybridised fragments were captured by streptavidin beads. Captured fragments were analysed by Agilent 2100 Bioanalyser to determine the magnitude of enrichment. High-throughput sequencing was then performed on each captured library using the HiSeq2000 system. Raw image files were processed by Illumina basecalling softare 1.7 with default parameters and the sequences of each sample were generated as 90/100 bp pair-end reads.
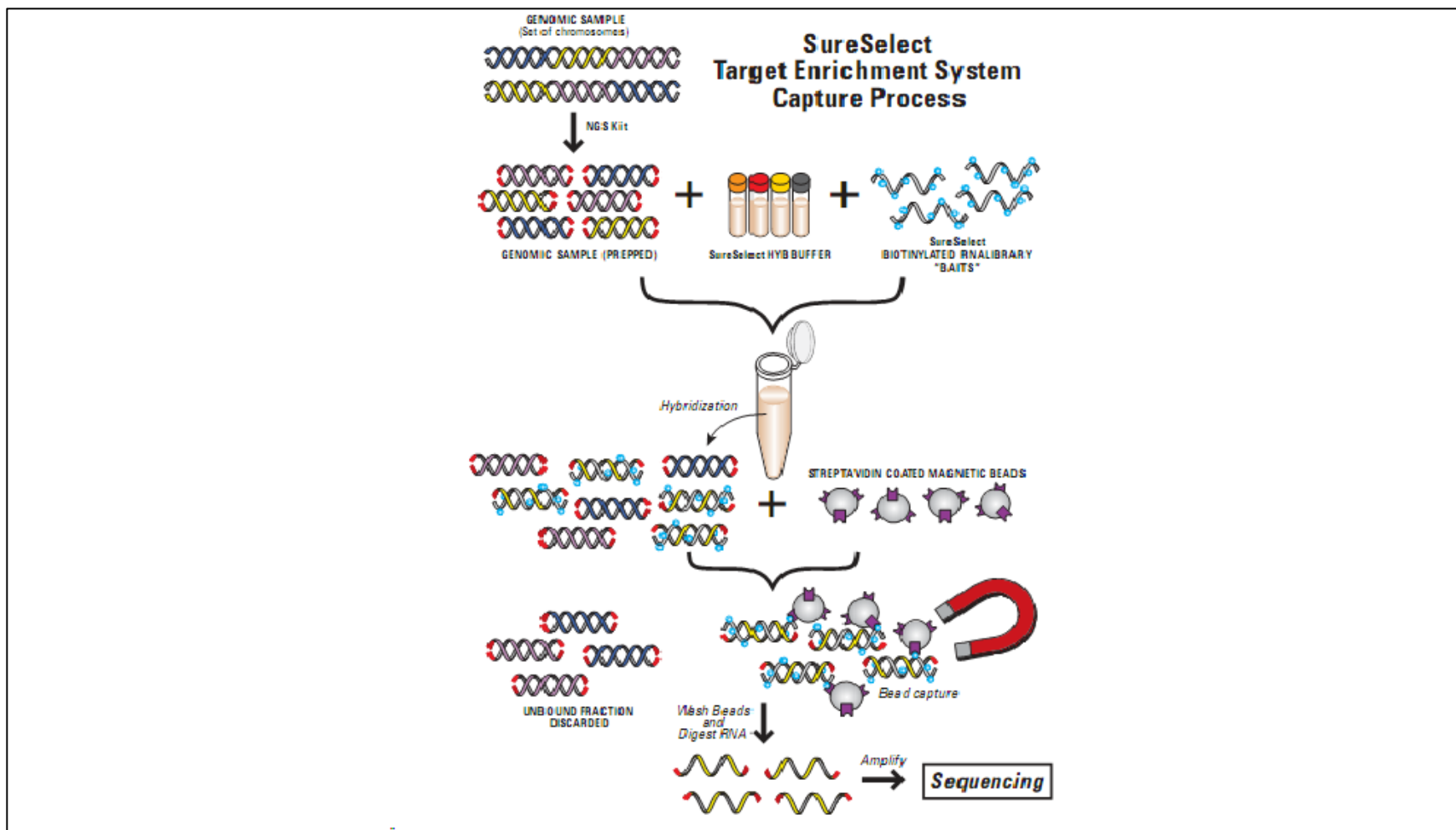
Figure 2-2: Agilent SureSelect system exome capture and sequencing protocol [271].

Bioinformatic analysis was carried out by BGI to determine the insertions and deletions (InDels), copy number variations, and single nucleotide polymorphisms. Data was cleaned by removing adapter sequence and low quality read from the raw data. Alignment was carried out using Burrows-Wheeler Aligner. The SKBR3-A and SKBR3-Par cell line samples were treated as a pair. Single nucleotide variants (SNVs), were detected by Varscan, InDels by SAMtools, and copy number variants (CNVs) by ExomeCNV.

2.15 *In vivo* experiments

All *in vivo* experiments were reviewed and approved by the DCU BioResource Advisory Group, the DCU Research Ethics Committee, and the Health Products Regulatory Authority.

2.15.1 Sample size calculation

Sample size calculations for the drug efficacy study were performed using the G*Power statistical software, in consultation with biostatisticians, Dr. Michael Parkinson and Dr. Tim Downing. Briefly, the desired minimum significant difference in tumour volume was < 20%. Using data from a previous *in vivo* study with HCC1954-L cells, the expected tumour volumes for untreated controls and lapatinib treated after 51 days was approximately 680 mm^3 and 600 mm^3, respectively. Therefore, a tumour volume of 500 mm^3 or less would be deemed a significant effect. Therefore, the minimum effect size for single agent lapatinib versus the lapatinib and LB-100 combination would be 1.25. The sample size calculation is described in Equation 1 below.

Equation 1: The effect size (dimensionless) was calculated using the mean untreated tumour volume (μ1) and desired maximum significant treatment tumour volume (μ2), divided by the variation of tumour volume (σ).

$$\frac{(\mu1 - \mu2)}{\sigma} = \frac{(600 - 500)}{80} = \frac{100}{80} = 1.25$$

The allocation ratio between groups was 1, a power of 80% was required and the error probability was set at 0.05. The tumour take rate was observed to be approximately 95%, data obtained from collaborators. Therefore, it was calculated that 12 animals were required per group and 60 animals in total for the drug efficacy study.

2.15.2 Tumour induction via subcutaneous injection

HCC1954-L cells were trypsinised, counted and resuspended to 5×10^6 and 1×10^7 cells/50 µL in serum-free RPMI-1640 medium. Cell suspension was combined with Cultrex (R&D Systems) in a 1:1 ratio on ice. This was then drawn into a syringe and a 25 gauge needle (BD) was attached. The animal was restrained by the scruff and held upright. The needle was inserted under the skin on the flank of the animal and 200 µL of the cell solution was injected. The mouse was then returned to its cage and monitored.

2.15.3 Tumour induction via mammary fat pad injection

HCC1954-L cells were trypsinised, counted and resuspended to 1×10^7 cells/mL in serum-free RPMI-1640 medium. The cell suspension was mixed with an equal volume of Cultrex (R&D Systems). This suspension was drawn into a 1 mL syringe and a 25 guage needle was attached. The mouse was anaesthetised with isoflurane, with O_2 as a carrier gas. The cell suspension (50 µL = 5×10^5 cells) was injected into the mammary fat pad of the fourth inguinal nipple by raising the nipple with a forceps and inserting the needle under the skin. The mouse was then given a subcutaneous injection of saline to aid recovery. The mouse was placed in a clean cage, which was partially on a heated mat, and monitored until full recovery.

2.15.4 Tumour measurements

The mouse was restrained by the scruff and held upright. Tumours were measured by height, width, and depth, using electronic calipers. Tumour volume was calculated by:

$$\text{Tumour volume} = \frac{(\text{Height x width x depth})}{1.9}$$

2.15.5 Oral gavage

Lapatinib solution was prepared in 0.5% hydroxypropylmethyl cellulose (HPMC)/0.1% Tween-80 in UHP water to 18.75 mg/mL (75 mg/kg) and sonicated for 15 mins. The solution was drawn into a 1 mL syringe and a bulb-tipped steel gavage needle was attached. The mouse was restrained and held upright. The tip of the gavage needle was dipped in filter-sterilised 1 g/mL sucrose solution. The needle was inserted along the roof of the mouth toward the stomach and 100 µL of lapatinib solution was injected. The needle was carefully removed and the mouse was monitored.

2.15.6 Intra-peritoneal injection

LB-100 was prepared under sterile conditions in PBS to 375 µg/mL (1.5 mg/kg). LB-100 was aliquoted and stored at -80°C before use. LB-100 was drawn into a 1 mL syringe and a 25 gauge needle was attached. The mouse was restrained by the scruff, inverted and held at a downward angle to avoid intestinal injection. The needle was inserted into the abdomen and 100 µL of LB-100 was injected. The needle was removed and the mouse was monitored for adverse response.

2.15.7 Tumour retrieval and processing

When mice were culled at the termination of study or due to adverse events, tumours were excised from the mouse. The tumour was then quickly divided into sections and preserved by liquid nitrogen flash freezing or formalin fixation. Flash frozen samples were stored at -80°C and formalin fixed samples were dehydrated in 50%, 70%, 90%, 100% ethanol, followed by 100% xylene, and then embedded in paraffin. FFPE blocks were stored at 4°C until sectioning. Some tumour material was also taken for cell culture. To do this, tumour tissue was digested in 300 U/mL collagenase/ 100 U/mL hyaluronidase in DMEM for 1 h, after which cells were centrifuged at 1500 rpm for 5 mins, re-suspended in RPMI-1640 supplemented with 10% FBS and 100 IU/mL penicillin and 100 µg/mL streptomycin, and allowed to attach in 25 cm^2 flasks.

2.16   Statistical analysis

P values were calculated (unless otherwise stated) using the student's t-test (two tailed with unequal variance). Analysis was performed on biological triplicates. $P < 0.05$ was considered significant.

Correlation co-efficient values were calculated using Spearman Rank test with two-tailed p value [272].

IC_{50} values were calculated using the dose effect analyser Calcusyn (Biosoft, Version 1.1). IC_{50} values were represented as an average of triplicate biological experiments ± the standard deviation.

For fixed-ratio assays, combination indices (CI) at the ED_{50} (effective dose of combination that inhibits 50% of growth) were determined using the Chou and Talalay equation, on CalcuSyn software (Biosoft) [273]. The combination index equation is based on the multiple drug-effect equation of Chou-Talalay derived from enzyme kinetic models. The equation determines only the additive effect rather than synergism or antagonism. Synergism is defined as a more than expected additive effect, and antagonism as a less than expected additive effect. Determination of synergy/antagonism used in this study was based on the recommended descriptions as shown in Table 2-9. As recommended by Chou *et al.*, the prerequisites for CI calculations included a dose-effect curve, at least four data points for each drug condition was used.

Table 2-9: Range of combinations index values that determine synergism or antagonism in drug combination studies analysed with the Combination Index method.

Range of CI	Symbol	Description
<0.10	+++++	Very strong synergism
0.10-0.30	++++	Strong synergism
0.31-0.70	+++	Synergism
0.71- 0.85	++	Moderate synergism
0.86-0.9	+	Slight synergism
0.91- 1.10	±	Nearly additive
1.11-1.20	_	Slight antagonism
1.21-1.45	_ _	Moderate antagonism
1.45-3.30	_ _ _	Antagonism
3.30- 10.00	_ _ _ _	Strong antagonism
>10.00	_ _ _ _ _	Very strong antagonism

3 The role of PP2A in acquired lapatinib resistant breast cancer

3.1 Introduction

Previous work in our laboratory produced two lapatinib resistant cell lines, SKBR3-L and HCC1954-L [148, 154]. The SKBR3-L cell line was generated by Dr Brigid Browne by treating SKBR3 cells for six months with 250 nM lapatinib. The HCC1954-L cells were established by Dr Martina McDermott by treating HCC1954 cells for six months with 1 µM lapatinib. Untreated SKBR3-Par and HCC1954-Par were maintained alongside the lapatinib-treated cells. In this study, these cell lines were further characterised to determine their sensitivity to other HER2-targeted therapies, including the novel HER family tyrosine kinase inhibitors neratinib and afatinib, in lapatinib resistant breast cancer.

To identify potential mediators of resistance, the SKBR3-L cells were previously examined for proteomic and phospho-proteomic alterations compared to the parental cell line [154]. In this analysis, levels of phosphorylated (Thr56) eukaryotic elongation factor 2 (eEF2) were found to be down-regulated; this was validated in the HCC1954-L cell line. eEF2 is a monomeric GTPase that is involved in protein synthesis and is inhibited by Thr56 phosphorylation. Lapatinib treatment of SKBR3-Par cells caused an increase in phospho-eEF2 levels, whereas in SKBR3-L cells phospho-eEF2 levels were not altered following lapatinib treatment. This suggested that lapatinib cannot inhibit eEF2-mediated protein synthesis in the SKBR3-L cell line and that eEF2 may therefore play a role in acquired lapatinib resistance. Analysis of the numerous signalling pathways that regulate phosphorylation of eEF2 revealed that protein phosphatase 2A (PP2A) is the key regulator of eEF2 activity in SKBR3-L cells and PP2A activity was shown to be increased in both SKBR3-L and HCC1954-L lapatinib resistant cell lines. PP2A is a trimeric holoenzyme that regulates multiple survival pathways [154].

In this study, PP2A was examined as a novel therapeutic target to overcome lapatinib resistance. The effects of and mechanism of action of two PP2A inhibitors, okadaic acid and LB-100, were assessed, alone and in combination with HER2-targeted therapies. Okadaic acid is a lab-grade inhibitor of PP2A and LB-100 is a PP2A inhibitor that is currently in clinical investigation.

3.2   Characterisation of lapatinib resistant cell lines

3.2.1   SKBR3-L and HCC1954-L cells are resistant to lapatinib

Lapatinib is given to patients orally at a dosage of 1.25 g daily. The pharmacokinetics of lapatinib is dependent on the patient's fasting state. Peak plasma concentrations range from 2.54 ± 0.84 µg/mL (4.37 ± 1.44 µM) to 0.91 ± 0.52 µg/mL (1.57 ± 0.894 µM) when fasted [274]. With this in mind, cell lines with an IC_{50} value of 1 µM were deemed lapatinib resistant. Both SKBR3-L and HCC1954-L cell lines were confirmed to be resistant to lapatinib at clinically relevant concentrations (Figure 3-1). The lapatinib IC_{50} value for SKBR3-Par cells was 0.05 ± 0.02 µM and 2.37 ± 0.58 µM for SKBR3-L cells. This represents a 46-fold decrease in sensitivity to lapatinib. The lapatinib IC_{50} value for the HCC1954-L cell line was 1.67 ± 0.34 µM. This is 5.2-fold greater than the lapatinib IC_{50} value in HCC1954-Par cells, 0.32 ± 0.19 µM. IC_{50} values are summarised in Table 3-1.
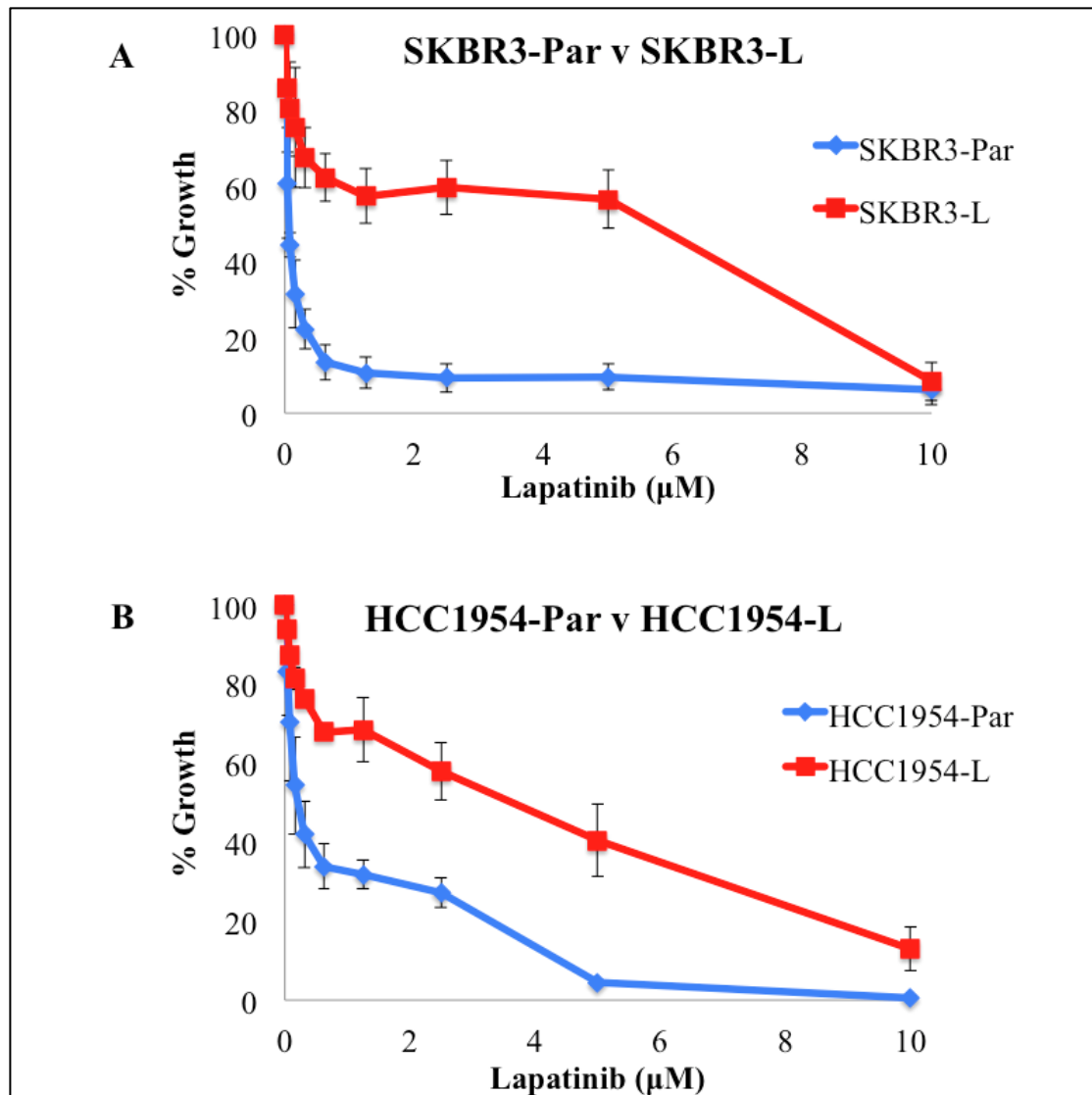
Figure 3-1: Proliferation of (A) SKBR3-L and (B) HCC1954-L cells after 5 days of treatment with lapatinib (0 – 10 μM) was examined by acid phosphatase assay. Percentage growth was calculated relative to untreated control cells. Error bars represent standard deviation of biological triplicate experiments.

3.2.2 SKBR3-L and HCC1954-L cells have reduced sensitivity to afatinib and neratinib

The pan-HER inhibitors, afatinib and neratinib, have been shown to be effective against trastuzumab-resistant HER2-positive breast cancer [108, 123]. Therefore, to assess the potential of the irreversible pan-HER inhibitors in lapatinib-resistant breast cancer, both acquired lapatinib resistant cell lines and their respective parental cell

lines were assessed for sensitivity to afatinib and neratinib (Figure 3-2). The parental cell lines, SKBR3-Par and HCC1954-Par, were both highly sensitive to afatinib and neratinib. The afatinib IC_{50} values for SKBR3-Par and HCC1954-Par cells were 10.9 $\pm$ 3.4 nM and 15.0 $\pm$ 4.6 nM, respectively, and the neratinib IC_{50} values for these cell lines were 3.4 $\pm$ 1.1 nM and 26.1 $\pm$ 1.2 nM, respectively. In comparison, the SKBR3-L and HCC1954-L cell lines showed significantly reduced sensitivity to both pan-HER inhibitors. The afatinib IC_{50} values for SKBR3-L and HCC1954-L cells were 152.0 $\pm$ 12.1 nM and 1.13 $\pm$ 0.18 μM, respectively, and neratinib IC_{50} values were 77.5 $\pm$ 9.6 nM and 272.9 $\pm$ 109.6 nM, respectively. IC_{50} values are summarised in Table 3-1.
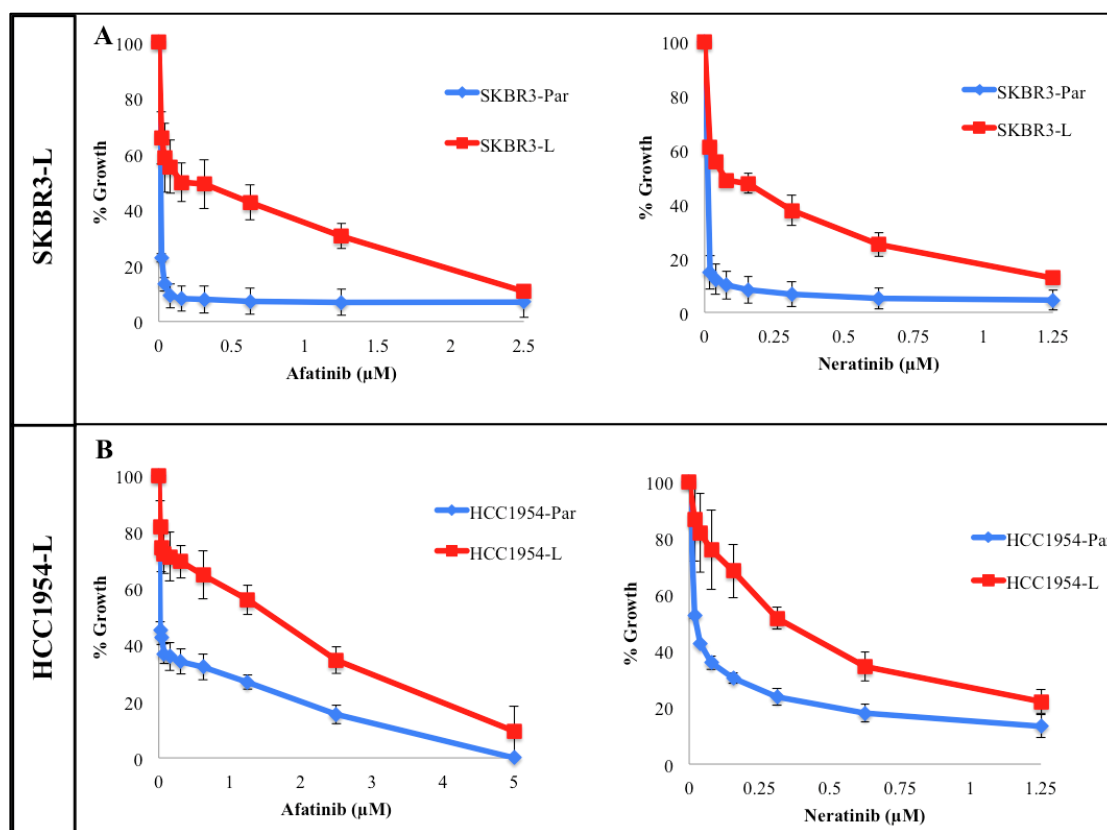
Figure 3-2: Proliferation of (A) SKBR3-L and (B) HCC1954-L cells after 5 days of treatment with afatinib or neratinib was examined by acid phosphatase assay. Percentage growth was calculated relative to untreated control cells. Error bars represent standard deviation of biological triplicate experiments.

3.2.3 Response to trastuzumab and pertuzumab in SKBR3-L and HCC1954-L cells

A trastuzumab-based regimen is standard of care in first-line treatment of metastatic and early stage HER2-positive breast cancer and trastuzumab treatment after disease progression on lapatinib has been investigated in a small clinical study [275, 276]. Furthermore, the addition of pertuzumab to trastuzumab has shown remarkable clinical efficacy and may become standard of care for patients with metastatic disease [67]. Therefore, the lapatinib resistant and parental cell lines were assessed for their sensitivity to trastuzumab and pertuzumab. SKBR3-Par cells were sensitive to trastuzumab *in vitro*; with $28.9 \pm 2.1\%$ growth inhibition relative to untreated controls after 5 days of 10 µg/mL treatment ($p = 1.8 \times 10^{-5}$). In comparison, the SKBR3-L cells were significantly less sensitive to trastuzumab ($p = 0.008$), with $15.1 \pm 4.3\%$ growth inhibition. Both cell lines showed a similar response to 10 µg/mL pertuzumab (SKBR3-Par $= 14.2 \pm 1.0\%$ growth inhibition and SKBR3-L $= 8.2 \pm 4.6\%$ growth inhibition, $p = 0.09$). Pertuzumab enhanced response to trastuzumab in SKBR3-Par cells ($42.2 \pm 2.2\%$ compared to $4.1 \pm 7.0\%$ growth inhibition, $p = 0.0016$), which was not observed in the SKBR3-L cell line ($p = 0.08$) (Figure 3-3).

In contrast to SKBR3-Par cells, HCC1954-Par cells are innately resistant to trastuzumab. In HCC1954-Par cells 10 µg/mL trastuzumab inhibited growth by $6.8 \pm 7.1\%$. Similarly, HCC1954-Par displayed resistance to 10 µg/mL pertuzumab ($5.6 \pm 10.1\%$ growth inhibition) and trastuzumab plus pertuzumab ($6.0 \pm 4.1\%$ growth inhibition). The HCC1954-L cells maintained this resistance to trastuzumab, pertuzumab, and trastuzumab plus pertuzumab ($4.4 \pm 1.5\%$, $7.9 \pm 3.6\%$, and $-7.2 \pm 3.3\%$ growth inhibition, respectively) (Figure 3-5). Responses to all HER2-targeted therapies are summarised Table 3-1.
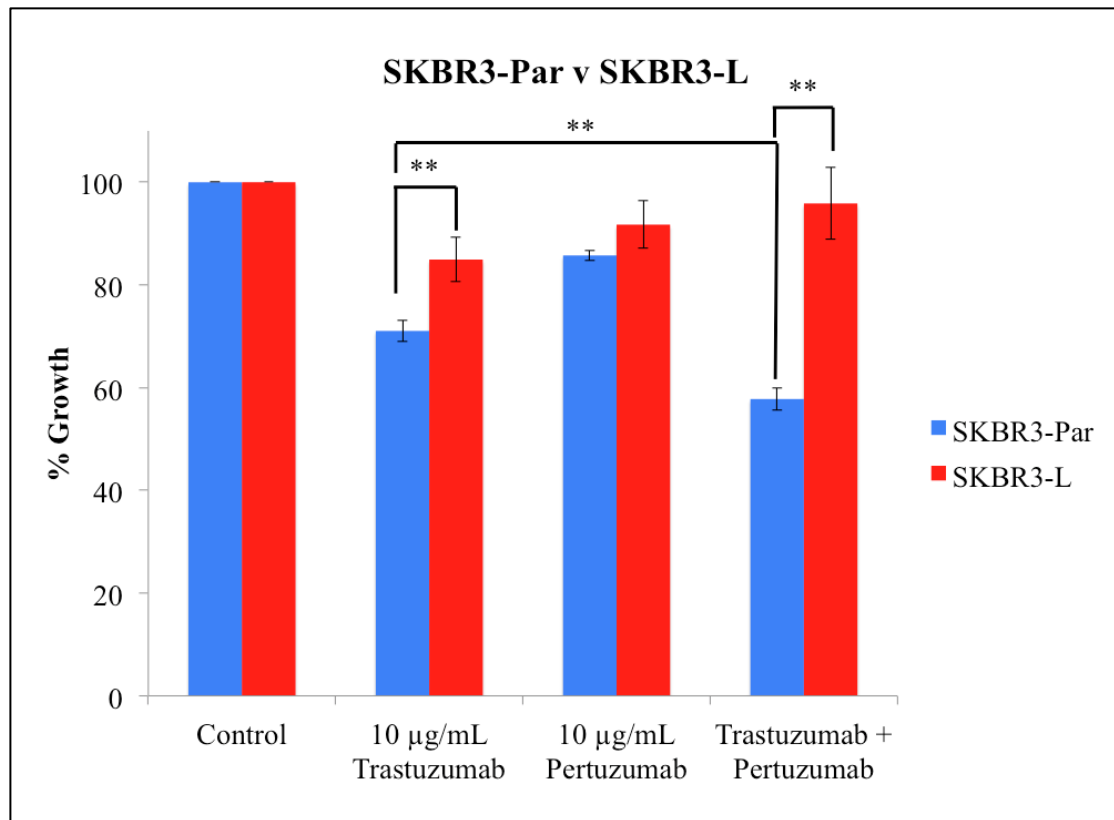
Figure 3-3: Proliferation of SKBR3-Par and SKBR3-L cells treated for 5-days with 10 *μ*g/mL trastuzumab, 10 *μ*g/mL pertuzumab, or trastuzumab plus pertuzumab was measured by acid phosphatase assay. Error bars represent standard deviation of biological triplicate experiments. The Student's t test was used to determine statistical significance. ** denotes a p value < 0.01.
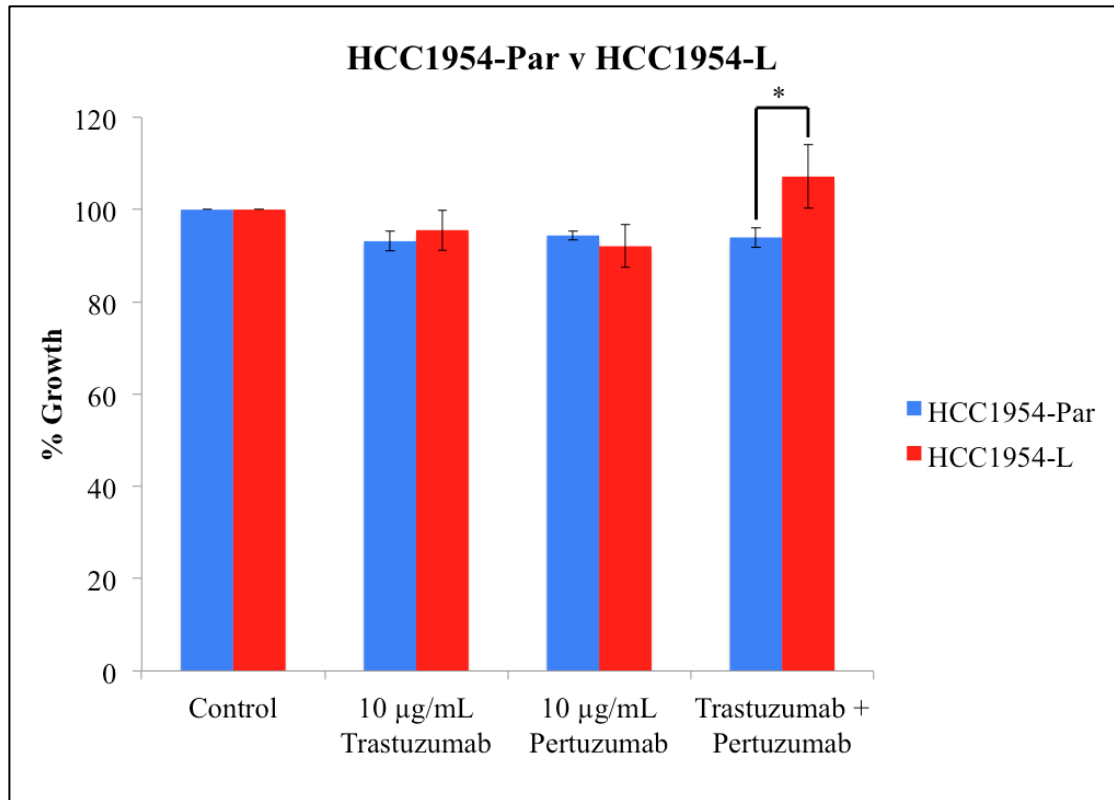
Figure 3-4: Proliferation of HCC1954-Par and HCC1954-L cells treated for 5-days with 10 μg/mL trastuzumab, 10 μg/mL pertuzumab, or trastuzumab plus pertuzumab was measured by acid phosphatase assay. Error bars represent standard deviation of biological triplicate experiments. The Student's t test was used to determine statistical significance. * denotes a p value < 0.05.

Table 3-1: Lapatinib resistant and parental cell line response to HER2-targeted therapies.

	SKBR3-L	SKBR3-Par	HCC1954-L	HCC1954-Par
Lapatinib IC_{50} value (μM)	2.37 ± 0.58	0.05 ± 0.02	1.67 ± 0.34	0.32 ± .019
Afatinib IC_{50} value (nM)	152.0 ± 12.1	10.9 ± 3.4	1130.0 ± 180.0	15.0 ± 4.6
Neratinib IC_{50} value (nM)	77.5 ± 9.6	3.4 ± 1.1	272.9 ± 109.6	26.1 ± 1.2
% Growth inhibition with 10 μg/mL trastuzumab	15.1 ± 4.3	28.9 ± 2.1	4.4 ± 1.5	6.8 ± 7.1
% Growth inhibition with 10 μg/mL pertuzumab	8.2 ± 4.6	14.2 ± 1.0	7.9 ± 3.6	5.6 ± 10.1
% Growth inhibition with 10 μg/mL trastuzumab and pertuzumab	4.1 ± 7.0	42.2 ± 2.2	-7.2 ± 3.3	6.0 ± 4.1

3.3 SKBR3-L and HCC1954-L cells are sensitive to okadaic acid

SKBR3-L and HCC1954-L cells were previously shown to have increased PP2A activity relative to their parental cell line [148, 154]. Both lapatinib resistant cell lines and their parental cell lines were tested for sensitivity to 3 nM okadaic acid, a lab-grade PP2A inhibitor, by acid phosphatase assay (Figure 3-5 A and B). Both SKBR3-L and HCC1954-L cell lines were more sensitive to okadaic acid compared to their respective parental cell lines ($p = 0.03$ and 0.04, respectively). Combined treatment with lapatinib and okadaic acid enhanced the growth inhibitory effect in SKBR3-L and HCC1954-L cells ($p = 0.03$ and 0.01, respectively) (Figure 3-6 A and C). Trastuzumab did not significantly alter the growth effect of okadaic acid in either cell line ($p = 0.17$ and 0.99, respectively) (Figure 3-6 B and D).
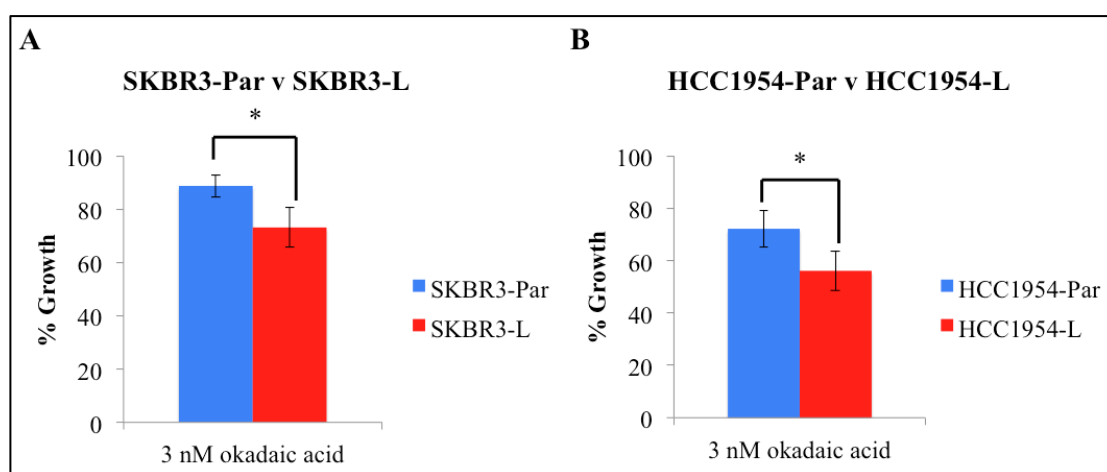
Figure 3-5: Proliferation of SKBR3-Par, SKBR3-L (A), HCC1954-Par, and HCC1954-L (B) after 5 days of treatment with 3 nM okadaic acid was examined by acid phosphatase assay. Percentage growth was calculated relative to untreated control cells. Error bars represent standard deviation of biological triplicate experiments. The Student's t test was used to determine statistical significance. * denotes a p value of < 0.05.
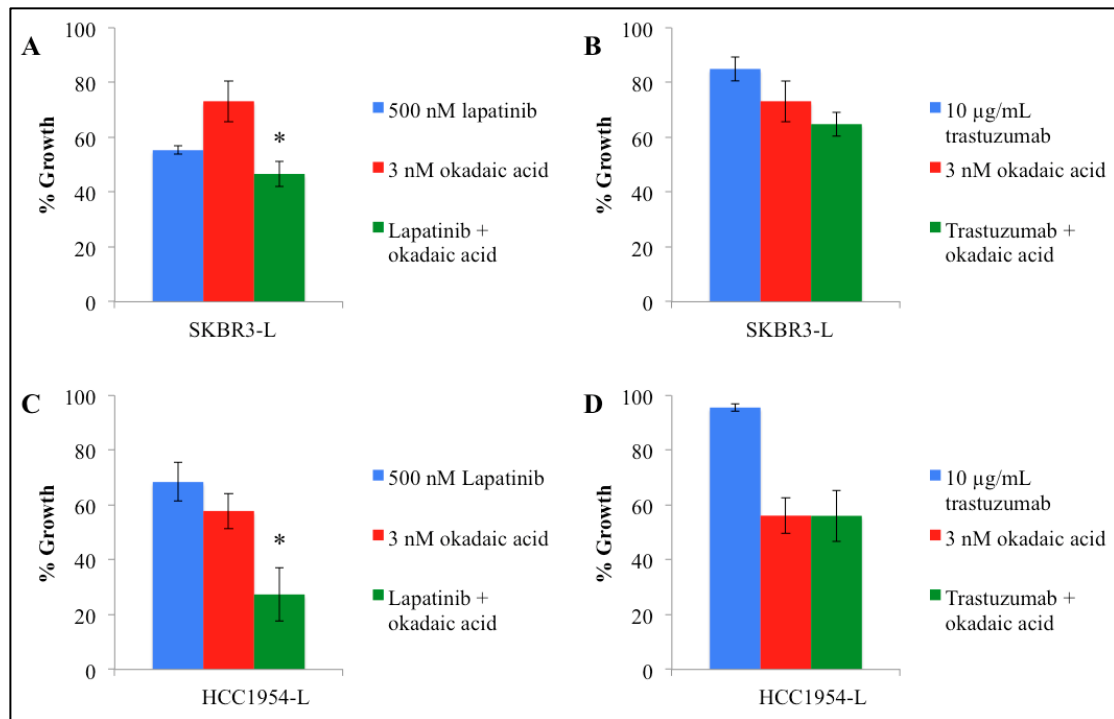
Figure 3-6: Proliferation of SKBR3-L after 5 days of treatment with 500 nM lapatinib, 3 nM okadaic acid, lapatinib plus okadaic acid (A) or 10 μg/mL trastuzumab, okadaic acid, or trastuzumab plus okadaic acid (B) was examined by acid phosphatase assay. Proliferation of HCC1954-L after 5 days of treatment with 500 nM lapatinib, 3 nM okadaic acid, lapatinib plus okadaic acid (C) or 10 μg/mL trastuzumab, okadaic acid, or trastuzumab plus okadaic acid (D) was examined by acid phosphatase assay. Percentage growth was calculated relative to untreated control cells. Error bars represent standard deviation of biological triplicate experiments. The Student's t test was used to determine statistical significance. * denotes a p value of < 0.05.

3.4   The effect of okadaic acid on cell cycle progression

SKBR3-L proliferation was inhibited by the combination of okadaic acid and lapatinib (Figure 3-6). To determine if okadaic acid combined with lapatinib was cytostatic or cytocidal, cell cycle assays were performed. SKBR3-L cells were treated with 500 nM lapatinib, 3 nM okadaic acid, or lapatinib plus okadaic acid for 48 h. The percentage of the cell population in each phase of the cell cycle was measured by propidium iodide staining and flow cytometry analysis. Lapatinib alone (500 nM) induced G1 arrest ($51.8 \pm 1.6\%$ compared to $41.8 \pm 2.9\%$ for untreated cells). OA alone induced a small increase in the sub-G1 population ($12.8 \pm 6.3\%$ versus $8.9 \pm 3.4\%$ for untreated cells) and the combination induced an increase in the sub-G1 fraction ($23.1 \pm 8.5\%$) compared to either lapatinib ($9.1 \pm 6.7\%$, $p = 0.044$) or OA ($12.8 \pm 6.3\%$, $p = 0.083$) alone (Figure 3-7).
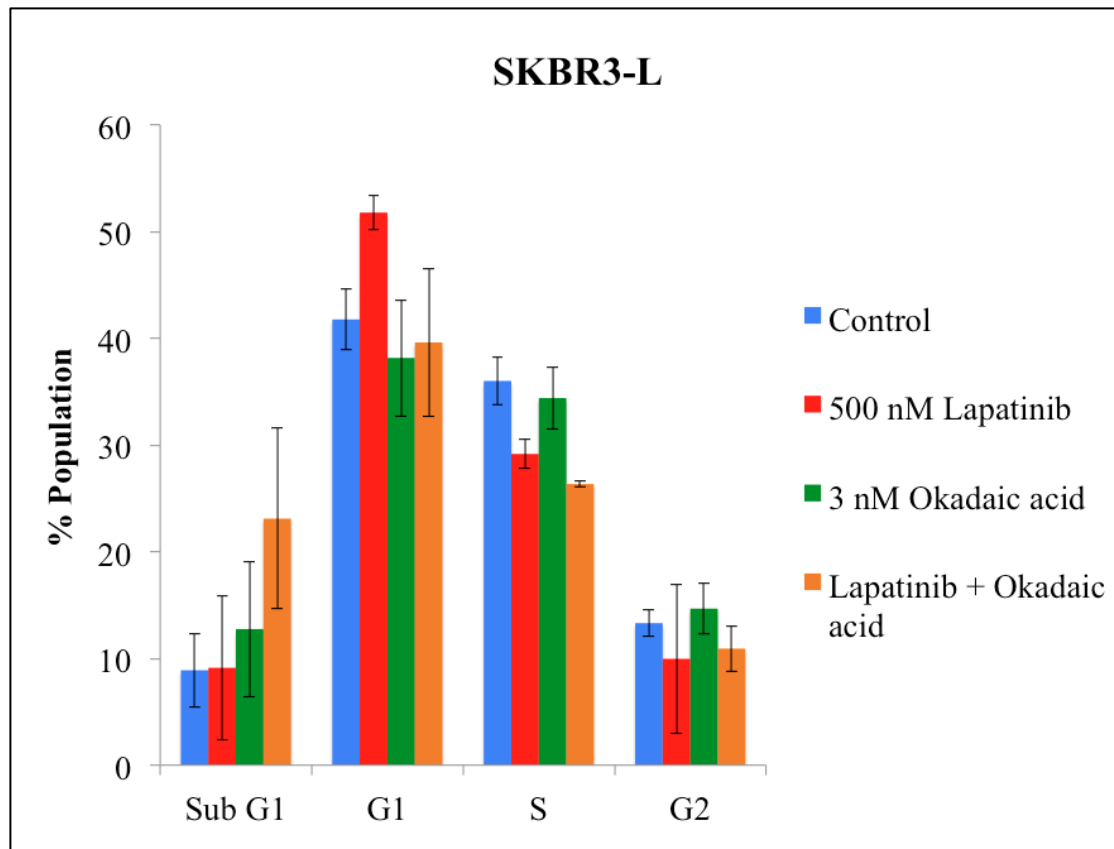
Figure 3-7: SKBR3-L cells were treated with 500 nM lapatinib, 3 nM okadaic acid, or lapatinib plus okadaic acid for 48 h. Cell cycle progression was measured by flow cytometry. Cell cycle stage was calculated using ModFit software. Error bars represent standard deviation of biological triplicate experiments. The Student's t test was used to determine statistical significance.

## 3.5 PP2A subunit expression in lapatinib resistant cell lines

PP2A is a holoenzyme, composed of three subunits: the structural A subunit, the regulatory B subunit, and the catalytic C subunit. Expression levels of the two isoforms of the catalytic subunit, PPP2CA and PPP2CB, and the levels of the catalytic subunit phosphorylation and methylation were measured by Western blotting (Figure 3-8Figure 3-8). Total levels of either catalytic subunit isoform were not significantly altered in HCC1954-L cells compared to HCC1954-Par cells ($p = 0.19$ and 0.66, respectively). Both post-translational modifications were decreased in the lapatinib resistant cell lines ($p = 0.015$ and 0.045, respectively). The lower levels of phosphorylated PPP2CA suggests that PP2A activity is increased in the HCC1954-L

cells, which was previously observed [154]. The methylation levels affect the substrate specificity of the holoenzyme and the decreased methylation would suggest that the lapatinib resistant cell line may have different substrate targets to the parental cells.
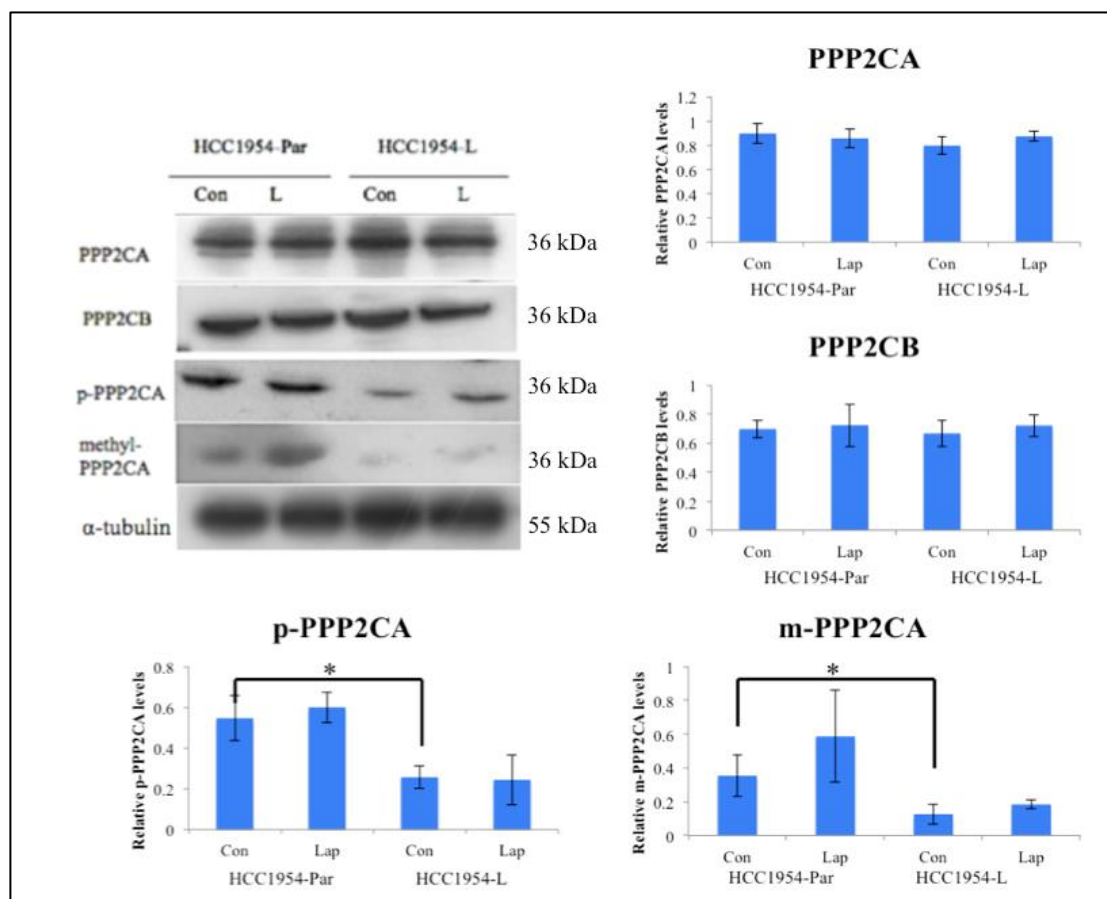
Figure 3-8: Western blotting of PPP2CA, PPP2CB, phosphor-PPP2CA and methyl-PPP2CA in HCC1954-Par and HCC1954-L cells untreated (Con) and treated with 1 μM lapatinib (Lap). Densitometry was carried out with LiCor Odyssey 3.0. Error bars represent standard deviation of triplicate experiments. Blot image shown is representative of triplicate blots. Tubulin was used as a loading control. The Student's t test was used to determine statistical significance. * denotes a p value of < 0.05.

3.6   The effect of PPP2CA siRNA knockdown on HCC1954-L proliferation

In order to ensure the growth inhibition effect of PP2A inhibition was not an off-target effect of the okadaic acid, HCC1954-L cells were reverse transfected with anti-PP2A catalytic subunit A, PPP2CA, siRNA (Figure 3-10). PPP2CA is the dominant catalytic subunit that carries out the phosphatase activity of the holoenzyme and is the substrate of okadaic acid [277]. The effectiveness of PPP2CA knockdown in HCC1954-L cells by anti-PPP2CA siRNA was measured by Western blotting after 72 h of treatment. PPP2CA protein expression was significantly reduced relative to scrambled siRNA treated cells (61.2% decrease in protein expression) (p = 0.047) (Figure 3-9). Lapatinib treatment did not significantly alter the effectiveness of PPP2CA knockdown (p = 0.77).

To measure the growth effects of PPP2CA siRNA, cells were treated with transfection reagent (Trans-IT X2), anti-PPP2CA siRNA, or anti-kinesin siRNA for 24 h, after which medium was changed. Cells were then treated with DMSO or 500 nM lapatinib for a further 72 h. Efficient transfection was confirmed using an anti-kinesin siRNA. Kinesin knockdown resulted in a 88.2 ± 3.4% growth inhibition. Anti-PPP2CA siRNA caused a significant decrease in cell growth compared to scrambled siRNA control (p = 0.015). Lapatinib plus anti-PPP2CA siRNA increased growth inhibition (57.9 ± 1.2% growth inhibition) compared to anti-PPP2CA siRNA alone (43.8 ± 10.5 % growth inhibition) but this difference did not achieve statistical significance (p = 0.08). This may be due to the shorter assay time of four days and lapatinib treatment for only the last three days.
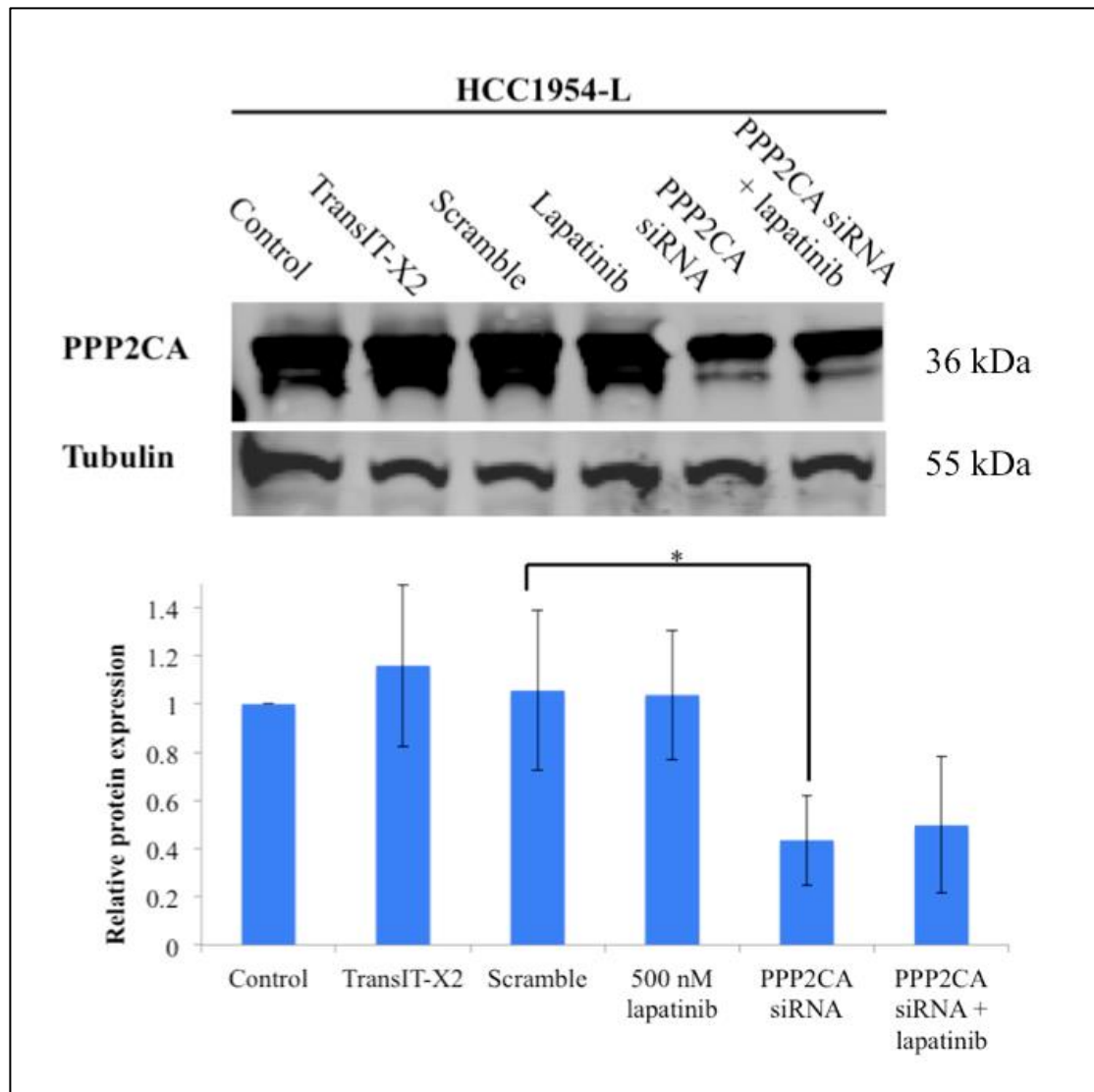
Figure 3-9: Western blotting of PPP2CA in HCC1954-L cells treated with Trans-IT X2, scrambled siRNA, 500 nM lapatinib, anti-PPP2CA siRNA, or anti-PPP2CA siRNA plus lapatinib. Densitometry was carried out with LiCor Odyssey 3.0. Error bars represent standard deviation of triplicate experiments. Blot image shown is representative of triplicate blots. Tubulin was used as a loading control. The Student's t test was used to determine statistical significance. * denotes a p value of < 0.05.
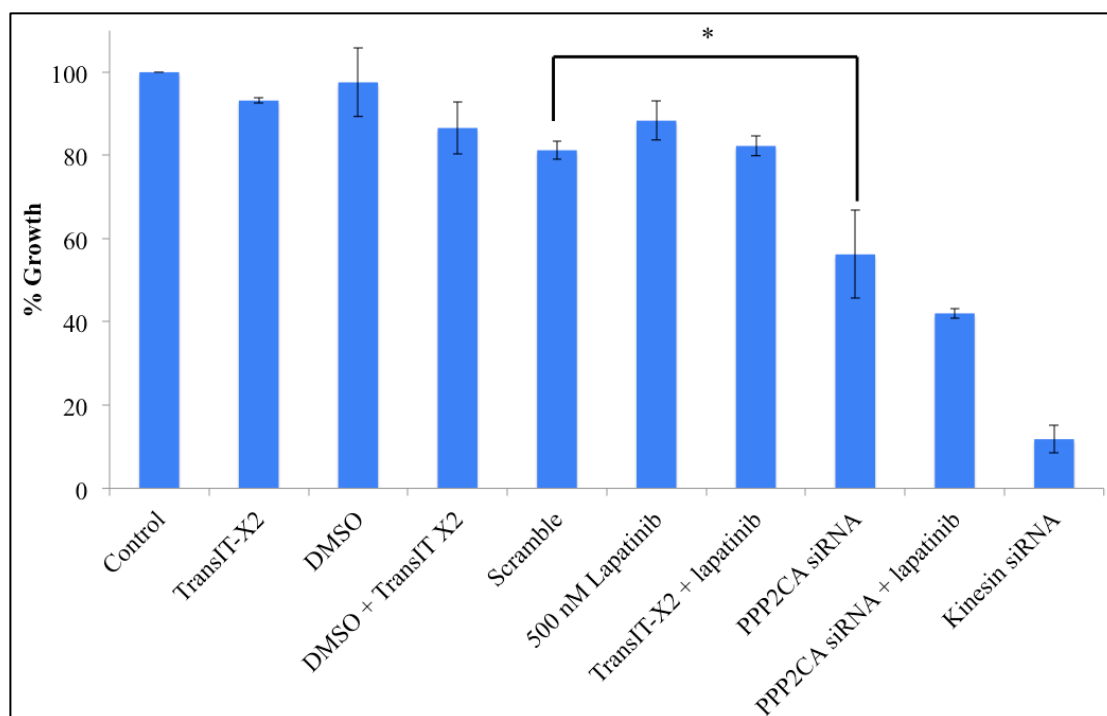
Figure 3-10: HCC1954-L cells were treated with TransIT-X2 transfection reagent, anti-PPP2CA siRNA, or anti-kinesin siRNA. After 24 h, medium was removed and fresh medium, DMSO, or 500 nM lapatinib was added. After a further 72 h, proliferation was measured by trypan blue exclusion cell counting. Error bars represent standard deviation of biological triplicate experiments. * denotes a p value of < 0.05.

3.7   PP2A activation decreases lapatinib sensitivity

In order to assess if increasing PP2A activity alters the response of lapatinib-naive cells to lapatinib, SKBR3-Par and HCC1954-Par cells were treated with FTY720, a PP2A activator [278], and then treated with serial dilution concentrations of lapatinib from 5 μM. 24 h pre-treatment of SKBR3 cells with 2.5 μM FTY720 resulted in a 5.3 fold increase in the lapatinib IC_{50} value. The lapatinib IC_{50} value of FTY720-pretreated SKBR3-Par cells was 136.1 ± 2.3 nM, compared to 25.8 ± 3 nM in FTY720-untreated SKBR3-Par cells ($p = 8.9 \times 10^{-7}$) (Figure 3-11 A). FTY720 treatment also decreased lapatinib sensitivity in HCC1954-Par cells, increasing the lapatinib IC_{50} value 2.1-fold, from 582 ± 31 nM to 1.22 ± 0.1 μM ($p = 7.8 \times 10^{-4}$)

(Figure 3-11 B). This suggests that increased PP2A activity causes decreased sensitivity to lapatinib.
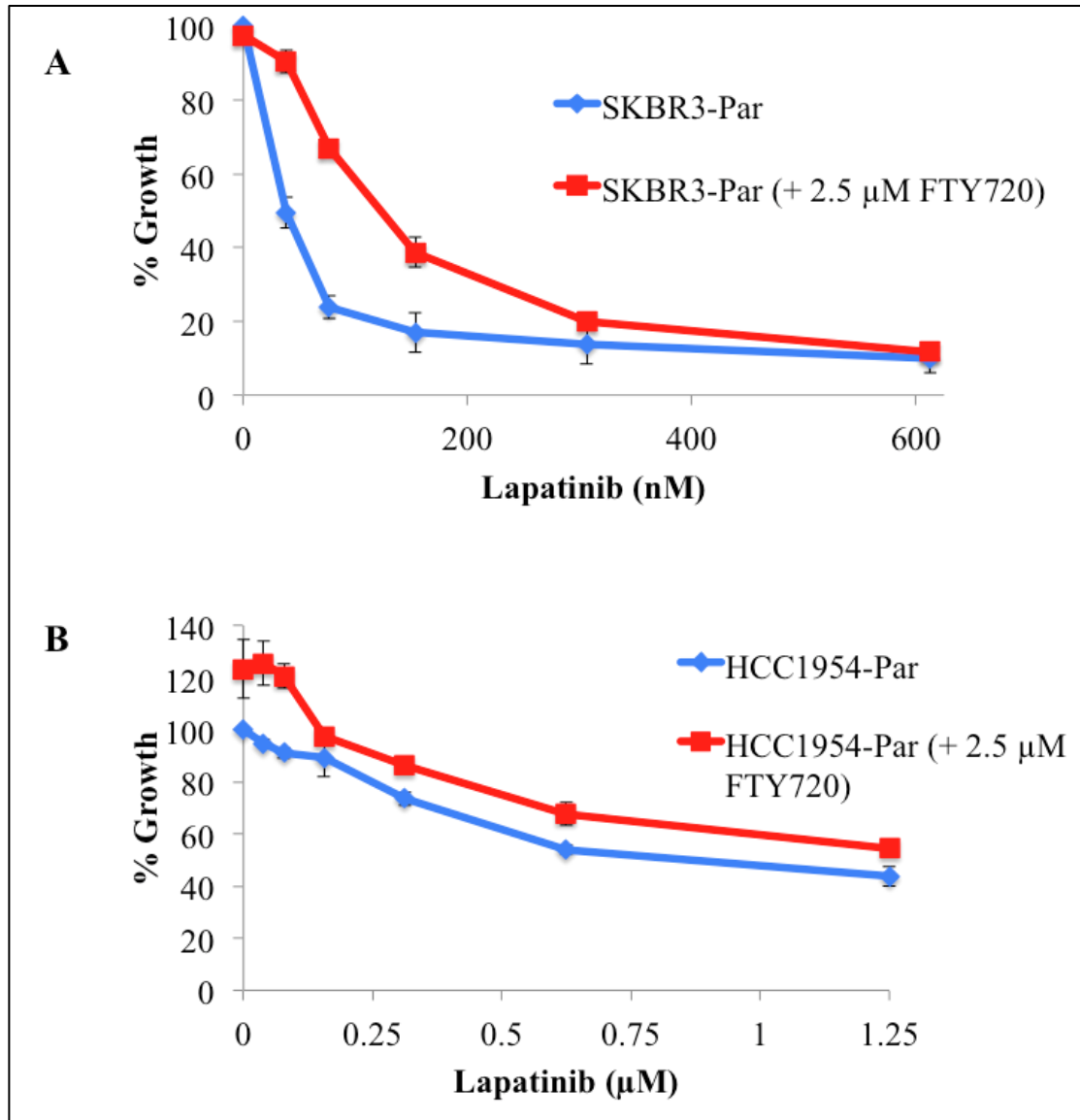
Figure 3-11: (A) SKBR3-Par and (B) HCC1954-par cells treated with 2.5 μM FTY720 for 24 h, followed by lapatinib treatment for five days. FTY720-treated cells were compared to an untreated control. Error bars are representative of biological triplicate results.

3.8   Okadaic acid blocks development of lapatinib resistance

As increased PP2A activity can decrease lapatinib sensitivity and lapatinib treatment can increase PP2A activity [154], the potential of inhibiting PP2A in conjunction with lapatinib treatment to prevent the development of lapatinib resistance was investigated. SKBR3 cells were treated twice weekly with 250 nM lapatinib, 3 nM okadaic acid, or lapatinib plus okadaic acid. The two endpoints of the assay were when the control cells became confluent (14 days), as a comparison for baseline lapatinib sensitivity, and when lapatinib resistant cells emerged and actively proliferated (28 days). At 14 days when control cells were confluent, lapatinib caused a 95% reduction in cell growth compared to control cells. Okadaic acid caused 52% growth inhibition and the combination treatment caused similar inhibition as lapatinib alone (98%). After a further 14 days of treatment, lapatinib-treated cells had started to grow in tight colonies and were now at 30% of the control cell number at day 14. In contrast, the growth of cells treated with lapatinib plus okadaic acid was still significantly inhibited ($p = 3.5 \times 10^{-5}$) (Figure 3-12).
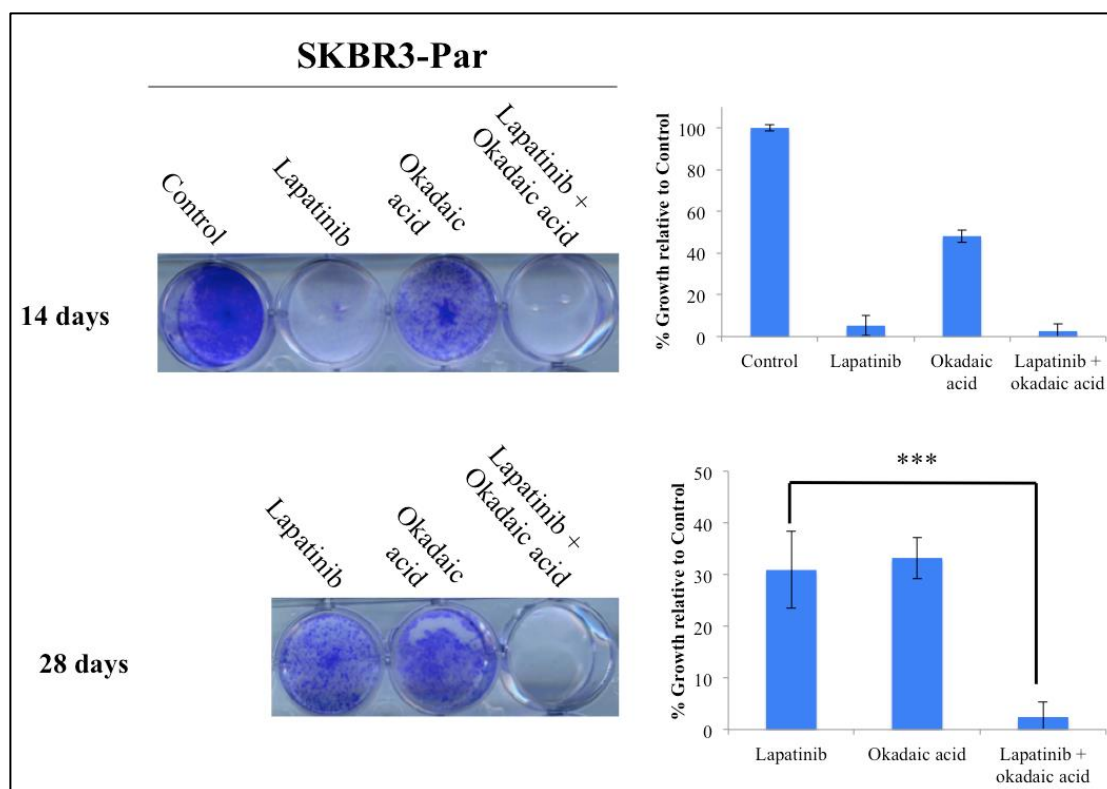
Figure 3-12: SKBR3-Par cells were treated twice weekly with 250 nM lapatinib, 3 nM okadaic acid, and lapatinib plus okadaic acid until control cells and lapatinib-treated cells approached confluency. Images represent triplicate experiments. Graphs represent absorbance levels of eluted crystal violet relative to control. Error bars represent standard deviation of triplicate assays. The Student's t test was used to determine statistical significance. *** denotes p < 0.001.

This experiment was repeated with the HCC1954-Par cells (Figure 3-12). As HCC1954 cells are less sensitive to lapatinib compared to SKBR3 cells, HCC1954 cells were treated with 1 μM lapatinib in this assay. HCC1954 cells were sensitive to both single agents and had an enhanced response to the combination (p = 0.03). After the additional week of treatment, HCC1954 cells began to actively grow again in okadaic acid (p = 0.005). Importantly, the combination treatment did not become resistant and had significantly less growth compared to either single agent (p = 0.001).
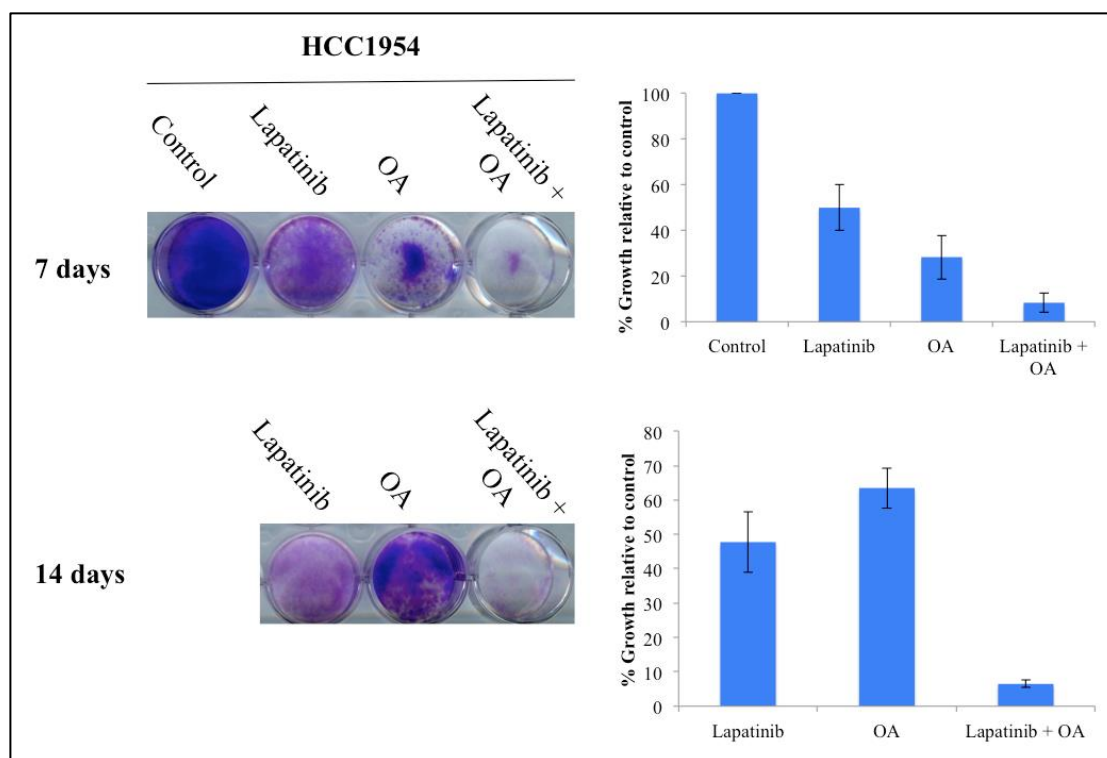
Figure 3-13: HCC1954-Par cells were treated twice weekly with 1 *μ*M lapatinib, 3 nM okadaic acid, and lapatinib plus okadaic acid until control cells and lapatinib-treated cells approached confluency. Images represent triplicate experiments. Error bars represent standard deviation of triplicate assays. Student's t test used to determine statistical significance.

3.9 RPPA analysis of lapatinib and okadaic acid treated HCC1954-L cells

PP2A dephosphorylates a myriad of proteins [279]. In order to understand the signalling effects of PP2A inhibition, alone and in combination with lapatinib, HCC1954-L cells treated with 500 nM lapatinib, 3 nM okadaic acid, and lapatinib plus okadaic acid for 18 h were examined by reverse phase protein array (RPPA) analysis. RPPA experiment was carried out by Dr. Mattia Cremona. HCC1954-L cells were chosen for this experiment as they showed a greater combination effect of okadaic plus lapatinib than the SKBR3-L cell line.

Lapatinib treatment significantly altered the total or phosphorylated levels of 10 proteins (Table 3-2). As lapatinib is an EGFR/HER2 inhibitor, it is unsurprising HER family member levels and activity was altered with lapatinib treatment. Phosphorylated HER2 (Y1248) and HER3 (Y1289) were both significantly decreased

(p = 0.016 and 0.047, respectively). Total protein levels of EGFR were also decreased compared to DMSO-treated cells (p value = 0.009). Downstream of HER2, Akt and Akt2 levels were significantly increased. Phosphorylated Akt (S473 and T308) were slightly reduced but this change was not significant. Interestingly, 18 h lapatinib treated caused increases in levels of the RTK MET. Grb2-associated binding protein 1 (GAB1) phosphorylation was also decreased. GAB1 is an adapter protein that interacts with several RTKs, including EGFR and MET [280, 281]. This may indicate after the 18 h treatment, downstream signalling may be suppressed. Previous work in our lab, showed decreased Akt and ERK 1/2 phosphorylation after 24 h of lapatinib treatment [154].

Eighteen hour 3 nM okadaic acid treatment significantly altered only two phosphorylated protein levels and decreased total levels of one protein, Akt2 (Table 3-3). Okadaic acid caused significant decrease in Src (Y416) levels (p = 0.035) and increased p38 MAPK (T180) (p = 0.039). The RPPA analysis examined 67 total or phosphorylated protein levels. However, PP2A regulates a large amount of proteins outside of the pathways encompassed in this analysis. PP2A inhibition with okadaic acid may be altering proteins outside of the remit of the RPPA platform used.

The combination of 500 nM lapatinib plus 3 nM okadaic acid caused 15 protein expression and activation changes, five of these were common to the lapatinib treatment (Akt, EGFR Y1068, HER2 Y1248, GAB1 Y627, NFκB p65 S536) and one with okadaic acid treatment (Src Y416) (Table 3-4). Combination treatment showed decreased phosphorylation of EGFR (Y1063 and Y1172) (p = 0.003 and 0.0001, respectively), HER2 (Y1248) (p = 0.0025), and HER3 (Y1289) (p = 0.006). Downstream from HER family member signalling, combination treated HCC1954-L cells showed significant decreases in phosphorylation of MAPK (T202/Y204) (p = 0.027), MEK 1/2 (S217) (p = 0.0007), Shc (Y317) (p = 0.04), Src (Y416) (p = 0.016), total and phosphorylated levels of mTOR (S2448) (p = 0.042 and 0.019, respectively) and total Raf levels (p value = 0.003). Total levels of the pro-angiogenic receptor, VEGFR2, was also decreased (p = 0.042). Akt2 levels were increased with lapatinib and decreased with okadaic acid, combination treatment negated these changes and total Akt levels were significantly increased to similar levels to lapatinib alone treatment.

These changes indicate that the combination of PP2A inhibition and EGFR/HER2 inhibition have an enhanced effect at inhibiting survival signalling.

Table 3-2: Statistically significant alterations in HCC1954-L cells treated with lapatinib versus DMSO control by RPPA analysis.

DMSO v Lapatinib

Protein	Phosphorylation site	Fold change	p value
EGFR	-	0.37	0.009
GAB1	Y627	0.47	0.008
HER2	Y1248	0.74	0.016
HER3	Y1289	0.84	0.047
Akt2	-	1.40	0.034
Akt	-	1.50	0.027
GSKβ	-	1.64	0.029
MET	-	2.13	0.040
PKCα	-	2.43	0.016
NFκB p65	S536	2.48	0.007

Table 3-3: Statistically significant alterations in HCC1954-L cells treated with okadaic acid versus DMSO control by RPPA analysis.

DMSO v Okadaic acid

Protein	Phosphorylation site	Fold change	p value
Akt2	-	0.11	0.0004
Src	Y416	0.78	0.0350
p38 MAPK	T180	1.62	0.0390

Table 3-4: Statistically significant alterations in HCC1954-L cells treated with lapatinib plus okadaic acid versus DMSO control by RPPA analysis.

DMSO v Lapatinib + Okadaic acid

Protein	Phosphorylation site	Fold change	p value
EGFR	Y1068	0.41	0.003
MEK 1/2	S217	0.41	0.001
GAB1	Y627	0.49	0.017
EGFR	Y1173	0.68	0.001
HER2	Y1248	0.73	0.003
mTOR	-	0.74	0.042
HER3	Y1289	0.75	0.006
MAPK	T202/Y204	0.76	0.027
Src	Y416	0.76	0.016
Shc	Y317	0.76	0.040
RAF	-	0.78	0.003
mTOR	S2448	0.79	0.019
VEGFR2	-	0.86	0.042
Akt	-	1.39	0.048
NFκB p65	S536	2.99	0.001

PANTHER Pathway
Total # Genes: 12   Total # pathway hits: 78

Click to get gene list for a category:
- Alzheimer disease-amyloid secretase pathway (P00003)
- Angiogenesis (P00005)
- Angiotensin II-stimulated signaling through G proteins and beta-arrestin (P05911)
- Apoptosis signaling pathway (P00006)
- B cell activation (P00010)
- CCKR signaling map (P06959)
- Cadherin signaling pathway (P00012)
- EGF receptor signaling pathway (P00018)
- Endothelin signaling pathway (P00019)
- FGF signaling pathway (P00021)
- Gonadotropin-releasing hormone receptor pathway (P06664)
- Hypoxia response via HIF activation (P00030)
- Inflammation mediated by chemokine and cytokine signaling pathway (P00031)
- Insulin/IGF pathway-mitogen activated protein kinase kinase/MAP kinase cascade (P00032)
- Integrin signalling pathway (P00034)
- Interferon-gamma signaling pathway (P00035)
- Interleukin signaling pathway (P00036)
- PDGF signaling pathway (P00047)
- Parkinson disease (P00049)
- Ras Pathway (P04393)
- T cell activation (P00053)
- TGF-beta signaling pathway (P00052)
- Toll receptor signaling pathway (P00054)
- VEGF signaling pathway (P00056)
- p53 pathway by glucose deprivation (P04397)

**Chart tooltips are read as: Category name (Accession): # genes; Percent of gene hit against total # genes;
Percent of gene hit against total # Pathway hits

Figure 3-14: Pathway analysis of HCC1954-L cells treated with lapatinib plus okadaic acid using PANTHER software.

3.10 Sensitivity of lapatinib resistant cell lines to LB-100

Although okadaic acid is a potent PP2A inhibitor, it is not safe as a therapeutic treatment [237, 282]. However, several PP2A inhibitors have been investigated in clinical trials. LB-100 (Lixte, Biotechnology), a therapeutic PP2A inhibitor, has recently been tested in a Phase I clinical trial in solid tumours and has been shown to enhance response to chemotherapy and radiotherapy in pre-clinial studies [196, 258, 259, 264]. Both lapatinib resistant cell lines and their parental cell lines were tested for sensitivity to LB-100 (Figure 3-15). Similar to PP2A inhibition with okadaic acid, SKBR3-L and HCC1954-L cell lines were significantly more sensitive to LB-100 compared to their respective parental cell lines. The LB-100 IC_{50} value for SKBR3-L cells was 2.13 ± 0.20 μM compared to 5.38 ± 0.60 μM for SKBR3-Par cells. The LB-100 IC_{50} values for HCC1954-L and HCC1954-Par cells were 2.31 ± 0.19 μM and 5.32 ± 0.82, respectively. Furthermore, lapatinib plus LB-100 was synergistic in the HCC1954-L and SKBR3-L cells (CI value at $ED_{50} = 0.68 \pm 0.26$ and 0.56 ± 0.13, respectively) (Figure 3-16).
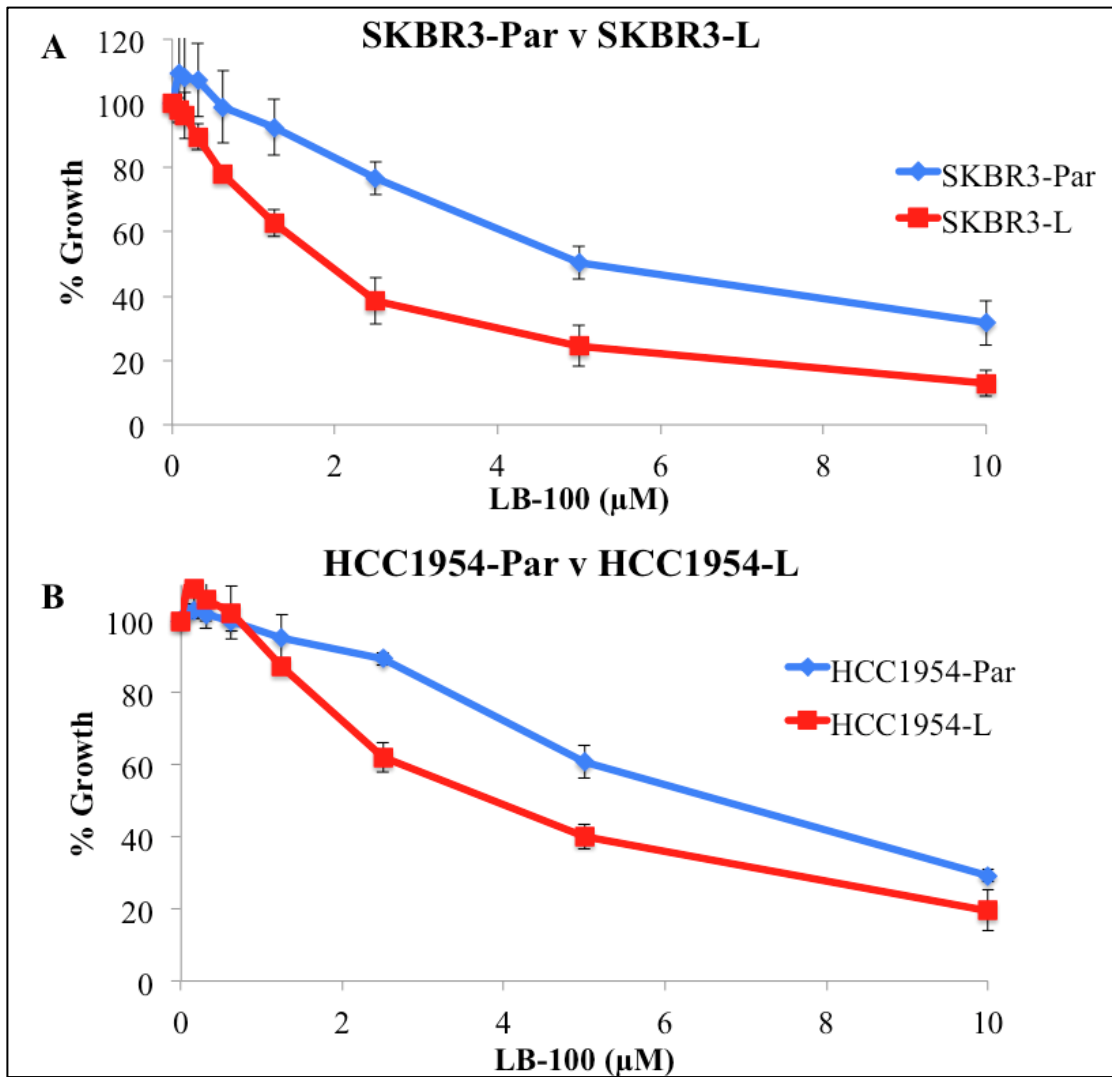
Figure 3-15: Proliferation of (A) SKBR3-Par and SKBR3-L and (B) HCC1954-Par and HCC1954-L treated with LB-100 for 5 days was measured by acid phosphatase assay. Error bars represent standard deviation of biological triplicate experiments.
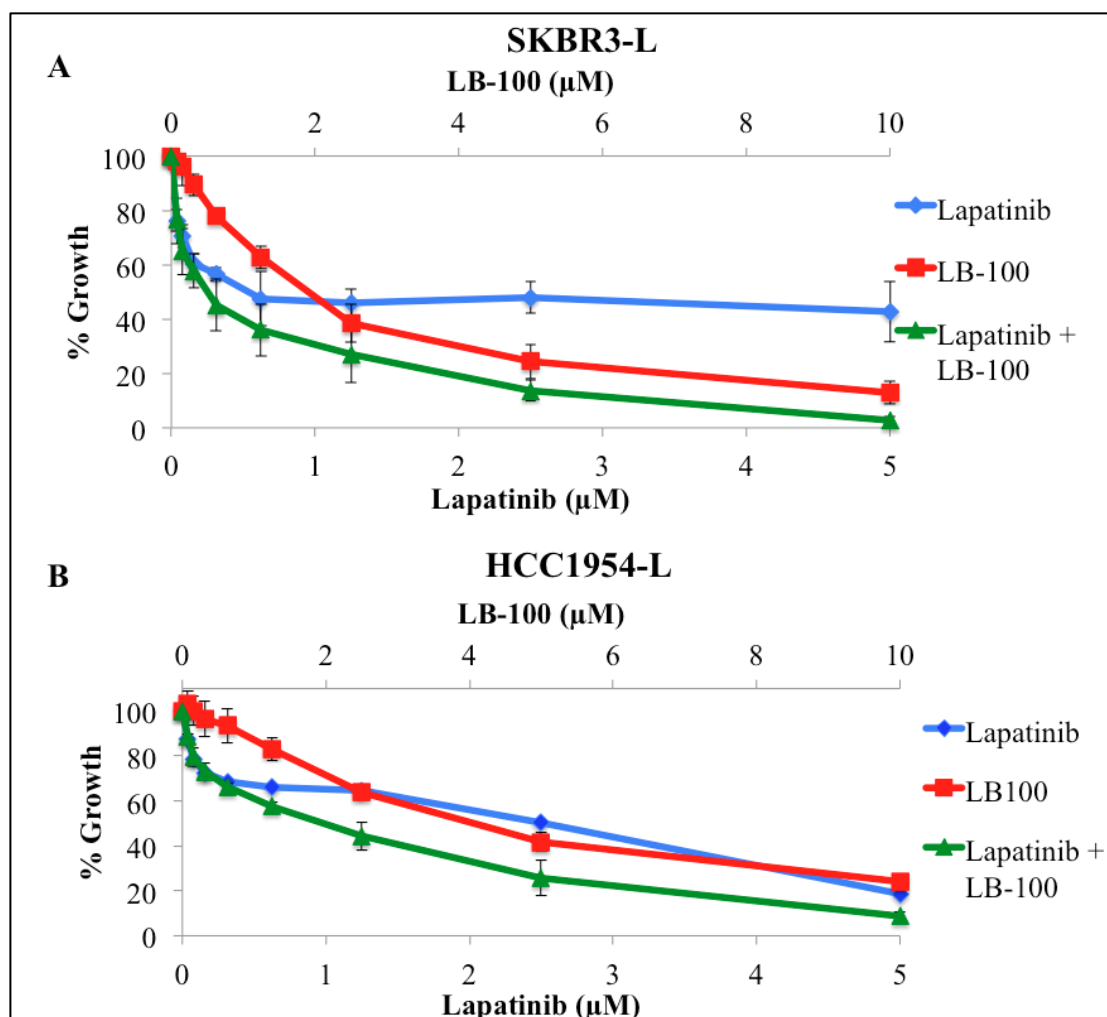
Figure 3-16: Proliferation of (A) SKBR3-L and (B) HCC1954-L treated with lapatinib, LB-100, or lapatinib plus LB-100 for 5 days was measured by acid phosphatase assay. Error bars represent standard deviation of biological triplicate experiments.

3.11 Assessment of sensitivity to LB-100 in 3D growth assays

In addition to examining the effect of LB-100 alone and in combination with lapatinib in 2D adherent culture, SKBR3-L and HCC1954-L cells were tested in 3D Matrigel growth assays (Figure 3-17). This is more representative of the *in vivo* tumour environment.

Both cells lines maintained lapatinib resistance in 3D conditions following 7-day treatment. The lapatinib IC$_{50}$ values for SKBR3-L and HCC1954-L cells were 1.02 ± 0.21 μM and 1.68 ± 0.37 μM. SKBR3-L displayed altered response to LB-100.

SKBR3-L cells were significantly less sensitive to LB-100 compared to adherent conditions (LB-100 IC_{50} value = 11.6 ± 0.46 µM versus 2.13 ± 0.2 µM in 2D assay). Lapatinib and LB-100 did not enhance response to lapatinib (CI value at ED_{50} = 0.95 ± 0.49). The LB-100 IC_{50} value was also reduced in HCC1954-L cells, 5.00 ± 0.12 µM compared to 2.31 ± 0.19 µM. However, lapatinib plus LB-100 was synergistic in HCC1954-L cells in 3D (CI value at ED_{50} = 0.51 ± 0.07). LB-100 IC_{50} values and CI at ED_{50} values are summarised in Table 3-5.
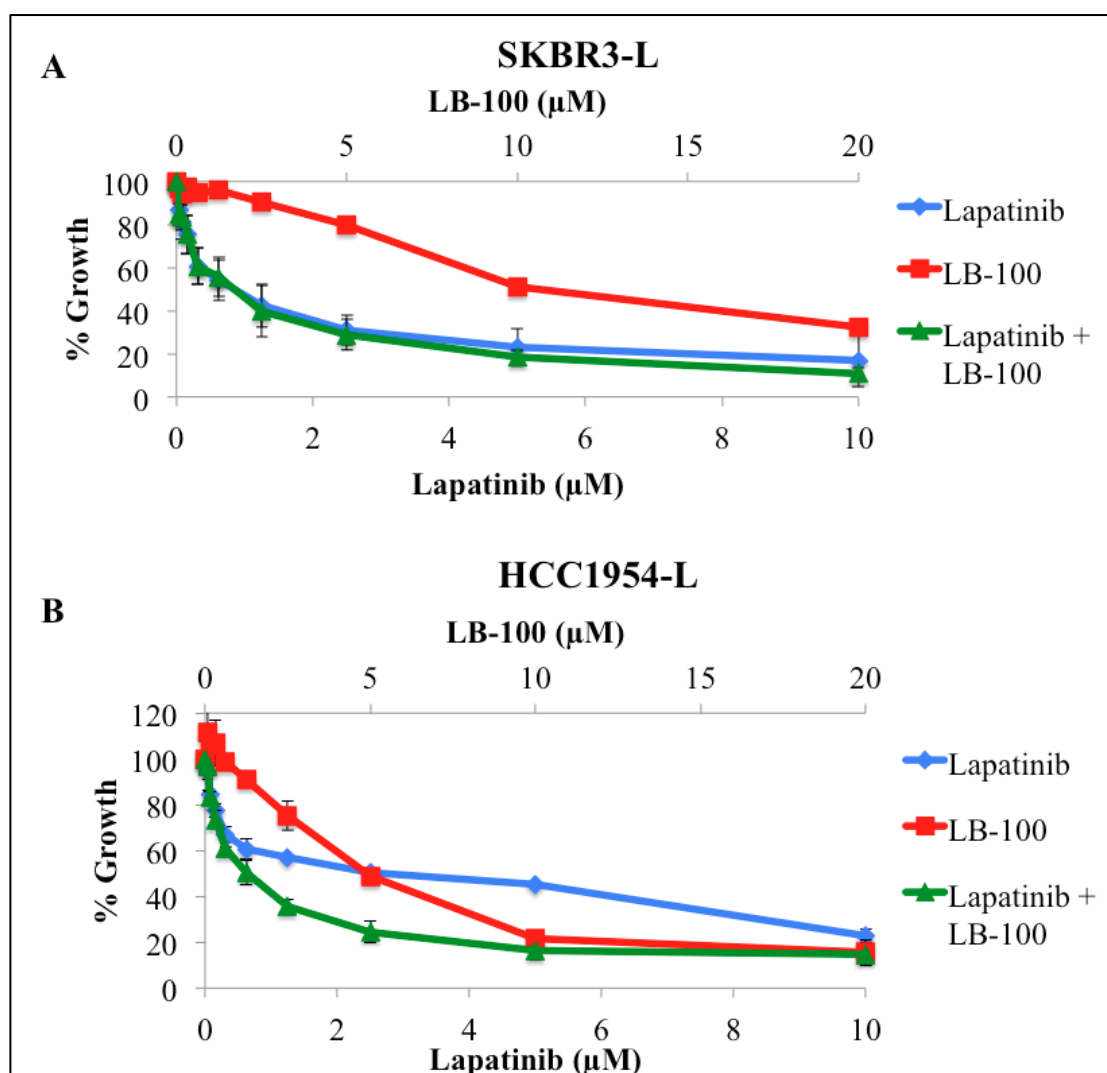
Figure 3-17: Proliferation of (A) SKBR3-L and (B) HCC1954-L treated with lapatinib, LB-100, or lapatinib plus LB-100 for 7 days in 3D growth conditions was measured by Presto blue assay. Error bars represent standard deviation of triplicate experiments.

Table 3-5: LB-100 response in SKBR3-L and HCC1954-L cells

	SKBR3-L	SKBR3-Par	HCC1954-L	HCC1954-Par
LB-100 IC$_{50}$ 2D assay (μM)	2.12 ± 0.20	5.38 ± 0.60	2.31 ± 0.19	5.32 ± 0.82
Lapatinib + LB-100 CI 2D assay	0.56 ± 0.13	-	0.68 ± 0.26	-
LB-100 IC$_{50}$ 3D assay (μM)	11.6 ± .046	-	5.0 ± 0.12	-
Lapatinib + LB-100 CI 3D assay	0.95 ± 0.49	-	0.51 ± 0.07	-

3.12 The effect of lapatinib and LB-100 on cell cycle progression

SKBR3-L and HCC1954-L cells were treated with lapatinib, LB-100, and lapatinib plus LB-100 for 48 h and cell cycle progression was analysed by flow cytometry (Figure 3-18 and Figure 3-19). Lapatinib alone caused G1 arrest in SKBR3-L (41.8 ± 2.5% versus 55.3 ± 8.7%) (p = 0.01) and HCC1954-L cells (28.2 ± 0.6% versus 37.2 ± 0.3%) (p = 1.6 x 10^{-5}). LB-100 increased the SubG1 population of SKBR3-L cells (p = 0.019). The combination of lapatinib and LB-100 did not significantly increase the Sub G1, apoptotic population compared to LB-100 alone (23/8 ± 8.5% versus 22.6 ± 6.1%) (p = 0.82). In the HCC1954-L cell line model, LB-100 significantly induced apoptosis (p = 0.046), which was enhanced in combination with LB-100 (Sub G1 with LB-100 = 10.7 ± 1.6% compared to 15.3 ± 2.2% with combination) (p = 0.046).
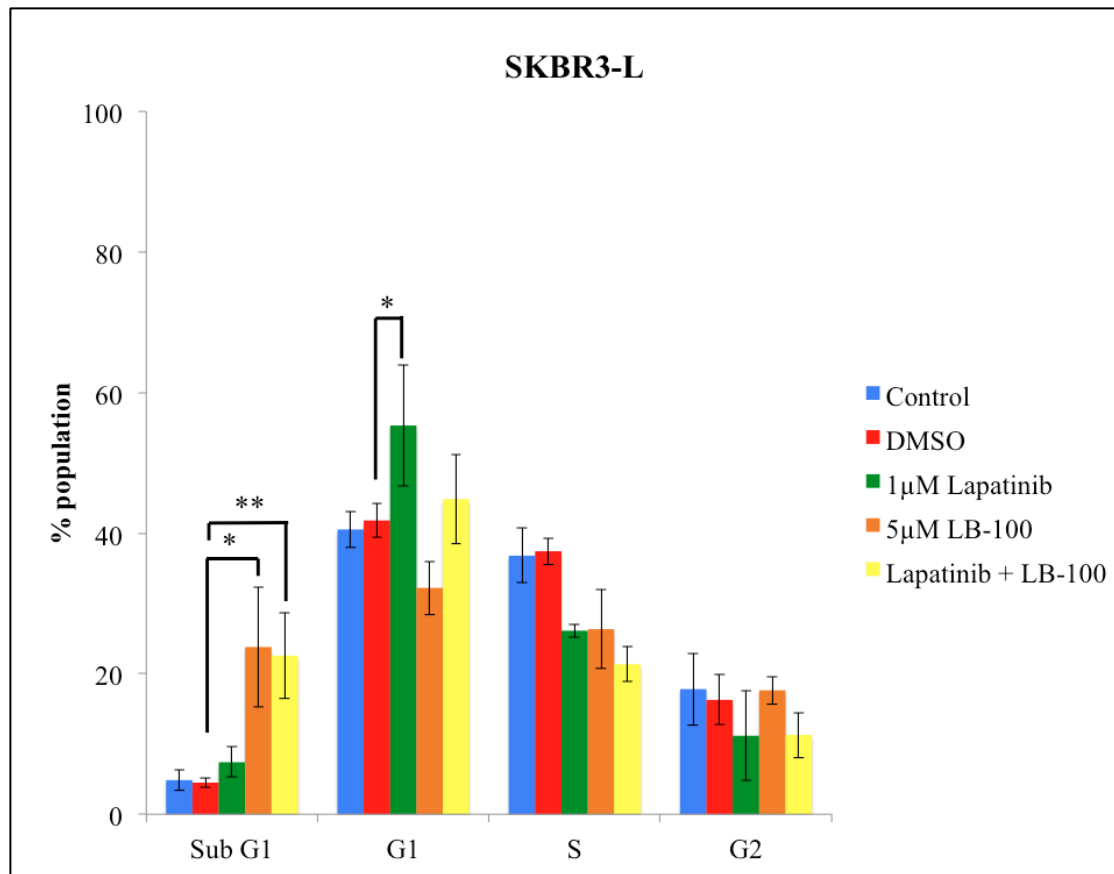
Figure 3-18: Percentage population of SKBR3-L cells treated with 1 μM lapatinib, 5 μM LB-100, lapatinib plus LB-100 in SubG1, G1, S, and G2 phases of the cell cycle. Cell cycle analysis was performed using the Guava EasyCyte and analysed using ModFit LT software. Error bars represent standard deviation of triplicate experiments. The Student's t test was used to determine statistical significance. * denotes p < 0.05, ** denotes p < 0.01.
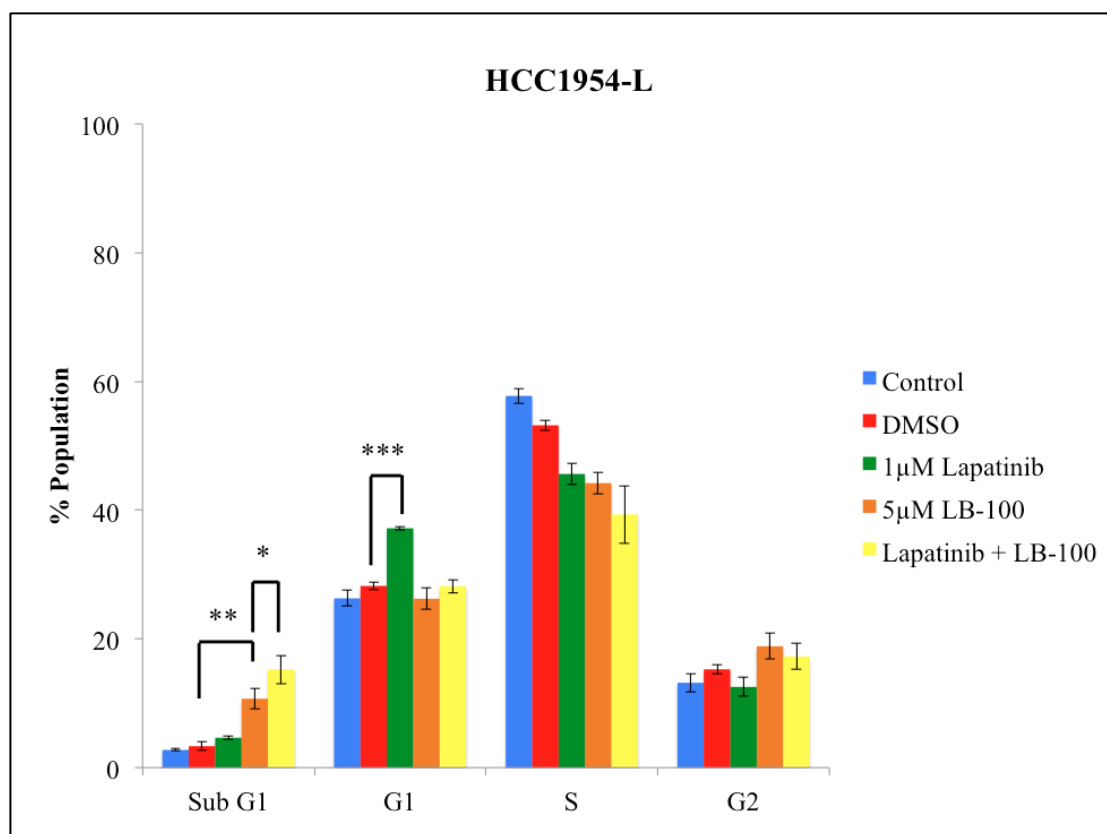
Figure 3-19: Percentage population of HCC1954-L cells treated with 1 μM lapatinib, 5 μM LB-100, lapatinib plus LB-100 in SubG1, G1, S, and G2 phases of the cell cycle. Cell cycle analysis was performed using the Guava EasyCyte and analysed using ModFit LT software. Error bars represent standard deviation of triplicate experiments. The Student's t test was used to determine statistical significance. * denotes $p < 0.05$, ** denotes $p < 0.01$, * denotes $p < 0.001$.**

3.13 The effect of LB-100 plus neratinib on lapatinib resistant cells

As discussed in Section 3.2.1, lapatinib resistant cell lines have reduced sensitivity to neratinib; and LB-100 has been shown to enhance response to lapatinib. It was hypothesised that LB-100 may enhance the effect of neratinib in lapatinib resistant breast cancer. Proliferation assays showed that neratinib plus LB-100 is synergistic in HCC1954-L cells with a CI value at ED_{50} of 0.61 ± 0.04 (Figure 3-20). Similar to lapatinib plus LB-100, neratinib plus LB-100 did not show an additive effect in the SKBR3-L cells (Figure 3-21).
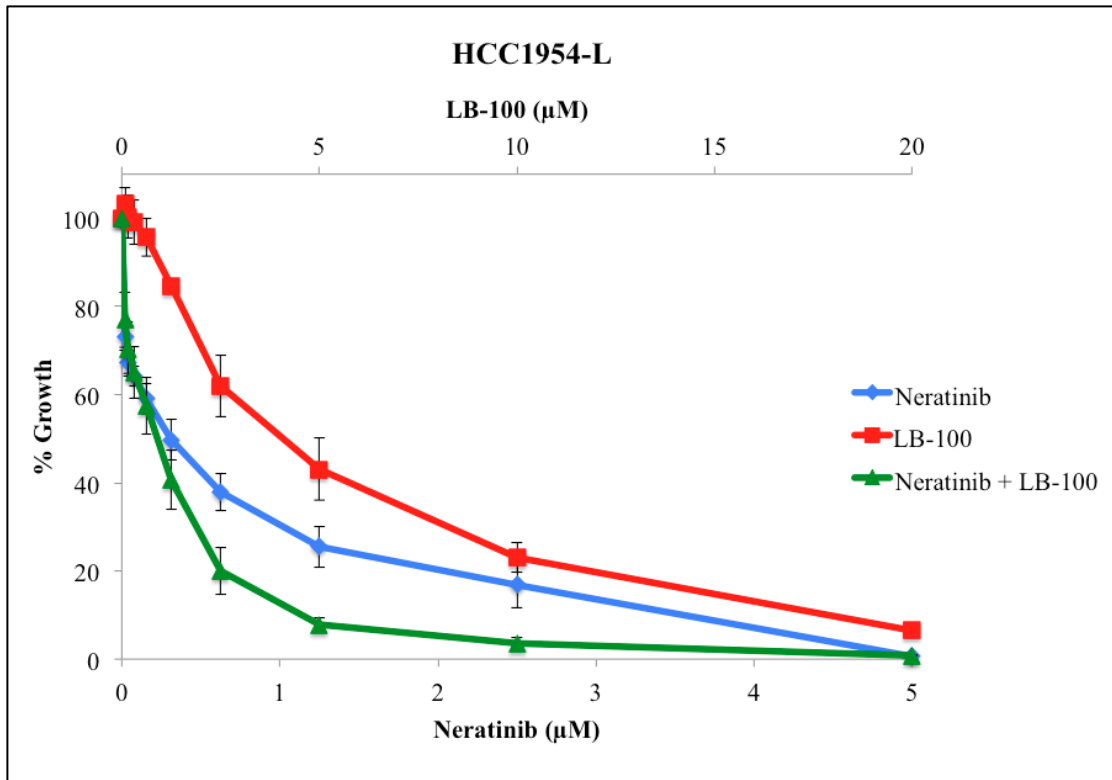
Figure 3-20: Proliferation of HCC1954-L treated with 0-5 *μ*M neratinib, 20 *μ*M LB-100, or neratinib plus LB-100 (1:4 ratio) for 5 days was measured by acid phosphatase assay. Error bars represent standard deviation of biological triplicate experiments.
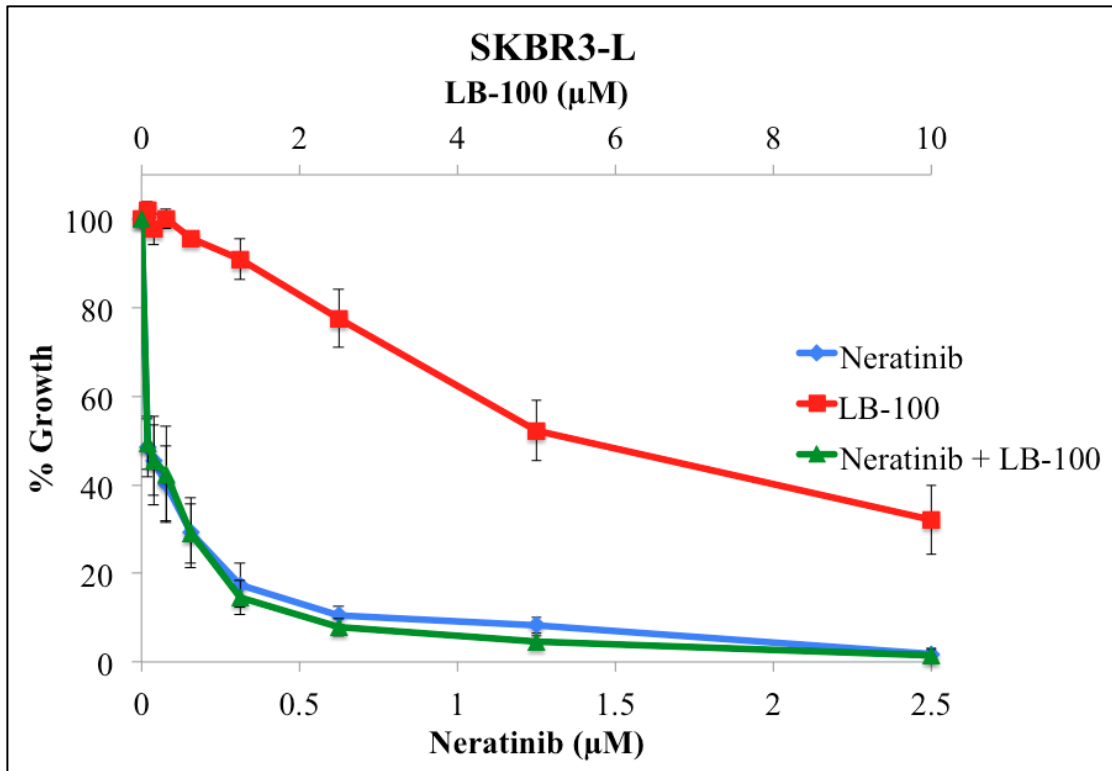
**Figure 3-21: Proliferation of SKBR3-L treated with 0-2.5 μM neratinib, 10 μM LB-100, or neratinib plus LB-100 (1:4 ratio) for 5 days was measured by acid phosphatase assay. Error bars represent standard deviation of biological triplicate experiments.**

3.15 Summary

Both acquired lapatinib resistant cell lines, SKBR3-L and HCC1954-L, were cross-resistant to the pan HER irreversible inhibitors, neratinib and afatinib, and to both monoclonal antibodies, trastuzumab and pertuzumab. This suggests that another therapeutic strategy other than targeting HER2 may be required to overcome resistance.

PP2A represents a potential novel therapeutic target to overcome lapatinib resistance. Previous work in our lab and the data generated in this study suggest that the development of lapatinib resistance may increase PP2A activity [154]. This increased PP2A activity contributes to the lapatinib resistant phenotype, as activating PP2A decreased lapatinib sensitivity in both parental cell lines. Lapatinib resistant cell lines were more sensitive to PP2A inhibition by okadaic acid and LB-100, compared to the parental cells. RPPA analysis showed that inhibition with lapatinib plus okadaic acid significantly reduced cell survival signalling in HCC1954-L cells, with down-regulation of EGFR, HER2 and HER3 phosphorylation and downstream signalling components such as phosphorylated Shc, GAB1, MEK 1/2, MAPK, and Src. LB-100 enhanced the effect of lapatinib in HCC1954-L cells in adherent and 3D conditions. LB-100 caused induction of apoptosis in both SKBR3-L and HCC1954-L cells, which was further enhanced with lapatinib in the HCC1954-L cell line. The combination of lapatinib and PP2A inhibition was also able to prevent the development of lapatinib resistance in short-term resistance assays. These data taken together suggest that the combination of lapatinib and LB-100 may be effective in both lapatinib resistant and lapatinib naive HER2-positive breast cancer.

4 Assessment of LB-100 in lapatinib resistant breast cancer *in vivo*

4.1   Introduction

The efficacy of LB-100 alone and in combination with lapatinib was assessed *in vitro* in 2D and 3D conditions in two lapatinib resistant cell lines (Section 3.10 and 3.11). The HCC1954-L cell line showed *in vitro* sensitivity to LB-100 and had a synergistic response to lapatinib plus LB-100. Similar responses were observed in 3D growth conditions. HCC1954 and HCC1954-L cells have been demonstrated to grow *in vivo* [283]. Therefore, HCC1954-L cells were chosen as the cell line model to progress to *in vivo* assessment of LB-100 in combination with lapatinib. LB-100 has been tested *in vivo* alone and in combination with chemotherapy and radiotherapy [259, 264, 265]. However, LB-100 has not been previously administered with HER2-targeted therapies.

The objectives of this study were (i) to optimise tumour growth conditions for the HCC1954-L cells in mice; (ii) to examine the safety of lapatinib and LB-100 *in vivo*; (iii) to determine if HCC1954-L cells retain the therapeutic targets of LB-100 and lapatinib; (iv) to determine if HCC1954-L cells maintain lapatinib resistance *in vivo;* and (v) to investigate the effect of LB-100 and lapatinib on HCC1954-L xenograft tumour growth *in vivo*.

4.2   Optimisation of HCC1954-L tumour growth

4.2.1   Pilot study to determine optimum cell number

In order to assess the optimum cell number for tumour growth, six 8-week old, female SCID mice were subcutaneously inoculated bilaterally with HCC1954-L cells, with 1 x 10^7 cells (higher cell number) injected on the left side and 5 x 10^6 cells (lower cell number) on the right. Cells were injected in a 1:1 ratio with extracellular matrix. Mice were 17.5 ± 0.5 g in weight at the time of tumour inoculation.

Tumours were allowed to develop and, when of sufficient size, were measured with calipers. Both cell numbers caused tumour growth (Figure 4-1). Individual tumour growth is represented in Figure 4-2 A and B. After 10 days, four of six mice had palpable tumours but were too small to measure. Mice implanted with the higher cell number had measurable tumours by day 21 (21.8 ± 7.6 mm^3, n = 5) and, after an additional 6 days, three of the lower cell number implant tumours were measurable

$(16.7 \pm 5.1 \text{ mm}^3)$. The average tumour volume 49 days after implantation was $248.3 \pm 25.6 \text{ mm}^3$ and $169.8 \pm 34.1 \text{ mm}^3$ for the higher and lower cell number, respectively. The take rate for both cell numbers was 5 out of 6 (83.3%). Although, the higher cell number implant tumours developed earlier and were larger by day 49, the lower cell number implant tumours surprisingly had a shorter doubling time. The tumour doubling time for the tumours implanted at higher cell number was 7.56 ± 0.99 days. The tumour doubling time for the lower cell number was 6.01 ± 1.01 days (Figure 4-3Figure 4-3). Doubling time was caluclated for each individual tumour as described in Section 2.16.
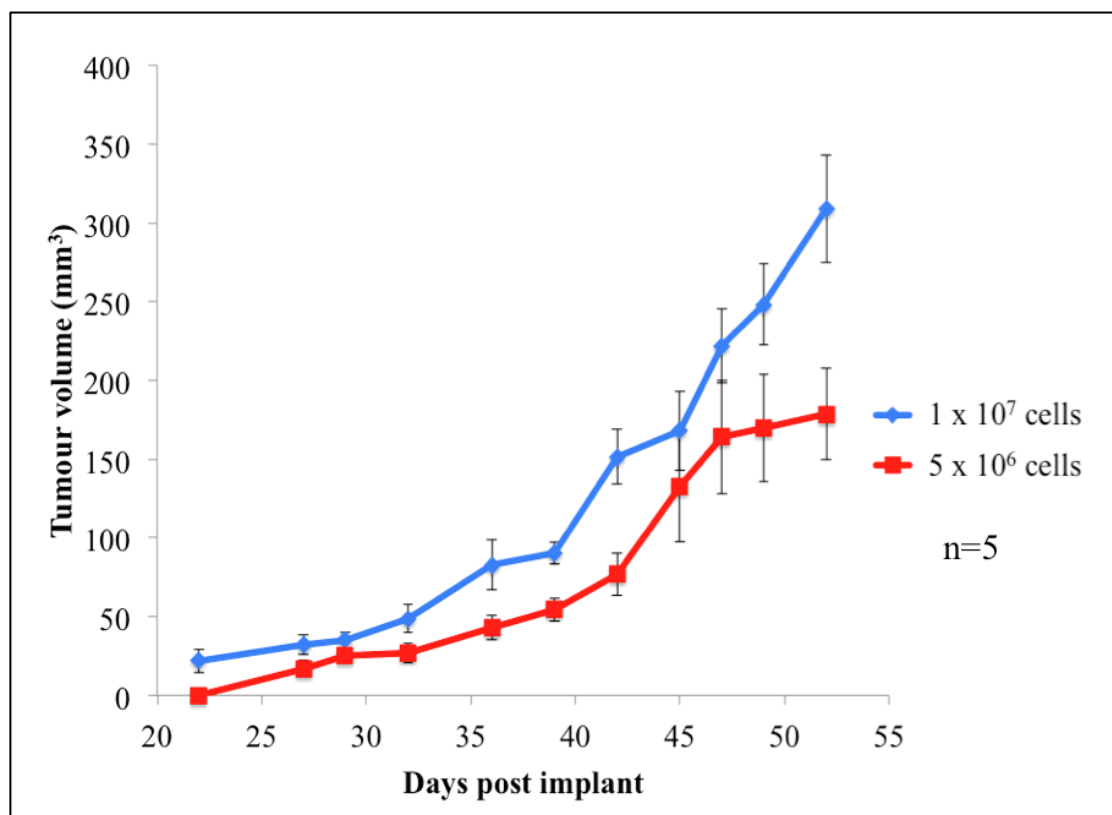
Figure 4-1: Average tumour growth of HCC1954-L cells in mice (n=5) bilaterally implanted with 1×10^7 cell implant (blue) and 5×10^6 cell implant (red). Tumour dimensions were measured by calipers and tumour volume was calculated as (Height x Width x Depth)/1.9. Error bars represent standard error of the mean of at least four tumours.
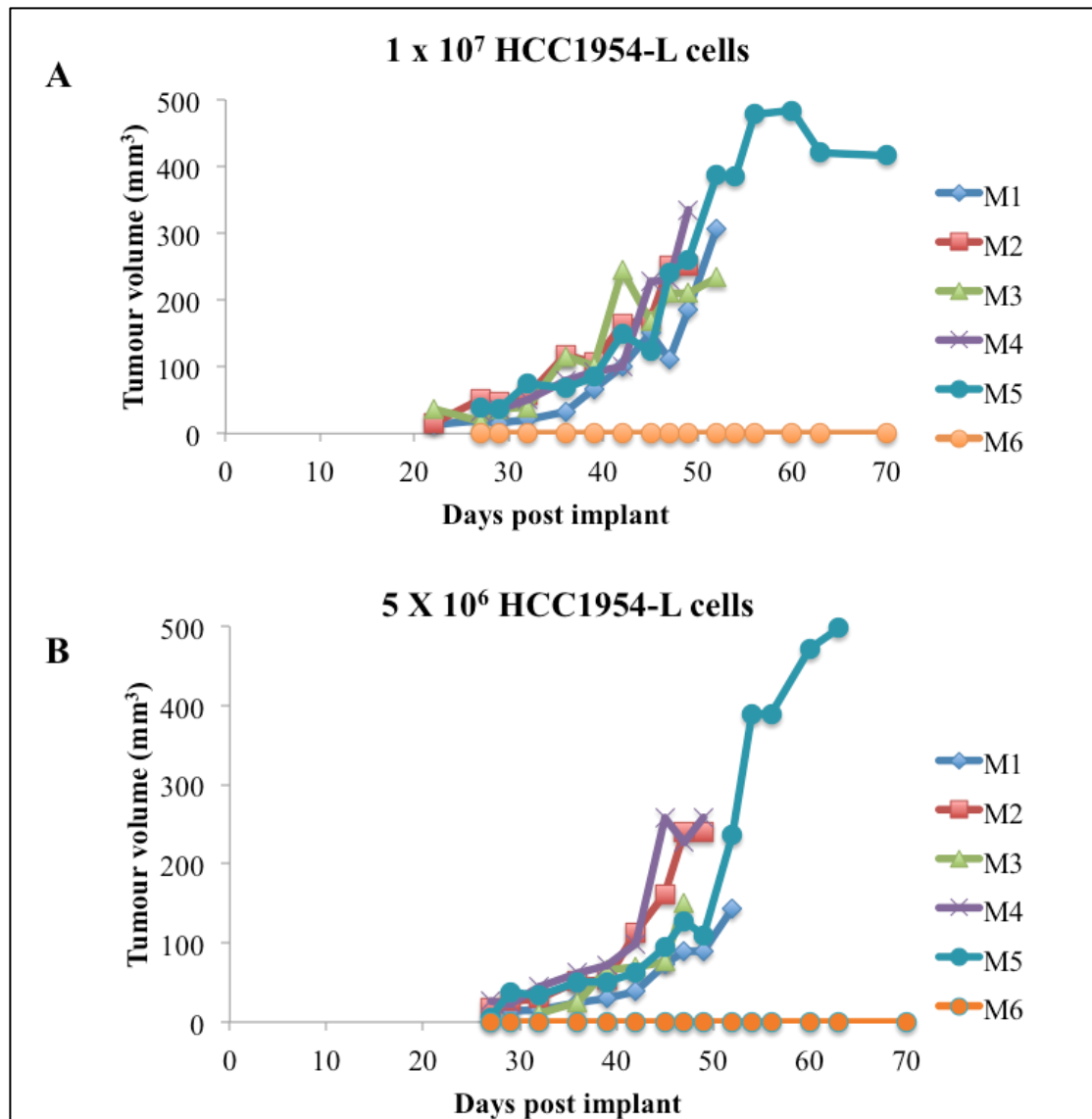
Figure 4-2: Individual growth rate of HCC1954-L cells in SCID mice implanted with (A) 1 x 10^7 and (B) 5 x 10^6 cells/mouse. Tumour dimensions were measured by calipers and tumour volume was calculated as (Height x Width x Depth)/1.9.
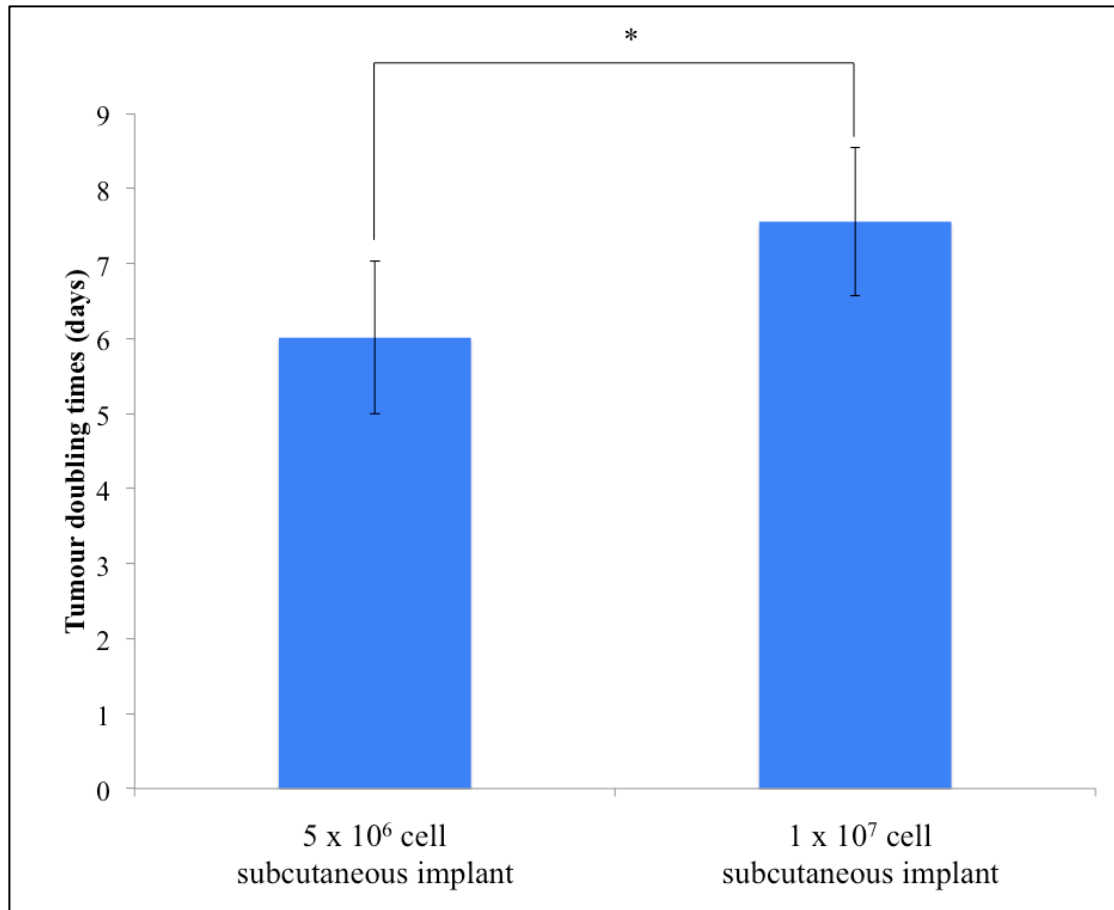
Figure 4-3: Tumour doubling time for 1 x 10^7 and 5 x 10^6 cell implant tumours. Doubling time was calculated as described in Section 2. Error bars represent standard deviation of five tumours. The Student's t test was used to determine statistical significance. * denotes p ≤ 0.05.

4.2.2 The effect of tumour burden on general health

The health of all mice was monitored daily and mouse body weight was used as an indicator of overall health of the animal. Mice with bilateral tumour implantation were weighed twice weekly and no significant effect of implantation of cells and growth on mouse weight was observed. Mice were 17.5 ± 0.5 g at implantation and 19.1 ± 1.0 g at day 47 (Figure 4-4).
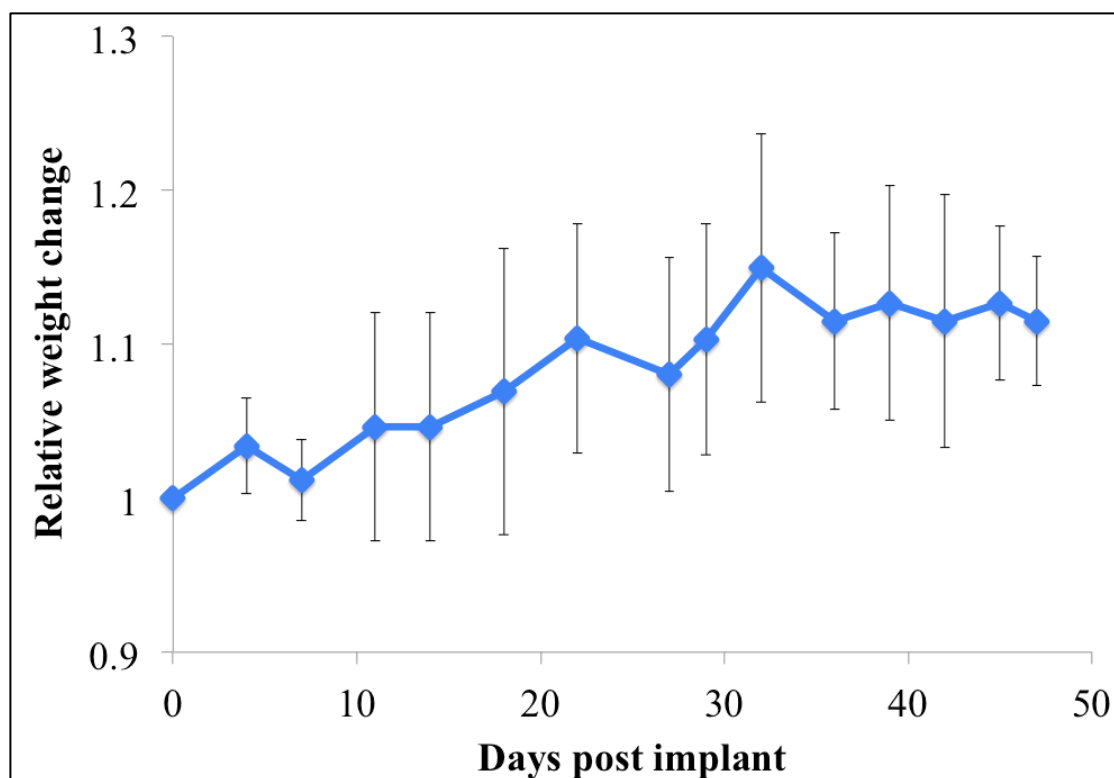
Figure 4-4: The weight of each mouse was normalised to its weight at tumour implantation and measured throughout the study. Error bars represent standard deviation (n = 5).

To assess the safety of the combination of lapatinib plus LB-100 six mice on study were randomized into two groups; group A were untreated and group B were administered lapatinib daily Monday to Friday and LB-100 Monday, Wednesday, and Friday (Table 4-1). Treatment began on day 47.

Table 4-1: Randomisation of animals for treatment groups.

Groups for pilot study of combination	
Control	Treatment
M1	M3
M5	M4
M6	M2

However, due to skin ulceration which occurred predominantly in the mice implanted with 1×10^7 cells (Figure 4-5), the pilot study had to be terminated early and treatment

was stopped after just 6 days. Skin ulceration can occur when tumour cells or tissue are implanted subcutaneously. This is seen by a loss of skin integrity, hair loss over the tumour, and skin breakage. This can be due to large tumour size, fast tumour growth, or changes in internal tumour pressure [284].

Skin ulceration began on Day 36 post implantation in M3. All of the higher cell number tumours and one of the lower cell number tumours developed skin ulceration. When the skin broke over the tumours, the animal was culled for humane reasons. The first mouse culled due to ulceration was on day 52 (M2) and three more were culled on day 53. The study was terminated on day 70 with one animal remaining.
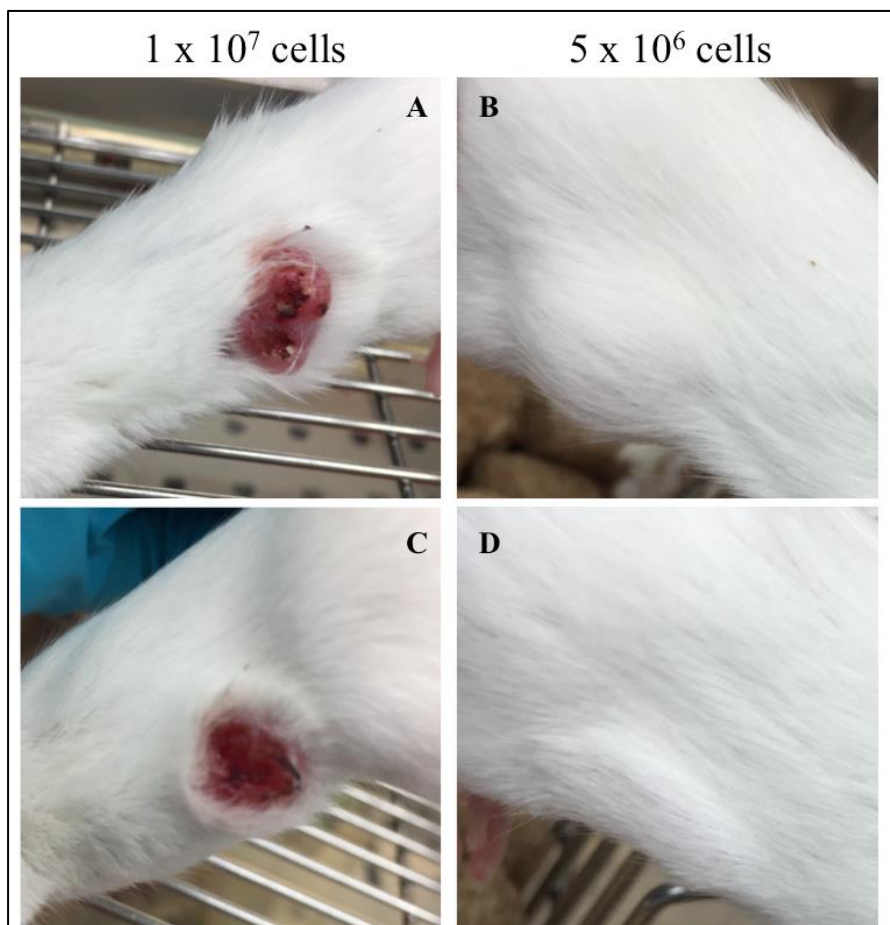
Figure 4-5: Images of skin ulceration and hair loss on mice implanted with 1 x 10^7 cells (A and C) and 5 x 10^6 cells (B and D). A and B are images of M4, C and D are of M2.

This pilot study confirmed the tumorigenesis of the HCC1954-L cells but suggested that 5 x 10^6 cells may be a better cell number for implantation due to the skin ulceration occurring in of all the mice implanted with 1 x 10^7 cells. However, the average tumour volume achieved at day 53, in the five mice with measurable tumours, was 178.7 ± 29.3 mm^3. This would be too small to assess any differences in tumour size with treatment in a drug efficacy study. Therefore, an additional pilot study was proposed to further assess implantation of 5 x 10^6 cells and to determine if skin ulceration would occur at a larger tumour size in mice implanted with 5 x 10^6 cells.

4.2.3   Pilot study to test 5 x 10^6 cell subcutaneous implantation

Six female SCID mice were injected subcutaneously in the flank, with 5 x 10^6 HCC1954-L cells, in a 1:1 ratio with extracellular matrix. At implantation, the animals were on average 21.5 ± 0.5 g in weight. 15 days after implantation, measurable tumours developed (Figure 4-6). The average volume of these tumours was 80.9 ± 8.5 mm^3. Unfortunately, skin ulceration again occurred. This time after 21 days, ulceration occurred in three of the six mice inoculated, with a further mouse developing ulceration on day 22. Therefore, this pilot study was ended as humane endpoints were reached in 4 of 6 animals, with final average tumour volumes of 128.0 ± 38.8 mm^3.

It was concluded from these two pilot studies that subcutaneous injection of HCC1954-L cells at either 1 x 10^7 or 5 x 10^6 cells/implant was not recommended for drug efficacy testing.
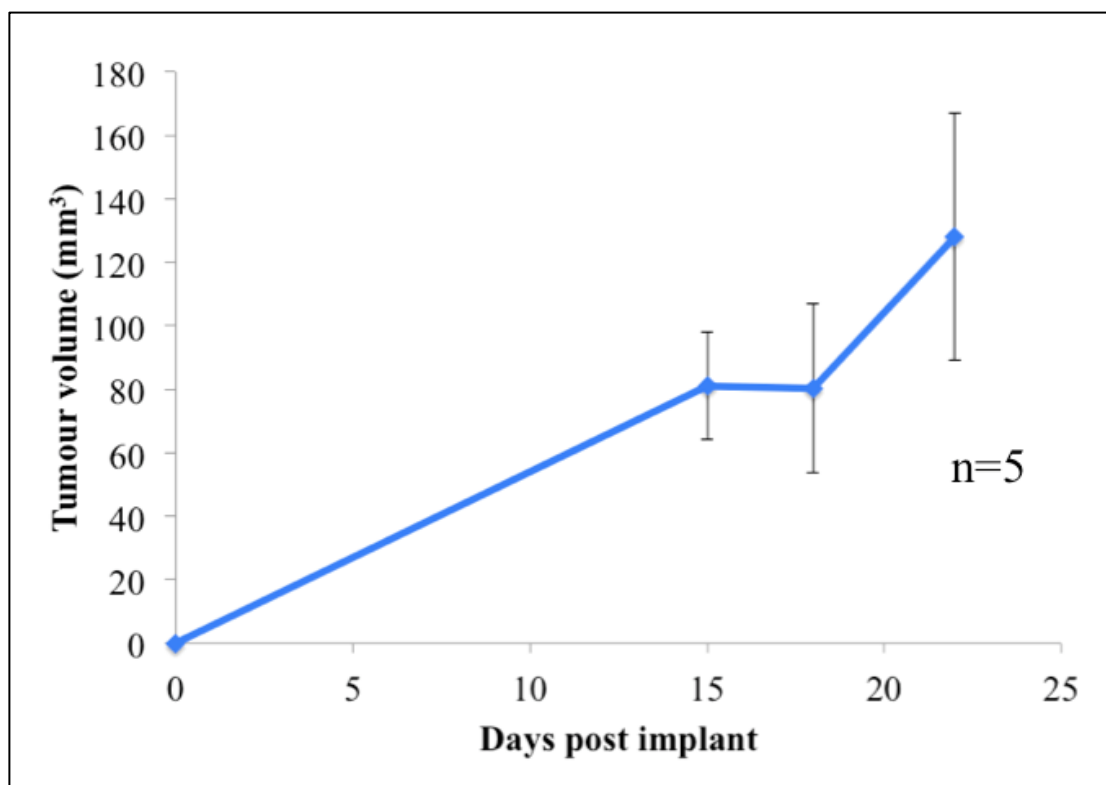
Figure 4-6: Individual growth rate of HCC1954-L cells in SCID mice (n=5) unilaterally implanted with 5 x 10^6 cells/mouse. Tumour dimensions were measured by calipers and tumour volume was calculated as (Height x Width x Depth)/1.9.

### 4.2.4 Mammary fat pad implantation of HCC1954-L cells

As skin ulceration limited the achievable tumour volumes in the previous pilot studies, the site of implantation, the cell number, and the strain of mouse were altered. The site of implantation was changed to the mammary fat pad. It was hypothesised that moving the site of implantation further from the skin would reduce the occurrence of skin ulceration. The mammary fat pad also provides a milieu more reflective of the tumour microenvironment in patients [285]. As the change of implantation involved injection of cells directly into a small organ, the cell number and injection volumes were decreased to 5 x 10^5/50 µL per injection. The strain of mouse was changed from SCID to BALB/c nude mice. This was due to a recommendation from collaborators who reported a lower frequency of skin

118

ulcerations when HCC1954 cells were implanted in the mammary fat pad of BALB/c nude (personal communication, Dr Ian Miller and Prof Annette Byrne, Royal College of Surgeons in Ireland).

Mice implanted with HCC1954-L in the mammary fat pad developed xenograft tumours (Figure 4-7 and 4-8), with measurable tumours after 13 days (M1 and M3, average tumour volume = 2.9 ± 1.2 mm^3). By day 59, four of six mice were tumour bearing (Figure 4-9 and 4-10). Therefore, the tumour take rate was 66.7%. One additional tumour developed at day 90 (tumour volume = 40.4 mm^3). However, this tumour was not located in the mammary fat pad and was subcutaneous. This was most likely due to inaccurate injection. This tumour was excluded in mammary fat pad tumour growth analysis. The maximum average achieved was 545.0 ± 190.1 mm^3 at day 85. This includes the largest tumour achieved, 1074.5 mm^3, in M6. This mouse was culled as the tumour height (14.7 mm) approached the maximum allowed limit of 15 mm. Individual mammary fat pad HCC1954-L tumour growth is represented in Figure 4-10. The average tumour doubling time was 7.6 ± 2.6 days.

Skin ulceration did not occur on any tumours. However, hemorrhagic areas occurred on the largest tumour (M6) (Figure 4-11), which occurred at day 83 as the tumour approached size limits. These tumours were highly vascularised. This can especially be observed in Figure 4-11.

Figure 4-7: Images of individual mammary fat pad tumours on day 76.
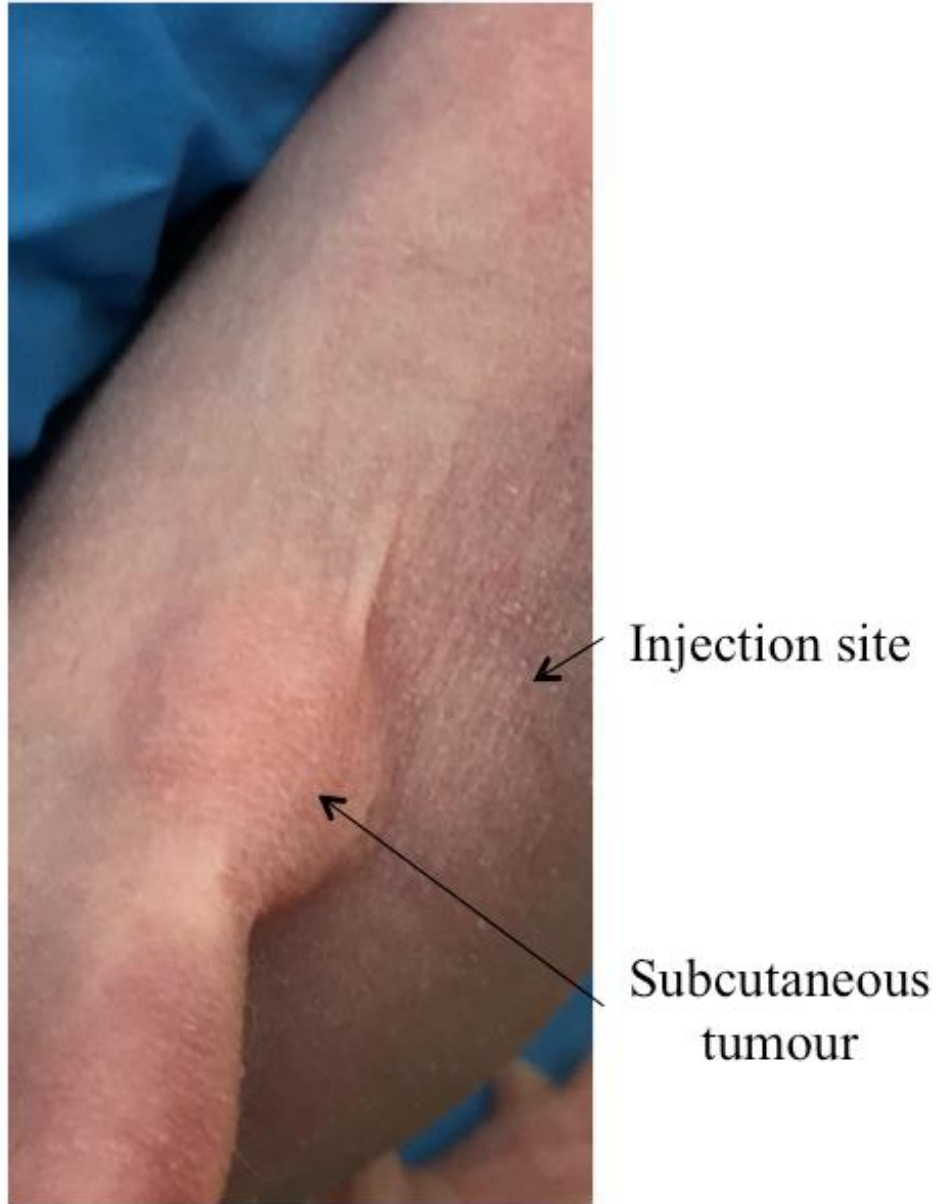
Figure 4-8: Image of HCC1954-L tumour that developed subcutaneously rather than in the mammary fat pad.
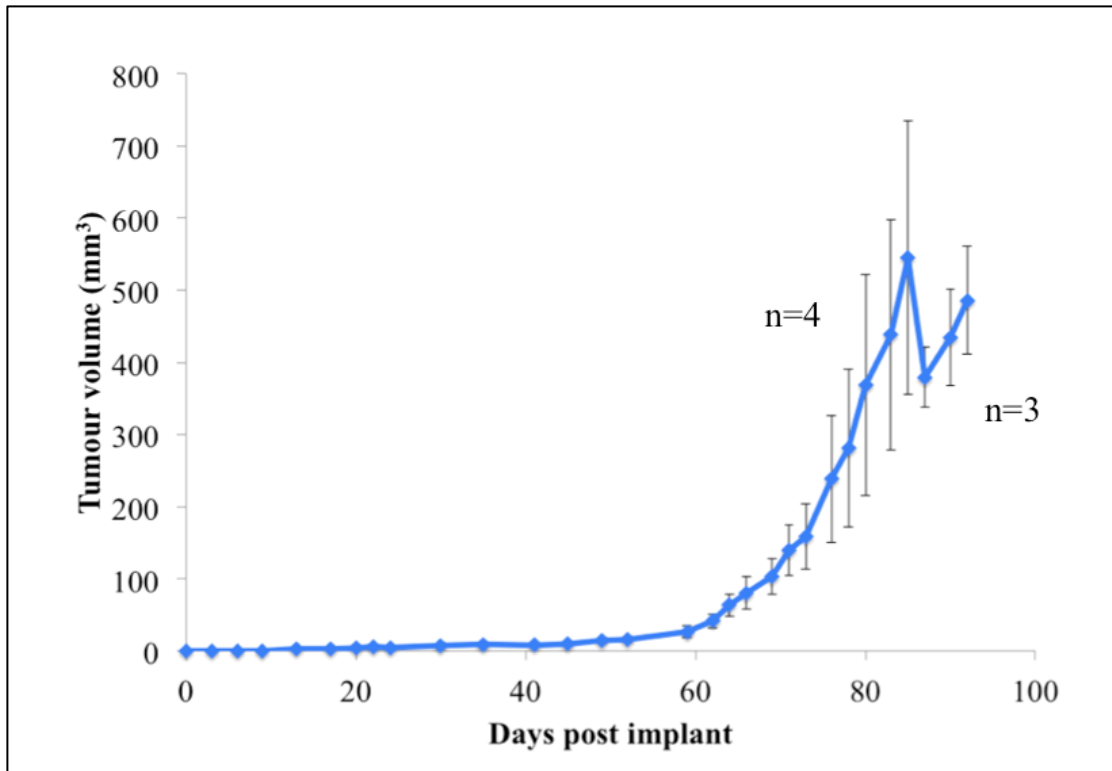
Figure 4-9: Average tumour volume of mammary fat pad implanted HCC1954-L cells measured by calipers. Error bars represent standard error of the mean, n = 4 up to day 85; n = 3 from day 87 to 92.
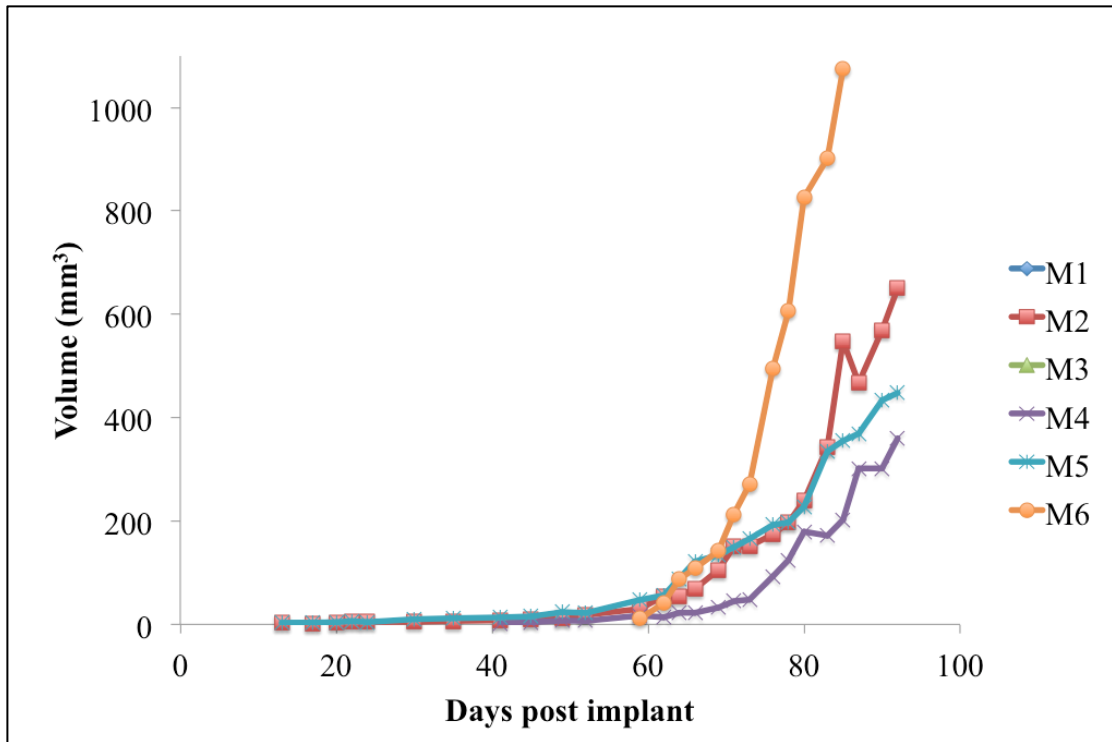
Figure 4-10: Individual tumour volumes of mammary fat pad implanted HCC1954-L cells.

M6 at day 83

Figure 4-11: Image of HCC1954-L mammary fat pad tumour of M6, 83 days post-implantation. Hemorrhagic areas observed in black regions on tumour.

4.3 HCC1954-L cells maintain lapatinib resistance *ex vivo*

After euthanasia, tumours were retrieved and part of the tumour was taken for primary cell culture. Two of the four tumours taken for primary culture, continued to grow *ex vivo* (M1 and M3) (Figure 4-12). Both samples were tested by 5-day acid phosphatase assay for sensitivity to lapatinib, LB-100, and the combination of lapatinib and LB-100 (Figure 4-13Figure 4-13). Both cell populations maintained resistance to lapatinib. The IC_{50} values for M1 and M3 were 2.23 µM and 1.39 µM, respectively. This is similar to IC_{50} values achieved in previous 2D and 3D assays of HCC1954-L cells. Similarly, *ex vivo* HCC1954-L cells maintained a similar response to LB-100. LB-100 IC_{50} values were 5.28 µM and 3.81 µM. Importantly, the synergy previously observed with lapatinib and LB-100 was replicated with the *ex vivo* HCC1954-L cells, with CI values of 0.67 and 0.79.
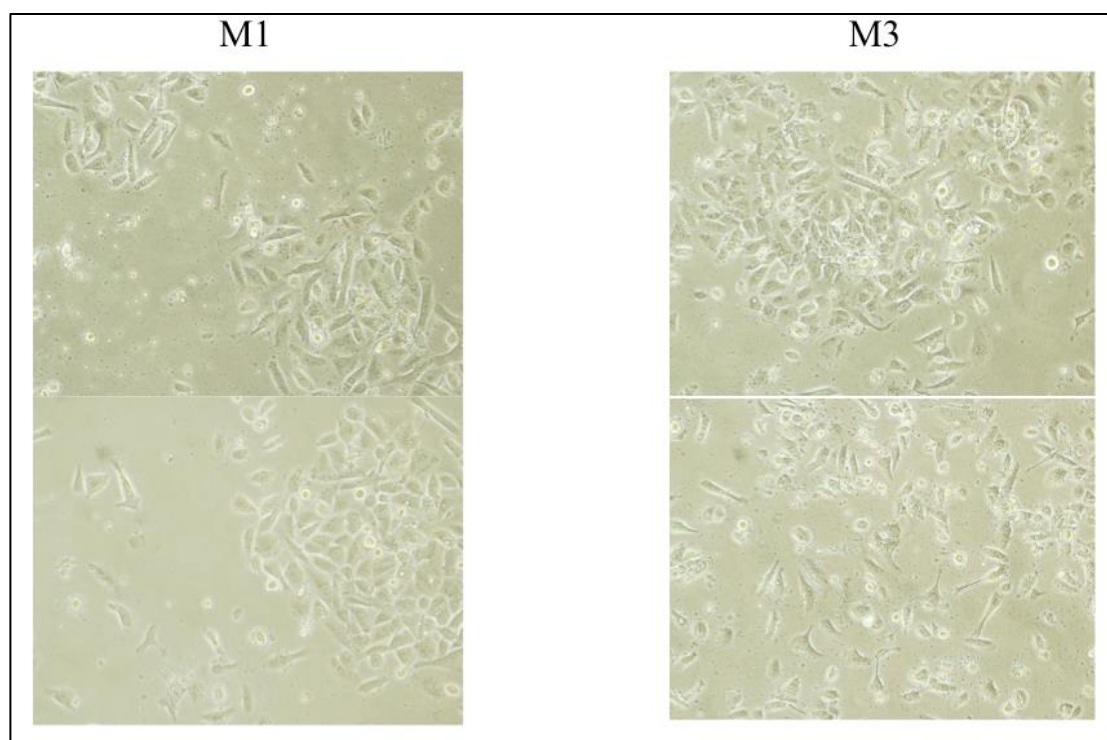
Figure 4-12: Representative images of *ex vivo* HCC1954-L cells in culture after tumour retrieval. Images were taken at 200X magnification.

124
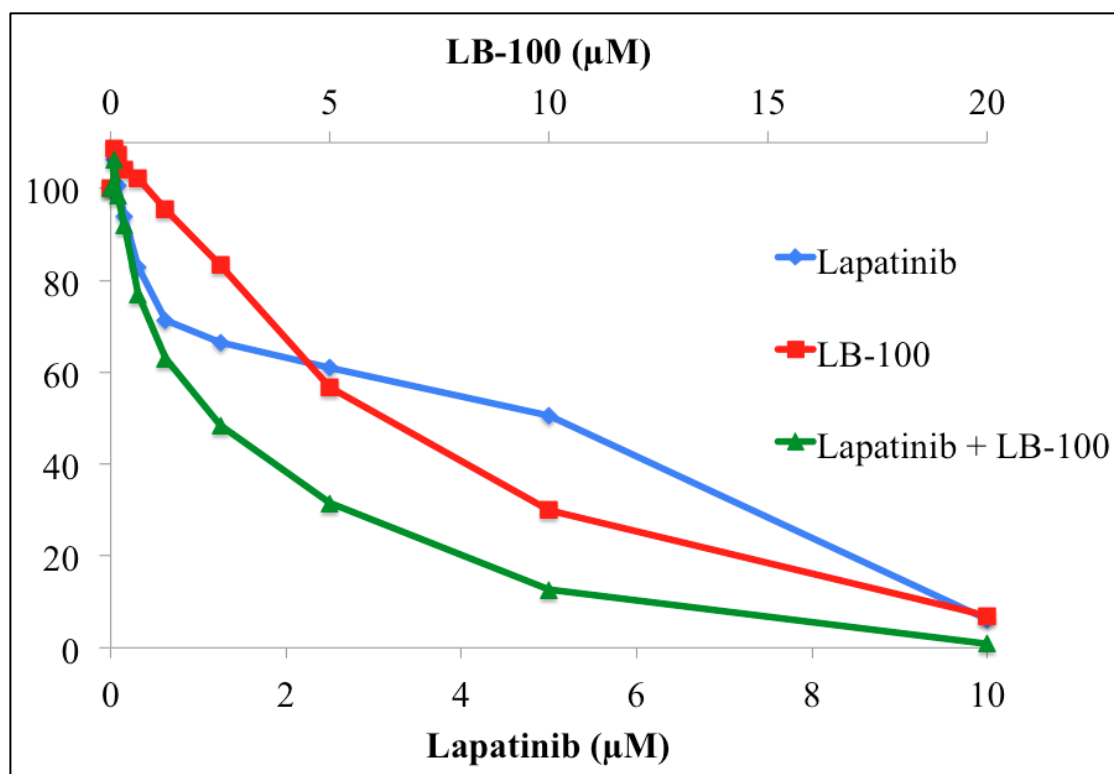
Figure 4-13: Sensitivity of the *ex vivo* HCC1954-L cells to lapatinib, LB-100, and lapatinib plus LB-100 was assessed by 5-day acid phosphatase assay. The data shown is an average of two *ex vivo* samples.

4.4 Assessment of the side effects of LB-100 and lapatinib *in vivo*

Due to the problems with ulceration and the requirement to change mouse strain and implantation site a decision was made to perform a separate toxicity study using six BALB/c nude mice, which were divided into two groups (untreated control and lapatinib plus LB-100 treatment group). The three mice on treatment received lapatinib and LB-100 for 45 days. All six mice were checked for adverse events and weighed three times per week. The lapatinib plus LB-100 did not have a significant effect on body weight (p = 0.42) (Figure 4-14 and Figure 4-15). As lapatinib inhibits both HER2 and EGFR, it has been shown to cause skin rashes, redness or peeling of skin, and hair loss [286, 287]. Repeated intra-peritoneal injection can also cause skin necrosis at the site of injection [288]. Therefore, mice were monitored for signs of skin damage. To minimise damage from repeated intra-peritoneal injection, the injection site was alternated between left and right sides for each injection. All mice

on treatment had no signs of necrosis or skin rashes (Figure 4-16). LB-100 has been shown to cause dyspnea (shortness of breath) in humans. No breathing difficulties were observed in mice treated with LB-100 and lapatinib.
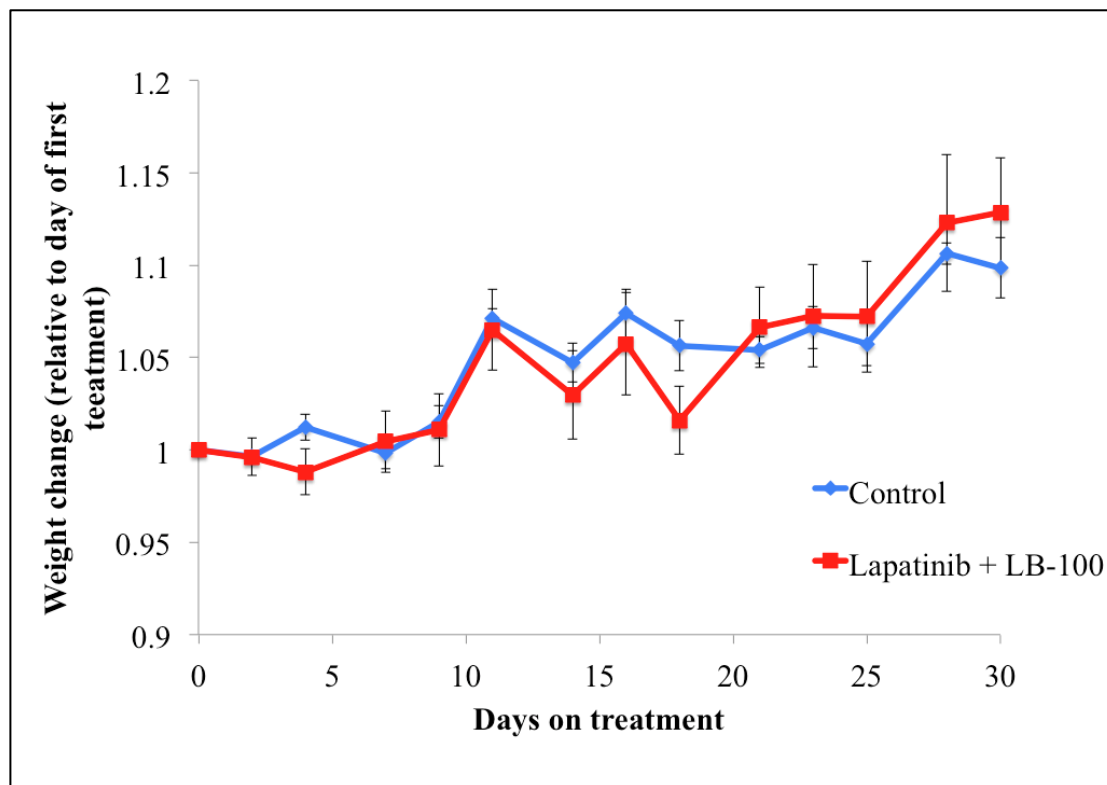
Figure 4-14: Relative weight change of BALB/c nude mice treated Monday – Friday with LB-100 and Monday, Wednesday, and Friday with lapatinib (Red) or untreated (Blue). Error bars represent standard error of the mean with three animals per group. The Student's t test was used to determine statistical significance.
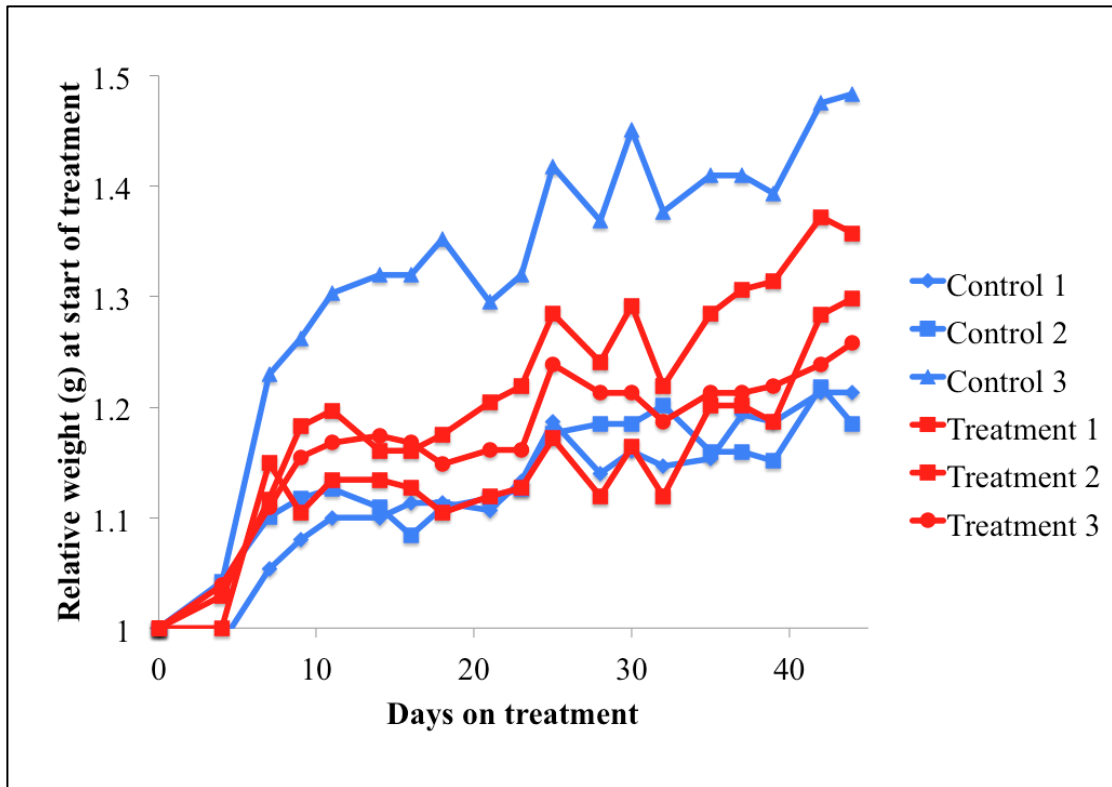
Figure 4-15: Relative weight change of individual BALB/c nude mice treated Monday – Friday with LB-100 and Monday, Wednesday, and Friday with lapatinib (Red) or untreated (Blue).
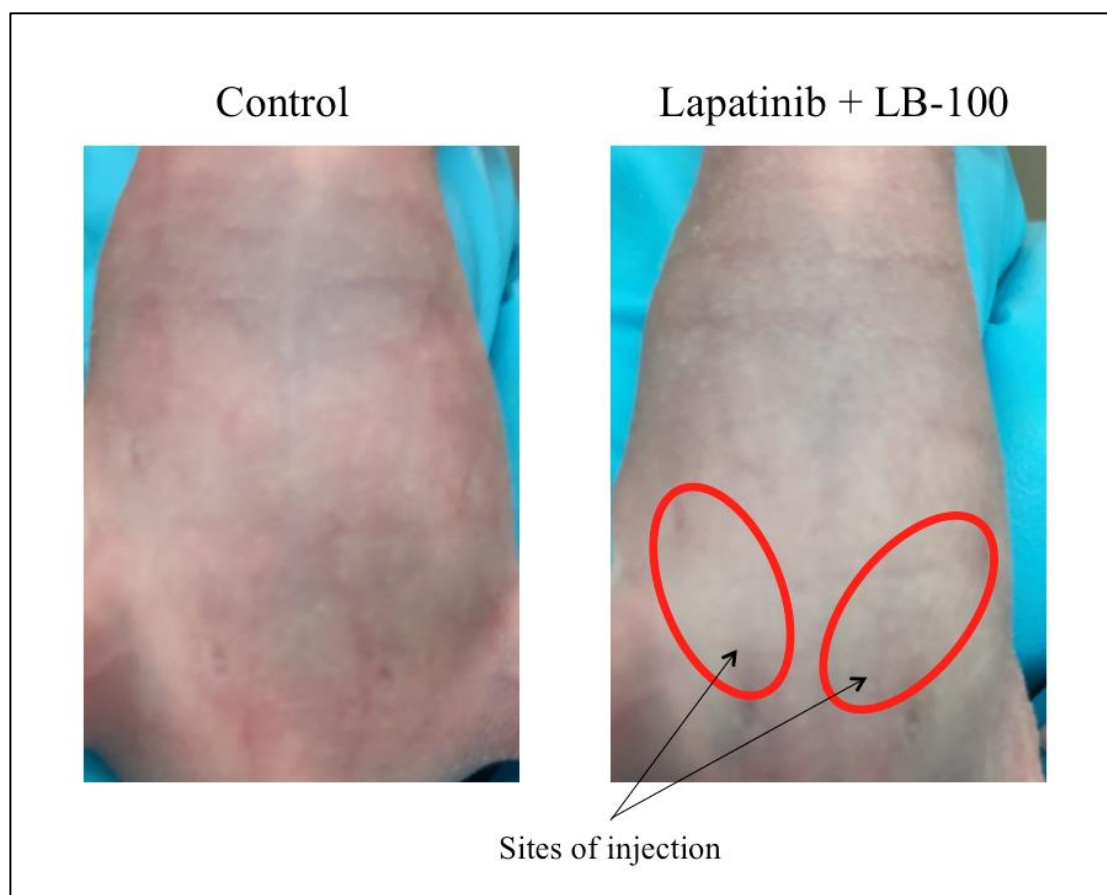
Figure 4-16: Images representative of the abdomen of control and treated mice taken after 39 days on treatment.

4.5 Pharmacodynamic effects of lapatinib and LB-100 on HCC1954-L cells *in vivo*

Prior to the early termination of the first pilot study of subcutaneous implantation of HCC1954-L cells, animals were divided into two groups of three with one group receiving lapatinib plus LB-100. Treatment was ended after six days and no effect on tumour growth was observed. However, tumours were retrieved post-mortem and analysed for changes in total and phosphorylated levels of eEF2, as a marker for PP2A activity. This was also compared to basal levels in HCC1954-L cells grown *in vitro* (Figure 4-17). Total levels of eEF2 were unchanged between *in vitro* grown HCC1954-L and HCC1954-L cells *in vivo*. Phosphorylated eEF2 was slightly decreased in *in vivo* cells. The tumour from a mouse treated with lapatinib and LB-100 showed a significant increase in phospho-eEF2 levels compared to an untreated

HCC1954-L tumour sample. In order to to ensure that the protein expression *in vivo* was due to HCC1954-L cells, the expression of human mitochondria was examined by immunohistochemistry (Figure 4-18). HCC1954-L tumour tested positive for human mitochondria similar to cells grown *in vitro*. *In vivo* samples showed some positive staining in negative controls, which was due to sample preparation.
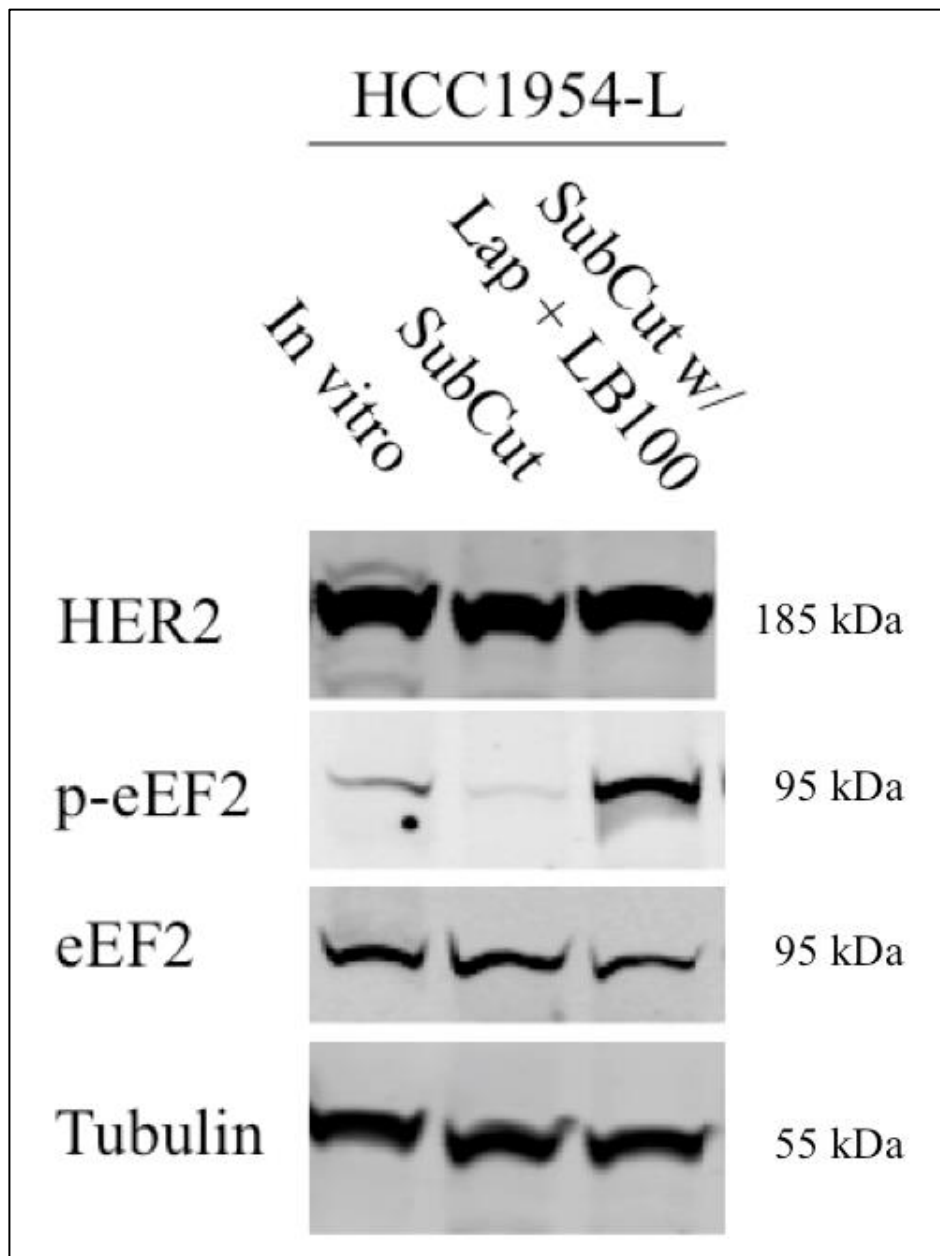
Figure 4-17: Western blotting of total and phosphorylated eEF2 levels in HCC1954-L cells grown *in vitro*, *in vivo*, and *in vivo* with lapatinib plus LB-100 treatment. Tubulin was used as a loading control. Blot shown representative of individual *in vivo* tumours.
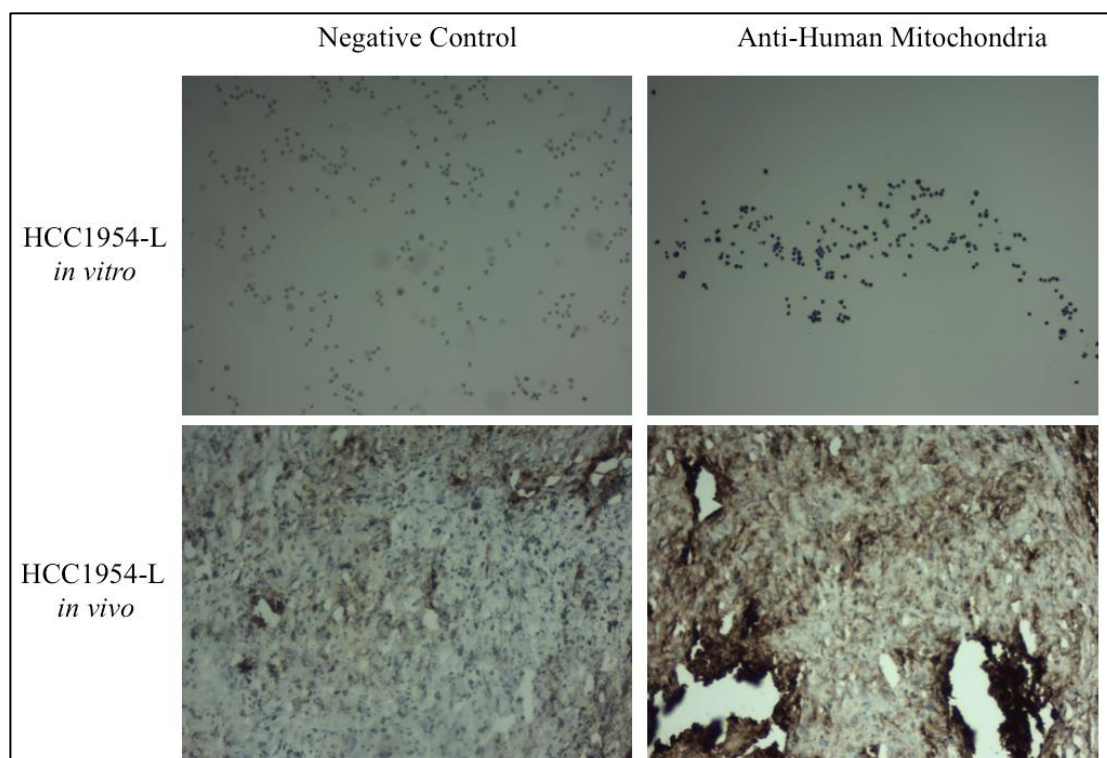
Figure 4-18: Immunohistochemistry of HCC1954-L cells grown *in vitro* and *in vivo* in SCID mice for human mitochondria (200X magnification).

4.6 Summary

HCC1954-L cells were demonstrated to grow *in vivo* following both subcutaneous and mammary fat pad implantation. However, skin ulceration limited the length of study and achievable tumour volumes following subcutaneous implantation. All mice implanted with 1 x 10^7 cells and one mouse implanted with 5 x 10^6 cells ulcerated in the bilateral pilot study. The 5 x 10^6 cell implantation was repeated. However, ulceration also occurred before tumour volumes, which would allow for the observation of drug effect changes, were reached. Importantly, implantation in the mammary fat pad of BALB/c nude mice did not result in the development of skin ulceration.

The combination of lapatinib and LB-100 was shown to be safe in BALB/c nude mice on long-term treatment, with no significant side effects observed. Preliminary data suggest that LB-100 is active *in vivo* and inhibits PP2A activity in HCC1954-L tumours.

Thus the conditions for evaluating the efficacy of lapatinib plus LB-100 *in vivo* have been optimised and this will be performed using HCC1954-L cells mammary fat pad xenografts in BALB/c nude mice.

5 PP2A in innate resistance to HER2-targeted therapy

5.1 Introduction

As Chapter 3 showed, PP2A is a potential mediator of lapatinib resistance in two lapatinib-resistant HER2-positive breast cancer cell lines. Clinically, lapatinib resistance can emerge after an initial response to lapatinib. However, HER2-positive breast cancer tumours can also have *de novo* resistance to lapatinib. Therefore, the possible role for PP2A in innate lapatinib resistance merited investigation. In this study, a panel of HER2-positive breast cancer cell lines with varying sensitivities to HER2-targeted therapies were examined for sensitivity to okadaic acid and LB-100 and expression levels of PP2A subunits.

5.2 HER2-positive breast cancer cell line panel response to lapatinib and trastuzumab

A panel of HER2-positive breast cancer cell lines was assessed for lapatinib by 5-day acid phosphatase proliferation assay (Table 5-1). Of the 10 cell lines tested, three cell lines were classified as lapatinib resistant, with an IC_{50} value greater than 1 µM. Trastuzumab sensitivity was taken from [184] (Table 5-2). Six of the 11 cell lines were classified as trastuzumab resistant using the fold change cut-off of $\leq$ 1.2. Response to lapatinib was shown to correlate with response to trastuzumab (p = 0.004) (Figure 5-1).

Table 5-1: Lapatinib IC$_{50}$ values of a panel of HER2-positive breast cancer cell lines.

Lapatinib IC$_{50}$ values (nM)	
EFM192A	20.2 ± 18.6
BT474	23.9 ± 19.6
SKBR3	25.9 ± 2.9
HCC1419	63.1 ± 29.7
HCC1569	242.0 ± 8.7
MDA-MB-361	323.5 ± 50.8
HCC1954	582.0 ± 31.0
JIMT-1	1416.0 ± 371.9
UACC732	3180.0 ± 939.0
MDA-MB-453	5186.3 ± 1542.8

Table 5-2: Trastuzumab response in panel of HER2-positive breast cancer cell lines taken from [184]. **Fold change was calculated from the ratio of doubling time in the presence of trastuzumab divided by the doubling time in the absence of drug.**

	Fold change with 10 μg/mL trastuzumab	
	Average	StDev
BT474	5.00	1.05
EFM192A	1.86	0.54
UACC812	1.49	0.27
SKBR3	1.45	0.09
MDA-MB-361	1.21	0.22
HCC1419	1.18	0.02
UACC732	1.17	0.01
JIMT-1	1.15	0.1
HCC1954	1.08	0.1
MDA-MB-453	1.04	0.04
HCC1569	1.04	0.06
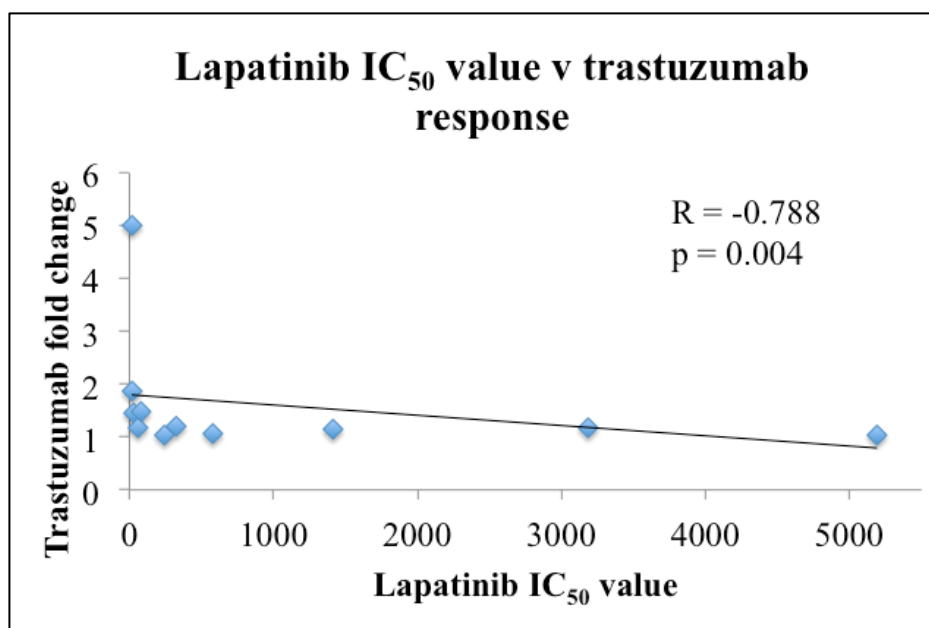
Figure 5-1: Lapatinib IC$_{50}$ values versus growth fold change with 10 μg/mL trastuzumab of HER2-positive breast cancer cell lines. R values and p values were calculated using Spearman rank correlation.

5.3 Okadaic acid sensitivity in HER2-positive breast cancer panel

In order to determine the relationship between HER2-targeted therapy resistance and sensitivity to PP2A inhibition, the panel of HER2-positive breast cancer cell lines was assessed for sensitivity to 5 nM okadaic acid (Figure 5-2). Okadaic acid caused growth inhibition in all cell lines tested, which indicates that PP2A may not be playing a tumour suppressor role in these cell lines. Correlation between response to okadaic acid and lapatinib or trastuzumab sensitivity was examined using Spearman rank correlation analysis. Sensitivity to okadaic acid was found to positively correlate with resistance to both lapatinib (p = 0.01) and trastuzumab (p = 0.01) (Figure 5-3 A and B).
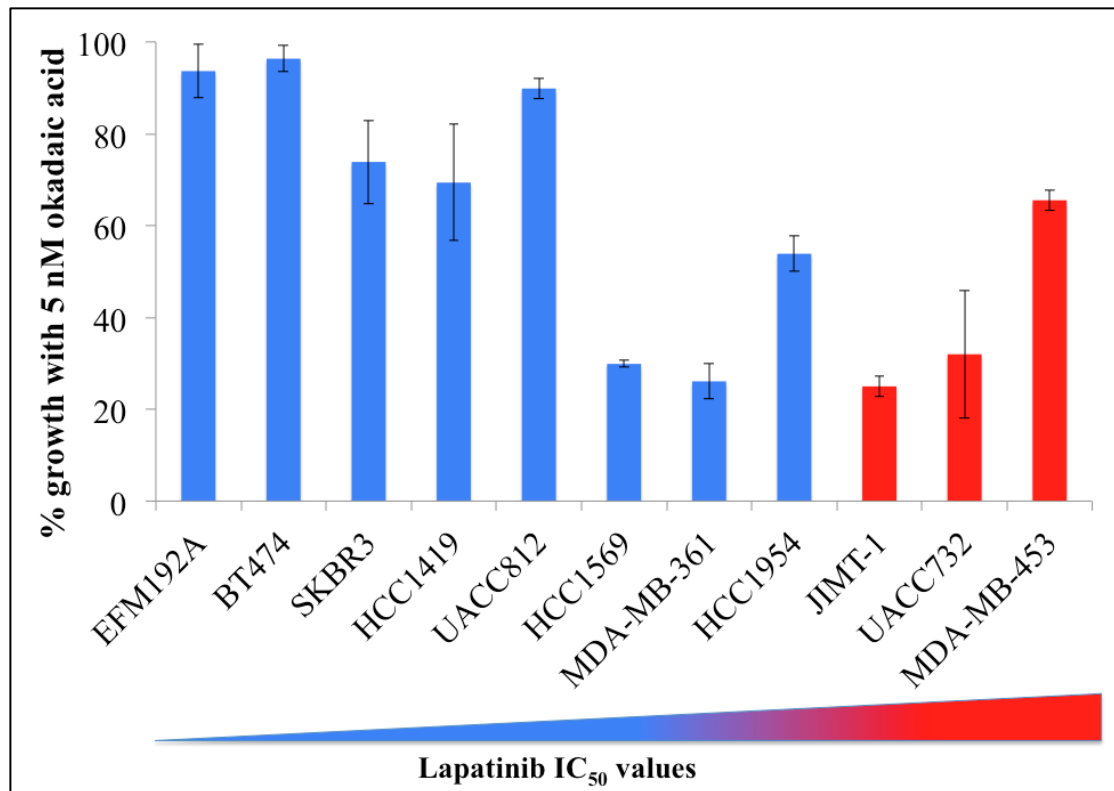
Figure 5-2: Proliferation of cell lines following 5-days of 5 nM okadaic acid treatment. Cell lines were ranked by lapatinib sensitivity. Percentage growth was calculated relative to untreated control and error bars represent standard deviation of biological triplicate experiments.
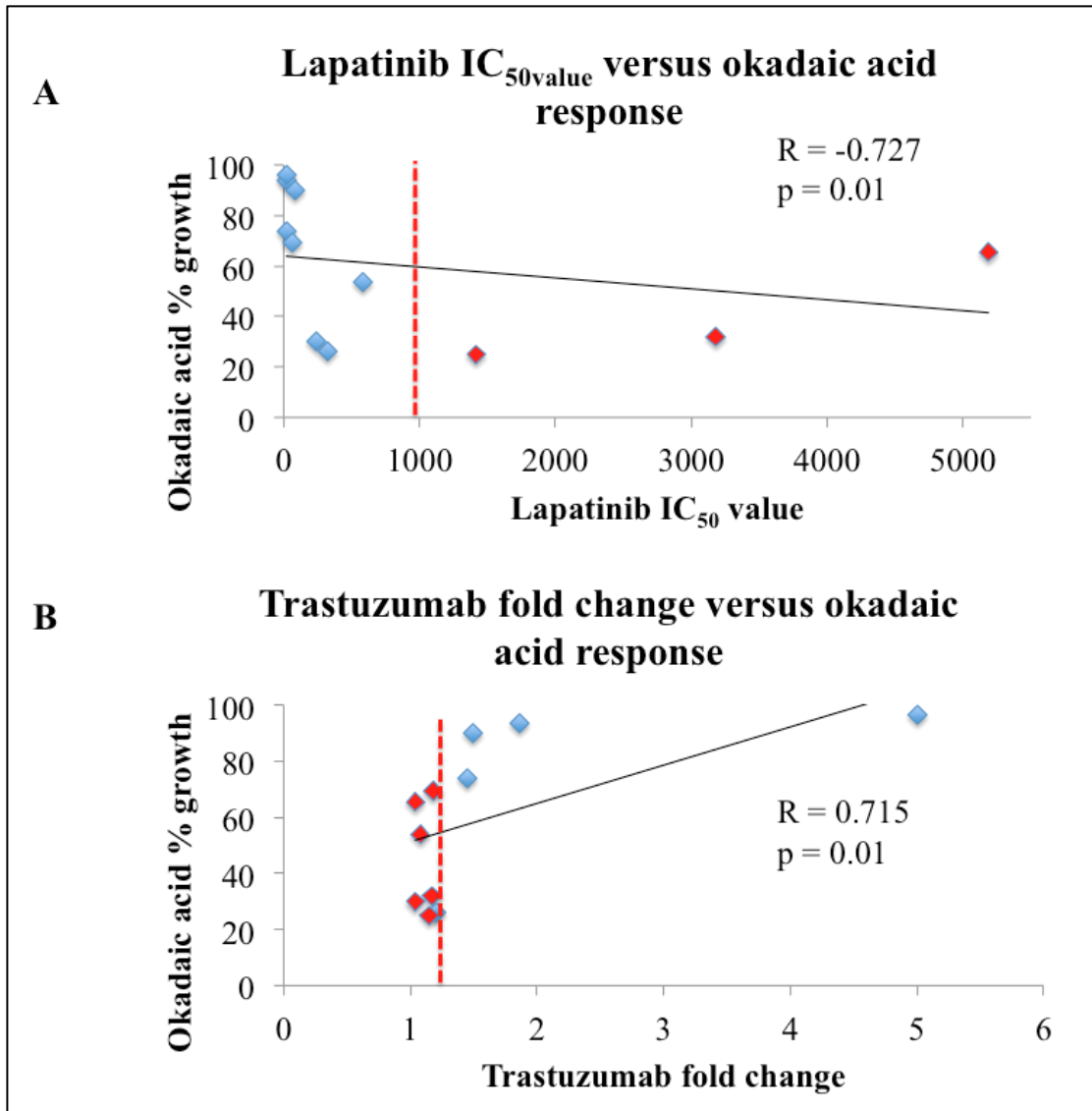
Figure 5-3: Relationship between (A) lapatinib IC$_{50}$ values or (B) trastuzumab response and growth response with 5 nM okadaic acid treatment. Blue dots indicate cell lines sensitive to trastuzumab or lapatinib and red dots indicate resistance. R values and p values were calculated using Spearman rank correlation.

5.3.1.1   <u>The effect of lapatinib plus okadaic acid on innately resistant cell lines</u>

The combination of lapatinib and okadaic acid had an additive effect in both the SKBR3-L and HCC1954-L cells (Section 3.3). The three cell lines innately resistant to both trastuzumab and lapatinib were tested for sensitivity to 500 nM lapatinib, 5 nM okadaic acid, and lapatinib plus okadaic acid. Two of the three cell lines showed a significant enhancement in growth inhibition, the MDA-MB-453 cells (p value = 0.0001) and the UACC-732 cells (p value = 0.02) (Figure 5-4). The combination had a slight but significant antagonistic effect in the JIMT-1 cells, with a 6.3% increase in percentage growth with the combination compared to okadaic acid alone (p value = 0.015). A selection of five lapatinib sensitive cell lines was assessed for their sensitivity to lapatinib plus okadaic acid. The combination of lapatinib plus okadaic acid significantly decreased cellular proliferation in one of the five cell lines, HCC1569 cells (p = 0.0005) (Figure 5-5). In summary, lapatinib plus okadaic acid had an additive effect in three of eight cell lines and an antagonistic effect was only observed in one cell line.
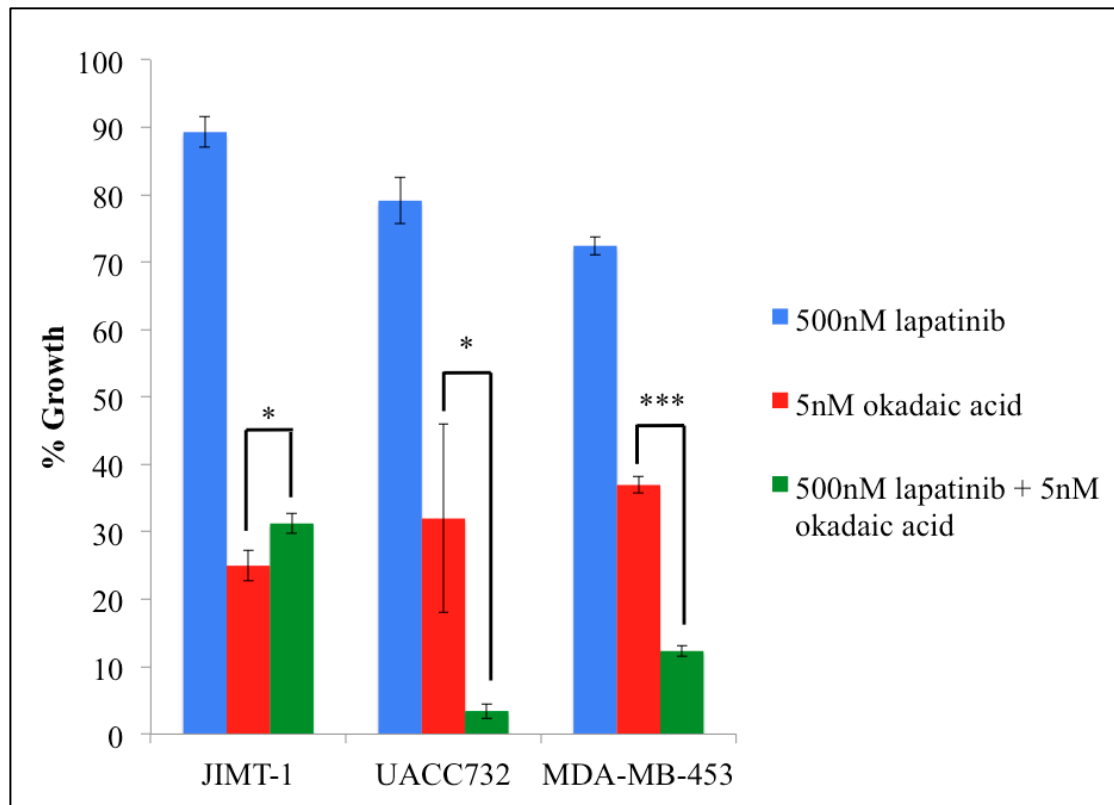
Figure 5-4: Proliferation of JIMT-1, UACC-732, and MDA-MB-453 cells following 5-day treatment with 500 nM lapatinib, 5 nM okadaic acid, and lapatinib plus okadaic acid. Error bars represent standard deviation of biological triplicate experiments. Percentage growth is relative to untreated control cells. The Student's t test was used to determine statistical significance. * denotes a p value of < 0.05, * denotes a p value of < 0.001.**
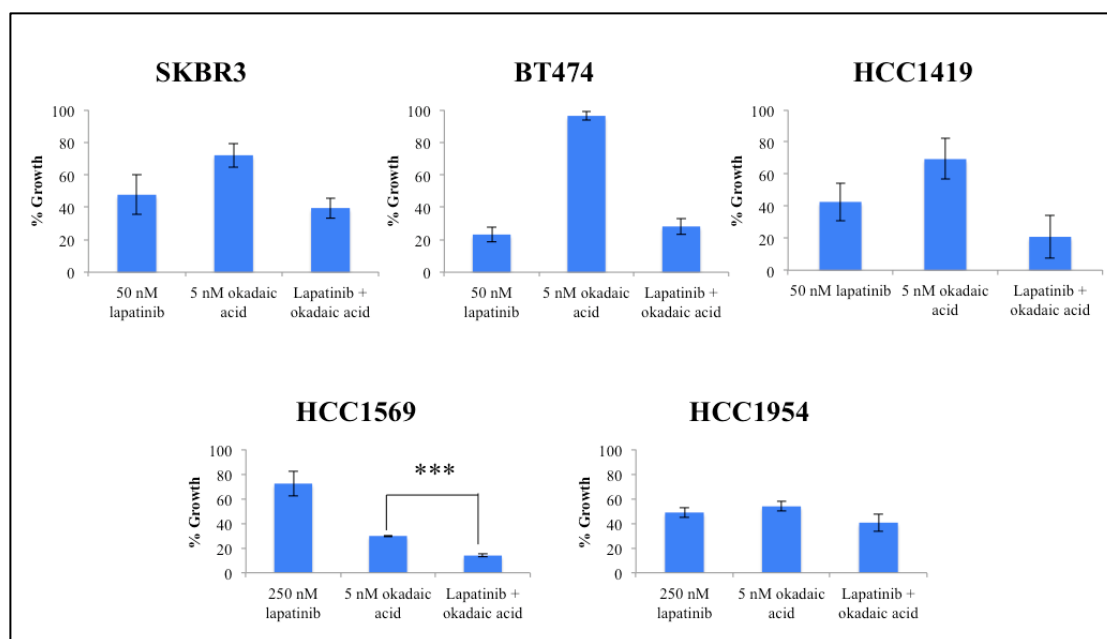
Figure 5-5: Proliferation of SKBR3, BT474, and HCC1419 treated with 50 nM lapatinib, 5 nM okadaic acid, and lapatinib plus okadaic acid, and HCC1569 and HCC1954 treated with 250 nM lapatinib, 5 nM okadaic acid, and lapatinib plus okadaic acid. Error bars represent standard deviation of biological triplicate experiments. Percentage growth is relative to untreated control cells. The Student's t test was used to determine statistical significance. * denotes p < 0.001.**

5.4 LB-100 sensitivity in HER2-positive breast cancer panel

LB-100 is the PP2A inhibitor that has made the most clinical progression and is the chosen candidate PP2A inhibitor for acquired lapatinib resistance. Therefore, LB-100 was also tested in the panel of HER2-positive breast cancer cell lines; this would indicate the sensitivities of the cell lines to a more clinically relevant inhibitor (Figure 5-6). Unexpectedly, LB-100 sensitivity did not correlate with sensitivity to okadaic acid (Figure 5-7 and Table 5-3). This may be due to differences in phosphatase inhibitory potency, chemical structure, or off-target effects [289]. LB-100 is a cantharidin derivative. Although both okadaic acid and cantharidin most selectively inhibit PP2A, they also inhibit other phosphatases at high concentrations. LB-100 response also did not correlate with either lapatinib or trastuzumab sensitivity (Figure 5-8 and 5-9).
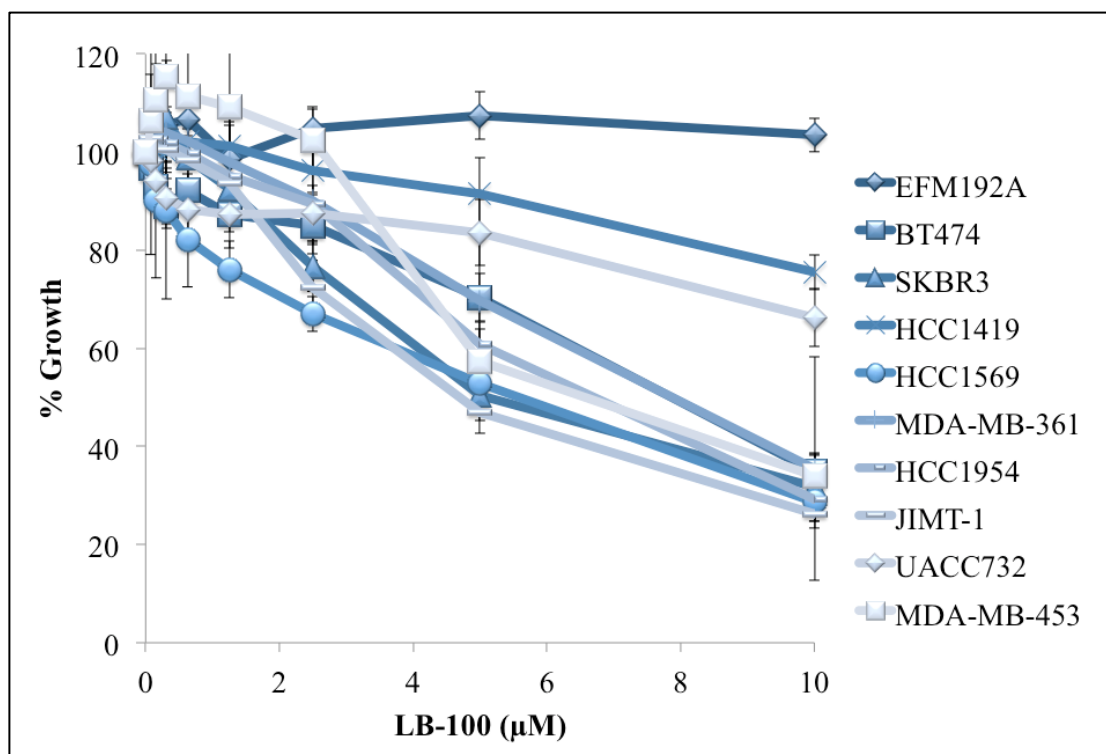
Figure 5-6: Proliferation of 11 HER2-positive breast cancer cell lines treated with 0-10 μM LB-100. Error bars represent standard deviation of biological triplicate experiments. Lighter series are more resistant to lapatinib.

Table 5-3: LB-100 IC$_{50}$ values for HER2-positive breast cancer cell lines.

LB-100 IC$_{50}$ value (μM)	
EFM192A	> 20
BT474	7.04 ± 3.56
SKBR3	5.38 ± 0.46
HCC1419	> 20
HCC1569	5.28 ± 0.46
MDA-MB-361	8.22 ± 2.26
HCC1954	5.32 ± 0.82
JIMT-1	4.96 ± 0.68
UACC732	19.34 ± 3.68
MDA-MB-453	6.87 ± 0.39
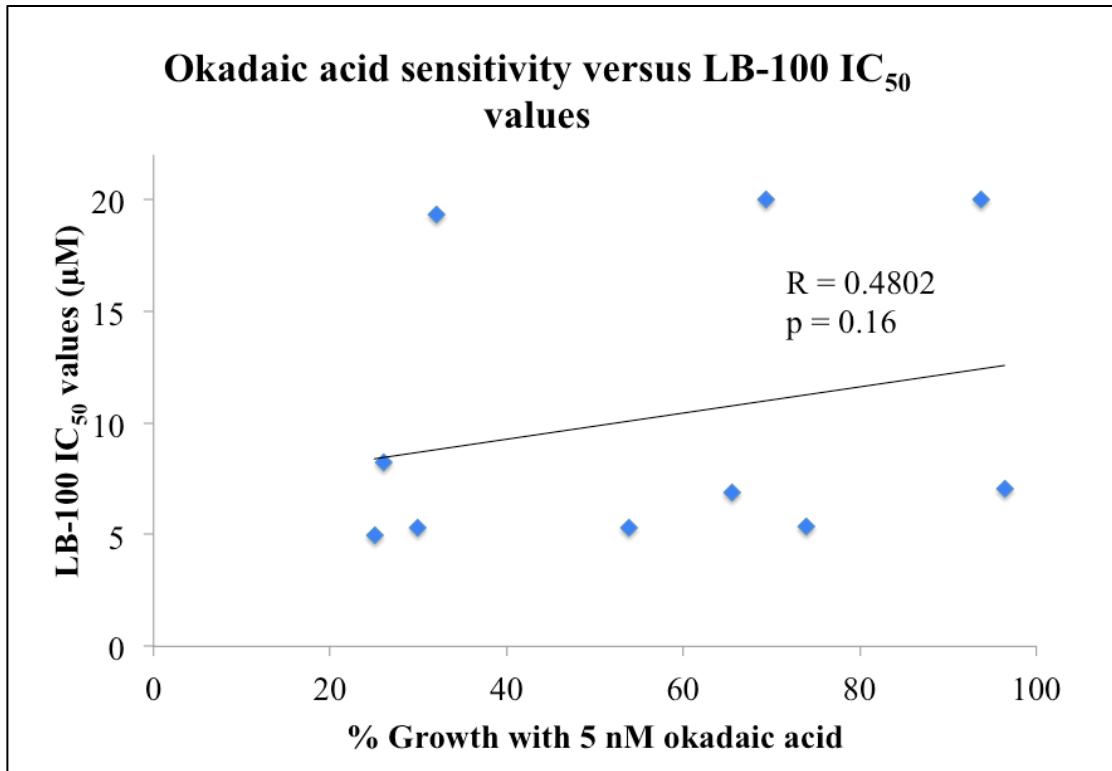
Figure 5-7: Relationship between percentage growth with 5 nM okadaic acid relative to untreated controls and LB-100 IC$_{50}$ values of the panel of HER2-positive breast cancer cell lines. R values and p values were calculated using Spearman rank correlation.
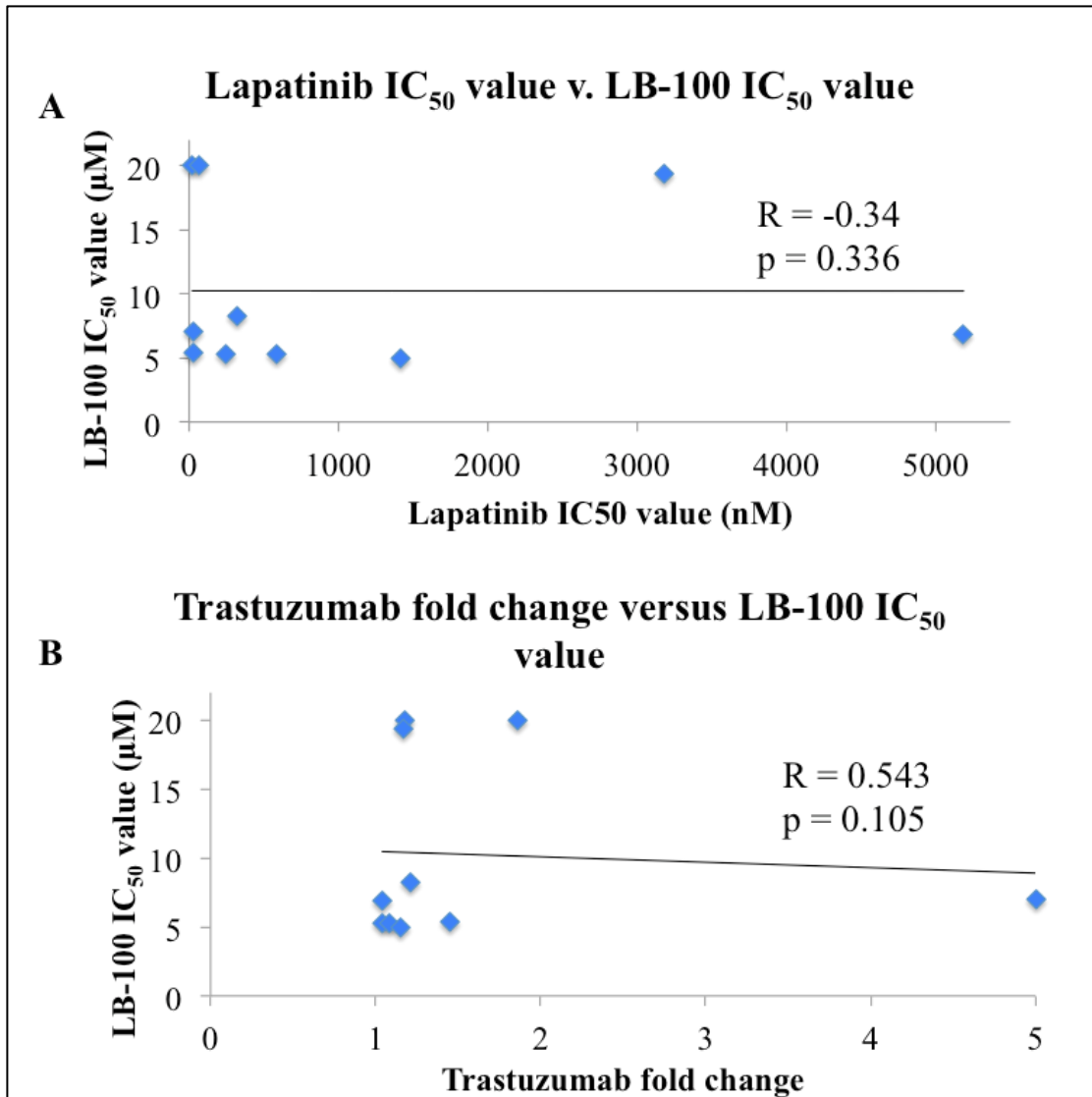
Figure 5-8: Relationship between LB-100 IC$_{50}$ values and (A) lapatinib IC$_{50}$ values and (B) trastuzumab-induced fold change in growth rate of the panel of HER2-positive breast cancer cell lines. R values and p values were calculated using Spearman rank correlation.

5.4.1.1 The effect of lapatinib plus LB-100

Although LB-100 sensitivity did not correlate with innate resistance to HER2-targeted therapies, we hypothesised that LB-100 may enhance lapatinib treatment in innately resistant cell lines. The three lapatinib resistant cell lines were evaluated for sensitivity to the combination therapy (Figure 5-9). Synergy was observed in one of the three cell lines tested, the MDA-MB-453 cells (CI value = 0.65 ± 0.16). An additive effect was not observed in either JIMT-1 or UACC732 cells (CI values = 1.21 ± 0.29 and 1.25 ± 0.21 respectively).
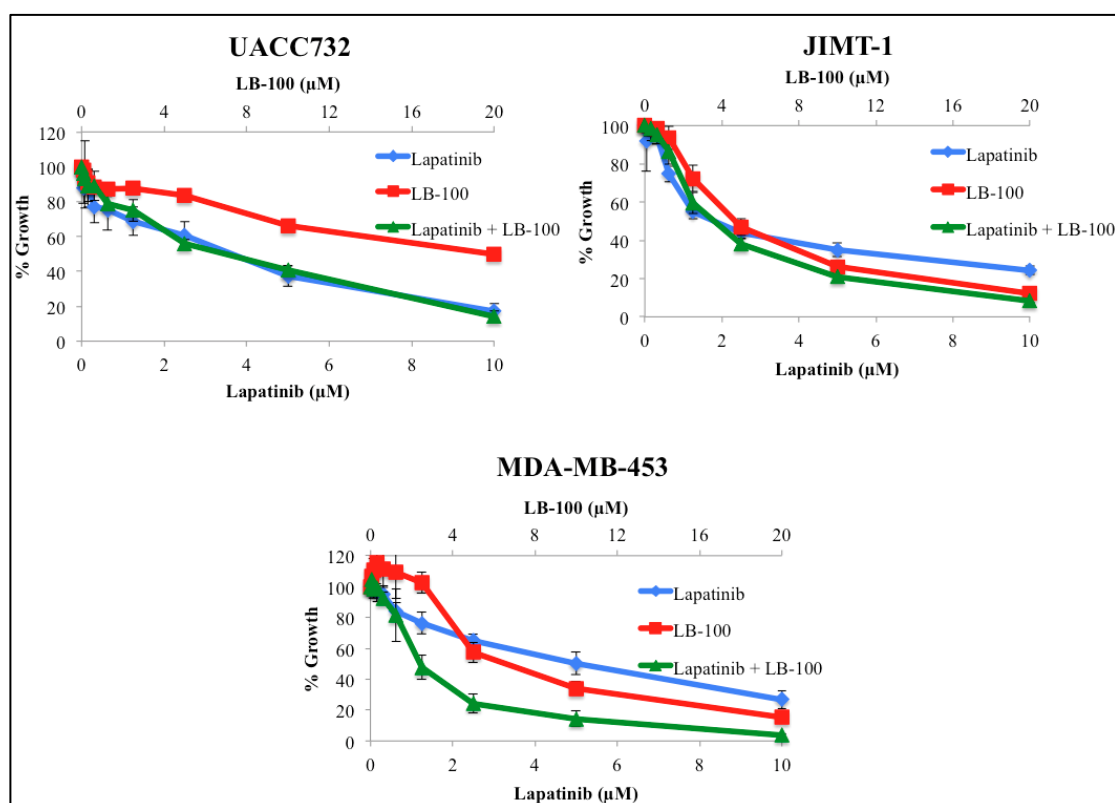
Figure 5-9: Proliferation of MDA-MB-453, JIMT-1, and UACC732 with lapatinib, LB-100, and lapatinib plus LB-100. Error bars represent standard deviation of biological triplicate experiments.

5.5 PP2A subunit expression in HER2-positive breast cancer cell lines

Alterations in PP2A subunit expression occurs in several cancer types [290, 291]. In order to examine if PP2A subunit expression is altered in HER2-positive breast cancer cell lines, both isoforms of the catalytic and structural subunits were assessed in the panel of cell lines (n=10). The catalytic subunits PPP2CA and PPP2CB did not correlate with sensitivity to either lapatinib or trastuzumab (p = 0.33 and 0.16 respectively) (Figure 5-10). Likewise, the expression levels of PPP2R1A and PPP2R1B also did not correlate with lapatinib (p = 0.244 and 0.96) or trastuzumab sensitivity (p = 0.185 and 0.444) (Figure 5-11).
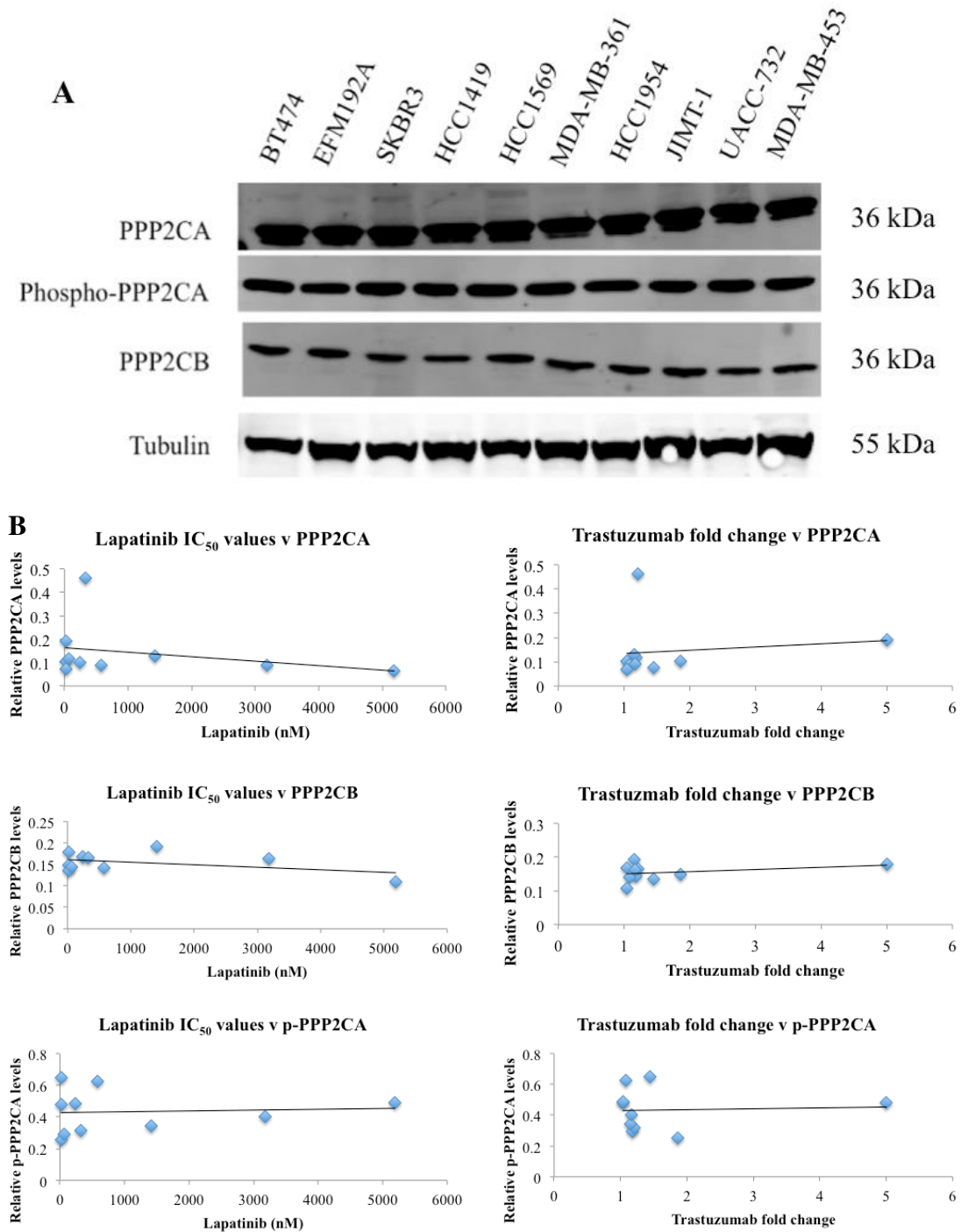
Figure 5-10: (A) Western blotting of PPP2CA, phospho-PPP2CA, and PPP2CB levels in a panel of HER2-positive breast cancer cell lines. Tubulin was used as a loading control. Blots shown are representative of triplicate blots. (B) R values and p values were calculated using Spearman rank correlation.to determine the relationship between total/phospho-PPP2CA, PPP2CB and lapatinib or trastuzumab sensitivity.
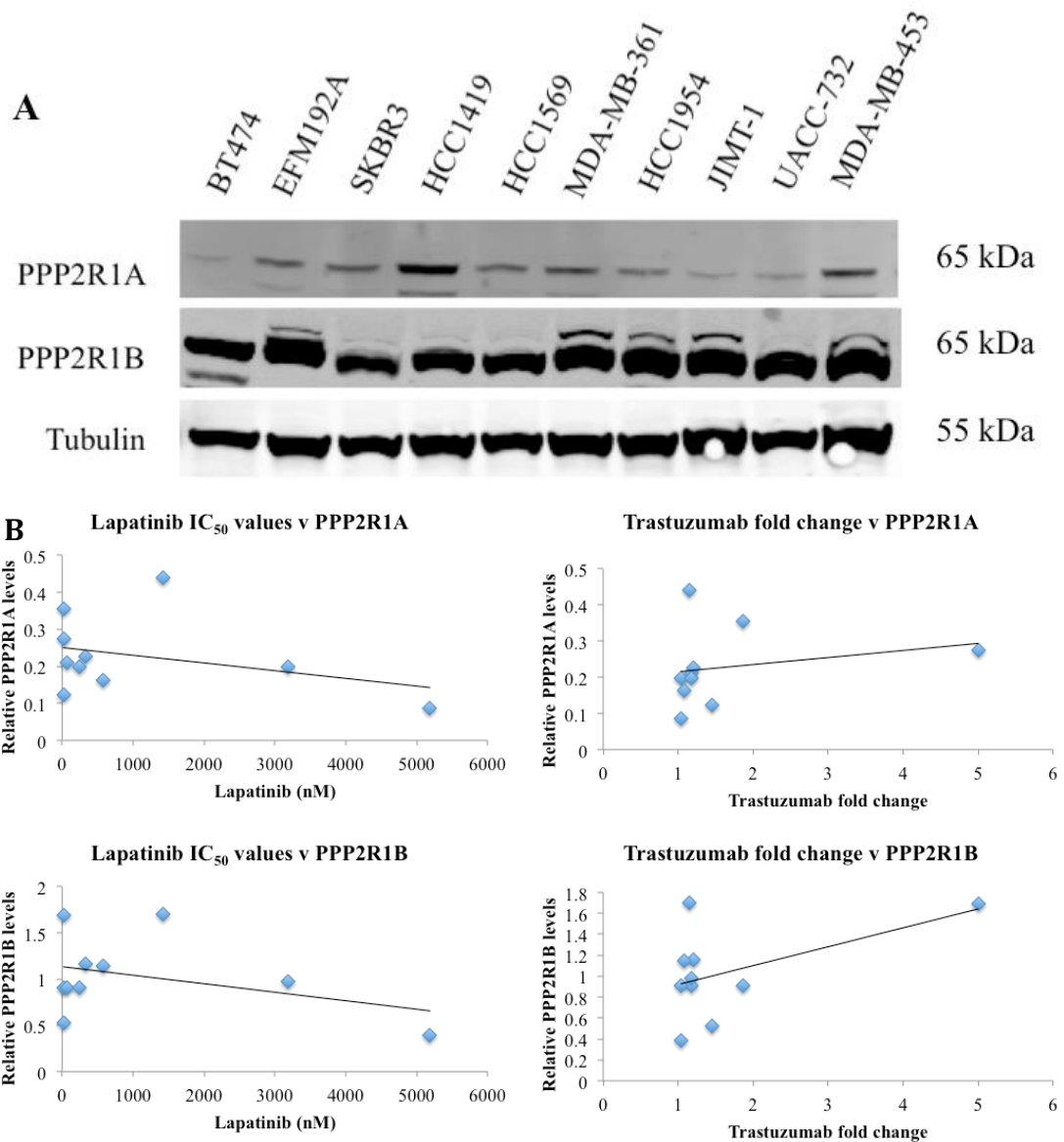
Figure 5-11: (A) Western blotting of PPP2R1A and PPP2R1B levels in a panel of HER2-positive breast cancer cell lines. Tubulin was used as a loading control. Blots shown are representative of triplicate blots. (B) R values and p values were calculated using Spearman rank correlation to determine the relationship between PPP2R1A or PPP2R1B and lapatinib or trastuzumab sensitivity.

5.6 Analysis of PP2A subunit expression in HER2-positive breast cancer patients

5.6.1.1 Correlation between PP2A subunit expression and survival

The expression of the PP2A catalytic and structural subunit isoforms was assessed in HER2-positive breast cancer patients and the association with overall and disease-free survival was examined. This analysis was done using the publicly available database BreastMark (http://glados.ucd.ie/BreastMark) [292]. This was carried out to validate the lack of correlation between PP2A subunit levels and HER2-targeted therapy response in the panel of HER2-positive cell lines. This database uses gene expression and survival data from 26 datasets, corresponding to approximately 17,000 genes and 4,738 breast cancer patients. In this study, the patient cohort was restricted to HER2-positive breast cancer patients. For each PP2A subunit, a Kaplan Meier curve was plotted. Patient samples with high and low expression of each subunit were stratified using the median and the 25th and 75th percentiles.

The mRNA expression of the α and β subunits of both the catalytic and structural subunits did not show a positive or negative correlation with survival outcomes (Figure 5-12 – 5-15). The p values for each PP2A subunit and survival outcome are summarised in Table 5-4. This is in agreement with the analysis of PP2A catalytic and structural subunit expression and the lack of a relationship with trastuzumab or lapatinib sensitivity.
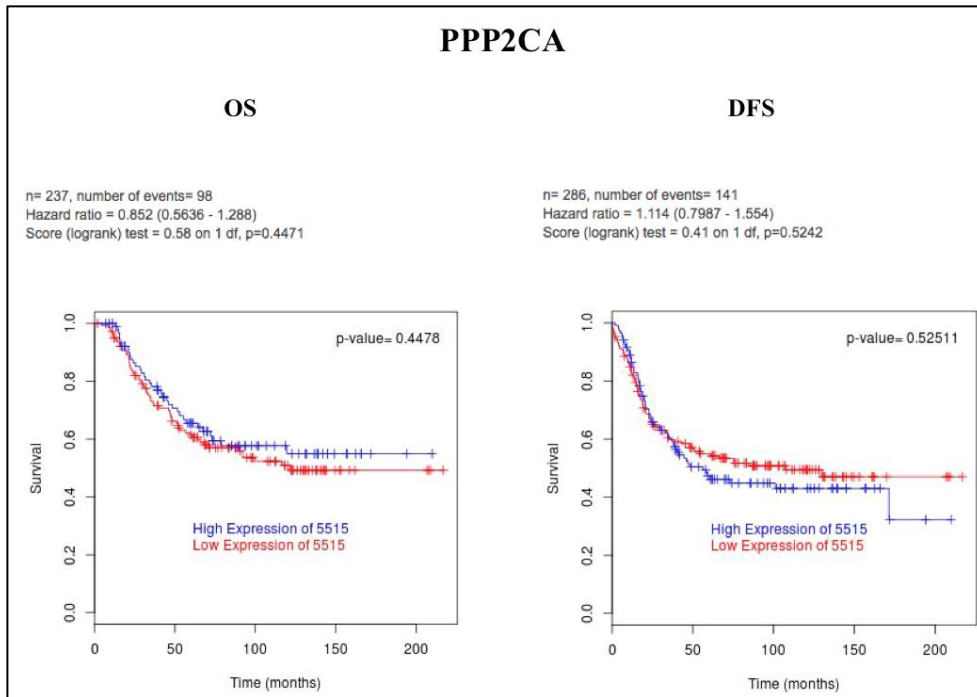
Figure 5-12: Kaplan Meier survival curves based on PAM50 classifier for OS and DFS with high and low expression of PPP2CA.
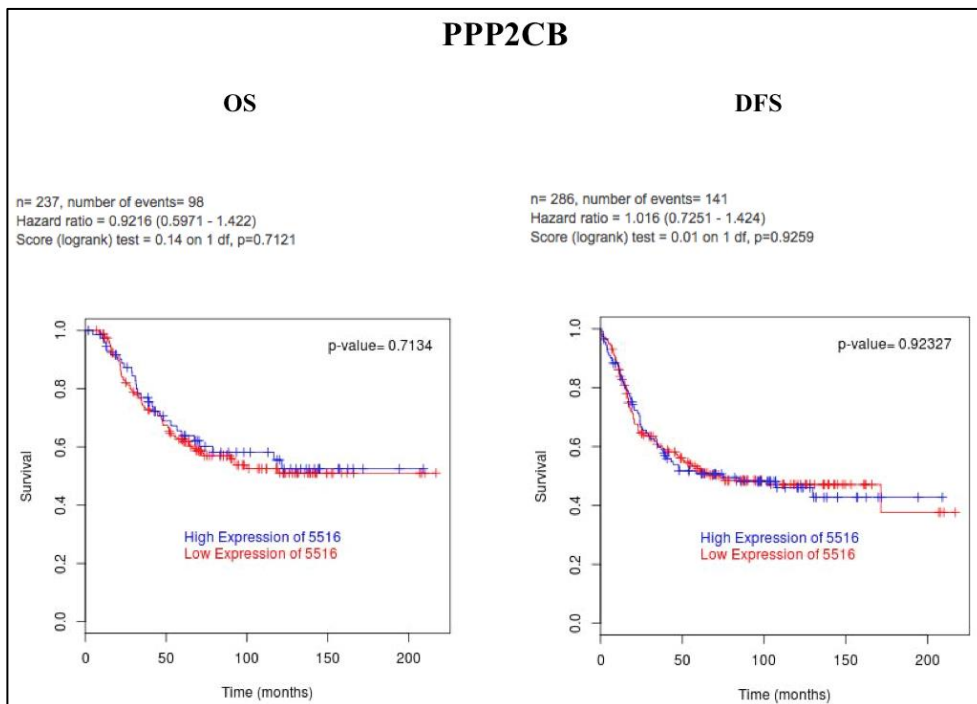
Figure 5-13: Kaplan Meier survival curves based on PAM50 classifier for OS and DFS with high and low expression of PPP2CB.
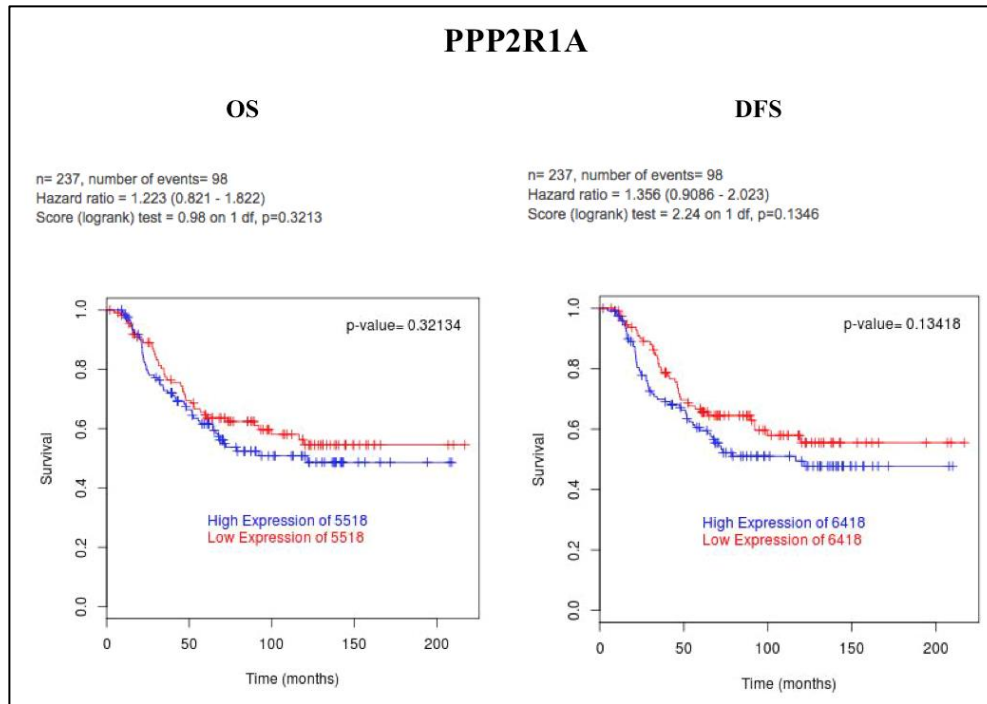
Figure 5-14: Kaplan Meier survival curves based on PAM50 classifier for OS and DFS with high and low expression of PPP2R1A.
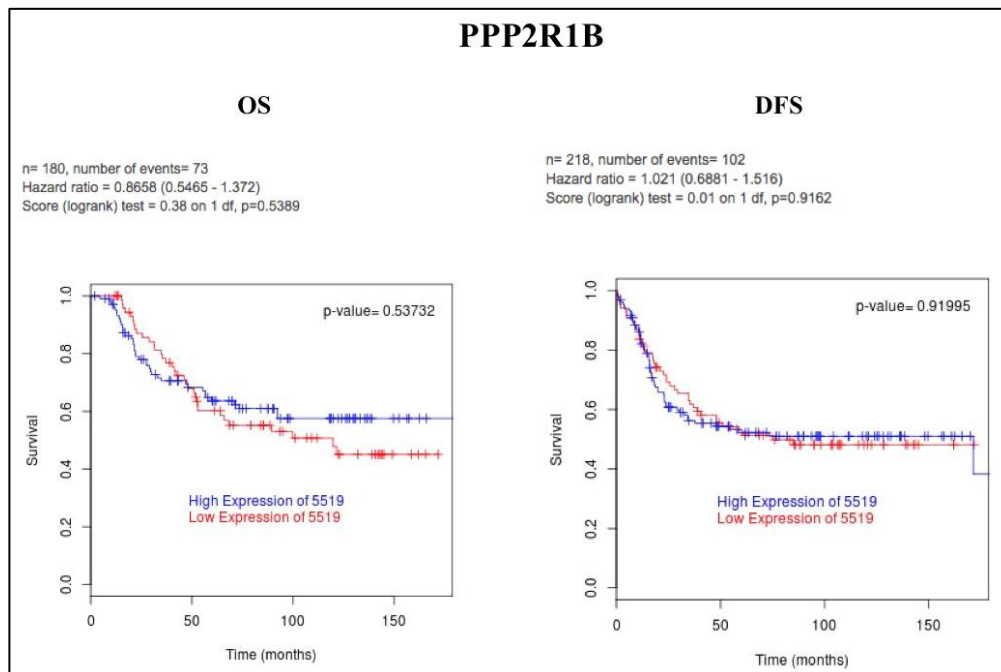
Figure 5-15: Kaplan Meier survival curves based on PAM50 classifier for OS and DFS with high and low expression of PPP2CA.

5.6.1.2 <u>Correlation between PP2A endogenous inhibitor expression and survival</u>

As PP2A catalytic and structural subunit expression did not correlate with survival, the gene expression levels of the PP2A inhibitor proteins CIP2A and SET were assessed. CIP2A and SET both interact with PP2A and reduce its phosphatase activity. Increased expression of both of these proteins has been previously associated with cancer progression [293]. However, in the BreastMark HER2-positive breast cancer dataset, high level expression of SET did not impact survival outcome (p for OS = 0.134 and DFS = 0.353) and high levels of CIP2A levels correlated with improved overall survival (p = 0.005) (Figure 5-16 and 5-17). CIP2A expression did not significantly impact DFS (p = 0.129). In contrast, in another breast cancer survival analysis, CIP2A was correlated with positive lymph node status and higher levels of proliferation markers. The correlation between low expression of CIP2A and improved OS in the BreastMark dataset may indicate that PP2A activity is increased in the patient tumours with poorer survival outcomes.
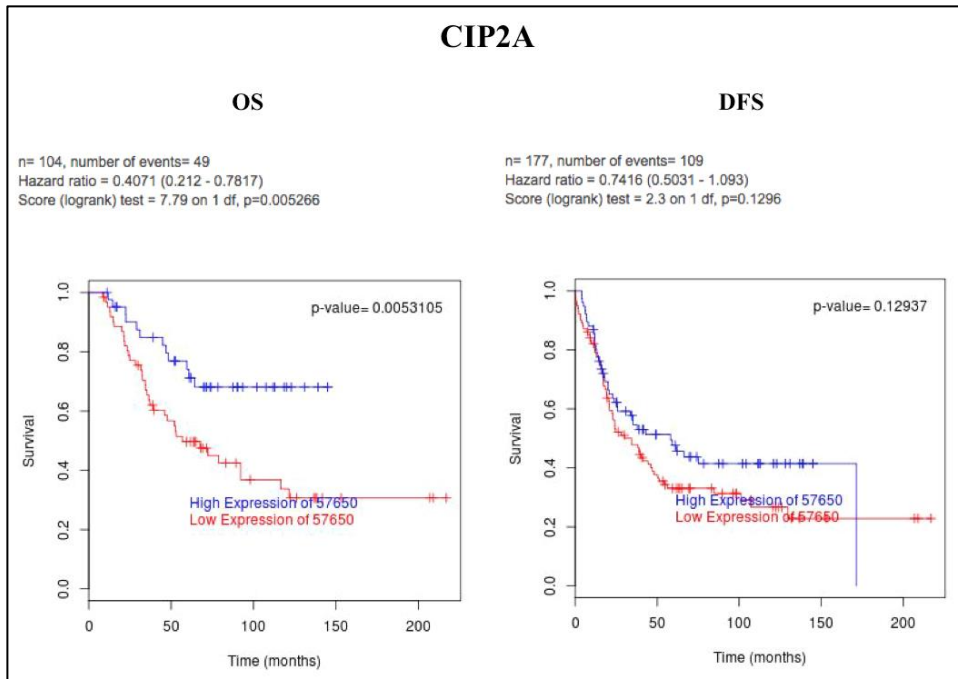
Figure 5-16: Kaplan Meier survival curves based on PAM50 classifier for OS and DFS with high and low expression of CIP2A.
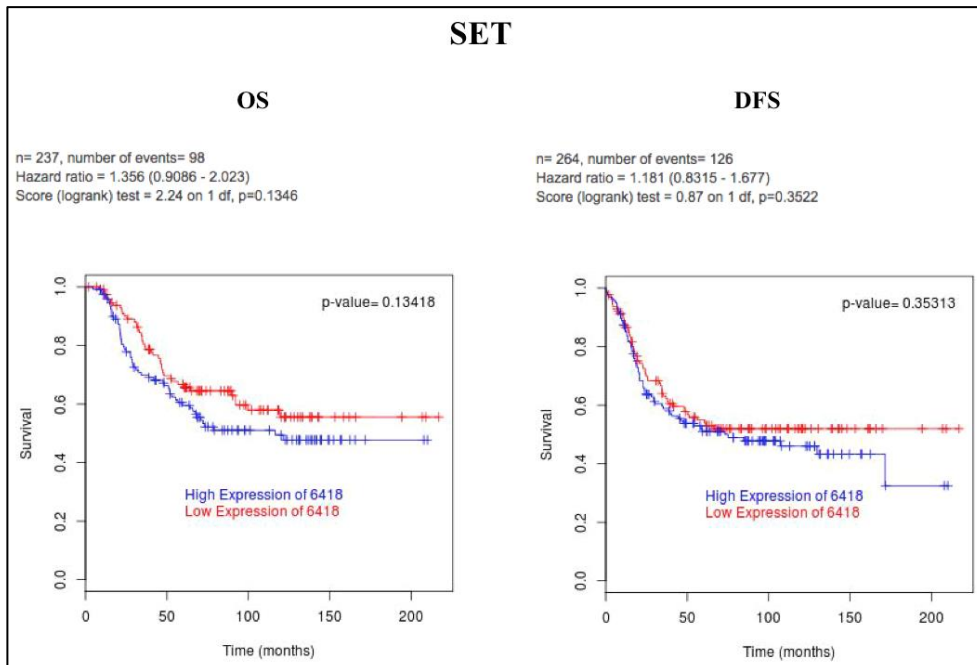
Figure 5-17: Kaplan Meier survival curves based on PAM50 classifier for OS and DFS with high and low expression of SET.

Table 5-4: Significance levels of correlation between PP2A catalytic and structural subunits/PP2A inhibitors and OS and DFS.

Gene	Overall survival (p value)	Disease-free survival (p value)
PPP2CA	0.448	0.525
PPP2CB	0.713	0.923
PPP2R1A	0.321	0.134
PPP2R1B	0.537	0.920
SET	0.134	0.353
CIP2A	0.005	0.129

5.7 Summary

Not all HER2-positive breast cancers have an initial response to HER2-targeted therapies and *de novo* resistance is a common clinical occurrence. This is also reflected in immortalised HER2-positive breast cancer cell lines. The panel of cell lines assessed had a variety of sensitivities to trastuzumab and lapatinib, with three cell lines displaying innate resistance to lapatinib and five cell lines resistant to trastuzumab. Okadaic acid caused varying some level of growth inhibition in all cell lines tested, indicating that PP2A is not playing a tumour suppressor role in these cell lines. The sensitivity to okadaic acid positively correlated with both trastuzumab and lapatinib resistance.

LB-100 was also examined in the panel of HER2-positive breast cancer cell lines. Interestingly LB-100 sensitivity did not correlate with response to okadaic acid or lapatinib or trastuzumab sensitivity.

There was no relationship observed between PP2A catalytic and structural subunit expression levels in the HER2-positive breast cancer cell lines and their HER2-targeted therapy sensitivity. Likewise, mRNA levels of the catalytic and structural isoforms did not correlate with survival outcomes in the HER2-positive breast cancer patients. However, high levels of the PP2A inhibitor protein CIP2A did correlate with positive patient outcomes.

6 The role of Src in resistance to afatinib and neratinib

6.1 Introduction

Despite advances in the treatment of HER2-positive breast cancer with HER2-targeted therapies, the majority of patients with metastatic HER2-positive breast cancer develop progressive disease with resistance to HER2 targeted therapies. Irreversible HER family inhibitors are in various stages of clinical development and represent novel HER2-targeting strategy for these patients.

Afatinib (Giotrif) is an anilinoquinazoline-derivative which functions as an irreversible pan-HER inhibitor, covalently binding to Cys797 of EGFR, Cys805 of HER2 and Cys803 of HER4, and rendering the receptors inactive [118]. Afatinib was FDA-approved for the treatment of non-small cell lung cancer in 2014 and is currently in phase III clinical trials in breast cancer [129]. Afatinib has shown efficacy in HER2-positive breast cancer *in vitro* and *in vivo* [123]. Canonici *et al*. showed an additive effect for the combination of trastuzumab and afatinib in trastuzumab-sensitive cell lines [123]. This study also showed that a cell line model of acquired trastuzumab resistance was sensitive to afatinib, with afatinib also restoring sensitivity to trastuzumab.

Likewise, neratinib (Nerlynx) is an irreversible HER family tyrosine kinase inhibitor that has shown activity in HER2-positive breast cancer in the pre-clinical and clinical setting [108]. In addition, following the phase III ExteNET trial, in which neratinib improved invasive disease free survival after relapse on trastuzumab, neratinib is FDA approved for the treatment of early stage HER2-positive breast cancer [294].

Using afatinib and neratinib resistant cell line models of HER2-positive breast cancer, the aim of this study was to examine the mechanisms by which these cells develop resistance, and to determine a therapeutic strategy to overcome or prevent resistance to irreversible pan-HER inhibitors.

6.2   Development of the afatinib-resistant SKBR3-A cell line

The afatinib resistant cell line model, SKBR3-A, was developed by Dr. Alexandra Canonici through continuous long-term exposure of the HER2-positive breast cancer cell line SKBR3 to afatinib. The SKBR3 cells were treated twice weekly with 150 nM afatinib until resistance developed (Figure 6-1 A). An age-matched, parental cell line (SKBR3-Par) was cultured alongside the treated cells. No significant morphological changes were observed in the afatinib resistant cell line compared to the parental cell line (Figure 6-1 B and C). SKBR3-A cells were significantly less sensitive to afatinib, with an afatinib IC_{50} value of 197.7 ± 53.8 nM compared to 10.9 ± 3.4 nM in the parental cell line. Pharmacokinetic studies of afatinib dosed at 40 mg per day show a peak plasma concentration of 38 ng/mL or 78.2 nM nM [128, 295]. Therefore, the cut-off concentration for afatinib sensitivity for this study was set at 80 nM. SKBR3-A cells are resistant to afatinib at clinically relevant concentrations.
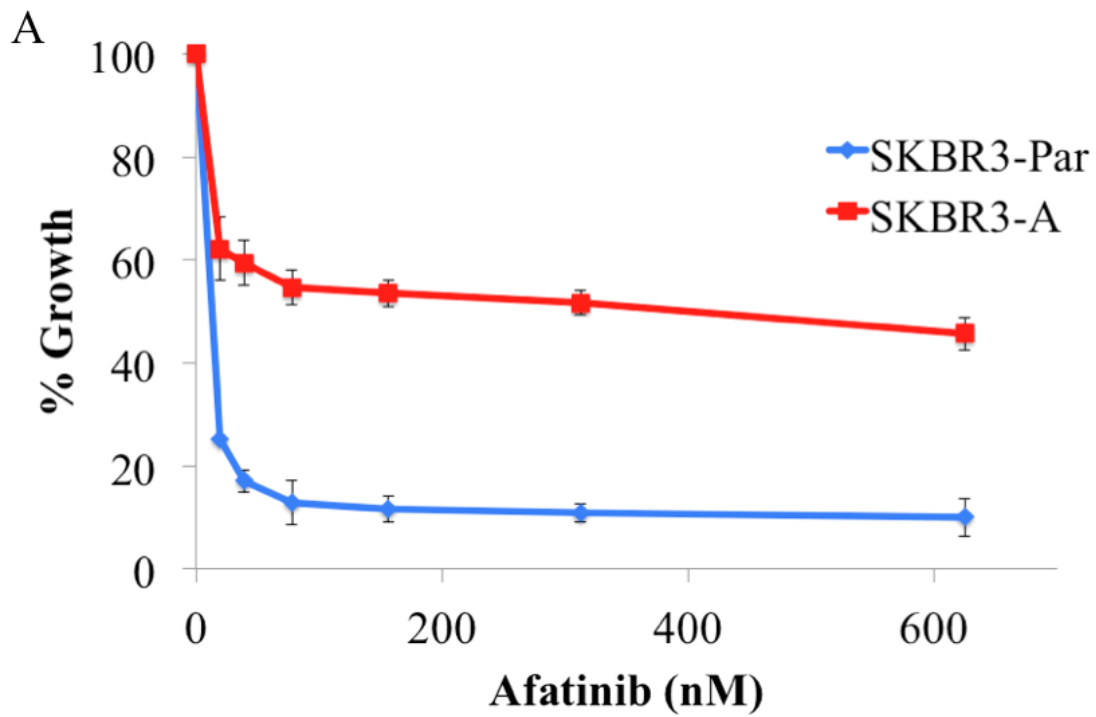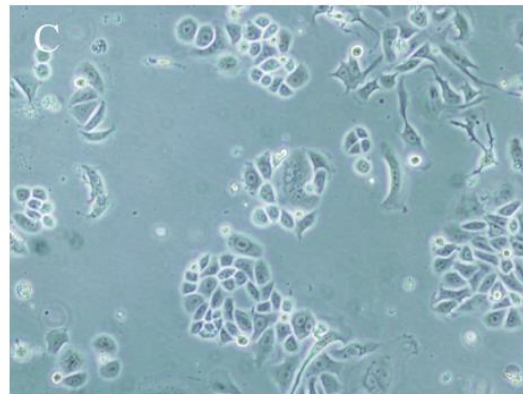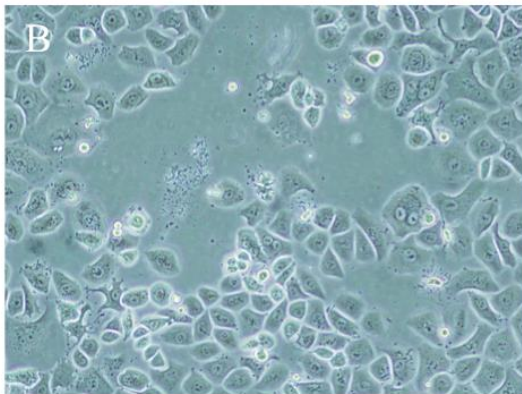
Figure 6-1: Proliferation of SKBR3-Par and SKBR3-A cells following 5-day treatment with afatinib (0 – 625 nM). Percentage growth was calculated relative to untreated control and error bars represent standard deviation of biological triplicate experiments. Images taken of SKBR3-A cells and SKBR3-Par cells at 400X magnification.

6.2.1 Effect of HER2-targeted therapies on SKBR3-A and SKBR3-Par

The SKBR3-A cells were also tested for cross-resistance to other HER2-targeted therapies. Parental SKBR3 cells are highly sensitive to the HER2-specific monoclonal antibody trastuzumab, the dual-targeting (EGFR/HER2) reversible TKI lapatinib, and the irreversible pan-HER TKIs afatinib and neratinib. SKBR3-A cells displayed cross-resistance to lapatinib and neratinib after five days of treatment (Figure 6-2 A and B). The SKBR3-A lapatinib IC_{50} was 1530.0 ± 380.0 nM compared to 51.0 ± 23.0 nM for SKBR3-Par cells (30-fold resistance) and the neratinib IC_{50} value was 114.0 ± 31.1 nM compared to 3.4 ± 1.1 nM (38-fold resistance). SKBR3-A cells were also assessed for altered sensitivity to trastuzumab, pertuzumab and the combination of monoclonal antibodies (Figure 6-3). The SKBR3-Par cell line showed $28.9 \pm 2.1\%$ growth inhibition following five days of trastuzumab treatment (10 μg/mL). In contrast, SKBR3-A cell growth was inhibited by $9.7 \pm 2.1\%$ (p = 0.0003). Pertuzumab also had a reduced anti-proliferative effect on SKBR3-A cells compared to the parental cell line, $-3.1 \pm 6.3\%$ compared to $14.2 \pm 1\%$ (p = 0.009). The enhanced combination effect observed in SKBR3-Par cells ($42.2 \pm 2.2\%$ growth inhibition) was also not seen in the SKBR3-A cells ($-10.7\% \pm 8.9\%$ growth inhibition) (p = 0.0005). Sensitivity of the SKBR3-A and SKBR3-Par cells to each of the HER2-targeted therapies is summarised in Table 6-1.
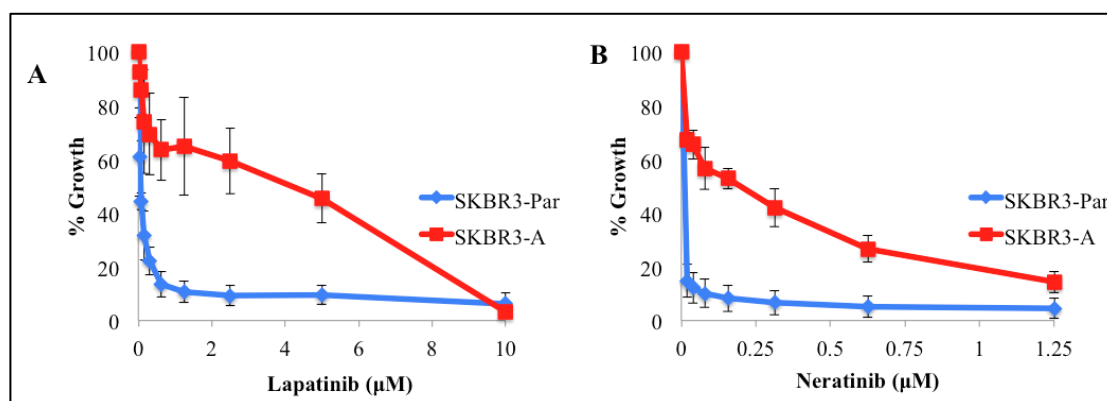
Figure 6-2: Proliferation of SKBR3-Par and SKBR3-A cells following 5-day treatment with A) 0 – 10 μM lapatinib and B) 0 – 1.25 μM neratinib. Percentage growth was calculated relative to untreated control and error bars represent standard deviation of biological triplicate experiments.
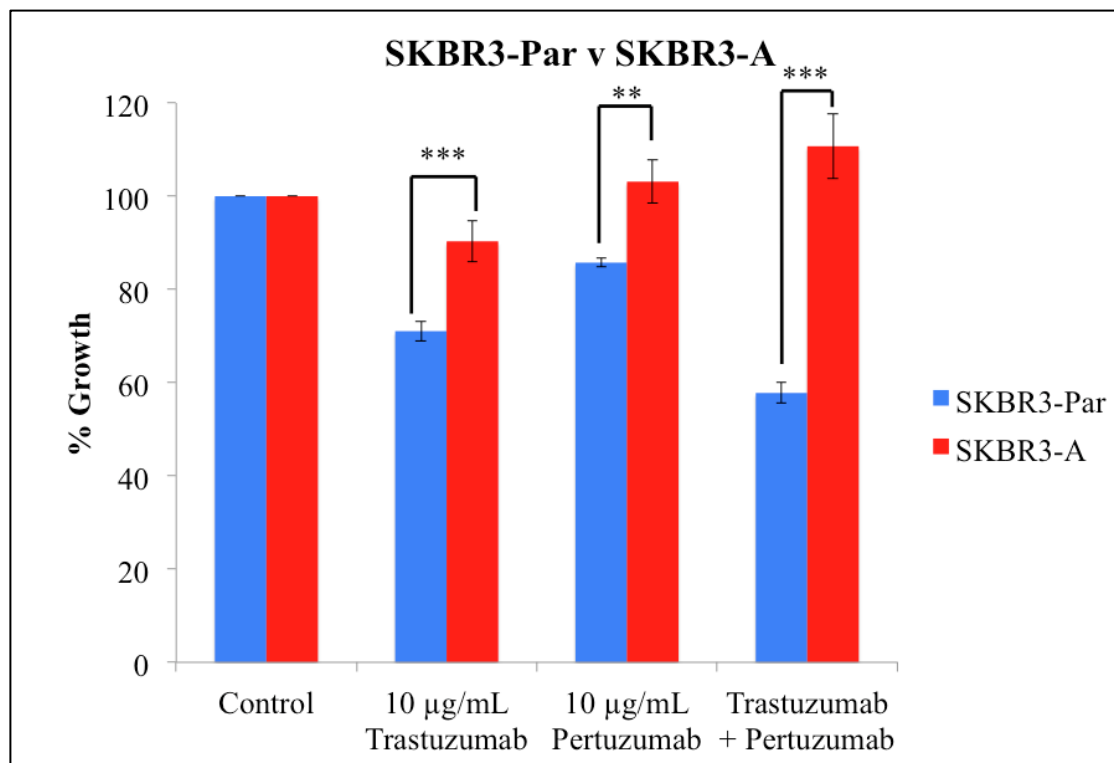
Figure 6-3: Proliferation of SKBR3-Par and SKBR3-A cells following 5-day treatment with 10 *μ*g/mL trastuzumab, 10 *μ*g/mL pertuzumab, trastuzumab plus pertuzumab. Percentage growth was calculated relative to untreated control and error bars represent standard deviation of biological triplicate experiments. The Student's t test was used to determine statistical significance. ** denotes a p value of < 0.01, * denotes P < 0.001.**

Table 6-1: SKBR3-A versus SKBR3-Par TKI IC$_{50}$ values and % growth inhibition following treatment with 10 μg/mL trastuzumab and/or pertuzumab.

Cell line	SKBR3-Par	SKBR3-A
Afatinib IC$_{50}$ (nM)	10.9 ± 3.4 nM	197.7 ± 53.8
Lapatinib IC$_{50}$ (nM)	51.0 ± 23.0	1530.0 ± 380.0
Neratinib IC$_{50}$ (nM)	3.4 ± 1.1	114.0 ± 31.1
% Growth inhibition 10 μg/mL trastuzumab	28.9 ± 2.1	9.7 ± 2.1
% Growth inhibition 10 μg/mL pertuzumab	14.2 ± 1	-3.1 ± 6.3
% Growth inhibition trast + pert	42.2 ± 2.2	-10.7 ± 8.9

6.3 Molecular characterisation of SKBR3-A cell line

6.3.1 Genetic profiling of SKBR3-A cells versus SKBR3-Par cells

Cancers that have become resistant to HER2-targeted therapy have been shown to develop genetic mutations, which cause oncogenic signalling changes [170, 198, 208]. In order to assess genetic alterations between the resistant and parental cells, both SKBR3-A and SKBR3-Par cell lines underwent whole exome sequencing, performed by Beijing Genomic Institute [271] (as described in Section 2.14). This analysis provided copy number variations (CNVs), single nucleotide variations (SNVs), and insertions and deletions (InDels). In SKBR3-A cells, 19 InDels were observed conpared to the parental cells. Only one of these indels caused a frameshift in the protein coding sequence (Table 6-2). This was a frameshift in the lactase (LCT) gene. There were 150 unique SNVs observed, 48 of which occurred within genes and 34 with structural implications on proteins (Table 6-3). SKBR3-A cells had 168 unique CNVs compared to SKBR3-Par cells, with four significant deletions and 205 amplifications. A significant alteration was deemed as a copy number ratio greater than 1.4 and less than 0.4 (Table 6-4). The InDel changes did not indicate any

possible oncogenic changes. Interestingly, SKBR3-A cells did not display mutations or gene amplification of HER family members, which has been shown as a mechanism of resistance to HER2-targeted therapies [170, 296]. However, the CNV analysis showed alterations in several signalling pathways. A number of genes associated with EMT, which has been implicated in lapatinib resistance, had significantly increased copy number, including PDE4A, PDE4D, ITGB4, SPHK1, S100A9, and NR4A1 [297–301]. SKBR3-A cells also showed gene copy number amplification of ITPR4 and TNIK, which are involved in autophagy induction [302]. Autophagy can act as a mechanism of cell death and also cell survival and afatinib has been shown to induce autophagy [303]. Pathway analysis using PANTHER also showed changes in several signalling pathways (Figure 6-4). These pathway alterations include inflammation related signalling such as inflammation mediated by chemokine and cytokine signalling, CCKR pathway, and T cell activation. Growth factor signalling was altered including insulin/IGF, VEGF, and PDGF signalling.

Table 6-2: Somatic insertions and deletion in SKBR3-A compared to SKBR3-Par cells.

	Insertions/Deletions	
Gene name	**Gene description**	**Region**
CEP104	Centrosomal protein 104	3' UTR
FBXO28	Centromere protein 30	Intron
FBXO28	Centromere protein 30	Intron
ACMSD	Aminocarboxymuconate semialdehyde decarboxylase	Intron
LCT	Lactase	Frameshift
SESTD1	SEC14 and spectrin domain containing 1	Intron
USP49	Ubiquitin specific peptidase 49	Downstream gene
KIAA1244	Protein phosphatase 1, regulatory subunit 33	Intron
NMBR	Neuromedin B receptor	Intron
LRCH4	Leucine rich repeats and calponin homology domain containing 4	Intron
ST7	Suppression of tumorigenicity 7	Intron
DYRK4	Dual specificity tyrosine phosphorylation regulated kinase 4	Intron
LEMD3	LEM domain containing 3	Intron
ANP32A	Acidic nuclear phosphoprotein 32 family member A	3' UTR
AKAP13	A-kinase anchoring protein 13	Intron
DNAH17	Dynein axonemal heavy chain 17	Intron
ZNF791	Zinc finger protein 791	Intron

| PRPF31 | Pre-mRNA processing factor 31 | Intron |
| OFD1 | Centriole and centriolar satellite protein | Intron |

Table 6-3: Single nucleotide variants in SKBR3-A compared to SKBR3-Par cells.

Gene	Gene description	Mutation	Nucleotide change
CA6	Carbonic anhydrase 6	Missense	G☐A
HIVEP3	Human Immunodeficiency Virus Type I Enhancer Binding Protein 3	Silent	A☐C
NCF2	Neutrophil cytosolic factor 2	Missense	G☐C
CFH	Complement factor H	Missense	G☐A
NUP133	Nucleoporin 133	Missense	C☐A
LRPPRC	Leucine Rich Pentatricopeptide Repeat Containing	Silent	G☐A
FER1L5	Fer-1 Like Family Member 5	Missense	C☐A
GORASP2	Golgi Reassembly Stacking Protein 2	Silent	A☐T
ICOS	Inducible T-Cell Costimulator	Missense	A☐C
PRKAG3	Protein Kinase AMP-Activated Non-Catalytic Subunit Gamma 3	Missense	C☐G
ARPP21	CAMP Regulated Phosphoprotein 21	Missense	G☐C
LZTFL1	Leucine Zipper Transcription Factor Like 1	Silent	G☐A
CHRD	Chordin	Silent	C☐A
TNK2	Tyrosine Kinase Non Receptor 2	Missense	C☐A
KIAA1211	KIAA1211	Missense	C☐A
TCOF1	Treacle Ribosome Biogenesis Factor 1	Missense	A☐C
ZNF454	Zinc Finger Protein 454	Missense	G☐T
HIST1H3A	Histone Cluster 1 H3 Family Member A	Missense	G☐C
HIST1H2AD	Histone Cluster 1 H2A Family Member D	Missense	G☐T
FILIP1	Filamin A Interacting Protein 1	Missense	A☐T

MUC12	Mucin 12, Cell Surface Associated	Silent	T□A
GPR22	G Protein-Coupled Receptor 22	Silent	G□A
CNBD1	Cyclic Nucleotide Binding Domain Containing 1	Missense	T□G
MPDZ	Multiple PDZ Domain Crumbs Cell Polarity Complex Component	Missense	C□T
ZBTB6	Zinc Finger and BTB Domain Containing 6	Missense	C□T
ADARB2	Adenosine Deaminase, RNA Specific B2	Silent	G□A
ASAH2	Neutral Ceramidase	Missense	C□A
JMJD1C	Jumonji Domain Containing 1C	Missense	C□T
OR52B2	Olfactory Receptor Family 52 Subfamily B Member 2	Missense	G□T
OR9G4	Olfactory Receptor Family 9 Subfamily G Member 4	Missense	T□C
AHNAK	Neuroblast Differentiation-Associated Protein AHNAK	Missense	C□A
CCDC88B	Coiled-Coil Domain Containing 88B	Silent	C□T
GLB1L3	Galactosidase Beta 1 Like 3	Silent	C□T
METTL25	Methyltransferase Like 25	Missense	A□T
C14orf119	Chromosome 14 Open Reading Frame 119	Missense	C□G
PCNXL4	Pecanex-Like Protein 4	Missense	G□T
ZNF839	Zinc Finger Protein 839	Missense	A□G
AHNAK2	AHNAK Nucleoprotein 2	Missense	C□T
ZNF774	Zinc Finger Protein 774	Missense	G□T
STAT3	Signal Transducer And Activator Of Transcription 3	Silent	G□A
FASN	Fatty Acid Synthase	Missense	C□G

ATP8B1	ATPase Phospholipid Transporting 8B1	Missense	G☐C
HMHA1	Rho GTPase Activating Protein 45	Missense	A☐C
CACTIN	Cactin, Spliceosome C Complex Subunit	Missense	C☐A
ZNF845	Zinc Finger Protein 845	Missense	A☐T
THBD	Thrombomodulin	Silent	G☐A
ZNF341	Zinc Finger Protein 341	Missense	C☐G
SOGA1	Suppressor Of Glucose, Autophagy-Associated Protein 1	Silent	G☐A
DIAPH2	Diaphanous Related Formin	Silent	T☐C

Table 6-4: Copy number variations in SKBR3-A compared to SKBR3-Par cells. Copy number ratio is given as a relative number of gene copies in SKBR3-A cells to SKBR3-Par cells. A cut of >1.5 and < 0.35 copy ratio was used. Complete table of significant copy ratio changes in Appendix.

Gene	Gene description	Copy ratio
LSM5	LSM5 Homolog, U6 Small Nuclear RNA And MRNA Degradation Associated	0.350
STS	Steroid Sulfatase	0.394
STAC	SH3 And Cysteine Rich Domain	0.527
ITGA9	Integrin Subunit Alpha 9	0.581
TRPS1	Transcriptional Repressor GATA Binding 1	1.501
TFAP2C	Transcription Factor AP-2 Gamma	1.501
ZBTB33	Zinc Finger And BTB Domain Containing 33	1.502
COL14A1	Collagen Type XIV Alpha 1 Chain	1.506
QRICH2	Glutamine Rich 2	1.511
ZNFX1	Zinc Finger NFX1-Type Containing 1	1.514
EIF4G2	Eukaryotic Translation Initiation Factor 4 Gamma 2	1.520
TPD52L2	Tumor Protein D52 Like 2	1.524
F8	Coagulation Factor VIII	1.524
USP26	Ubiquitin Specific Peptidase 26	1.528
EPM2AIP1	EPM2A Interacting Protein 1	1.530
CASKIN2	CASK Interacting Protein 2	1.531
DCLK3	Doublecortin Like Kinase 3	1.531
TRANK1	Tetratricopeptide Repeat And Ankyrin Repeat Containing 1	1.531

MLH1	MutL Homolog 1	1.531
COL14A1	Collagen Type XIV Alpha 1 Chain	1.538
ATP6V0D2	ATPase H+ Transporting V0 Subunit D2	1.539
CNGB3	yclic Nucleotide Gated Channel Beta 3	1.539
ITPR1	Inositol 1,4,5-Trisphosphate Receptor Type 1	1.541
GRM7	Glutamate Metabotropic Receptor 7	1.541
DSCC1	DNA Replication And Sister Chromatid Cohesion 1	1.542
MSC	Musculin	1.542
TRPA1	Transient Receptor Potential Cation Channel Subfamily A Member 1	1.542
TERF1	Telomeric Repeat Binding Factor 1	1.542
STAU2	Staufen Double-Stranded RNA Binding Protein 2	1.542
TCEB1	Transcription elongation factor B polypeptide 1	1.542
JPH1	Junctophilin 1	1.542
PEX2	Peroxisomal Biogenesis Factor 2	1.542
STMN2	Stathmin 2	1.542
MRPS28	Mitochondrial Ribosomal Protein S28	1.542
TPD52	Tumor Protein D52	1.542
KCNB2	Potassium Voltage-Gated Channel Subfamily B Member 2	1.543
KCNB2	Potassium Voltage-Gated Channel Subfamily B Member 2	1.551
S100A9	S100 Calcium Binding Protein A9	1.551
BHLHE40	Basic Helix-Loop-Helix Family Member E40	1.553
RHBDF2	Rhomboid 5 Homolog 2	1.554
RDH10	Retinol Dehydrogenase 10	1.556

KIAA1210	KIAA1210	1.559
FLNA	Filamin A	1.560
STAU2	Staufen Double-Stranded RNA Binding Protein 2	1.565
HERPUD1	Homocysteine Inducible ER Protein With Ubiquitin Like Domain 1	1.565
COL14A1	Collagen Type XIV Alpha 1 Chain	1.567
MRPL13	Mitochondrial Ribosomal Protein L13	1.567
MTBP	MDM2 Binding Protein	1.567
ZACN	Zinc Activated Ion Channel	1.569
C17orf80	Chromosome 17 Open Reading Frame 80	1.570
MYO15B	Myosin XVB	1.574
MTBP	MDM2 Binding Protein	1.577
SEC16B	SEC16 Homolog B, Endoplasmic Reticulum Export Factor	1.579
PDE4D	Phosphodiesterase 4D	1.584
GPR112	G protein-coupled receptor 112	1.590
FOXK2	Forkhead Box K2	1.598
JPH1	Junctophilin 1	1.617
DLEC1	Deleted In Lung And Esophageal Cancer 1	1.628
SCN5A	Sodium Voltage-Gated Channel Alpha Subunit 5	1.628
SCN10A	Sodium Voltage-Gated Channel Alpha Subunit 10	1.628
CSRNP1	Cysteine And Serine Rich Nuclear Protein 1	1.628
CX3CR1	C-X3-C Motif Chemokine Receptor 1	1.628
RPSA	Ribosomal Protein SA	1.628
FAM104A	Family With Sequence Similarity 104 Member A	1.631

GPRC5C	G Protein-Coupled Receptor Class C Group 5 Member C	1.631
MYO15B	Myosin XVB	1.631
ITGB4	Integrin Subunit Beta 4	1.631
EXOC7	Exocyst Complex Component 7	1.631
SPHK1	Sphingosine Kinase 1	1.631
CYTH1	Cytohesin 1	1.631
RPTOR	Regulatory Associated Protein Of MTOR Complex 1	1.631
NPB	Neuropeptide B	1.631
TUFT1	Tuftelin 1	1.649
SCYL1	SCY1 Like Pseudokinase 1	1.670
TAF2	TATA-Box Binding Protein Associated Factor 2	1.682
DEPTOR	DEP Domain Containing MTOR Interacting Protein	1.682
PRKDC	Protein Kinase, DNA-Activated, Catalytic Polypeptide	1.712
NR4A1	Nuclear Receptor Subfamily 4 Group A Member 1	1.751
REEP2	Receptor Accessory Protein 2	1.834
HIST1H2BD	Histone Cluster 1 H2B Family Member D	1.866
TNIK	TRAF2 And NCK Interacting Kinase	1.892
KRT7	Keratin 7	1.921
HIST2H3A	Histone Cluster 2 H3 Family Member A	1.950
FLJ42969	Uncharacterized LOC441374	1.966
TXNRD1	Thioredoxin Reductase 1	2.055
CCDC57	Coiled-Coil Domain Containing 57	2.160
AADACL2	Arylacetamide Deacetylase Like 2	2.217

Figure 6-4: PANTHER pathway analysis of CNVs in SKBR3-A cells.

6.3.2 RPPA analysis of SKBR3-A cells versus SKBR3-Par

The levels of 73 proteins and phospho-proteins involved in key signalling pathways were examined in the SKBR3-A and SKBR3-Par cells by RPPA analysis. Applying a p-value of ≤ 0.05, the levels of five proteins/ phospho-proteins were significantly decreased and nine significantly increased in the SKBR3-A cells (Table 6-5Table 6-5).

SKBR3-A displayed changes in the levels of some members of the HER family and HER-family-related signalling proteins. SKBR3-A cells had decreased phospho-HER3 (Y1289) (fold change = 0.4, p = 0.0026), but had significantly increased levels of total EGFR (fold change = 2.02, p = 0.043). Phospho- and total-HER2 and HER4 levels were not significantly affected, although, several phospho-proteins downstream of HER family signalling were down-regulated. Levels of phospho-Akt (T308 and S473) (fold change = 0.44, p = 0.028, and fold change = 0.01, p = 0.022, respectively) were decreased compared to parental cells. However, total levels of the Akt isoform, Akt2, (fold change = 2.31, p = 0.0017) were significantly increased. The phosphorylated levels of the receptor scaffolding protein, Shc, (fold change = 0.41, p = 0.025) and MEK 1/2 (fold change = 0.19, p = 8 x 10^{-4}), a protein involved in the ERK signalling cascade, were decreased. The levels of the anti-apoptotic protein Bcl-2 (fold change = 4.14, p = 0.003) were significantly elevated, along with its activating phosphorylated from (S70) (fold change = 1.78, p = 0.027). Interestingly, the NR4A1 gene, which was found to be amplified in SKBR3-A cells by whole exome sequencing, can increase levels of EGFR and Bcl-2 levels [304].

The highest fold change (fold change = 4.41, p = 0.028) observed in the RPPA analysis was in levels of phosphorylated Src (Y416). Src is an oncogenic kinase that has been implicated in trastuzumab and lapatinib resistance in breast cancer and afatinib resistance in lung cancer [160, 204, 305]. Src is also a druggable target; dasatinib is an FDA-approved Src inhibitor used in the treatment of chronic myelogenous leukaemia and acute lymphoblastic leukaemia [220]. Therefore, Src was chosen as a candidate drug target to overcome afatinib resistance in HER2-positive breast cancer.

Table 6-5: Statistically significant alterations in SKBR3-A compared to SKBR3-Par cells by RPPA analysis.

Decreased protein level			
Antibody	**Phosphorylation site**	**Fold change**	**p value**
p-Akt	T308	0.44	2.8×10^{-2}
p-Shc	Y317	0.41	2.5×10^{-2}
p-HER3	Y1289	0.40	2.6×10^{-3}
p-MEK1/2	S217/221	0.19	8.0×10^{-4}
p-Akt	S473	0.01	2.2×10^{-4}

Increased protein level			
Antibody	**Phosphorylation site**	**Fold change**	**p value**
p-Src	Y416	4.41	2.8×10^{-2}
Bcl-2	-	4.14	3.0×10^{-3}
p53	-	2.46	2.0×10^{-3}
Akt2	-	2.31	1.7×10^{-3}
EGFR	-	2.02	4.3×10^{-2}
p-Bcl-2	S70	1.78	2.7×10^{-2}
p27	-	1.46	4.6×10^{-2}
p-AMPK	T172	1.40	1.5×10^{-2}
p38 MAPK	-	1.38	2.1×10^{-2}

6.3.2.1 Validation of phospho-Src and total EGFR levels in SKBR3-A cells

The increased levels of phospho-Src (Y416) and EGFR in SKBR3-A cells, which were observed by RPPA, were validated by Western blotting (Figure 6-5). Total Src levels were unchanged between the SKBR3-A and parental cell lines (p = 0.51). However, there was a significant increase in phosphorylated Src (Y416) levels (fold change = 2.38, p = 0.04). EGFR levels showed an increase but did not achieve statistical significance (fold change = 3.39, p = 0.08).
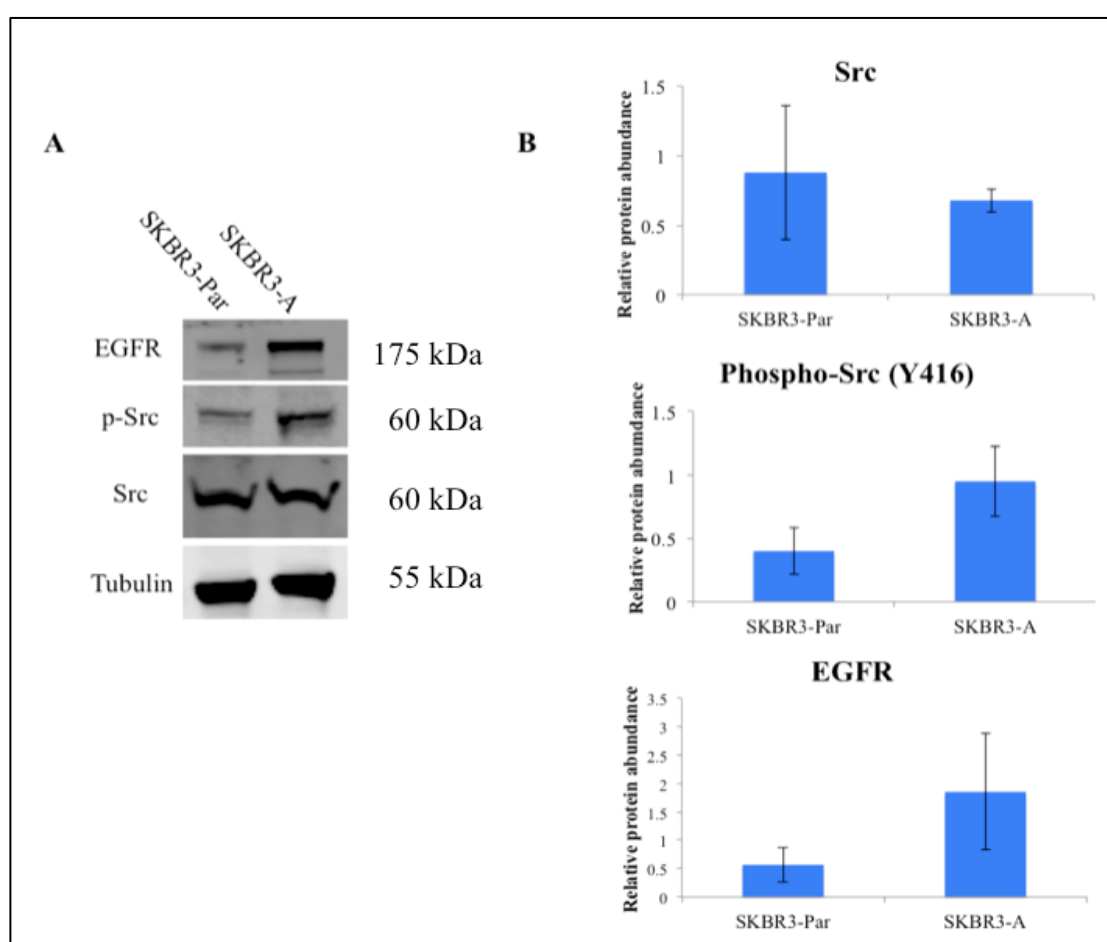
Figure 6-5 (A) Western blotting of SKBR3-Par and SKBR3-A cells for Src and phospho-Src (Y416) and EGFR. Blots shown are representative of triplicate blots. (B) Densitometry analysis of immunoblots of SKBR3-Par and SKBR3-A cells for total and phospho-Src and EGFR. Error bars represent standard deviation of biological triplicate experiments.

6.4 Assessment of SKBR3-A sensitivity to Src inhibition

The effect of the Src inhibitor dasatinib was assessed using a proliferation assay. SKBR3-A cells were moderately more sensitive to dasatinib compared to SKBR3-Par cells, with IC_{50} values of 1718.8 ± 901.8 nM and 2948.7 ± 441.7 nM respectively (Figure 6-6).
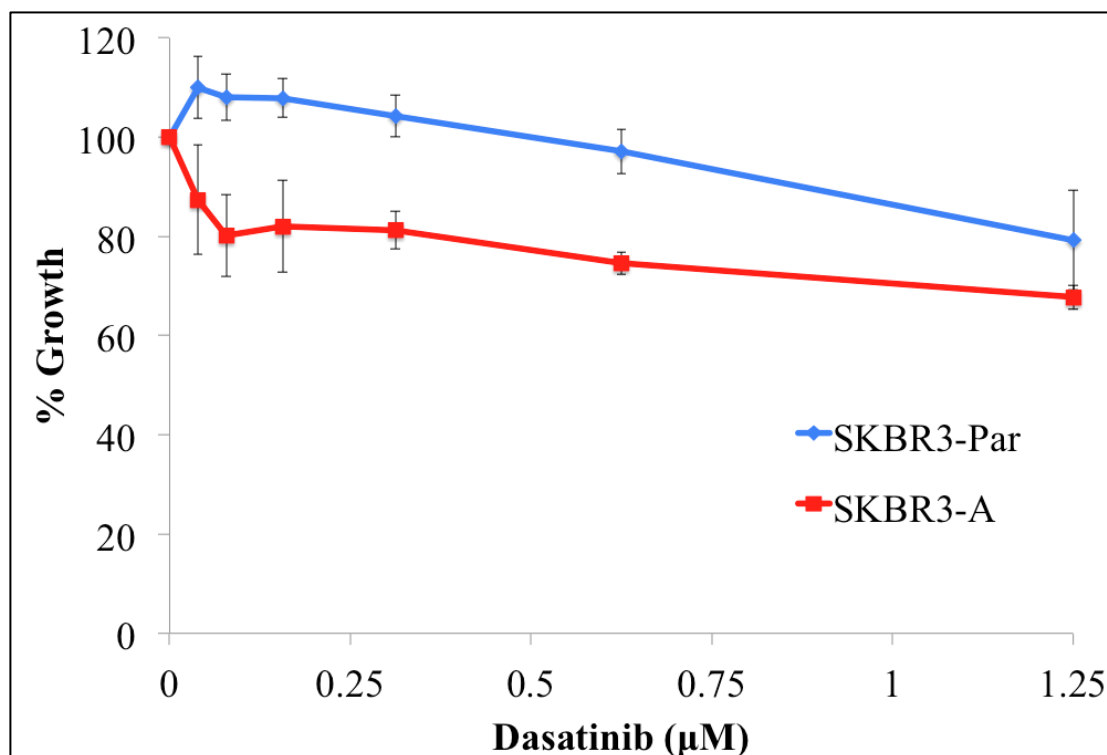
Figure 6-6: Proliferation of SKBR3-Par and SKBR3-A cells following 5-day treatment with dasatinib (0 – 1.25 μM). Percentage growth was calculated relative to untreated control and error bars represent standard deviation of biological triplicate experiments.

6.5 The effect of afatinib and dasatinib on SKBR3-A cells

In order to establish if the addition of Src inhibition would enhance the effect of afatinib, SKBR3-A cells were assessed for sensitivity to afatinib, dasatinib and afatinib plus dasatinib at a 1:2 ratio, in proliferation assays. The combination of afatinib and dasatinib was highly synergistic in SKBR3-A cells (CI value = 0.09 ± 0.06) (Figure 6-7).
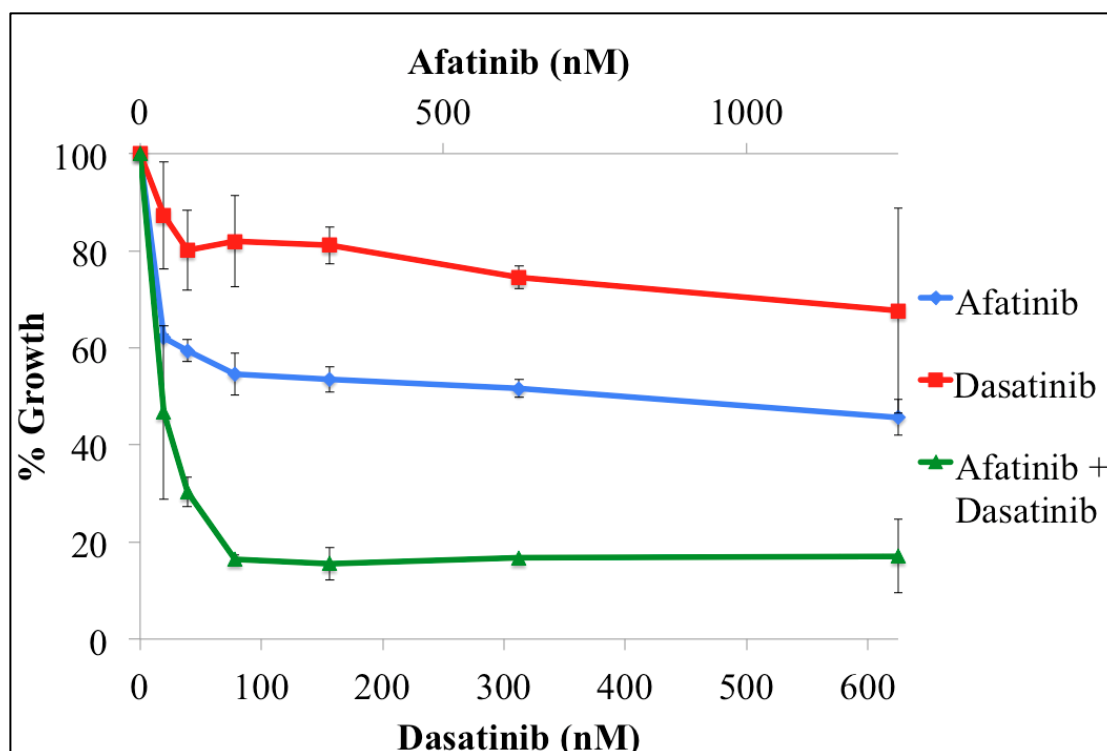
Figure 6-7: A) Proliferation of SKBR3-A cells following 5-day treatment with afatinib (0 – 625 nM), dasatinib (0 – 1250 nM) and 1:2 afatinib:dasatinib combination. Percentage growth was calculated relative to untreated control and error bars represent standard deviation of biological triplicate experiments.

6.5.1 Mechanism of action of afatinib and dasatinib combination in SKBR3-A cells

The anti-cancer effect of afatinib and dasatinib as single agents can occur through cell cycle arrest, apoptosis and/or autophagy [122, 303, 306–309]. Therefore, the combination was tested in SKBR3-A cells using assays for cell cycle apoptosis and autophagy.

6.5.1.1 The effect on cell cycle progression

SKBR3-A cells were treated with afatinib, dasatinib, and the combination to investigate alterations in cell cycle progression, using propidium iodide staining and flow cytometry. There was no significant induction of cell cycle arrest with either

inhibitor, alone or in combination (p values for G1: control v afatinib = 0.51, control v dasatinib = 0.41, control versus combination = 0.09, afatinib versus the combination = 0.36, dasatinib versus combination = 0.08) (Figure 6-8). Likewise, the subG1 population was not significantly changed following treatment. However, afatinib plus dasatinib increased the combined population of SubG1 and G1 (63.8 ± 2.7%) compared to either afatinib (56.5 ± 1.0%, p = 0.03) or dasatinib (48.3 ± 0.7%, p = 0.007) alone.
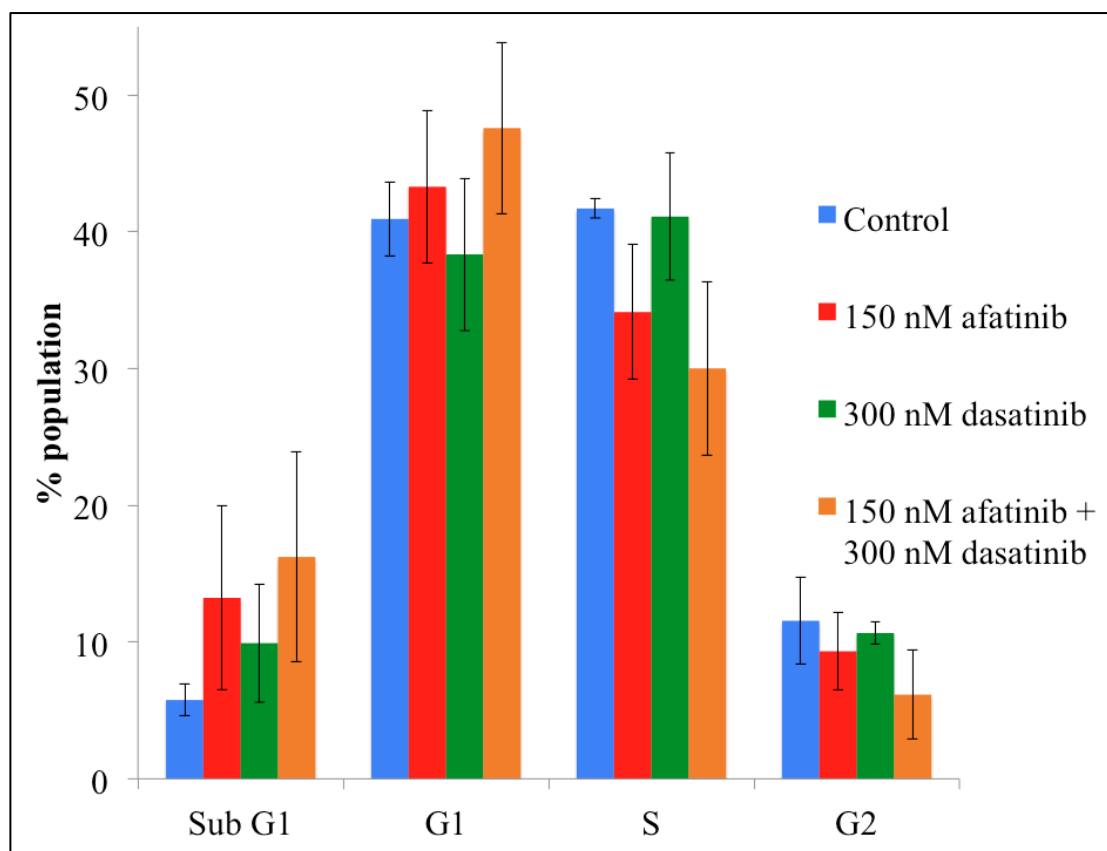
Figure 6-8: Cell cycle assays of SKBR3-A cells treated with afatinib, and/or dasatinib were examined by propidium iodide staining and flow cytometry. Error bars represent standard deviation of biological triplicate assays. The Student's t test was used to determine statistical significance.

6.5.1.2 <u>Apoptosis induction</u>

In order to determine if the combination of afatinib and dasatinib induces apoptosis, SKBR3-A cells treated with afatinib, dasatinib, or the combination were assessed for caspase 3/7 activation after 48 h of drug treatment using the Caspase-Glo 3/7 assay. Afatinib treatment alone resulted in decreased levels of caspase 3/7 activation ($p = 0.004$ compared to DMSO control). The combination of afatinib and dasatinib also decreased caspase 3/7 activation ($p = 0.007$ relative to DMSO), but did not significantly alter caspase 3/7 activity compared to afatinib treatment ($p = 0.3$) (Figure 6-9). The lack of subG1 population increase and caspase 3/7 activation, suggest that afatinib plus dasatinib does not induce apoptotic cell death.
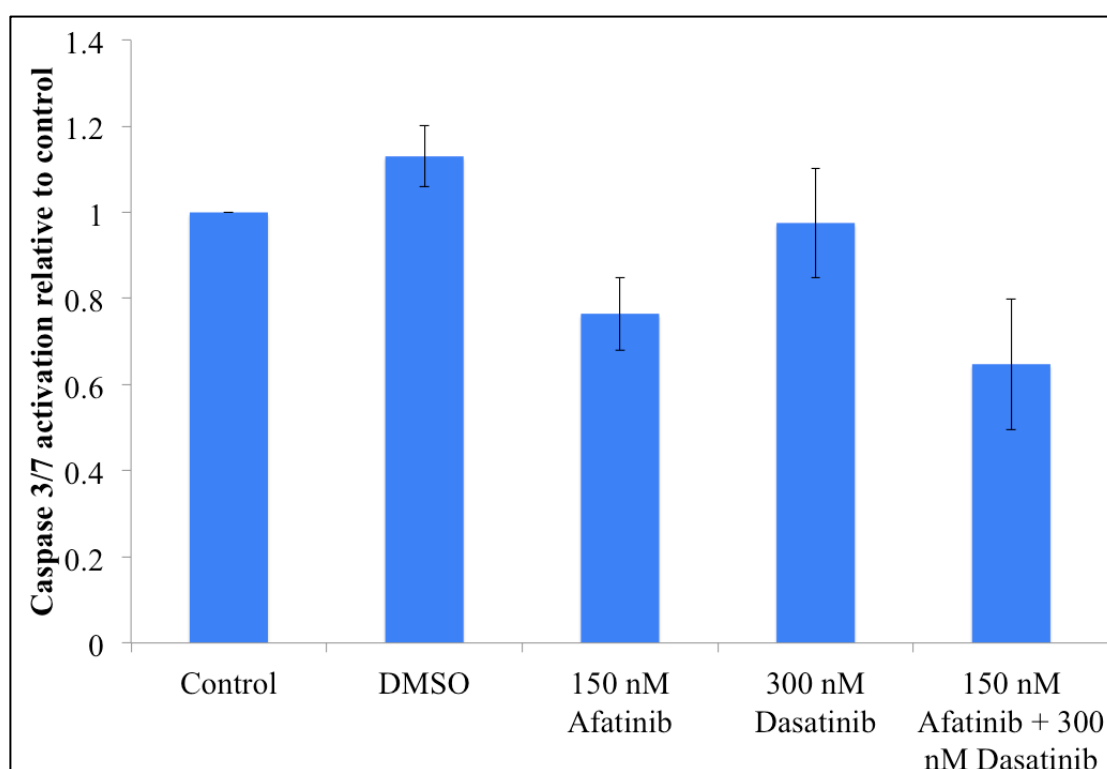
Figure 6-9: Caspase 3/7 activation in SKBR3-A cells following 48 h treatment with 150 nM afatinib, 300 nM dasatinib, or afatinib plus dasatinib. Error bars represent standard deviation of biological triplicate assays. Student's t test was used to determine statistical significance.

6.5.1.3 <u>Autophagy induction</u>

Both afatinib and dasatinib individually, have been shown to induce autophagy in other cell line models [303, 308]. Induction of autophagy was examined by treating SKBR3-A cells with 150 nM afatinib, 300 nM dasatinib or the combination for 2 days. Evidence of autophagy was then examined by fluorescent microscopy and fluorescent photospectrometry. Afatinib treatment alone stimulated a 13% increase in autophagy activity (p = 0.04). However, there was no increase in autophagy levels with the combination of afatinib plus dasatinib compared to afatinib alone (p = 0.21) (Figure 6-10).
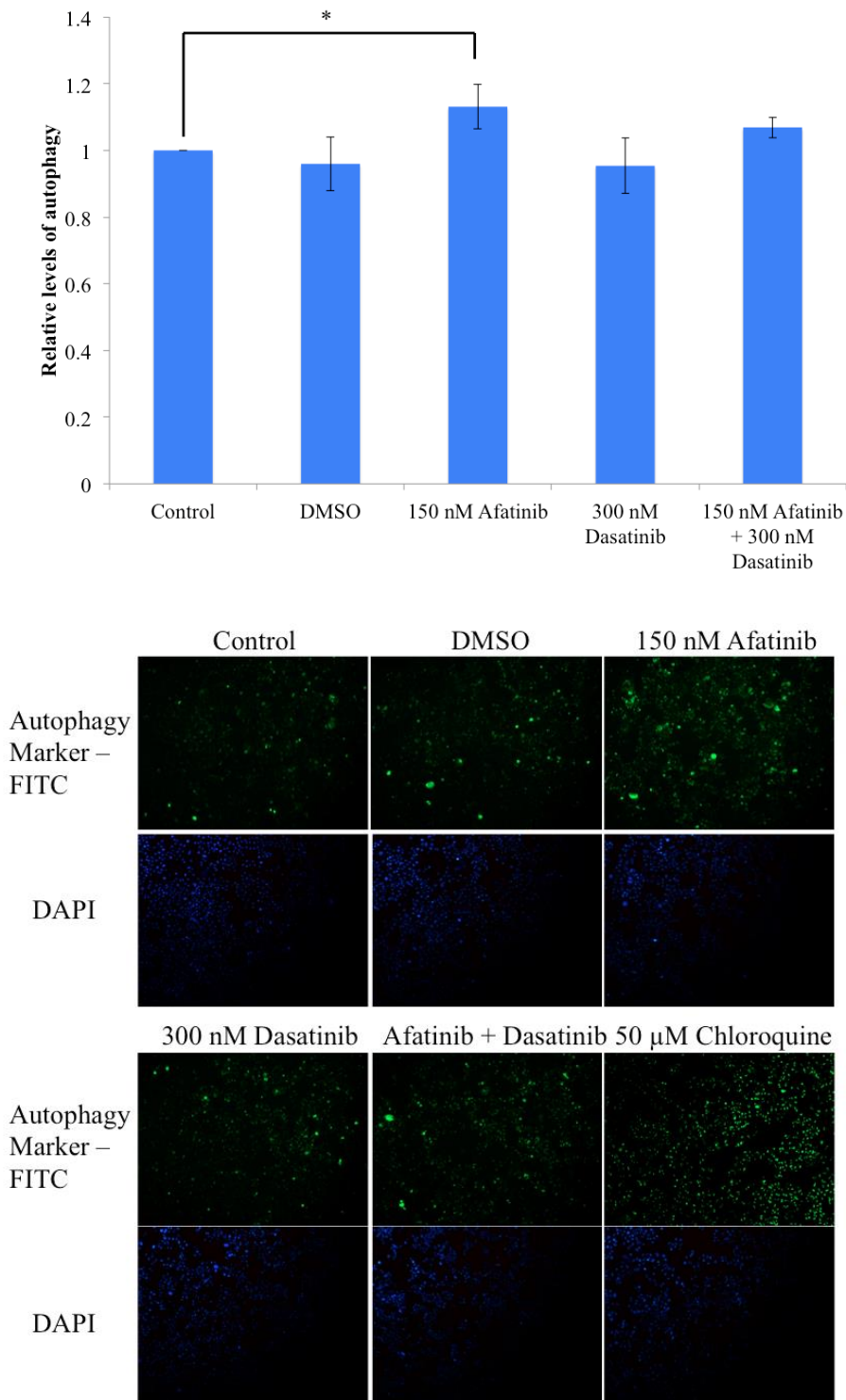
Figure 6-10: Autophagy levels in SKBR3-A cells treated with DMSO, 150 nM afatinib, 300 nM dasatinib, or the combination for 48 h, or 50 μM chloroquine for 24 h measured by fluorescent spectroscopy and immunofluorescence images. Error bars represent standard deviation of triplicate experiments. The Student's t test was used to determine statistical significance. * denotes p < 0.05.

6.5.1.4 <u>Necrosis</u>

Cells undergoing necrosis have been shown to secrete the nuclear protein HMGB1. Apoptotic cells can also passively release HMGB1; however, this is cell line dependent and may rely on DNA deacetylation [310, 311]. Extracellular HMGB1 was found to be elevated 3-fold in conditioned medium of SKBR3-A cells treated with afatinib and dasatinib for 48 h ($p = 0.039$) (Figure 6-11). Secreted HMGB1 levels were not significantly increased by either afatinib or dasatinib alone. This result suggests that afatinib in combination with dasatinib induces necrosis rather than apoptosis or autophagy.
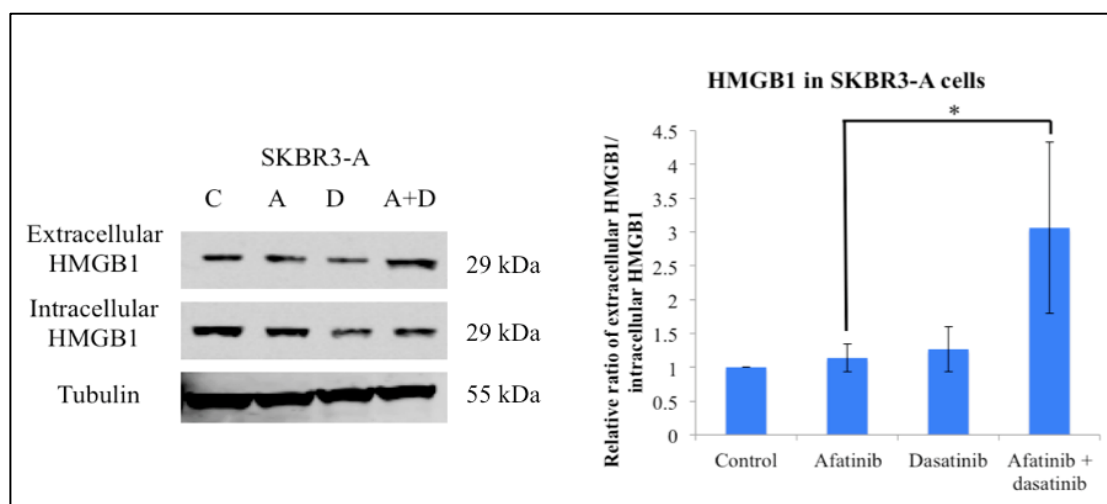
Figure 6-11: Western blotting of extracellular and intracellular HMGB1 in SKBR3-A cells treated with 150 nM afatinib, 300 nM dasatinib, afatinib plus dasatinib. Densitometry was carried out on triplicate assays. Blots shown are representative of triplicate blots. Tubulin was used as a loading control. The Student's t test was used to determine statistical significance. Error bars represent standard deviation of biological triplicate experiments. * denotes p < 0.05.

6.6 Assessment of afatinib plus dasatinib in other HER2-targeted therapy resistant cell lines

6.6.1 Afatinib plus dasatinib in trastuzumab-resistant cell lines

We have shown that Src is a potential mediator of afatinib resistance. Src has previously been implicated in trastuzumab and lapatinib resistance [160, 305]. Therefore, we hypothesised that afatinib-sensitive HER2-targeted therapy-naïve and trastuzumab-resistant cells may have an improved response to the combination of afatinib and dasatinib. A panel of trastuzumab-resistant cell lines (SKBR3-T, BT474-T, EFM192A-T) and their parental cells (SKBR3-Par, BT474, EFM192A) were assessed for sensitivity to afatinib and dasatinib. All six cell lines were highly sensitive to afatinib, with IC_{50} values < 20 nM (Table 6-6). Dasatinib was ineffective as a single agent; an IC_{50} value was not reached at 160 nM dasatinib in any of the six cell lines. Three of the six cell lines showed no growth inhibition with 160 nM dasatinib alone. BT474 cells were most sensitive to dasatinib with $68.2 \pm 7\%$ growth following treatment with 160 nM dasatinib. The trastuzumab resistant variant, BT474-T, was less sensitive to 160 nM dasatinib, with $91.5 \pm 10.1\%$ growth. The combination of afatinib and dasatinib did not enhance response to afatinib in the cell lines tested (Figure 6-12). However, SKBR3-T cell did show a small additive effect at 40 and 80 nM ($p = 0.008$ and 0.001, respectively).

Table 6-6: Afatinib IC_{50} values for trastuzumab-resistant and parental cell lines.

Afatinib IC_{50} values (nM)					
SKBR3-Par	SKBR3-T	BT474	BT474-T	EFM192A	EFM192A-T
6.6 ± 0.4	14.4 ± 1.9	4.3 ± 1.4	2.8 ± 1.5	8.4 ± 6.2	12.9 ± 5.1
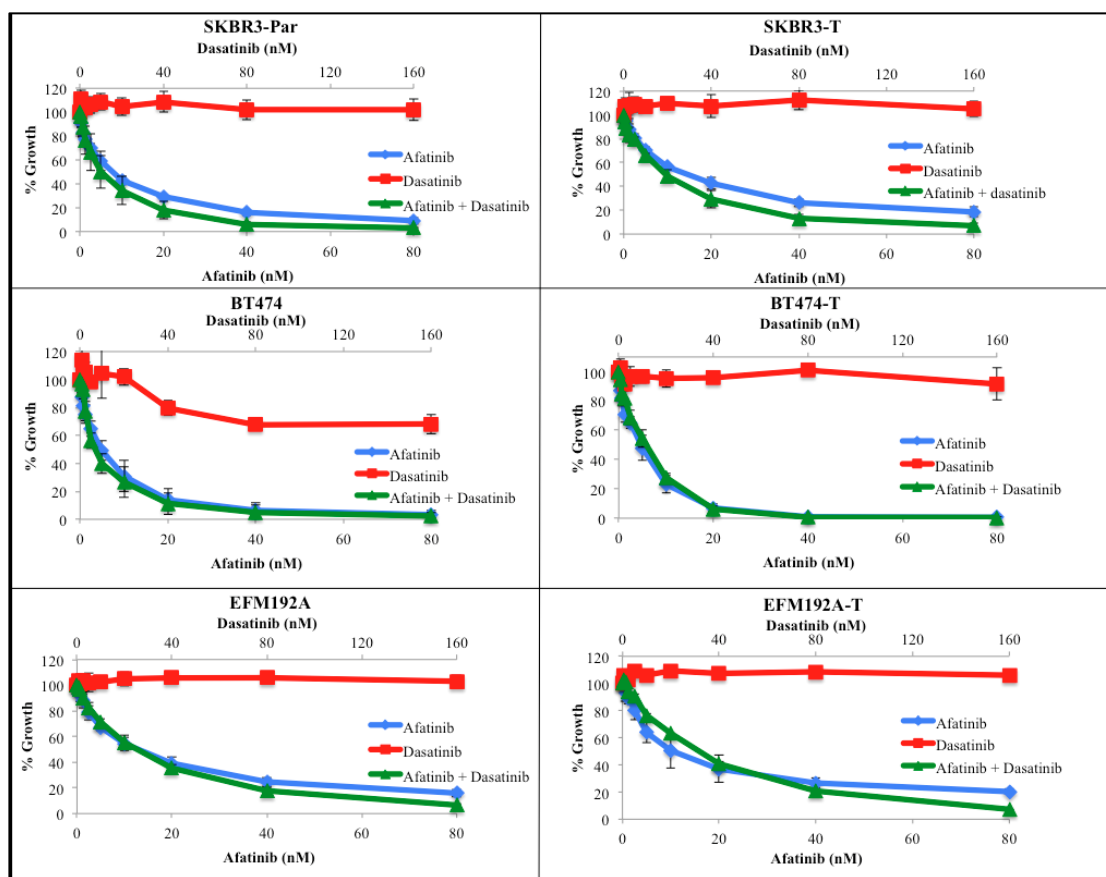
Figure 6-12: Proliferation of SKBR3-Par, SKBR3-T, BT474, BT474-T, EFM192A, and EFM192A-T with afatinib, dasatinib, and afatinib plus dasatinib treatment. Error bars represent standard deviation of biological triplicate experiments.

6.6.2 Afatinib plus dasatinib in lapatinib-resistant cell lines

As was previously shown, SKBR3-L cells are 13.9-fold less sensitive to afatinib compared to controls (Table 3-1). SKBR3-L cells are resistant to dasatinib (IC_{50} value > 10 μM). However, SKBR3-L cells showed enhanced response to the combination of afatinib and dasatinib similar to SKBR3-A cells (CI value = 0.12 ± 0.4) (Figure 6-13). This suggests the afatinib plus dasatinib combination could also be effective in lapatinib-refractory breast cancer.
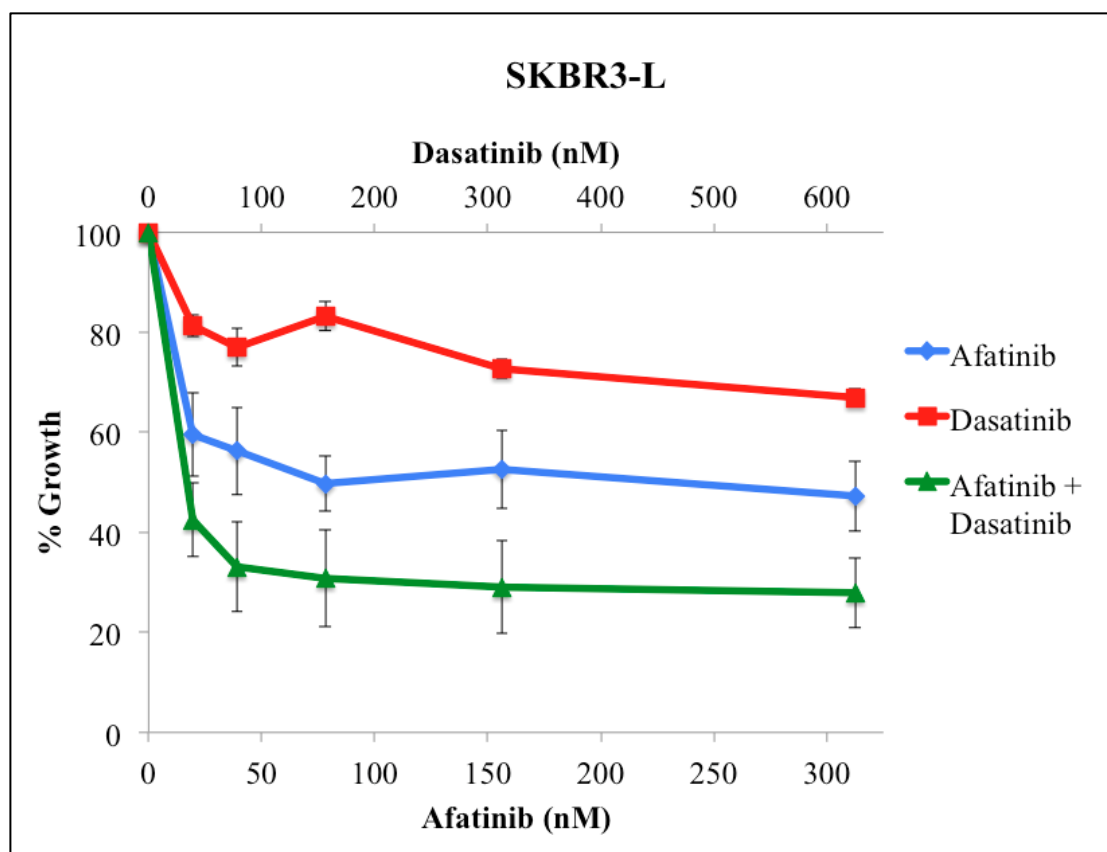
Figure 6-13: Proliferation of SKBR3-L cells treated with afatinib, dasatinib, or afatinib plus dasatinib. Error bars represent standard deviation of triplicate experiments.

6.7   Afatinib plus dasatinib in the prevention of afatinib resistance development

Although afatinib plus dasatinib did not enhance the effect of afatinib alone in the SKBR3, BT474, or EFM192A cell lines or the trastuzumab-resistant variants, the combination may have longer-term anti-cancer effects. Therefore, in order to assess if afatinib plus dasatinib can improve long term response to afatinib and prevent the development of afatinib resistance, the parental and resistant cell lines were treated twice weekly with 75 nM afatinib, 150 nM dasatinib, or the combination (as described in Section 2.9) (Figure 6-14 and 6-15). The concentrations chosen for afatinib and dasatinib are close to peak plasma levels [295, 312] and follow the 1:2 ratio that was used in five-day proliferation assays.

All cell lines were highly sensitive to 75 nM afatinib, with   all but the HCC1954 cell line achieving greater than 80% growth inhibition after two weeks. Untreated SKBR3, BT474, EFM192A, SKBR3-T and BT474-T cells became confluent at 14 days. At this point, the afatinib plus dasatinib treatment did not enhance growth inhibition compared to afatinib alone. Likewise, after 28 days when dasatinib treated cells became confluent, no difference was observed between afatinib alone and the combination. However, after 70 days of treatment, EFM192A, SKBR3, and SKBR3-T cells developed resistance to afatinib (% growth with afatinib = $20.5 \pm 1.0\%$, $20.5 \pm 6.2\%$, $14.3 \pm 4.3\%$ compared to $1.6 \pm 1.7\%$, $2.4 \pm 2.0\%$, and $3.2 \pm 2.1\%$, respectively). The BT474 cell lines did not develop resistance after 70 days. The % growth with afatinib was $3.9 \pm 0.6\%$ and $3.8 \pm 0.5\%$ with afatinib plus dasatinib in the BT474-T cell line.

HCC1954 cells displayed a synergistic response to afatinib plus dasatinib in 5-day proliferation assays. Therefore, these cells were also treated twice weekly with afatinib and dasatinib for longer-term treatment (Figure 6-14). Control cells became confluent after 7 days, with afatinib treatment causing a $58.3 \pm 6.9\%$ growth reduction. The second plate was treated for a further 7 days. The afatinib-treated cells were spread out, however, were at $38.9 \pm 13.7\%$ growth level of the untreated control cells at day 7. Importantly, afatinib plus dasatinib treated cells had $8.4 \pm 5.9\%$ growth relative to control at day 7, and this growth level was maintained until day 14 ($3.7 \pm 1.5\%$).
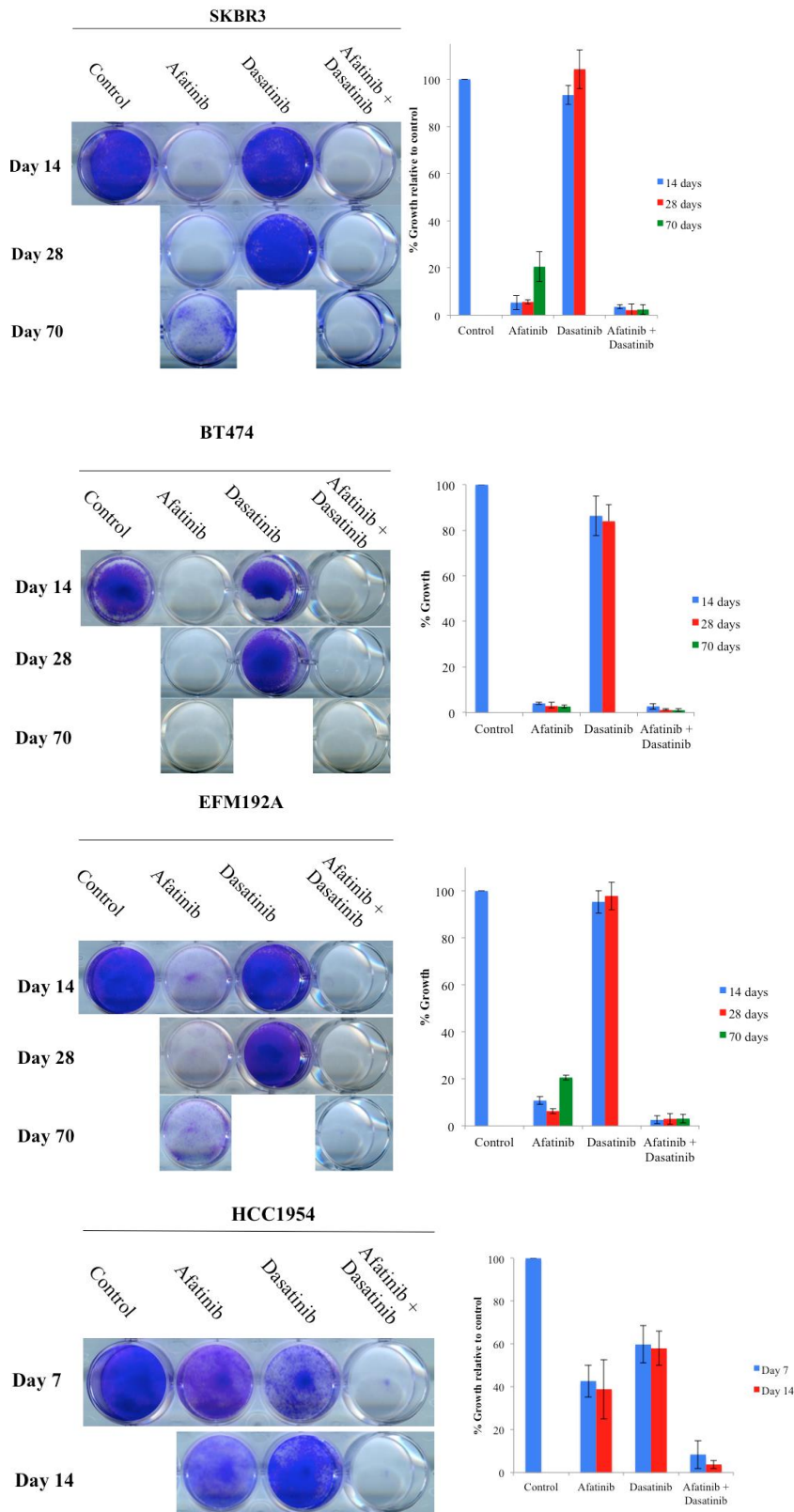
Figure 6-14: SKBR3, BT474, EFM192A, and HCC1954 cells were treated with 75 nM afatinib, 150 nM dasatinib, or afatinib plus dasatinib twice weekly until

untreated control cells became confluent (Plate 1) [each row represents one plate], dasatinib-treated cells became confluent (Plate 2), and afatinib-treated cells became confluent (Plate 3). Each image is representative of three biological assays.
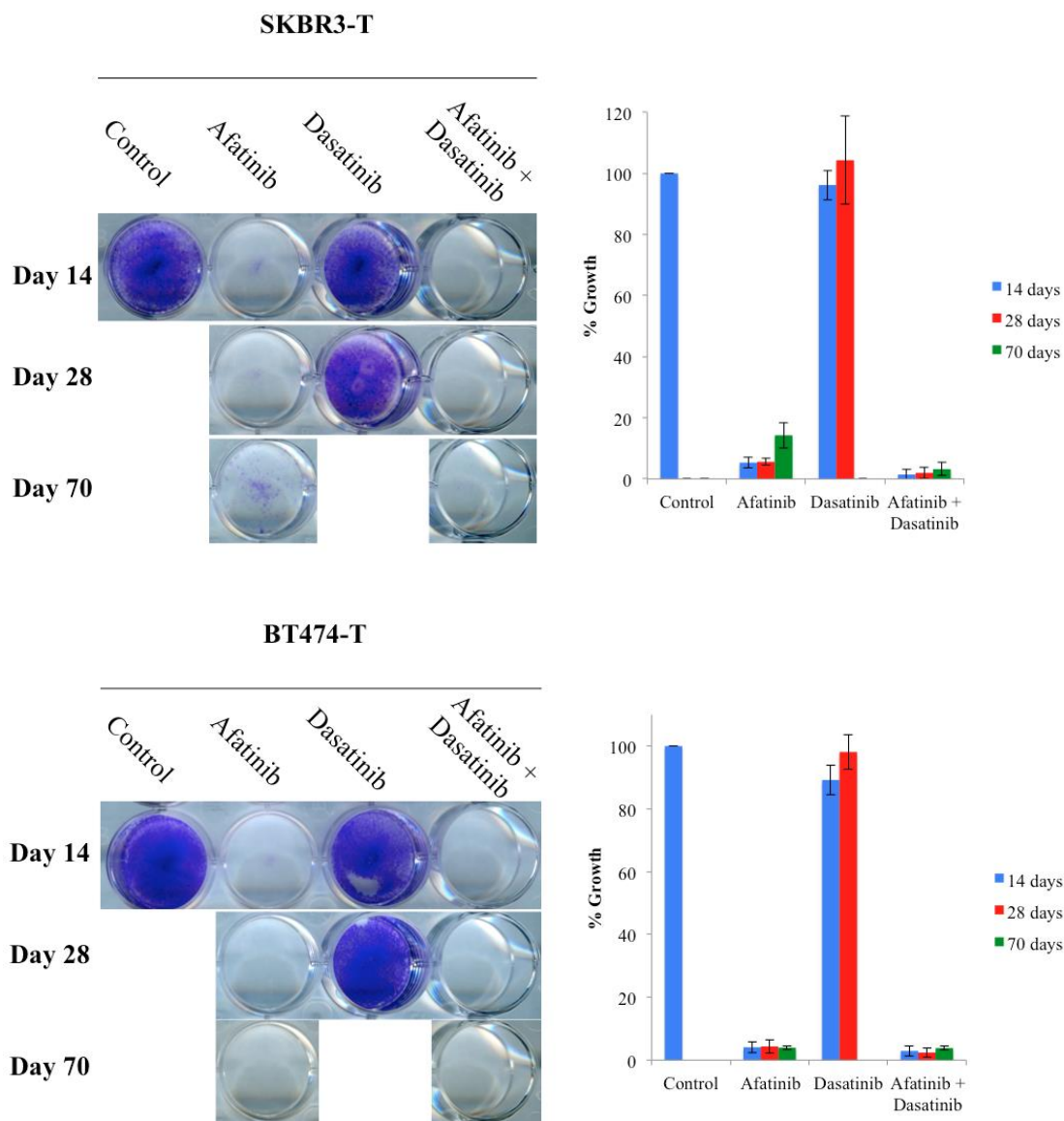
Figure 6-15: SKBR3-T and BT474-T cells were treated with 75 nM afatinib, 150 nM dasatinib, or afatinib plus dasatinib twice weekly until untreated control cells became confluent (Plate 1), dasatinib-treated cells became confluent (Plate 2) and afatinib-treated cells became confluent (Plate 3). Each image is representative of three biological triplicate assays.

6.8 The role of Src in neratinib resistance

6.8.1.1 Acquired neratinib resistant cell line

In order to test if the combination effect of afatinib and dasatinib was specific to afatinib, and as neratinib has now been approved for early-stage HER2-positive disease, the combination of neratinib and dasatinib was examined in a neratinib resistant model. The HCC1954-N cell line was developed by Dr. Susan Breslin and Prof. Lorraine O'Driscoll, Trinity College Dublin, by treating HCC1954 cells with 250 nM neratinib three times per week for 6 months, and gifted to the NICB. HCC1954-N cells were resistant to neratinib with an IC_{50} value of 781.8 ± 142.7 nM compared to 26.1 ± 1.2 nM for HCC1954-Par (Figure 6-16 A). Similar to the lapatinib and afatinib resistant cell lines, HCC1954-N cells were cross-resistant to the other tyrosine kinase inhibitors (Figure 6-16 B and C).
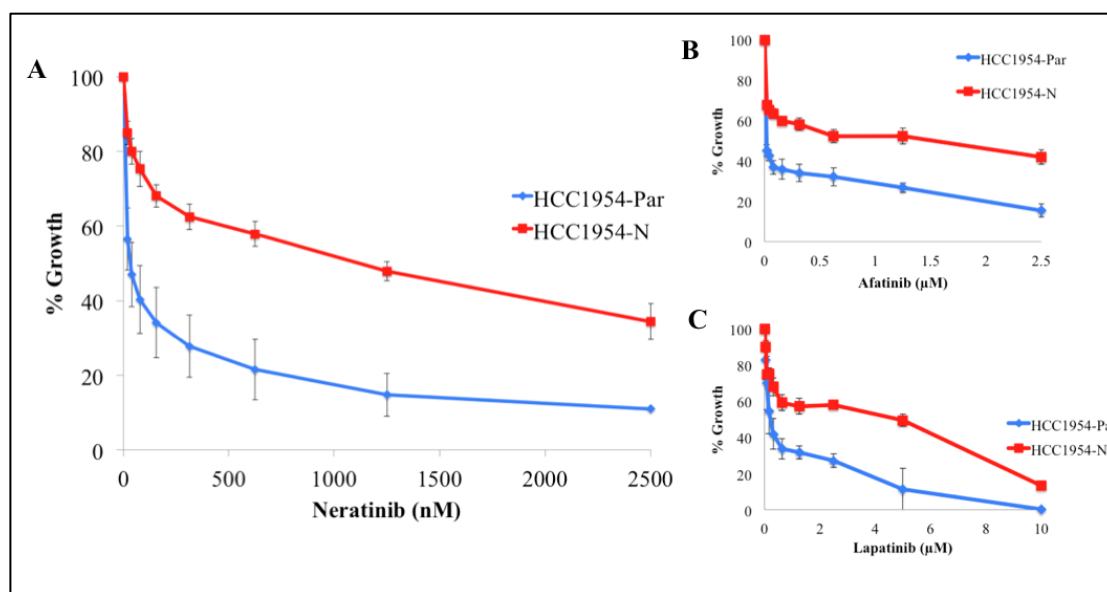
Figure 6-16: Proliferation of HCC1954-Par and HCC1954-N cells following 5 days of treatment with A) neratinib (0 – 2.5 μM), B) 0-2.5 μM afatinib, and C) 0-10 μM lapatinib. Error bars indicate standard deviation of triplicate biological experiments.

6.8.2 Dasatinib sensitivity in HCC1954-Par and HCC1954-N cells

The effect of dasatinib on HCC1954-Par and HCC1954-N cells was assessed by 5-day proliferation assays using the acid phosphatase method. HCC1954-N cells were less sensitive to dasatinib compared to HCC1954-Par cells. The dasatinib IC_{50} value for the HCC1954-N cells was 2086.2 ± 2324.9 nM and was 681.3 ± 170.8 nM for HCC1954-Par cells. However, dasatinib in combination with neratinib was highly synergistic in both parental (CI value = 0.09 ± 0.1) and resistant (CI value = 0.1 ± 0.03) cells (Figure 6-17 and Figure 6-18).

Neratinib and dasatinib were also assessed, as single agents and in combination, in HCC1954-N cells under 3D growth conditions. HCC1954-N cells were significantly more sensitive to neratinib in 3D conditions compared to 2D assays (IC_{50} value in 3D = 29.6 ± 3.9 versus 781.8 ± 142.7 nM in 2D). HCC1954-N cells were slightly more resistant to dasatinib in 3D culture (IC_{50} value in 3D = 3.1 ± 0.4 µM compared to 2.1 ± 2.3 µM in 2D). However, the combination of neratinib and dasatinib was also synergistic in 3D (CI value = 0.36 ± 0.02) (Figure 6-19).
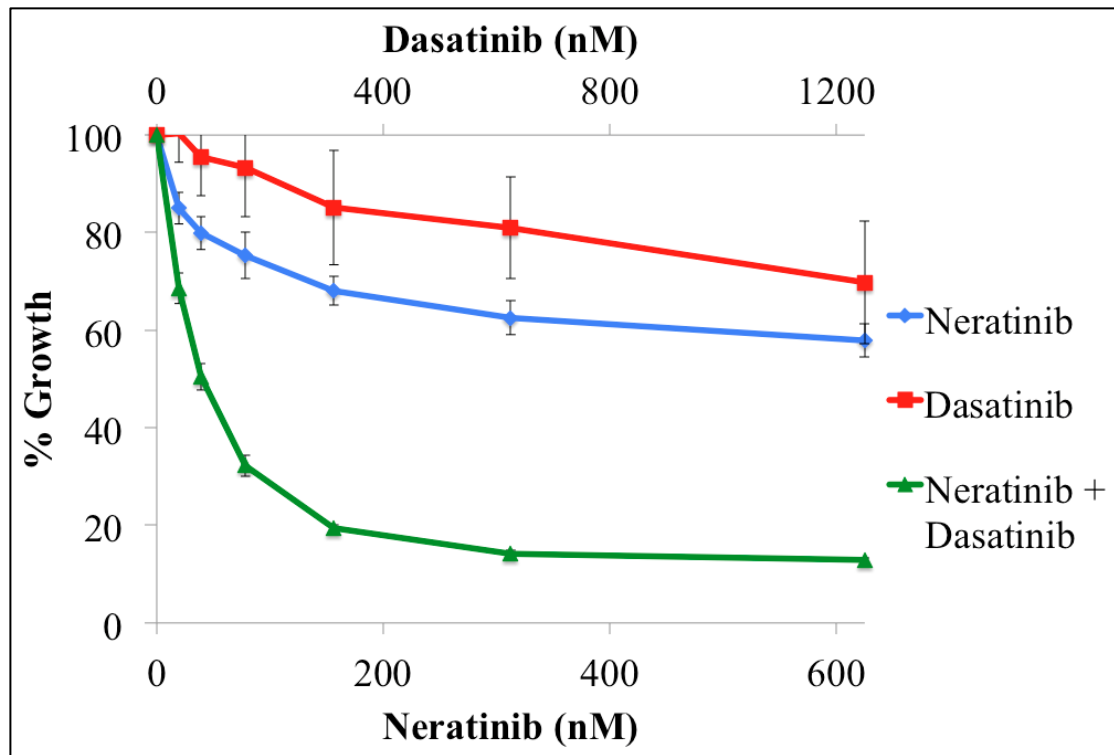
Figure 6-17: 2D acid phosphatase proliferation assays of HCC1954-N cells following 5 days of treatment with neratinib (0 – 625 nM), dasatinib (0 – 1250 nM), and 1:2 neratinib plus dasatinib. Error bars indicate standard deviation of triplicate biological experiments.
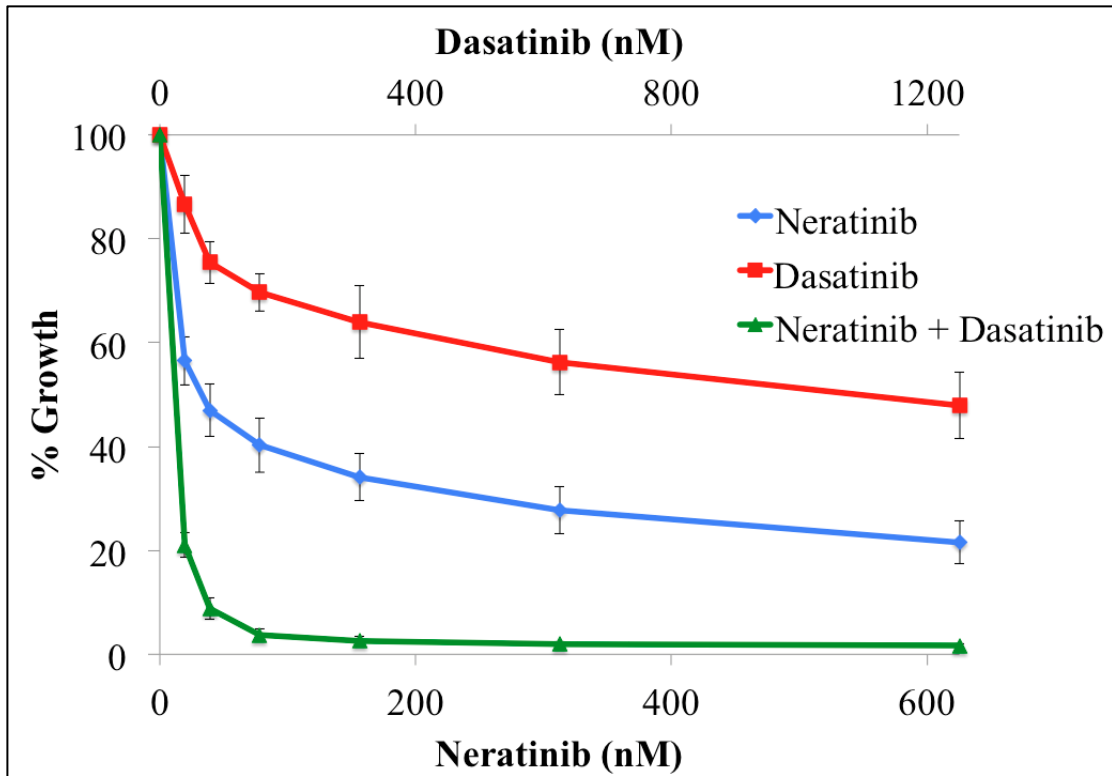
Figure 6-18: 2D acid phosphatase proliferation of HCC1954-Par cells following 5 days of treatment with neratinib (0 – 625 nM), dasatinib (0 – 1250 nM), and 1:2 neratinib plus dasatinib. Error bars indicate standard deviation of triplicate biological experiments.
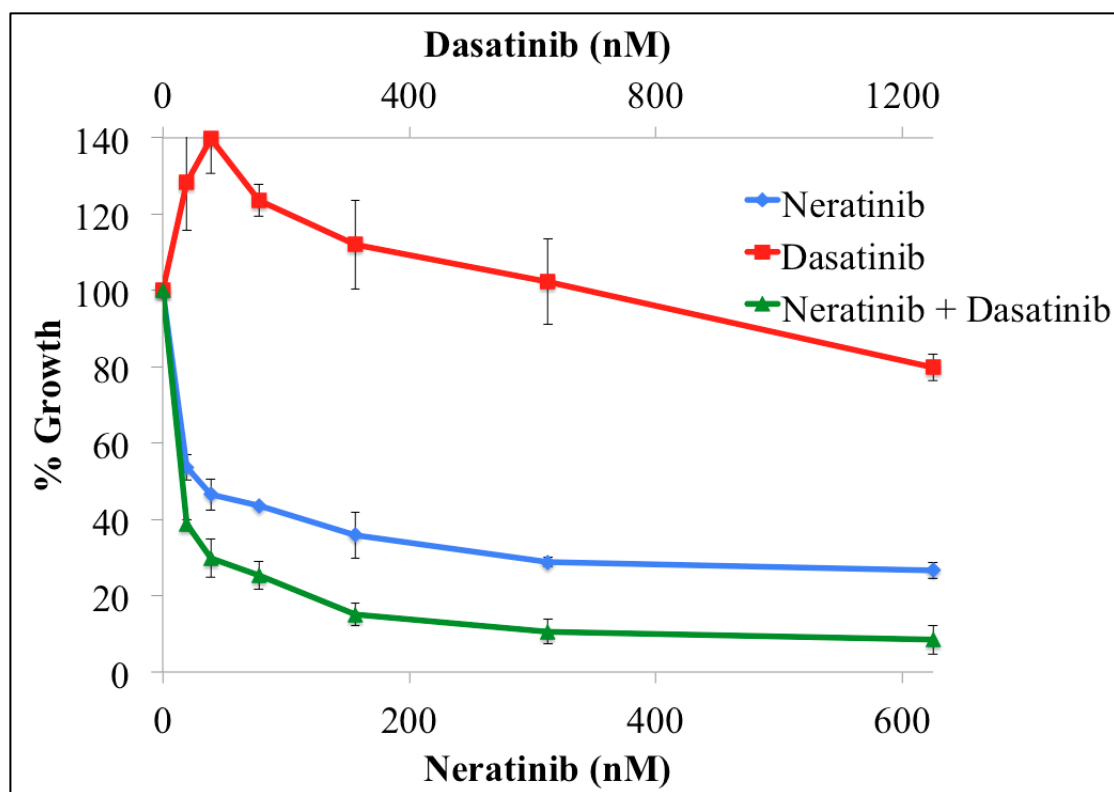
Figure 6-19: Proliferation of HCC1954-N cells, grown in 3D suspension in 4% Matrigel, following 7 days of treatment with neratinib (0 – 625 nM), dasatinib (0 – 1250 nM), and 1:2 neratinib plus dasatinib. Error bars indicate standard deviation of triplicate biological experiments.

6.8.3 Mechanism of cell death by neratinib and dasatinib

The induction of apoptosis by neratinib and dasatinib was examined in the HCC1954-N cells by investigating caspase 3/7 activation and by cell cycle analysis. Cell cycle analysis showed a highly significant increase in the sub G1 population in cells treated with the combination ($61.7 \pm 8.3\%$) compared to neratinib ($11.4 \pm 1.3\%$, $p = 0.018$) and dasatinib ($11.9 \pm 1.3\%$, p value $= 0.013$) (Figure 6-20). Both neratinib and dasatinib increased caspase 3/7 activity compared to control cells ($p = 0.04$ and 0.006, respectively). Neratinib plus dasatinib caused a significant increase in caspase 3/7 activation compared to both single agents ($p = 7 \times 10^{-5}$ relative to neratinib treatment, and 0.015 compared to dasatinib) (Figure 6-21).
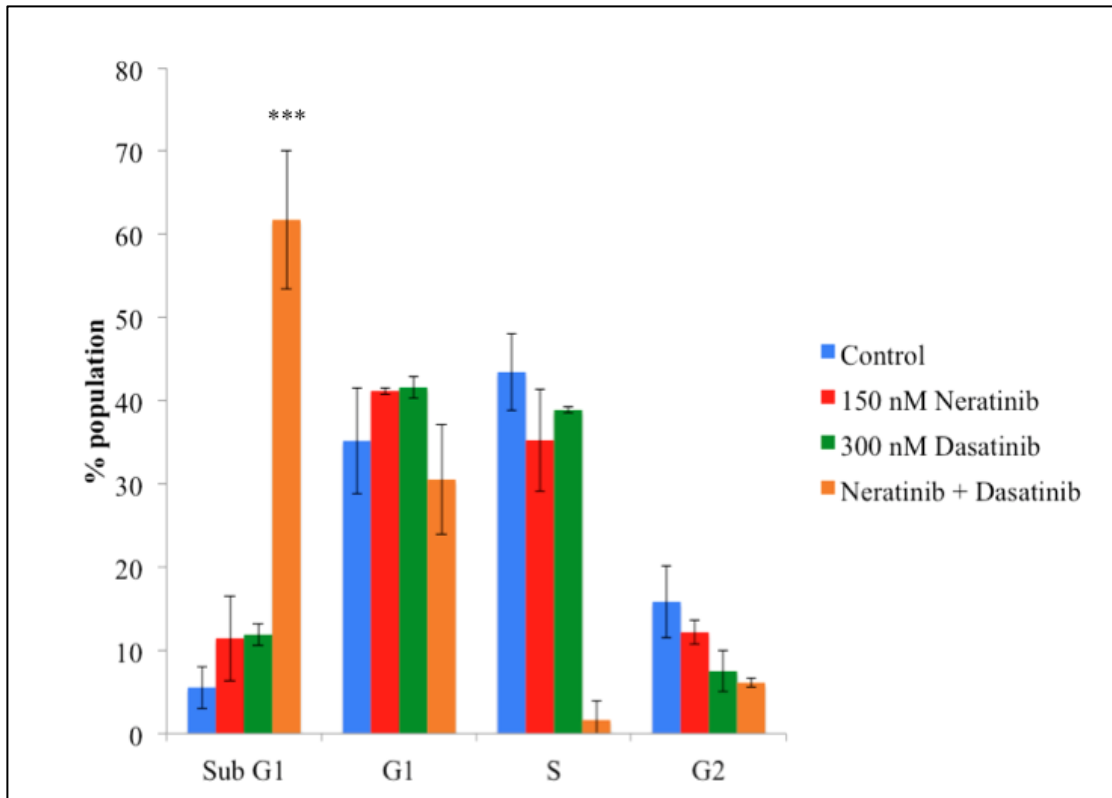
Figure 6-20: Cell cycle analysis was carried out on HCC1954-N cells treated with 150 nM neratinib, 300 nM dasatinib, and neratinib plus dasatinib for 72 h. Error bars represent standard deviation of biological triplicate experiments. The Student's t test was used to determine statistical significance. *** denotes a p value of < 0.001.
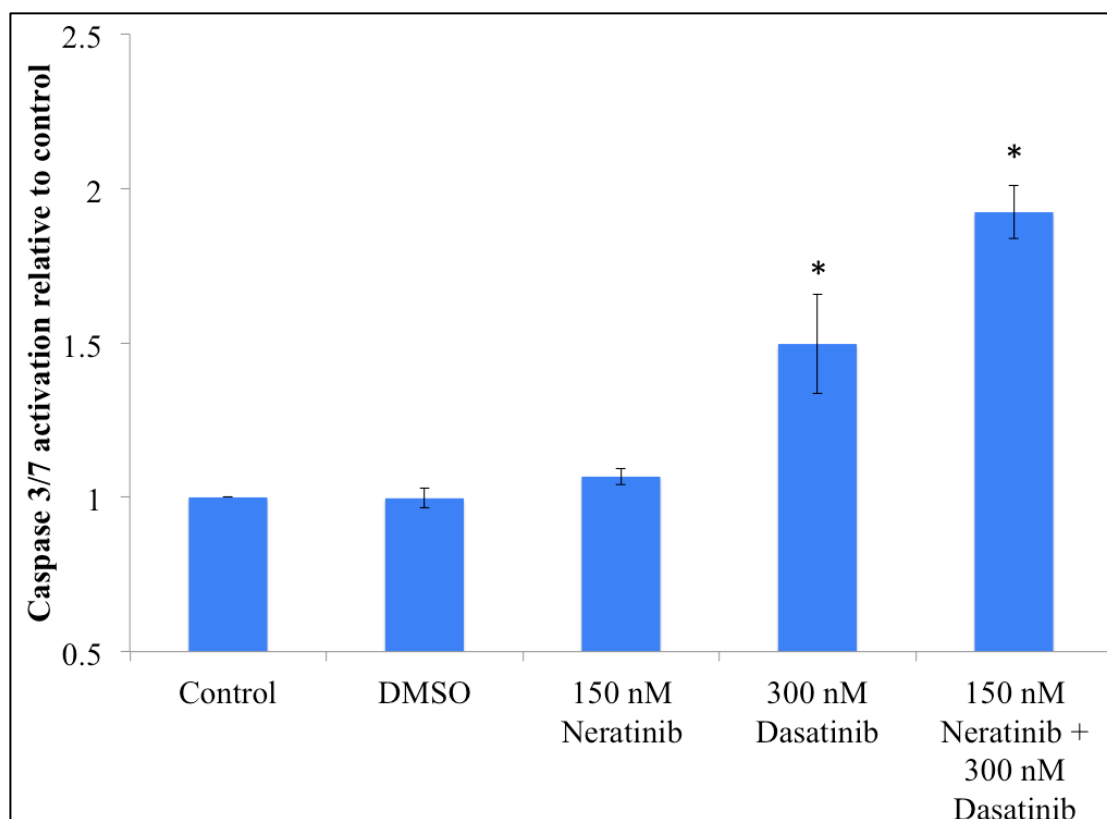
Figure 6-21: Caspase 3/7 activation in HCC1954-N cells treated with 150 nM neratinib, 300 nM dasatinib, and neratinib plus dasatinib. Error bars represent standard deviation of triplicate experiments. The Student's t test was used to determine statistical significance. * denotes p < 0.05.

6.9 Summary

Afatinib-sensitive cells developed resistance to afatinib following long-term treatment. SKBR3-A cells were cross-resistant to the HER2-targeted therapies trastuzumab, pertuzumab, lapatinib and neratinib. The SKBR3-A cell line showed alterations in key signalling pathways including down-regulation of Akt and MEK 1/2 activity and an up-regulation of EGFR levels and Src activity. The SKBR3-A cell line displayed multiple genetic changes. There were 168 unique CNVs, 34 SNVs with protein structural implications, and 1 frameshift InDel in a protein-coding region. These adaptations indicate the possibility of EMT and an increase in autophagy-related proteins. Interestingly, afatinib treatment increased levels of autophagy in SKBR3-A cells.

Src was selected as a therapeutic target to overcome afatinib resistance, as Src has previously been implicated in trastuzumab and lapatinib resistance and can be inhibited by the FDA-approved drug dasatinib. SKBR3-A cells were modestly more sensitive to dasatinib than the SKBR3-Par cells. Afatinib plus dasatinib was strongly synergistic in SKBR3-A cells. The effect of afatinib plus dasatinib was independent of apoptosis and autophagy and may be due to induction of necrosis.

The combination of afatinib plus dasatinib was tested in other models of HER2-targeted therapy resistance. SKBR3-L cells had reduced sensitivity to afatinib and were innately resistant to dasatinib. Nonetheless, strong synergy was observed with the combination. The trastuzumab-resistant cell lines, SKBR3-T, BT474-T, and EFM192A-T cells, were exquisitely sensitive to afatinib and did not show enhancement with five-day combination treatment. However, longer term treatment with afatinib and dasatinib prevented afatinib resistance development in SKBR3-T cells. This was also observed in SKBR3, EFM192A, and HCC1954 cells.

The synergy of pan-HER inhibition and Src inhibition was also replicated in the neratinib resistant HCC1954-N model. HCC1954-N cells were highly sensitive to neratinib plus dasatinib in 2D acid phosphatase assays and 3D growth assays.

The combination of afatinib or neratinib plus dasatinib showed promise in HER2-positive breast cancer *in vitro*, in both HER2-targeted therapy naive and resistant cell lines. Afatinib plus dasatinib overcame afatinib resistance, prevented afatinib resistance development in three of four treatment naive and one of two trastuzumab resistant cell lines, and showed efficacy against lapatinib resistant cells.

7 Discussion

7.1 Introduction

There are five HER2-targeted therapies approved for the treatment of HER2-positive breast cancer [34–36, 39, 313]. However, the optimal treatment window and order of HER2-targeted therapies has been a much debated topic and the emergence of resistance to these therapies is a significant issue. HER2-targeted therapy has dramatically improved the prognosis of patients with HER2-positive breast cancer, especially in early-stage disease. The disease-free survival rate after three years for patients with early-stage HER2-positive breast cancer treated with trastuzumab and pertuzumab is 92%, and for patients with node negative disease that increases to 97.5% [314]. The addition of neratinib to this setting may also further improve the disease-free survival of those patients [294]. There have also been incredible advances in the metastatic setting; median survival for patients with metastatic HER2-positive breast cancer with trastuzumab plus pertuzumab in the CLEOPATRA trial was 56.5 months [67]. The use of lapatinib plus capecitabine or T-DM1 provides additional second- or third-line therapy for these patients. Nonetheless, unfortunately, the majority of these patients still die of their disease. Therefore, there is a clinical need for novel treatment options for metastatic HER2-positive breast cancer patients. The aim of this study was to examine the mechanisms of resistance to currently approved HER2-targeted therapies and to identify novel therapies for those patients whose disease no longer respond to HER2-targeted agents.

7.2 Cross-resistance to HER2-targeted therapies

In vitro assessment of the sensitivity of cell line models of HER2-targeted therapy resistant breast cancer to HER-family targeting monoclonal antibodies (trastuzumab and pertuzumab), and TKIs (lapatinib, afatinib and neratinib) provides pre-clinical evidence that may inform the order in which HER2-targeted therapies should be administered and also allows evaluation of cross-resistance that may emerge following specific HER2 targeted therapies. The three trastuzumab-resistant cell lines tested in this study were sensitive to afatinib, with IC_{50} values < 20 nM (Figure 6-12). Trastuzumab-resistant cell lines have previously been shown to be sensitive to the irreversible pan-HER inhibitors afatinib neratinib, and dacomitinib [108, 123, 315]

The TKI sensitivity in trastuzumab-resistant cells indicates that the irreversible TKIs could be active as a second-line therapy in metastatic disease after cells become refractory to trastuzumab, similar to lapatinib. Clinical examination of neratinib in the ExteNET trial showed that neratinib enhanced the clinical benefit when given after adjuvant trastuzumab in early-stage HER2-positive breast cancer and showed a 2.3% improvement in 2-year iDFS in a sub-population that had developed trastuzumab resistance [294]. Likewise, afatinib showed some single agent clinical benefit in a trastuzumab-refractory setting. In a phase II clinical trial afatinib monotherapy 46% of patients achieved clinical benefit, with 10% PR [128].

Trastuzumab is given as first-line therapy for metastatic breast cancer and, following the results of the CLEOPATRA trial, pertuzumab may soon be added to first-line trastuzumab as standard-of-care [275, 316]. In this study, the effectiveness of trastuzumab, pertuzumab or the dual combination was assessed in HER2-targeted therapy naive cells and cells with acquired lapatinib or afatinib resistance. The combination of the HER2 antibodies can have an additive anti-proliferative effect, which was seen in the SKBR3-Par cells (Figure 3-3). This was previously observed in BT474 cells, which are also innately sensitive to trastuzumab alone [66]. Notably, however, the combination had no effect on the innately trastuzumab-resistant cell line HCC1954-Par. This was also found in both the SKBR3-L and HCC1954-L cell lines (Figures 3-3 and 3-4). A caveat to this observation is that only the anti-proliferative effect of the antibody combination was assessed here. In another study, the innately trastuzumab- and lapatinib-resistant JIMT-1 cells were shown to be more sensitive to trastuzumab plus pertuzumab due to an increase in NK cell mediated ADCC [317].

Both acquired lapatinib resistant cell lines also had reduced sensitivity to the irreversible pan-HER inhibitors afatinib and neratinib (Figure 3-2). The HCC1954-L cell line was cross-resistant to afatinib and neratinib at reported maximum plasma concentrations (80 nM and 150 nM respectively). The SKBR3-L cells achieved an afatinib IC_{50} value greater than the resistance cut-off. However, the neratinib IC_{50} value was below the cut-off but was still 22.7-fold less sensitive to neratinib (Table 7-1). This result is also consistent with the clinical evidence of reduced effectiveness of neratinib in lapatinib-refractory breast cancer compared to lapatinib-naive disease [114]. In a phase I/II clinical trial, the ORR with neratinib treatment was 64% for the

lapatinib-naïve and 57% for the lapatinib pre-treated patients, with median PFS of 40.3 and 35.9 weeks, respectively. Likewise, in clinical investigation of afatinib plus vinorelbine versus trastuzumab plus vinorelbine, the afatinib-containing regimen did not show superiority in trastuzumab- or lapatinib-refractory breast cancers [318]. The LUX-Breast 3 clinical trial of afatinib plus vinorelbine versus the investigator's choice of therapy demonstrated the investigator's choice had a higher PFS and patient benefit rate [129].

Despite the clinical potential of the irreversible pan-HER inhibitors in HER2-positive breast cancer, resistance may develop. For example, afatinib resistance commonly occurs in lung cancer. In a small trial of 24 NSCLC patients, 23 patients developed progressive disease [319]. The SKBR3-A cells developed cross-resistance to trastuzumab alone, pertuzumab alone, and the combination of the antibodies, similar to the SKBR3-L cells (Figure 6-3). However, afatinib resistance also conferred resistance to lapatinib (IC_{50} value > 1 μM) (Figure 6-2). Afatinib is approved in NSCLC and, although lapatinib is not approved in this setting, the EGFR-targeted TKIs, gefitinib and erlotinib are [320, 321]. Reduced sensitivity to afatinib was also observed in lung cancer after progression following gefitinib or erlotinib in the LUX-Lung 1 trial [322]. Similar to the lapatinib resistant SKBR3-L, SKBR3-A cells had a significant reduction in neratinib sensitivity reflected in a 33.5-fold increase in IC_{50} value (Figure 6-2). Nevertheless, this was still just below the maximum plasma concentration of neratinib. Similarly, the HCC1954-N cell line was cross-resistant to both lapatinib and afatinib (Figure 6-16). The results from this study suggest that HER2-targeted TKIs should be given after trastuzumab treatment and that treatment with a HER-targeted TKI might have reduced efficacy after other HER2-targeted TKI treatment. Other pre-clinical studies have also observed cross-resistance in HER2-targeted TKI resistant cell lines. Using the irreversible pan-HER inhibitor dacomitinib, Kalous *et al*. showed that an SKBR3-L cell line was less sensitive to dacomitinib than the parental cells. Interestingly, SKBR3-T cells were as sensitive to dacomitinib as their parental cells [315], mirroring the results observed with afatinib in this study and in that of Canonici, *et al*. [123].

Table 7-1: Fold change of HER2-targeted therapy response in SKBR3-L, HCC1954-L, and SKBR3-A cell lines.

Fold change relative to parental cell lines	SKBR3-L	HCC1954-L	SKBR3-A
10 μg/mL trastuzumab	1.2	1.0	1.3
10 μg/mL pertuzumab	1.1	1.0	1.2
Trastuzumab plus pertuzumab	1.7	1.1	1.9
Lapatinib IC$_{50}$	47.4	5.2	30.6
Neratinib IC$_{50}$	22.8	10.4	33.5
Afatinib IC$_{50}$	13.9	75.3	58.1

In summary, HER2-targeted therapy treatment affects future sensitivity to other HER2-targeted therapy agents. These results suggest that there is a role for HER2-targeted TKIs as a second-line therapy following progression on monoclonal antibody therapies, which is consistent with the approved use of lapatinib in this setting. However, the data indicates that irreversible TKIs might have reduced impact following lapatinib or other irreversible TKI treatment. Future work should examine the possible sensitivity of resistant models to T-DM1, the only other approved HER2-targeted therapy not examined in this study. The cytotoxic component of this trastuzumab-based antibody drug conjugate could offer a potential treatment strategy for both monoclonal antibody- and TKI-refractory disease.

The reduced sensitivity of HER2-targeted TKI resistant breast cancer cell lines to other HER2-targeted therapies indicates that a novel therapeutic target is required for these patients with metastatic disease that has acquired resistance to the TKIs. That led us to examine the lapatinib, afatinib and neratinib resistant cell lines for targetable alterations. PP2A was selected as the potential target in lapatinib resistance and Src was assessed in afatinib and neratinib resistance.

7.3 PP2A in acquired lapatinib resistance

We have previously shown that lapatinib treatment elevated phosphorylated (p-) eEF2 levels in SKBR3-Par cells, but not in SKBR3-L cells [154]. Both SKBR3-L and HCC1954-L cells showed decreased p-eEF2 levels and increased PP2A activity compared to parental cells. eEF2 is a phosphatase substrate of PP2A [323]. Thr56 phosphorylation of eEF2 prevents ribosomal binding, thereby preventing global protein translation within the cell [323, 324]. Another study has also shown that lapatinib treatment stimulated an increase in PP2A activity in a lapatinib-sensitive HER2-positive breast cancer cell line [193]. Therefore, increased PP2A activity may be a stress response to lapatinib treatment.

PP2A plays a critical role in cell growth and development and several studies indicate PP2A may have a tumour suppressor role [226, 228, 290]. Contrary to this, other studies have shown an anti-apoptotic and anti-proliferative effect, suggesting the phosphatase has an oncogenic function [325–327]. This starkly contrasting behaviour may be due to the multi-faceted activity of PP2A in the cell, the complexity of its trimeric holoenzyme composition, or cell line variations [190, 328].

Compared to their parental cell lines, both SKBR3-L and HCC1954-L cells were more sensitive to PP2A inhibitors, okadaic acid and LB-100 (Figures 3-5 and 3-14). Importantly, PP2A inhibition enhanced the anti-proliferative effect of lapatinib.
In order to determine if the growth inhibition with okadaic acid and LB-100 was inhibitor-specific, siRNA knockdown was employed (Section 3.6). Knockdown of the PP2A catalytic subunit PPP2CA, which carries out the majority of the holoenzyme's phosphatase activity [225], resulted in a significant reduction of HCC1954-L proliferation. The combination of siRNA PPP2CA knockdown and lapatinib also caused a minor enhancement, although not statistically significant compared to the siRNA alone (Section 3.6). Another study examining the effect of PP2A inhibition in HER2-positive breast cancer showed that PPP2CA knockdown in both BT474 and SKBR3 cells caused apoptosis [325]. These results combined give further evidence that inhibiting PP2A can suppress HER2-positive breast cancer cell growth.

To further validate the role of PP2A and lapatinib resistance, PP2A activity was increased in lapatinib sensitive cells using FTY720 (Section 3.7). FTY720 is a sphingosine derivative that activates PP2A [329]. FTY720 activates PP2A through several mechanisms; it can inhibit SET-PP2A binding, down-regulate CIP2A and cause de-phosphorylation of PP2A Tyr307 [231, 330, 331]. FTY720 (2.5 µM) has previously been shown to increase PP2A activity and disrupt SET:PP2A binding in cancer cell lines and was therefore chosen as the concentration to be used [332, 333]. Activation of PP2A in the SKBR3-Par and HCC1954-Par cells using FTY720 reduced lapatinib sensitivity by 5.4- and 2.1-fold. Conversely, another study of lapatinib resistance showed that knockdown of CIP2A increased sensitivity to lapatinib [197]. In this study, a BT474-L cell line was generated by lapatinib treatment for 5 months up to a concentration of 5 µM lapatinib. This cell line had up-regulation of CIP2A, along with increased phosphorylated levels of HER2, Akt, and mTOR. Increased CIP2A, in the BT474-L cell line and CIP2A-transfected SKBR3 cells, reduced sensitivity to lapatinib [197]. The discrepancy in the effect of PP2A activation on lapatinib response between the Zhao *et al*. study and the results described herein (Section 3.7) may be due to variations in the cell lines used or differences in the mechanism of PP2A activation employed. The lapatinib resistant model of their study used BT474-L cells. The BT474 cell lines are ER-positive and this may impact the role PP2A is playing in the cells. Increased ER can increase expression of the PP2A inhibitor SET [334]. FTY720 activates PP2A by several mechanisms and can directly bind to the PP2A inhibitors SET, CIP2A, and ANP32A [330, 335]. Therefore, the effect of FTY720 may be due to interactions with PP2A inhibitors other than CIP2A. In addition, the experiment in this PhD project used pre-treatment with FTY720 rather than combinatorial treatment, which may prevent antagonistic effects of lapatinib plus FTY720. Future work could examine the binding affinity of SET:PP2A in lapatinib resistant cell lines and in lapatinib-treated parental cell lines. The relationship between PP2A and CIP2A and ANP32A should also be examined.

7.3.1 Mechanism of action of lapatinib plus PP2A inhibition

As PP2A can affect the activity of a myriad of proteins [190, 192], RPPA analysis was used to determine the pathway alterations in the HCC1954-L cells treated with 3 nM okadaic acid with or without 500 nM lapatinib (Section 3.9) (Figure 7-1). RPPA allows for ~80 proteins to be analysed in samples simultaneously. The concentration of okadaic acid used (3 nM) was chosen to ensure phosphatase inhibition was specific to PP2A [289]. The combination of okadaic acid and lapatinib increased phospho-eEF2 levels most at 18 h, compared to 4, 6, and 24 h treatment. Treatment with 3 nM okadaic acid for 18 h showed minimal changes to key signalling pathways, including HER family signalling, Bcl-2 family members, STAT3 signalling, and caspase/PARP cleavage. The phosphorylation states of two proteins were altered: Src (Y416) and p38 MAPK (T180). The decreased levels of phosphorylated Src was unexpected as PP2A inhibition by okadaic acid has been shown to increase phosphorylated Src (Y416) in cell-free experiments [336]. However, higher concentrations of okadaic acid were used in that study, which may be a reason for the different effect in the lapatinib-resistant cells. The two cell lines may also have different levels of the regulatory subunits. It is possible that further alteration to PP2A substrates would be seen at a later timepoint. PP2A is a known regulator of p38 MAPK phosphorylation [337]. Previous studies demonstrated that chemical inhibition of PP2A caused p38 MAPK phosphorylation, which inhibited apoptosis induction. This anti-apoptotic effect was not observed in the HCC1954-L cells as okadaic acid and LB-100 treatment decreased cell proliferation and induced apoptosis (Sections 3.3, 3.10 and 3.12). The apoptotic effect of PP2A inhibition may be due to the inhibition of eEF2 and, therefore, the down-regulation of protein synthesis. Inhibition of eEF2 has previously been shown to inhibit cell growth in colon cancer cell lines and eEF2 is over-expressed in colon cancer and head and neck squamous cell carcinoma [338, 339].

RPPA analysis of 18 h 500 nM lapatinib treatment showed inactivation of HER2 and HER3 and down-regulation of total levels of EGFR in HCC1954-L cells. This is consistent with previous reporting of the HER family inhibitory activity of lapatinib [88, 340]. Interestingly, lapatinib also induced increased activation of NFκB p65 and MET. NFκB p65 has previously been shown to be up-regulated by lapatinib in breast cancer [341] and activation of NFκB can confer lapatinib resistance [342]. MET has

also been previously implicated in lapatinib resistance [343]. These increases may be a stress response by the resistant cells to overcome the effect of lapatinib.

Importantly, the combination of okadaic acid and lapatinib caused a significant increase in inhibition of survival signalling pathways. The inhibition of EGFR, HER2, and HER3 activity, along with inactivation of downstream signalling components such as mTOR, ERK 1/2, MEK 1/2, and Src was observed. PP2A, with B56 regulatory subunit composition, negatively regulates ERK phosphorylation [344], but inhibition of PP2A in combination with lapatinib inhibited ERK 1/2 phosphorylation. The down-regulation of MEK 1/2 and ERK 1/2 acitivity may be due to the up-stream inhibition of Src or decreased total levels of RAF, which activates MEK1/2, which was also observed in the RPPA analysis [345].

Notably, HCC1954-L cells are more sensitive to lapatinib plus okadaic acid than SKBR3-L cells (Figure 3-6) and previous investigations in our lab showed that HCC1954-L cells had increased levels of phosphorylated Akt and ERK compared to HCC1954-Par cells [346]. The opposite trend is observed in SKBR3-L cells. The enhanced growth inhibition observed with the combination of lapatinib and okadaic acid in HCC1954-L cells may be due to the additional inhibition of Akt and ERK signalling.

Lapatinib plus okadaic acid did not abrogate the increased activation of NFκB p65 that was seen with lapatinib alone treatment. As NFκB p65 can stimulate cell proliferation and prevent apoptosis [341, 347], this may be a potential mechanism of resistance to treatment. Conversely, okadaic acid treatment of PANC-1 cells induced apoptosis by activating NFκB. NFκB caused up-regulation of the pro-apoptotic genes TNF-α, TRAILR1, and TRAILR2 [348]. Further work should examine the role of NFκB p65 in lapatinib and PP2A inhibitor response.
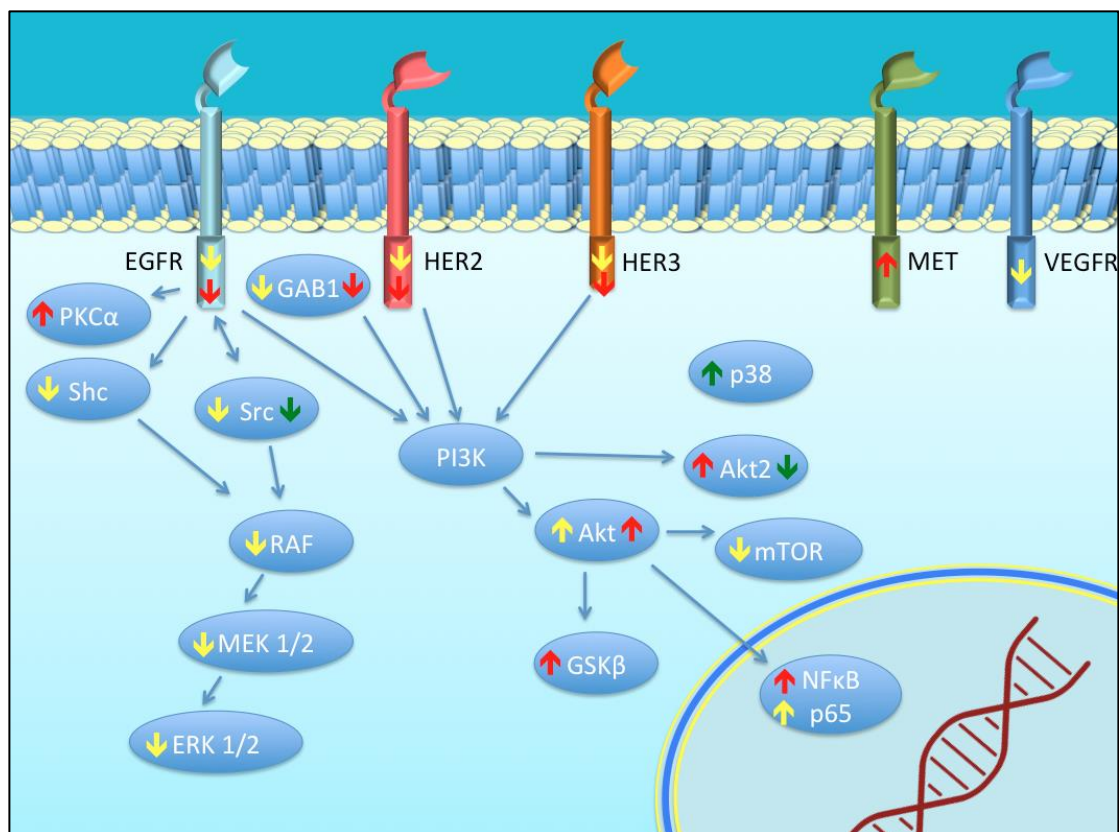
Figure 7-1: Representation of pathway alterations of HCC1954-L cells observed in RPPA analysis. Red arrows indicate lapatinib treatment, green arrows indicate okadaic acid treatment, and yellow arrows represent lapatinib plus okadaic acid (Pathway adapted from [349])**.**

7.3.2 PP2A expression in lapatinib resistant cells

The composition of the PP2A holoenzyme governs the localisation and substrate specificity of the molecule. The α isoforms of the catalytic subunits are dominant and 90% of PP2A holoenzymes contain the α isoforms [225, 350]. Changes to subunit composition can therefore lead to significantly altered function and could contribute to lapatinib resistance.

Analysis of both lapatinib resistant cell lines by Western blotting showed no alteration in total levels of either catalytic subunit isoform (Section 3.5). However, post-translational modifications of PPP2CA were altered in the HCC1954-L cells. Phosphorylation of PPP2CA inhibits the phosphatase activity of the enzyme [351]. As PP2A activity was increased in these cells, it was unsurprising that Y309

phosphorylation was decreased. Methylation of PPP2CA was also decreased in the lapatinib resistant cell line. PPP2CA methylation affects the regulatory subunits that can bind to the dimer [352]. Methylation levels were significantly decreased in HCC1954-L cells compared to their parental cells. Phosphorylation and methylation of PP2A catalytic subunit may be a marker of lapatinib resistance and, therefore, future work should examine phospho- and methyl-PPP2CA in lapatinib-resistant HER2-positive breast cancer patient samples.

7.3.3 LB-100 in lapatinib resistance

Although there are several chemical inhibitors of PP2A, including okadaic acid, fostriecin, and cantharidin [353–355], many of these inhibitors cannot be used clinically due to severe toxicities. However, LB-100 shows promise as a clinical PP2A inhibitor. A phase I clinical trial of LB-100 showed that the drug was safe and tolerable [268]. Pre-clinical studies demonstrated that LB-100 enhances response to chemotherapy and radiotherapy [262, 263]. LB-100 has also shown some efficacy in overcoming resistance to the EGFR-targeted therapy, gefitinib, in pre-clinical models of EGFR-mutant NSCLC. Two acquired gefitinib-resistant cell lines showed improved response to gefitinib in combination with LB-100, which was also replicated in *in vivo* examination [267]. In this study, SKBR3-L and HCC1954-L cells were 2.5- and 2.3-fold more sensitive to LB-100 than their respective parental cell lines. The IC$_{50}$ values achieved in the lapatinib resistant cell lines are similar to those observed in other cancer cell line models [265, 266, 356]. Both cell lines showed reduced LB-100 sensitivity in 3D conditions. However, synergy with lapatinib was maintained in the HCC1954-L cell line. Interestingly, a similar effect was also observed with LB-100 in combination with neratinib, as synergy was observed in the HCC1954-L cells. This is of particular interest as neratinib is now approved for the treatment of early-stage HER2-positive breast cancer [39]. To provide clinically relevant pre-clinical data, future work should examine the efficacy of LB-100 in trastuzumab resistant cell lines and the potential of LB-100 with lapatinib or neratinib in acquired trastuzumab resistant models. Future studies should also attempt to understand why there is a reduced response to LB-100 in 3D conditions. Cantharidin

efficacy has been shown to be influenced by calcium and phosphate transporters [357], these may be altered in 3D conditions.

Previous studies by other groups have shown that LB-100 can induce apoptosis, mitotic catastrophe, G1 cell cycle arrest, and G2/M cell cycle arrest [260, 266, 356]. LB-100 in combination with DNA-chelating chemotherapy enhances DNA damage by preventing cell cycle arrest. This forced cell cycle progression allows for additional DNA damage by DNA-chelating agents [260, 265, 356]. Combination treatment of LB-100 with cisplatin showed an induction of apoptosis [260]. This was also observed in hepatocellular carcinoma in combination with the VEGFR inhibitor sorafenib [266]. In the lapatinib-resistant cell lines, LB-100 alone significantly induced apoptosis, evident from cell cycle analysis (Section 3.12), and the combination with lapatinib further enhanced this effect in the HCC1954-L cells. Lapatinib alone instigated G1 cell cycle arrest in both SKBR3-L and HCC1954-L cells. This G1 cell cycle arrest was down-regulated by the combination with LB-100 in both cell lines. This suggests LB-100 was driving the arrested cells into apoptosis, similar to that observed in previous studies by other laboratories [260, 266].

7.3.4 PP2A inhibition prevented lapatinib resistance development

Although short-term growth assays are a useful tool for screening potential anti-cancer drugs, longer-term clonogenic assays provide a better insight into what can be expected *in vivo* [358]. Resistance development assays were carried out to examine the efficacy of okadaic acid and LB-100 in preventing the development of lapatinib resistance (Section 3.8 and 3.14). Twice weekly treatment of SKBR3 and HCC1954 cells with lapatinib with or without okadaic acid or LB-100 showed that PP2A inhibition can prevent the development of lapatinib resistance *in vitro*. After 2-4 weeks, growth of SKBR3 and HCC1954 cells continued in the presence of lapatinib, but this recommencement of growth did not occur with the addition of a PP2A inhibitor.

In summary, PP2A is a mediator of the lapatinib resistant phenotype in both the SKBR3-L and HCC1954-L cells. Both cell lines were more sensitive to PP2A inhibition with okadaic acid and LB-100. This PP2A inhibition also enhanced

lapatinib response, primarily in the HCC1954-L cell line. Lapatinib plus okadaic acid significantly inhibited survival signalling; an effect that was not observed with either inhibitor alone.

LB-100 showed pre-clinical efficacy in the lapatinib resistant HER2-positive breast cancer, particularly in the HCC1954-L model (Figure 7-2). LB-100 alone and in combination with lapatinib or neratinib inhibited HCC1954-L proliferation. From this, an *in vivo* assessment of lapatinib plus LB-100 was proposed to further investigate the clinical potential of LB-100 in lapatinib-resistant HER2-positive breast cancer.
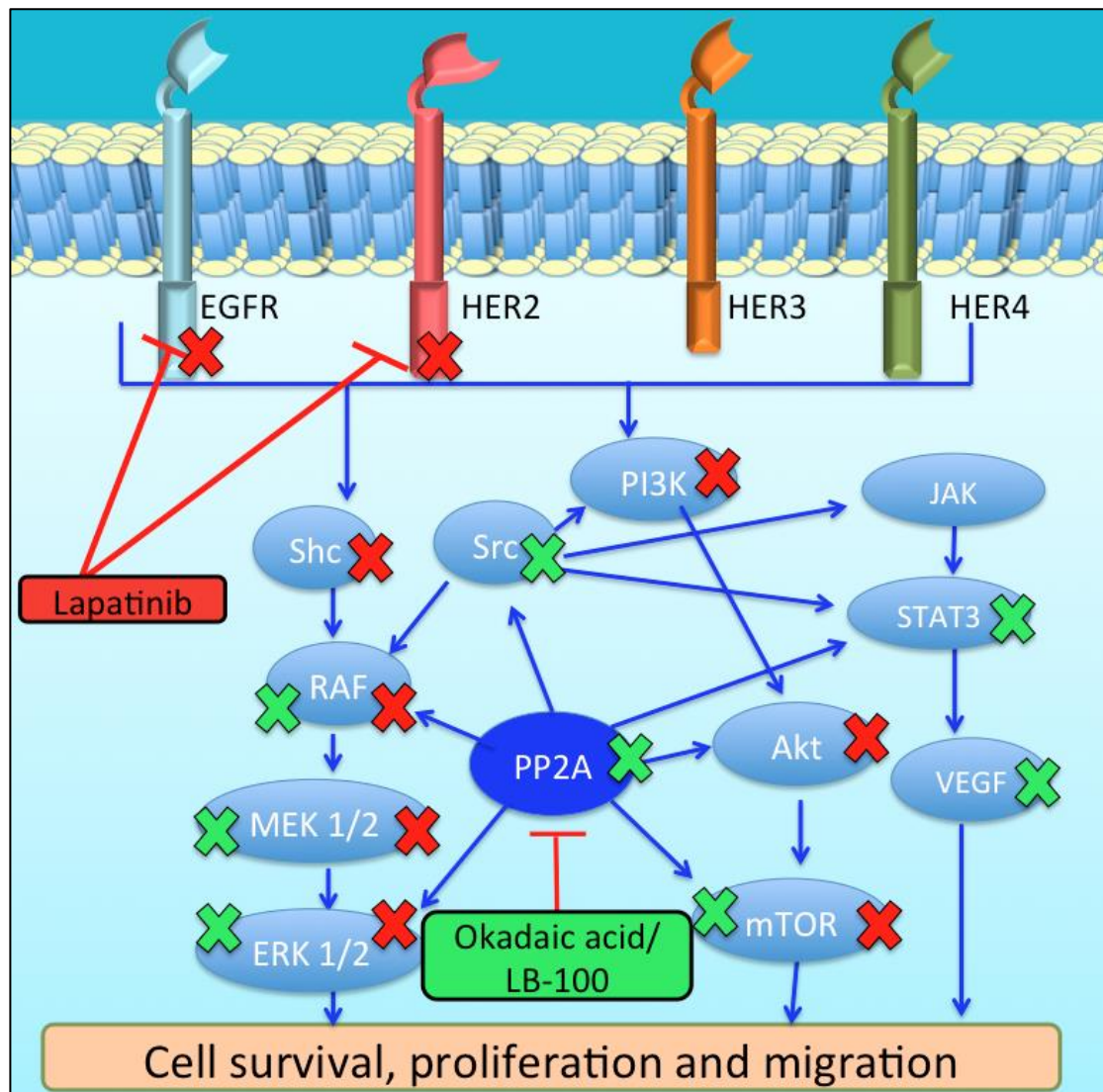
Figure 7-2: Lapatinib plus PP2A inhibition in HER family member signalling (Pathway adapted from [349])**. Red X indicates inhibition by lapatinib. Green X indicates inhibition by okadaic acid/LB-100.**

7.4   Lapatinib resistance *in vivo*

7.4.1   Maintenance of lapatinib resistance phenotype *in vivo*

Although numerous acquired lapatinib resistant cell line models have been developed, not all of these can be used for *in vivo* assessment of candidate drugs to overcome resistance. This can be due to the low tumourigenicity of the cell lines in mice or loss of the resistant phenotype when withdrawn from lapatinib treatment. The SKBR3-L cell line is not a good *in vivo* model for both of these reasons. Previous work from our group showed that withdrawal of lapatinib treatment resulted in increased sensitivity to lapatinib in SKBR3-L. In contrast, the lapatinib IC_{50} value of the HCC1954-L did not significantly change after three months without lapatinib; the IC_{50} value following one week of lapatinib withdrawal was 2.73 ± 0.05 μM and after 12 weeks it was 2.63 ± 0.16 μM [148]. In comparison, the SKBR3-L cell line had a 7.6-fold decrease in lapatinib IC_{50} value 14 weeks after lapatinib withdrawal, rendering the cells sensitive to lapatinib [346]. Although lapatinib resistance in HCC1954-L cells was shown to be maintained *in vitro*, it was not known if the resistant phenotype would be maintained *in vivo*. The *ex vivo* experiments showed that lapatinib resistance was retained by HCC1954-L after 12 weeks *in vivo* growth in the absence of lapatinib treatment (Figure 4-13). Importantly, this work also demonstrated that *in vivo* conditions did not significantly affect the synergy observed between lapatinib and LB-100 in HCC1954-L.

Implantation of cancer cell lines into mouse models can impact on the expression of RTKs, such as HER2, insulin receptor, and IGF-1R [359]. Therefore, prior to assessment of lapatinib plus LB-100 against HCC1954-L, the maintenance of the respective targets needed to be confirmed. This was achieved by analysing HER2 and phospho-eEF2 levels in HCC1954-L xenografts and comparing them to levels found *in vitro*; no differences were observed between *in vitro* and *in vivo* samples (Figure 4-17). Previously, LB-100 has been shown to inhibit PP2A in a glioblastoma model at a dose of 1.5 mg/kg, the same concentration used in this study [356]. In order to examine if LB-100 was also effective in the *in vivo* HCC1954-L model, tumour tissue was removed post-mortem from a mouse treated with 75 mg/kg lapatinib plus 1.5 mg/kg LB-100. Phosphorylated eEF2 levels were up-regulated in a treated sample (Figure 4-17). As protein samples were taken from extracted tumours, it is possible

mouse cells were also extracted. However, HER2 levels were similar to that of the HER2-amplified HCC1954-L cells. In addition, the relative levels of phospho-eEF2 to both α-tubulin and HER2 levels indicate that the increased phospho-eEF2 is due to the effect of LB-100 on the tumour cells.

7.4.2 Lapatinib plus LB-100 is non-toxic in BALB/c nude mice

If the combination of lapatinib plus LB-100 resulted in high levels of toxicity, it would be difficult to support the progression of this combination to clinical assessment. Although LB-100 has been examined *in vivo* previously [258, 261, 265, 356], it has not been tested in combination with HER2-targeted therapy. Assessment of LB-100 alone by Lu *et al*. inhibited PP2A but did not cause systemic toxicities after 21 days of consecutive treatment [356]. Likewise, 1.5 mg/kg LB-100 in combination with doxorubicin showed no toxicity in animals after 11 days of treatment [360]. We tested 75 mg/kg lapatinib plus 1.5 mg/kg LB-100 in non-tumour-bearing mice for 30 days, with lapatinib given daily Monday-Friday by oral gavage and LB-100 administered by IP injection Monday, Wednesday, and Friday (Section 4.4). The drug regimen scheduled in treatment holidays at weekends to allow for recovery from treatments. Thirty days was chosen as the duration of treatment as this would allow the establishment and maintenance of long-term peak plasma concentration of lapatinib and LB-100. Lapatinib has previously been shown to reach peak plasma levels after 5 to 7 days in humans and has a half-life of approximately 24 h [361]. Despite the short half-like of LB-100, its maximum PP2A inhibition occurs 2-4 h after infusion [194]. This 30-day treatment regimen was chosen to give an indication of the expected adverse events of this combination *in vivo*. The most common adverse events related to lapatinib in humans are diarrhoea and skin rashes [362] and LB-100 has been shown to impair renal function [268]. These side effects, along with the adverse effects of the drug administration, were monitored by weight measurement and observation for skin damage. The absence of such side effects suggest that the combination of lapatinib and LB-100 could be tolerated in a pre-clinical model, which adds support to the rationale for testing this combination in a phase I clinical trial.

212

7.4.3   Mammary fat pad is optimal for HCC1954-L cells *in vivo*

The first objective of the *in vivo* assessment of lapatinib plus LB-100 in a model of lapatinib resistance was to optimise the tumour growth conditions for HCC1954-L cells in mice. The two pilot studies examining HCC1954-L growth in SCID mice with sub-cutaneous implantation (Sections 4.2.1 and 4.2.2) confirmed that HCC1954-L cells form tumours *in vivo*. However, best practice and adherence to animal welfare regulation meant that the occurrences of skin ulceration on the tumours terminated these studies prior to any investigation of the effect of the drug combination on xenograft tumour growth. Skin ulceration can occur due to rapid tumour expansion, haemorrhagic development, continuous abrasion, tumour type, or cell line predisposition to cause ulceration [363]. This has been observed in several cell line models when implanted sub-cutaneously including the ovarian cancer cell line A2780 and the pancreatic cancer cell line AR42J [284]. This skin ulceration can be painful to the animal and cause loss of skin integrity and injection. Therefore, extensive skin ulceration requires humane termination [284, 363].

Mammary fat pad implantation allowed for greater maximum tumour volume compared to the sub-cutaneous injections (545.0 ± 190.1 mm^3 compared to 248.3 ± 25.6 mm^3) without incidence of skin ulceration. Although sub-cutaneous injection is a more simple procedure and avoids the need for anaesthetic, mammary fat pad implantation allows for a more accurate recreation of the tumour microenvironment, increases the metastatic potential of the developing tumours, and reduces the likelihood of skin ulceration [285, 364, 365]. One disadvantage of the procedure is the accuracy and technical proficiency required to inject cells into the murine mammary fat pad. In this mammary fat pad implant pilot study, the take rate was 66.7%, with an additional tumour developing subcutaneously (Section 4.2.4). Importantly, skin ulceration did not occur in any of the six mice tested. The only tumour-related side effect was haemorrhagic areas developing at a large tumour volume in one mouse (Figure 4-11). Adverse haemorrhagic events at this volume should not interfere with a drug efficacy study of lapatinib plus LB-100 as expected tumour volume differences between treatment arms would be expected below the volume at which the haemorrhagic necrosis occurred.

There is little information in the literature relating to the occurrence of skin ulceration with implanted HCC1954 cells. Some studies briefly mention the development of

tumour ulceration but do not give details of percentage occurrences or the size of tumours at ulceration [366, 367].

In summary, the HCC1954-L cell line showed high tumourigenic potential both in sub-cutaneous and mammary fat pad injection. The lapatinib resistant cell line maintained its HER2 and phospho-eEF2 levels *in vivo* and lapatinib resistance was preserved despite the absence of lapatinib treatment for over three months. Unfortunately, skin ulceration of sub-cutaneous implanted tumours hampered the further study of lapatinib plus LB-100 *in vivo*. As skin ulceration did not occur in the mammary fat pad model, future work should use this model to test the efficacy of the drug combination. This study should also examine the metastatic potential of the HCC1954-L cell line and evaluate the *in vivo* mechanisms of lapatinib plus LB-100.

7.5   PP2A in innate lapatinib resistance

As the acquired lapatinib resistant cells were more sensitive to okadaic acid and LB-100 than their parental cell lines (Sections 3.2 and 3-10), the role of PP2A in innate lapatinib resistance was examined (Section 5.3). Previous work in our research group showed that there was a relationship between lower levels of phospho-eEF2 and innate lapatinib resistance in a panel of HER2-positive breast cancer cell lines [346]. In this study, the sensitivity of the HER2-positive cell lines to okadaic acid was shown to correlate with both lapatinib and trastuzumab sensitivity (Figure 5-3). The cytotoxic effect of okadaic acid in cancer cell lines has been examined in a number of studies. Okadaic acid has shown anti-proliferative activity in osteosarcoma, pancreatic cancer, and breast cancer cell lines [327, 368, 369]. Okadaic acid induced apoptosis and cell differentiation in three breast cancer cell lines: MDA-MB-231, MCF7, and AU565 [368, 370]. Okadaic acid may also induce increased expression of Fas receptor and ligand and also affects sensitivity to TRAIL [239, 371]. In contrast, okadaic acid has also demonstrated pro-growth activity in prostate and pancreatic cell lines [331, 372]. In this study, okadaic acid enhanced the anti-proliferative effect of lapatinib in two of three lapatinib-resistant cell lines (Figure 5-4).

As discussed earlier, LB-100 has been examined in a phase I clinical trial and was shown to be safe and tolerable [268] and, in this study, has shown efficacy in acquired lapatinib resistant HER2-positive breast cancer [154]. However, when LB-100 sensitivity was assessed in a panel of HER2-positive cell lines naive to any HER2-targeted therapy, sensitivity to LB-100 did not correlate with either lapatinib or trastuzumab resistance (Figure 5-8). The difference in okadaic acid and LB-100 sensitivity may be due to the differences in potency and selectivitiy of the molecules. LB-100 is a cantharidin derivative and therefore has different selectivity to PP2A [289]. The associated transporter proteins of LB-100 have not yet been investigated. Okadaic acid uptake is regulated by OATP1B3 and p-glycoprotein [373, 374]. LB-100 may be regulated by different transporter molecules.

LB-100 enhanced lapatinib in the HCC1954-L cells and synergy was also observed in the innately lapatinib and trastuzumab resistant MDA-MB-453 cell line (Figure 5-9), but slight antagonism was observed in the JIMT-1 and UACC732 cell lines. The MDA-MB-453 cells showed a similar enhancement with okadaic acid. However, the additive effect observed with okadaic acid plus lapatinib was lost with LB-100.

Alterations in PP2A subunit levels have been observed in several cancer types [277]. This may occur through mutation of the structural subunit, which decreases holoenzyme assembly [375]. This study showed that there was no relationship between PP2A catalytic and structural subunit expression and sensitivity to lapatinib or trastuzumab (Figure 5-10). This indicates that the mediator of okadaic acid and HER2-targeted therapy response is independent from PP2A expression in HER2-positive breast cancer cell lines. The lack of a relationship between PP2A expression and HER2-targeted therapy response was mirrored by the absence of a correlation between high expression of PP2A catalytic or structural subunits and HER2-positive breast cancer patient survival response (Figure 5-12 – 5-17). Interestingly, low levels of the PP2A inhibitor protein CIP2A were associated with improved overall survival. CIP2A levels has previously been reported to correlate with poor prognosis in breast cancer [231]. Future work should examine the expression of CIP2A in the panel of HER2-positive breast cancer cell lines and evaluate the relationship between CIP2A levels and HER2-targeted therapy response. Methylation levels of PP2A and PP2A activity should also be evaluated in the HER2-positive breast cancer cell lines.

7.6   Analysis of afatinib resistant cell line model

In addition to evaluating the potential of PP2A as a novel target for the treatment of HER2-positive breast cancer, the afatinib resistant SKBR3-A cells, which were generated by Dr. Alexandra Canonici in our research group, were examined in order to identify additional novel targets in the treatment of HER-targeted TKI resistance. Acquired resistance to afatinib has not previously been investigated in HER2-positive breast cancer. All pre-clinical investigations of afatinib resistance have focused on the emergence of resistance in NSCLC using cell lines to develop resistant models to afatinib *in vitro* and *in vivo* [170, 198, 204, 319, 376–378].

An afatinib resistant breast cancer cell line model, SKBR3-A was developed in our lab by Dr Alexandra Canonici. In order to investigate the mechanisms by which the SKBR3-A cells become resistant to afatinib and the other HER2-targeted therapies tested, the afatinib-resistant and parental cells were analysed by whole exome sequencing and RPPA.

7.6.1   HER family member alterations

The acquisition of EGFR- or HER2-mutations is the most commonly occurring resistance mechanism in afatinib-resistant NSCLC models. EGFR L858R, V843I and T790M mutations and EGFR exon insertions have all been associated with afatinib resistance [201, 378, 379]. However, the SKBR3-A cell line did not develop secondary HER family member mutations (Table 6-3), insertions or deletions (Table 6-2), or gene copy number alterations (Table 6-4); indicating afatinib resistance in a HER2-positive breast cancer model utilises alternative mechanisms to those described in lung cancer. Other previously reported afatinib resistance mechanisms were also examined in the SKBR3-A cells by RPPA and whole exome sequencing analysis. The SKBR3-A cells did not display MET amplification, which has been shown to occur in afatinib-resistant lung cancer (Table 6-5) [380]. RPPA analysis showed changes in HER family members. Total levels of EGFR were significantly increased and phosphorylated levels of HER3 (Y1289) were decreased in SKBR3-A cells. The results suggest that EGFR has a role to play in circumventing afatinib resistance in SKBR3 cells. This increased EGFR was also seen in previous work in our lab on the

lapatinib-resistant SKBR3-L cell line model [154]. Levels of HER2 were also slightly decreased in the SKBR3-A cells but this was not statistically significant. Increased EGFR levels, through amplification or mutation, is a common mechanism of resistance to HER2-targeted therapies and has been observed in our SKBR3-L, SKBR3-T, and SKBR3-TL cell lines [169, 198]. Alterations to EGFR, through increased levels or by mutation, has been shown to drive afatinib resistance in a lung cancer cell line model [377].

7.6.2 Downstream signalling changes

Reactivated signalling downstream of EGFR and HER2 can compensate for the effect of HER2-targeted therapies and several downstream kinases have been associated with afatinib, lapatinib, and trastuzumab resistance [153, 199, 202, 377]. RPPA analysis showed no significant increase in mTOR levels or S2448 phosphorylation. Likewise, phosphorylation of AKT (S473 and T308) and phosphorylated MEK 1/2 (S217/221) were down-regulated. This suggests that the afatinib resistant cells have become less dependent on Akt and ERK signalling. As discussed, total levels of EGFR were significantly increased, despite the absence of EGFR amplification (Figure 6-5 and Table 6-3). Phosphorylation of EGFR was increased but not statistically significantly. EGFR up-regulation has been observed in afatinib-resistant NSCLC cell lines [198]. However, this increase in EGFR caused constitutive activation of PI3K/Akt signalling, which was not observed in RPPA analysis of our afatinib-resistant HER2-positive breast cancer model. This is possible due to the lack of a similar increase in phospho-EGFR levels.

However, the RPPA data indicated increased activation of other signalling pathways. Despite down-regulation of PI3K/AKT and ERK signalling, SKBR3-A cells had increased total p38 MAPK, phosphorylated AMPK (T172), AKT2, and phosphorylated Src (Y416) levels. All of these proteins are involved with EGFR activity, which may be driving compensatory signalling networks. P38 MAPK can act independently of EGFR and HER2 signalling and can act as an internal activator of EGFR, by phosphorylating EGFR Y845 [381, 382]. AKT2 activity is driven by EGFR signalling [383], which may account for the increased AKT2 in the SKBR3-A cells. Src kinase cross-talks with EGFR and has been associated with a variety of HER-

targeted therapies [157, 204, 305, 384, 385]. Src can be activated by EGFR through phosphorylation of Y416. Activated Src can then interact with EGFR and phosphorylate EGFR Y845 [386] and Src activation is more dependent on EGFR than HER2 signalling [160].

The gene copy number of nuclear receptor subfamily 4 group 1 (NR4A1) was significantly amplified in the SKBR3-A cells. NR4A1 is a transcription factor that has been implicated in several cancer types and is now being pursued as a potential anti-cancer drug target [301, 387–389]. Importantly, knockdown of NR4A1 caused decreased levels of EGFR and Bcl-2 and an increase in cleaved caspase-3 and PARP [387]. Thus increased expression of NR4A1 in the SKBR3-A cells may contribute to the increased levels of EGFR observed. Future work should further investigate the role of NR4A1 in afatinib resistance and in regulating EGFR in afatinib resistant cells.

7.6.3   Epithelial-mesenchymal transition

The development of a stem cell-like phenotype has previously been observed in afatinib resistant lung cancer cell lines [376]. In that study, 10 afatinib resistant cell lines were developed. Of those cell lines, three afatinib-resistant cell lines, (two originating from HCC4011 and one from HCC827) and a dual afatinib and crizotinib resistant HCC827 cell line showed increased vimentin, a mesenchymal marker, and down-regulated E-cadherin, an epithelial marker. In our study, whole exome sequencing showed amplification of several genes associated with EMT. The EMT-associated amplified genes include NR4A1, SPHK1, ITGB4, S100A9, and PDE4A [297–301]. The emergence of an EMT phenotype has also been observed in both trastuzumab and lapatinib resistance [189, 390]. Further investigation into the possible stem-like properties of afatinib resistant HER2-positive breast cancer cells may be warranted. This should be done by examining the protein levels of the EMT-associated genes altered in the exome sequencing and by assessing the mammosphere formation ability of the SKBR3-A and SKBR3-Par cell lines. Mammosphere assays indicate the stem cell potential of tumour cells. In this assay, cells are cultured in suspension in mammosphere medium (DMEM/F12, B27 supplement, and EGF). The number of spheroids > 50 μm formed after five days, relative to the cell seeding

density, indicates the stem cell progenitor activity. Disaggregation and reseeding of these spheroids for a secondary mammosphere assays then gives the self-renewal potential of the cells [391, 392].

7.6.4   Integrin level alterations

Integrin proteins are cell adhesion molecules that are involved in cancer progression, proliferation, and metastasis [393]. Whole exome sequencing of SKBR3-A cells show significant changes in the gene copy number of two integrins, integrin subunit alpha 9 (ITGA9) and integrin subunit beta 4 (ITGB4).

ITGA9 is a suspected tumour suppressor and its copy number ratio is decreased in SKBR3-A cells. ITGA9 has been shown to be down-regulated or hyper-methylated in lung, breast and nasopharyngeal cancer [394–396].

ITGB4 is an oncogenic integrin that has been shown to increase invasion of cancer cells [298, 397–399]. This gene was significantly amplified in SKBR3-A cells. ITGB4 promoted EMT and metastasis in pancreatic cancer and was a negative prognostic marker [298]. In hepatocellular carcinoma, ITGB4 is often over-expressed and has been demonstrated to induce an invasive and migratory phenotype. ITGB4 can also interact with EGFR, thereby activating FAK and AKT signalling [397]. As the SKBR3-A cells have over-expression of EGFR, ITGB4 may stimulate cell survival through interaction with EGFR. Levels of both integrin proteins should be evaluated in order to determine if they are having an effect on afatinib response.

7.6.5   Bcl-2 expression and activation

Bcl-2 is an anti-apoptotic protein found on the mitochondrial membrane. Bcl-2 family member proteins regulate intrinsic apoptosis. The eponymous Bcl-2 prevents apoptosis induction by blocking caspase 9 activation. Inhibition of Bcl-2 family members, MCL-1 and BIM, has been shown to overcome lapatinib resistance in cell line models of acquired resistance [91, 93, 400]. SKBR3-L and SKBR3-TL cells were previously shown in our lab to have decreased levels of the pro-apoptotic Bcl-2 family member BAX and increased levels of MCL-1 [401]. RPPA analysis of the SKBR3-A cells showed no significant alterations to BAX, MCL-1, the anti-apoptotic

Bcl-xL, or pro-apoptotic BIM. However, SKBR3-A cells had increased total and phosphorylated (S70) Bcl-2 levels.

Like the increase observed in EGFR levels, this up-regulation of Bcl-2 could be related to amplification of the transcription factor NR4A1, as NR4A1 has been shown to increase Bcl-2 expression [402]. Interestingly, when NR4A1 is exported out of the nucleus it binds to Bcl-2 to form a pro-apoptotic complex [403]. This has led to the development of NR4A1 mimetics and drugs that induce nuclear export [387, 404, 405]. This may be a therapeutic strategy to examine in this SKBR3-A cell line.

7.7   Dasatinib in afatinib resistant HER2-positive breast cancer

Src kinase was chosen as the best candidate target to overcome afatinib resistance, as phosphorylated Src (Y416) had a 4-fold increase in the RPPA data and a 2-fold increase by Western blotting. Src has been implicated in cell line models of lapatinib and trastuzumab resistance in HER2-positive breast cancer and afatinib resistance in NSCLC [160, 204, 305]. Dasatinib plus afatinib has also shown some potential in triple negative breast cancer in pre-clinical studies [406]. Dasatinib was chosen as the Src inhibitor for this study as saracatinib is not being further pursued for novel oncological use. In addition, afatinib plus dasatinib has completed phase I clinical testing to examine safety and tolerability in NSCLC at 30 mg afatinib plus 100 mg dasatinib [205]. Dasatinib has shown little activity in pre-clinical testing in HER2-positive breast cancer [210]. The triple negative breast cancer subtype proved more sensitive to dasatinib in pre-clinical models but did not show clinical efficacy in triple negative breast cancer patients as a single agent [312]. Following this outcome, further investigation of the clinical potential of dasatinib has been in combination with chemotherapy or another targeted therapy, with some positive results. For example, dasatinib showed an enhancing effect in combination with doxorubicin in triple negative breast cancer cells [407] and is currently being investigated in combination with trastuzumab and paclitaxel as first-line therapy in HER2-positive breast cancer [408].

In our study, SKBR3-A cells were more sensitive to the Src inhibitor dasatinib than the parental cell line (Figure 6-6). However, single agent dasatinib still had only modest activity in SKBR3-A cells. Our results suggest the therapeutic potential is in

the combination of afatinib plus dasatinib, which was strongly synergistic in the afatinib resistant model (Section 6.2.4). This anti-proliferative enhancement of Src inhibition and HER2-targeted therapies has been reported in both breast and lung cancer cell lines. Lapatinib plus saracatinib had a greater than additive effect in the innately lapatinib resistant JIMT-1 cell line [160]. One study showed that lapatinib plus dasatinib or afatinib plus dasatinib can act synergistically in the lapatinib/trastuzumab resistant MDA-MB-453 cell line, but showed antagonism in SKBR3 cells [409]. This antagonism was not observed in the SKBR3-Par or the trastuzumab- and lapatinib-resistant variants in our lab. However, the combination of afatinib plus dasatinib showed a slight enhancement in SKBR3-T cells and synergism in SKBR3-L cells.

This study shows that the combination of afatinib and dasatinib may also be a therapeutic approach to overcome and prevent the development of afatinib resistance in HER2-positive breast cancer. Interestingly, the synergistic growth inhibitory effect of the combination was apoptosis-independent (Figure 6-8 and 6-9). Dasatinib plus afatinib at concentrations causing approximately 80% growth inhibition caused no significant change in caspase 3/7 activation or increase in the subG1, apoptotic population. Both agents have been shown to cause cell cycle arrest and apoptosis in other cancer types [306, 309]. They are also known to stimulate autophagy [303, 308]. This led us to examine if the combination of afatinib and dasatinib caused induction of autophagy. Although afatinib treatment alone caused an increase in autophagy, the combination did not significantly enhance this effect (Figure 6-10). However, the RPPA data showed that the SKBR3-A cells had an increase in total and phosphorylated (activating) Bcl-2 levels. Bcl-2 has been implicated in cell death mechanism switching. In a study using Bcl-2 transfected HeLa cells, Bcl-2 prevented apoptotic cell death at low concentrations of H_2O_2 that caused apoptosis in control vector cells. Notably, at higher H_2O_2 concentrations, Bcl-2 transfected cells died at a greater rate than control cells as Bcl-2 prevented apoptosis induction but stimulated necrosis [410].

As the combination of afatinib and dasatinib did not result in increased levels of apoptosis or autophagy, necrosis was considered as a possible mechanism. Afatinib has been shown to induce apoptosis and necrosis in a retinoblastoma cell line, RB116 [411]. Afatinib in combination with paclitaxel has also caused tumour necrosis *in vivo*

[412]. We examined if afatinib plus dasatinib causes necrotic death in SKBR3-A cells by assaying the levels of secreted HMGB1 (Figure 6-11). HMGB1 is a chromatin protein that is bound to chromatin during apoptosis, but, when a cell undergoes necrosis, it is released into the extracellular matrix and signals to surrounding cells to elicit an inflammatory response [310, 413]. Extracellular HMGB1 was found to be elevated in afatinib plus dasatinib treated SKBR3-A cells relative to untreated controls and single agent treatment. A limitation of this experiment was that in order to distinguish HMGB1 through Western blotting, SKBR3-A cells were grown in serum-free conditions, which may alter the growth of the cells. However, this result combined with the cell cycle and caspase 3/7 activation experiments suggest that afatinib plus dasatinib induces non-apoptotic, necrotic cell death in this afatinib-resistant cell model. As HMGB1 release can cause immune cell activation [310], future work should examine the effect of extracellular HMGB1 on natural killer cell cytotoxicity against SKBR3-A cells. This would give insight into the possible advantageous immunological effect of afatinib plus dasatinib.

As well as looking for therapeutic strategies to overcome afatinib resistance, we also investigated ways of preventing the development of resistance. As HER2-positive breast cancer patients that could potentially receive afatinib would most likely have received previous HER2-targeted therapy, we examined the efficacy of afatinib alone and in combination with dasatinib in acquired trastuzumab resistant cell lines and a lapatinib resistant cell line model. A panel of HER2-targeted therapy-naïve cell lines were also examined as representatives of patients without prior HER2-targeted intervention. All HER2-targeted therapy-naïve cell lines and the three trastuzumab resistant cell lines were exquisitely sensitive to afatinib alone (IC$_{50}$ values < 15 nM) (Figure 6-12), while the lapatinib resistant model, as previously discussed in Section 7.2, was resistant to afatinib alone at clinically relevant concentrations. Similar to literature reports, the HER2-positive breast cancer cells tested with dasatinib alone in this study showed minimal to no growth inhibition [210].

Afatinib plus dasatinib was strongly synergistic in SKBR3-L cells (Figure 6-13). In contrast, the combination only slightly improved afatinib response in one HER2-targeting TKI-naïve cell line, the SKBR3-T cells and had a non-antagonistic but non-additive effect in the other cell lines tested. It is possible that in a five day assay, afatinib causes such growth inhibition that dasatinib cannot enhance growth inhibition

further in such a short timeframe. Thus, we then used a longer-term treatment format to assess growth response (Section 6.4). By treating cells twice weekly until cells become treatment refractory, the drug response can be measured across time as well as by growth inhibition. The benefit of addition of dasatinib was observed in four of the six cell lines tested. For example, SKBR3 cells, which showed no improvement in the five-day assay, began to actively grow again after approximately 70 days of afatinib treatment. In contrast, SKBR3 cells treated with afatinib plus dasatinib did not develop resistance by this point. This was also observed in the SKBR3-T, EFM192A and HCC1954 cell lines. Importantly, the HCC1954 cells, which showed an initial synergistic response to afatinib plus dasatinib, maintained their response in this repeated treatment assay over a longer timescale. BT474 and BT474-T cells did not show emergence of afatinib resistance following treatment with 80 nM afatinib. Unfortunately, SKBR3 cells show a low tumourigenic potential *in vivo* [414] and therefore the effect of afatinib plus dasatinib on the SKBR3-A cell line cannot be investigated *in vivo*. In order to further examine the potential of afatinib plus dasatinib an *in vivo* model should be generated.

The HCC1954-N cell line may provide an appropriately model for studying the combination of a pan-HER inhibitor and dasatinib *in vivo*; HCC1954 cells are tumourigenic and the combination of neratinib and dasatinib was synergistic in this model. However, there are a number of differences between the HCC1954-N and SKBR3-A. The HCC1954-N cells displayed a different mechanism of cell death to the SKBR3-A cells. Both cell cycle and caspase 3/7 activation showed that neratinib plus dasatinib significantly induces apoptosis (Figure 6-20 and 6-21). Notably, previous work by another group showed that the HCC1954-N have decreased levels of EGFR, HER2 and HER3 and had increased IGF-1R, which is unlike the SKBR3-A cells [151, 206]. This would indicate that alternate resistance mechanisms are being exploited in the HCC1954-N cell line. However, the response to neratinib plus dasatinib in both the resistant and parental cell lines suggests that this is a viable therapeutic combination (Figure 6-17 and 6-18). The synergy observed in the HCC1954-N cell model was also observed in a 3D environment (Figure 6-19).

Previous investigations into the mechanism of neratinib resistance in the HCC1954-N cell line model by the group that developed the cell line have implicated CYP3A4 activity, over-expression of Neuromedin U, and down-regulation of miR-630 [151,

165, 206]. CYP3A4 is a cytochrome P450 that metabolises approximately half of all marketed drugs, including neratinib [415]. Therefore, the elevated CYP3A4 activity in HCC1954-N cells may decrease intracellular neratinib accumulation. Pharmacokinetic analysis of neratinib in combination with the CYP3A inhibitor ketoconazole showed a 3.2-fold increase in neratinib C_{max} [416]. CYP3A4 may also be relevant to the potential of neratinib plus dasatinib. Dasatinib is also a substrate and weak inhibitor of CYP3A4 and dasatinib levels are increased by co-administration of ketoconazole [417]. This may explain the reduced inhibition of neratinib or dasatinib alone in HCC1954-N cells compared to HCC1954-Par cells (Figures 6-17 and 6-18). Neuromedin U confers neratinib resistance by interacting with Hsp27, which stabilises HER2. Neuromedin U can increase HER2 and EGFR expression and reduce sensitivity to HER2-targeted therapy [165]. As the neratinib and dasatinib are acting downstream of HER2, the combination may overcoming this resistance mechanism.

In summary, the combination of afatinib or neratinib plus dasatinib shows potential for the treatment of pan-HER inhibitor resistant HER2-positive breast cancer (Figure 7-3). The combination of afatinib and dasatinib was strongly synergistic in SKBR3-A cells and cell death was due to necrosis and independent of apoptosis and autophagy. Neratinib plus dasatinib was also highly synergistic in HCC1954-N cells and, in contrast to the afatinib resistant model, stimulated a significant induction of apoptosis. The addition of dasatinib to afatinib does not enhance response in cell lines highly sensitive to afatinib, in short-term treatment experiments. However, the combination can delay or block the emergence of afatinib resistance. One cell line model of afatinib resistance and one model of neratinib resistance were tested in this study. This should be expanded in order to ensure that this is not a cell line-dependent phenomenon. Further *in vivo* investigations are necessary to determine the potential therapeutic benefit of afatinib or neratinib in combination with dasatinib.
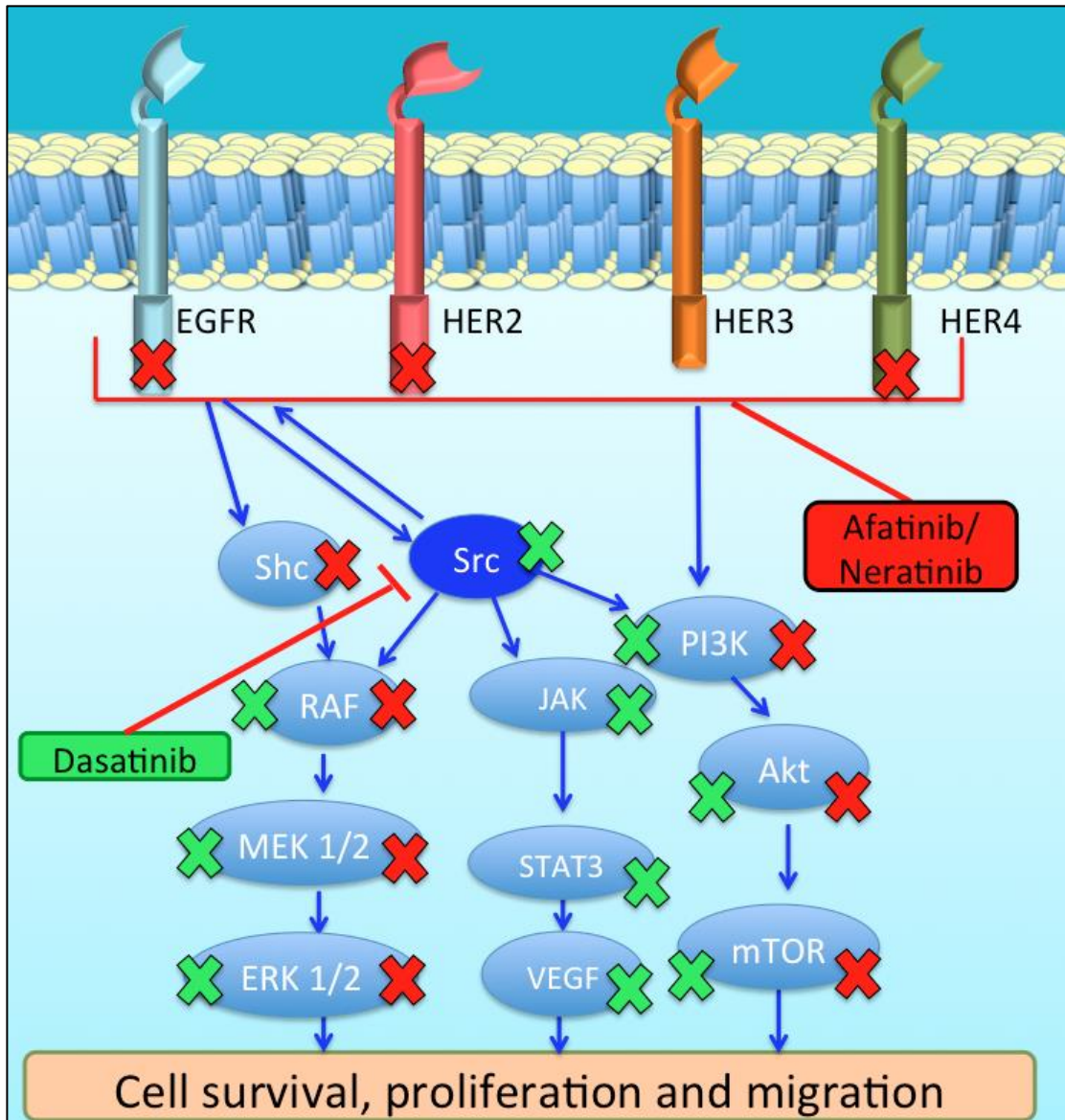
Figure 7-3: Afatinib/neratinib plus dasatinib in HER family member signalling (Pathway adapted from [349])**. Red X indicates inhibition by afainib/neratinib. Green X indicates inhibition by dasatinib.**

7.8 Summary

Acquired HER2-targeted therapy resistant cell lines represent a valid model of resistance observed in the clinic [148]. This study utilised seven HER2-targeted therapy resistant cell lines: three trastuzumab resistant, two lapatinib resistant, one afatinib resistant and one neratinib resistant cell line. These cell lines showed that the irreversible inhibitors afatinib and neratinib had a better efficacy against trastuzumab resistant cell lines than lapatinib resistant cell lines. Afatinib and neratinib resistant cell lines were insensitive to trastuzumab, pertuzumab, lapatinib and either pan-HER inhibitor, highlighting the need for novel targets for treatment-refractory HER2 positive breast cancer.

Both SKBR3-L and HCC1954-L cell lines were more sensitive to PP2A inhibition with okadaic acid and LB-100 compared to their parental cell lines. Okadaic acid and LB-100 in combination with lapatinib were both synergistic in HCC1954-L cells. PP2A inhibition and lapatinib caused apoptosis in both lapatinib-resistant cell lines. Importantly, combining PP2A inhibition with lapatinib in both SKBR3-Par and HCC1954-Par cell lines prevented the development of lapatinib resistance. Activation of PP2A using FTY720 also generated a less lapatinib sensitive phenotype in both parental cell lines. The proteomic analysis of HCC1954-L cells treated with okadaic acid and lapatinib by RPPA gave an insight into the molecular mechanism of action as combination therapy significantly inhibited downstream survival signalling compared to either single agent.

The optimal xenograft model of the HCC1954-L cell line was found to be mammary fat pad implantation. HCC1954-L cells caused skin ulceration on the tumour surface when implanted subcutaneously. This limited the size of the tumours and ultimately both subcutaneous implantation pilot studies were ended early for humane reasons. The mammary fat pad implantation did not display skin ulceration and will be the chosen model for future efficacy studies of LB-100 plus lapatinib. Preliminary study of the activity of LB-100 and lapatinib *in vivo* shows that the treatment can increase phospho-eEF2, indicating decreased PP2A activity, and the combination did not cause any adverse events in mice.

In a panel of HER2-positive breast cancer cell lines, sensitivity to okadaic acid correlated with resistance to both lapatinib and trastuzumab. Response to okadaic acid did not show any relationship to PP2A catalytic or structural subunit expression.

Likewise, PP2A expression had no relationship with lapatinib or trastuzumab sensitivity, showing that PP2A inhibition sensitivity is independent of PP2A catalytic and structural subunit expression. PP2A inhibition with LB-100 did not relate to HER2-targeted therapy or okadaic acid response. This indicates that LB-100 may have a different mechanism of action to okadaic acid in the panel of cell lines.

The SKBR3-A cell line represents an afatinib resistant model in HER2-positive breast cancer. This cell line showed increased EGFR and phosphorylated Src levels and - heightened sensitivity to the combination of afatinib and dasatinib. The combination caused a non-apoptotic, necrotic cell death in this model. The combination of afatinib and dasatinib prevented the development of afatinib resistance in five of seven cell lines tested.

Similarly, the neratinib resistant HCC1954-N cell line showed a synergistic response to the other pan-HER inhibitor neratinib plus dasatinib. In contrast to the SKBR3-A cells, the combination significantly induced apoptosis in these cells.

7.9 Conclusions

In conclusion, two novel approaches have been identified to overcome resistance to HER2-targeted therapies. Firstly, the combination of lapatinib plus LB-100 may be effective in acquired lapatinib resistant breast cancer, which will be further evaluated in *in vivo* efficacy testing. Levels of PP2A expression did not correlate with response to PP2A inhibition. Therefore, other potential biomarkers of response should be investigated, including methylated PP2A and PP2A substrate levels.

Secondly, afatinib or neratinib in combination with dasatinib has potential as a novel treatment strategy to block the emergence of TKI resistance in HER2-positive breast cancer. This combination could be evaluated clinically in two different settings: the combination may be effective as a second line-therapy in metastatic breast cancer after progression on trastuzumab or as a third line-therapy after the subsequent development of resistance to lapatinib.

8 References

1. Hanahan D, Weinberg RA, Francisco S: **The Hallmarks of Cancer**. 2000, **100**:57–70.

2. Hanahan D, Weinberg RA: **Hallmarks of cancer: the next generation.** *Cell* 2011, **144**:646–74.

3. **Cancer trends No. 29 - breast cancer** [http://www.ncri.ie/sites/ncri/files/pubs/bc_trends_21.pdf]

4. Linda A, Zuiani C, Girometti R, Londero V, Machin P, Brondani G, Bazzocchi M: **Unusual malignant tumors of the breast: MRI features and pathologic correlation**. *Eur J Radiol* 2010, **75**:178–184.

5. Pourteimoor V, Mohammadi-Yeganeh S, Paryan M: **Breast cancer classification and prognostication through diverse systems along with recent emerging findings in this respect; the dawn of new perspectives in the clinical applications**. *Tumor Biol* 2016, **37**:14479–14499.

6. Sorlie T, Tibshirani R, Parker J, Hastie T, Marron JS, Nobel A, Deng S, Johnsen H, Pesich R, Geisler S, Demeter J, Perou CM, Lønning PE, Brown PO, Børresen-Dale A-L, Botstein D: **Repeated observation of breast tumor subtypes in independent gene expression data sets.** *Proc Natl Acad Sci U S A* 2003, **100**:8418–23.

7. Sotiriou C, Wirapati P, Loi S, Harris A, Fox S, Smeds J, Nordgren H, Farmer P, Praz V, Haibe-Kains B, Desmedt C, Larsimont D, Cardoso F, Peterse H, Nuyten D, Buyse M, Van de Vijver MJ, Bergh J, Piccart M, Delorenzi M: **Gene expression profiling in breast cancer: understanding the molecular basis of histologic grade to improve prognosis.** *J Natl Cancer Inst* 2006, **98**:262–72.

8. Perou CM, Sørlie T, Eisen MB, van de Rijn M, Jeffrey SS, Rees C a, Pollack JR, Ross DT, Johnsen H, Akslen L a, Fluge O, Pergamenschikov a, Williams C, Zhu SX, Lønning PE, Børresen-Dale a L, Brown PO, Botstein D: **Molecular portraits of human breast tumours.** *Nature* 2000, **406**:747–52.

9. Sørlie T, Perou CM, Tibshirani R, Aas T, Geisler S, Johnsen H, Hastie T, Eisen MB, van de Rijn M, Jeffrey SS, Thorsen T, Quist H, Matese JC, Brown PO, Botstein D, Lønning PE, Børresen-Dale a L: **Gene expression patterns of breast carcinomas distinguish tumor subclasses with clinical implications.** *Proc Natl Acad Sci U S A* 2001, **98**:10869–74.

10. Dvorkin-Gheva A, Hassell JA: **Identification of a novel luminal molecular subtype of breast cancer.** *PLoS One* 2014, **9**:e103514.

11. Dawson S-J, Rueda OM, Aparicio S, Caldas C: **A new genome-driven integrated classification of breast cancer and its implications.** *EMBO J* 2013, **32**:617–28.

12. Goldhirsch A, Winer EP, Coates AS, Gelber RD, Piccart-Gebhart M, Thürlimann B, Senn H-J: **Personalizing the treatment of women with early breast cancer: highlights of the St Gallen International Expert Consensus on the Primary Therapy of Early Breast Cancer 2013.** *Ann Oncol* 2013, **24**:2206–23.

13. Kauraniemi P, Kallioniemi A: **Activation of multiple cancer-associated genes at the ERBB2 amplicon in breast cancer**. *Endocr Relat Cancer* 2006, **13**:39–49.

14. Schnitt SJ: **Classification and prognosis of invasive breast cancer: from morphology to molecular taxonomy.** *Mod Pathol* 2010, **23 Suppl 2**:S60-4.

15. Prat A, Parker JS, Karginova O, Fan C, Livasy C, Herschkowitz JI, He X, Perou CM: **Phenotypic and molecular characterization of the claudin-low intrinsic subtype of breast cancer.** *Breast Cancer Res* 2010, **12**:R68.

16. Farmer P, Bonnefoi H, Becette V, Tubiana-Hulin M, Fumoleau P, Larsimont D, Macgrogan G, Bergh J, Cameron D, Goldstein D, Duss S, Nicoulaz A-L, Brisken C, Fiche M, Delorenzi M, Iggo R: **Identification of molecular apocrine breast tumours by microarray analysis.** *Oncogene* 2005, **24**:4660–71.

17. Aertgeerts K, Skene R, Yano J, Sang B-C, Zou H, Snell G, Jennings A, Iwamoto K, Habuka N, Hirokawa A, Ishikawa T, Tanaka T, Miki H, Ohta Y, Sogabe S: **Structural analysis of the mechanism of inhibition and allosteric activation of the kinase domain of HER2 protein.** *J Biol Chem* 2011, **286**:18756–65.

18. Cho H, Mason K, Ramyar KX, Stanley AM: **Structure of the extracellular region of HER2 alone and in complex with the Herceptin Fab**. *Nature* 2003, **421**:756–60.

19. Roskoski R: **ErbB/HER protein-tyrosine kinases: Structures and small molecule inhibitors.** *Pharmacol Res* 2014, **87**:42–59.

20. Stein RA, Staros J V: **Evolutionary analysis of the ErbB receptor and ligand families.** *J Mol Evol* 2000, **50**:397–412.

21. Falls DL: **Neuregulins: functions, forms, and signaling strategies.** *Exp Cell Res* 2003, **284**:14–30.

22. Yarden Y, Sliwkowski MX: **Untangling the ErbB signalling network.** *Nat Rev Mol Cell Biol* 2001, **2**:127–37.

23. Shankaran H, Zhang Y, Tan Y, Resat H: **Model-based analysis of HER activation in cells co-expressing EGFR, HER2 and HER3.** *PLoS Comput Biol* 2013, **9**:e1003201.

24. Sliwkowski MX: **Ready to partner.** *Nat Struct Biol* 2003, **10**:158–9.

25. Brennan PJ, Kumogai T, Berezov A, Murali R, Greene MI: **HER2/Neu: mechanisms of dimerization/oligomerization**. *Oncogene* 2000, **19**:6093–6101.

26. Peles E, Lamprecht R, Ben-Levy R, Tzahar E, Yarden Y: **Regulated coupling of the Neu receptor to phosphatidylinositol 3'-kinase and its release by oncogenic activation.** *J Biol Chem* 1992, **267**:12266–74.

27. Britsch S, Li L, Kirchhoff S, Theuring F, Brinkmann V, Birchmeier C, Riethmacher D: **The ErbB2 and ErbB3 receptors and their ligand, neuregulin-1, are essential for development of the sympathetic nervous system**. *Genes Dev* 1998, **12**:1825–1836.

28. Moscoso LM, Chu GC, Gautam M, Noakes PG, Merlie JP, Sanes JR: **Synapse-associated expression of an acetylcholine receptor-inducing protein, ARIA/heregulin, and its putative receptors, ErbB2 and ErbB3, in developing mammalian muscle.** *Dev Biol* 1995, **172**:158–69.

29. Alroy I, Yarden Y: **The ErbB signaling network in embryogenesis and oncogenesis: signal diversification through combinatorial ligand-receptor interactions**. *FEBS Lett* 1997, **410**:83–86.

30. Ozcelik C, Erdmann B, Pilz B, Wettschureck N, Britsch S, Hübner N, Chien KR, Birchmeier C, Garratt AN: **Conditional mutation of the ErbB2 (HER2) receptor in cardiomyocytes leads to dilated cardiomyopathy.** *Proc Natl Acad Sci U S A* 2002, **99**:8880–5.

31. Press MF, Cordon-Cardo C, Slamon DJ: **Expression of the HER-2/neu proto-oncogene in normal human adult and fetal tissues.** *Oncogene* 1990, **5**:953–62.

32. Iwamoto R, Yamazaki S, Asakura M, Takashima S, Hasuwa H, Miyado K, Adachi S, Kitakaze M, Hashimoto K, Raab G, Nanba D, Higashiyama S, Hori M, Klagsbrun M, Mekada E: **Heparin-binding EGF-like growth factor and ErbB signaling is essential for heart function.** *Proc Natl Acad Sci U S A* 2003, **100**:3221–6.

33. Slamon D, Clark G, Wong S, Levin W, Ullrich A, McGuire W: **Human breast cancer: correlation of relapse and survival with amplification of the HER-2/neu oncogene**. *Science (80-)* 1987, **235**:177–182.

34. Research C for DE and: **Therapeutic Biologic Applications (BLA) - Trastuzumab Product Approval Information - Licensing Action 9/25/98**. .

35. Ryan Q, Ibrahim A, Cohen MH, Johnson J, Ko C, Sridhara R, Justice R, Pazdur R: **FDA drug approval summary: lapatinib in combination with capecitabine for previously treated metastatic breast cancer that overexpresses HER-2.** *Oncologist* 2008, **13**:1114–9.

36. Blumenthal GM, Scher NS, Cortazar P, Chattopadhyay S, Tang S, Song P, Liu Q, Ringgold K, Pilaro AM, Tilley A, King KE, Graham L, Rellahan BL, Weinberg WC, Chi B, Thomas C, Hughes P, Ibrahim A, Justice R, Pazdur R: **First FDA approval of dual anti-HER2 regimen: pertuzumab in combination with trastuzumab and docetaxel for HER2-positive metastatic breast cancer.** *Clin Cancer Res* 2013, **19**:4911–6.

37. Amiri-Kordestani L, Wedam S, Zhang L, Tang S, Tilley A, Ibrahim A, Justice R, Pazdur R, Cortazar P: **First FDA approval of neoadjuvant therapy for breast cancer: pertuzumab for the treatment of patients with HER2-positive breast cancer.** *Clin Cancer Res* 2014, **20**:5359–64.

38. Amiri-Kordestani L, Blumenthal GM, Xu QC, Zhang L, Tang SW, Ha L, Weinberg WC, Chi B, Candau-Chacon R, Hughes P, Russell AM, Pope Miksinski S, Chen XH, McGuinn WD, Palmby T, Schrieber SJ, Liu Q, Wang J, Song P, Mehrotra N, Skarupa L, Clouse K, Al-Hakim A, Sridhara R, Ibrahim A, Justice R, Pazdur R, Cortazar P: **FDA Approval: Ado-trastuzumab Emtansine for the Treatment of Patients with HER2-Positive Metastatic Breast Cancer.** *Clin Cancer Res* 2014.

39. Research AA for C: **Neratinib Approved for HER2+ Breast Cancer**. *Cancer Discov* 2017.

40. Nagata Y, Lan K-H, Zhou X, Tan M, Esteva FJ, Sahin AA, Klos KS, Li P, Monia BP, Nguyen NT, Hortobagyi GN, Hung M-C, Yu D: **PTEN activation contributes to tumor inhibition by trastuzumab, and loss of PTEN predicts trastuzumab resistance in patients.** *Cancer Cell* 2004, **6**:117–27.

41. Petricevic B, Laengle J, Singer J, Sachet M, Fazekas J, Steger G, Bartsch R, Jensen-Jarolim E, Bergmann M: **Trastuzumab mediates antibody-dependent cell-mediated cytotoxicity and phagocytosis to the same extent in both adjuvant and metastatic HER2/neu breast cancer patients.** *J Transl Med* 2013, **11**:307.

42. Collins DM, Gately K, Hughes C, Edwards C, Davies A, Madden SF, O'Byrne KJ, O'Donovan N, Crown J: **Tyrosine kinase inhibitors as modulators of trastuzumab-mediated antibody-dependent cell-mediated cytotoxicity in breast cancer cell lines**. *Cell Immunol* 2017, **319**:35–42.

43. Ram S, Kim D, Ober RJ, Ward ES: **The level of HER2 expression is a predictor of antibody-HER2 trafficking behavior in cancer cells.** *MAbs* 2014, **6**:1211–9.

44. Klos KS, Zhou X, Lee S, Zhang L, Yang W, Nagata Y, Yu D: **Combined trastuzumab and paclitaxel treatment better inhibits ErbB-2-mediated angiogenesis in breast carcinoma through a more effective inhibition of Akt than either treatment alone.** *Cancer* 2003, **98**:1377–85.

45. Le X-F, Claret F-X, Lammayot A, Tian L, Deshpande D, LaPushin R, Tari AM, Bast RC: **The role of cyclin-dependent kinase inhibitor p27Kip1 in anti-HER2 antibody-induced G1 cell cycle arrest and tumor growth inhibition.** *J Biol Chem* 2003, **278**:23441–50.

46. Hudziak RM, Lewis GD, Winget M, Fendly BM, Shepard HM, Ullrich A: **p185HER2 monoclonal antibody has antiproliferative effects in vitro and sensitizes human breast tumor cells to tumor necrosis factor.** *Mol Cell Biol* 1989, **9**:1165–72.

47. Fendly BM, Winget M, Hudziak RM, Lipari MT, Napier MA, Ullrich A: **Characterization of murine monoclonal antibodies reactive to either the human epidermal growth factor receptor or HER2/neu gene product.** *Cancer Res* 1990, **50**:1550–8.

48. Sarup JC, Johnson RM, King KL, Fendly BM, Lipari MT, Napier MA, Ullrich A, Shepard HM: **Characterization of an anti-p185HER2 monoclonal antibody that stimulates receptor function and inhibits tumor cell growth.** *Growth Regul* 1991, **1**:72–82.

49. Carter P, Presta L, Gorman CM, Ridgway JB, Henner D, Wong WL, Rowland AM, Kotts C, Carver ME, Shepard HM: **Humanization of an anti-p185HER2 antibody for human cancer therapy.** *Proc Natl Acad Sci U S A* 1992, **89**:4285–9.

50. Cobleigh MA, Vogel CL, Tripathy D, Robert NJ, Scholl S, Fehrenbacher L, Wolter JM, Paton V, Shak S, Lieberman G, Slamon DJ: **Multinational study of the efficacy and safety of humanized anti-HER2 monoclonal antibody in women who have HER2-overexpressing metastatic breast cancer that has progressed after chemotherapy for metastatic disease.** *J Clin Oncol* 1999, **17**:2639–48.

51. Slamon DJ, Leyland-Jones B, Shak S, Fuchs H, Paton V, Bajamonde A, Fleming T, Eiermann W, Wolter J, Pegram M, Baselga J, Norton L: **Use of chemotherapy plus a monoclonal antibody against HER2 for metastatic breast cancer that overexpresses HER2.** *N Engl J Med* 2001, **344**:783–92.

52. Gullo G, Zuradelli M, Sclafani F, Santoro A, Crown J: **Durable complete response following chemotherapy and trastuzumab for metastatic HER2-positive breast cancer.** *Ann Oncol* 2012, **23**:2204–5.

53. Dahabreh IJ, Linardou H, Siannis F, Fountzilas G, Murray S: **Trastuzumab in the Adjuvant Treatment of Early-Stage Breast Cancer: A Systematic Review and Meta-Analysis of Randomized Controlled Trials**. *Oncologist* 2008, **13**:620–630.

54. O'Sullivan CC, Smith KL: **Therapeutic Considerations in Treating HER2-Positive Metastatic Breast Cancer.** *Curr Breast Cancer Rep* 2014, **6**:169–182.

55. Romond EH, Perez EA, Bryant J, Suman VJ, Geyer CE, Davidson NE, Tan-Chiu E, Martino S, Paik S, Kaufman PA, Swain SM, Pisansky TM, Fehrenbacher L, Kutteh LA, Vogel VG, Visscher DW, Yothers G, Jenkins RB, Brown AM, Dakhil SR, Mamounas EP, Lingle WL, Klein PM, Ingle JN, Wolmark N: **Trastuzumab plus adjuvant chemotherapy for operable HER2-positive breast cancer.** *N Engl J Med* 2005, **353**:1673–84.

56. Pivot X, Romieu G, Debled M, Pierga J-Y, Kerbrat P, Bachelot T, Lortholary A, Espié M, Fumoleau P, Serin D, Jacquin J-P, Jouannaud C, Rios M, Abadie-Lacourtoisie S, Tubiana-Mathieu N, Cany L, Catala S, Khayat D, Pauporté I, Kramar A, PHARE trial investigators: **6 months versus 12 months of adjuvant trastuzumab for patients with HER2-positive early breast cancer (PHARE): a randomised phase 3 trial.** *Lancet Oncol* 2013, **14**:741–8.

57. Gyawali B, Niraula S: **Duration of adjuvant trastuzumab in HER2 positive breast cancer: Overall and disease free survival results from meta-analyses of randomized controlled trials**. *Cancer Treat Rev* 2017, **60**:18–23.

58. Cameron D, Piccart-Gebhart MJ, Gelber RD, Procter M, Goldhirsch A, de Azambuja E, Castro G, Untch M, Smith I, Gianni L, Baselga J, Al-Sakaff N, Lauer S, McFadden E, Leyland-Jones B, Bell R, Dowsett M, Jackisch C, Herceptin Adjuvant (HERA) Trial Study Team: **11 years' follow-up of trastuzumab after adjuvant chemotherapy in HER2-positive early breast cancer: final analysis of the HERceptin Adjuvant (HERA) trial.** *Lancet (London, England)* 2017, **389**:1195–1205.

59. Gianni L, Eiermann W, Semiglazov V, Lluch A, Tjulandin S, Zambetti M,

Moliterni A, Vazquez F, Byakhov MJ, Lichinitser M, Climent MA, Ciruelos E, Ojeda B, Mansutti M, Bozhok A, Magazzù D, Heinzmann D, Steinseifer J, Valagussa P, Baselga J: **Neoadjuvant and adjuvant trastuzumab in patients with HER2-positive locally advanced breast cancer (NOAH): follow-up of a randomised controlled superiority trial with a parallel HER2-negative cohort.** *Lancet Oncol* 2014.

60. Gianni L, Salvatorelli E, Minotti G: **Anthracycline cardiotoxicity in breast cancer patients: synergism with trastuzumab and taxanes**. *Cardiovasc Toxicol* 2007, **7**:67–71.

61. Wittayanukorn S, Qian J, Westrick SC, Billor N, Johnson B, Hansen RA: **Prevention of Trastuzumab and Anthracycline-induced Cardiotoxicity Using Angiotensin-converting Enzyme Inhibitors or β-blockers in Older Adults With Breast Cancer**. *Am J Clin Oncol* 2017:1.

62. Slamon D, Eiermann W, Robert N, Pienkowski T, Martin M, Press M, Mackey J, Glaspy J, Chan A, Pawlicki M, Pinter T, Valero V, Liu M-C, Sauter G, von Minckwitz G, Visco F, Bee V, Buyse M, Bendahmane B, Tabah-Fisch I, Lindsay M-A, Riva A, Crown J, Breast Cancer International Research Group TBCIR: **Adjuvant trastuzumab in HER2-positive breast cancer.** *N Engl J Med* 2011, **365**:1273–83.

63. Harbeck N, Beckmann MW, Rody A, Schneeweiss A, Müller V, Fehm T, Marschner N, Gluz O, Schrader I, Heinrich G, Untch M, Jackisch C: **HER2 Dimerization Inhibitor Pertuzumab - Mode of Action and Clinical Data in Breast Cancer**. *Breast Care* 2013, **8**:49–55.

64. Franklin MC, Carey KD, Vajdos FF, Leahy DJ, de Vos AM, Sliwkowski MX: **Insights into ErbB signaling from the structure of the ErbB2-pertuzumab complex.** *Cancer Cell* 2004, **5**:317–28.

65. Scheuer W, Friess T, Burtscher H, Bossenmaier B, Endl J, Hasmann M: **Strongly Enhanced Antitumor Activity of Trastuzumab and Pertuzumab Combination Treatment on HER2-Positive Human Xenograft Tumor Models**. *Cancer Res* 2009, **69**:9330–9336.

66. Nahta R: **The HER-2-Targeting Antibodies Trastuzumab and Pertuzumab Synergistically Inhibit the Survival of Breast Cancer Cells**. *Cancer Res* 2004, **64**:2343–2346.

67. Swain SM, Kim S-B, Cortés J, Ro J, Semiglazov V, Campone M, Ciruelos E, Ferrero J-M, Schneeweiss A, Knott A, Clark E, Ross G, Benyunes MC, Baselga J: **Pertuzumab, trastuzumab, and docetaxel for HER2-positive metastatic breast cancer (CLEOPATRA study): overall survival results from a randomised,**

double-blind, placebo-controlled, phase 3 study. *Lancet Oncol* 2013, **14**:461–471.

68. Baselga J, Cortés J, Kim S-B, Im S-A, Hegg R, Im Y-H, Roman L, Pedrini JL, Pienkowski T, Knott A, Clark E, Benyunes MC, Ross G, Swain SM: **Pertuzumab plus Trastuzumab plus Docetaxel for Metastatic Breast Cancer**. *N Engl J Med* 2012, **366**:109–119.

69. Sabatier R, Gonçalves A: **Pertuzumab (Perjeta®) approval in HER2-positive metastatic breast cancers**. *Bull Cancer* 2014, **101**:765–771.

70. **Five-year analysis of the phase II NeoSphere trial evaluating four cycles of neoadjuvant docetaxel (D) and/or trastuzumab (T) and/or pertuzumab (P). | 2015 ASCO Annual Meeting | Abstracts | Meeting Library** [http://meetinglibrary.asco.org/content/147709-156]

71. Gianni L, Pienkowski T, Im Y-H, Roman L, Tseng L-M, Liu M-C, Lluch A, Staroslawska E, de la Haba-Rodriguez J, Im S-A, Pedrini JL, Poirier B, Morandi P, Semiglazov V, Srimuninnimit V, Bianchi G, Szado T, Ratnayake J, Ross G, Valagussa P: **Efficacy and safety of neoadjuvant pertuzumab and trastuzumab in women with locally advanced, inflammatory, or early HER2-positive breast cancer (NeoSphere): a randomised multicentre, open-label, phase 2 trial.** *Lancet Oncol* 2012, **13**:25–32.

72. Lewis Phillips GD, Li G, Dugger DL, Crocker LM, Parsons KL, Mai E, Blättler WA, Lambert JM, Chari RVJ, Lutz RJ, Wong WLT, Jacobson FS, Koeppen H, Schwall RH, Kenkare-Mitra SR, Spencer SD, Sliwkowski MX: **Targeting HER2-positive breast cancer with trastuzumab-DM1, an antibody-cytotoxic drug conjugate.** *Cancer Res* 2008, **68**:9280–90.

73. Junttila TT, Li G, Parsons K, Phillips GL, Sliwkowski MX: **Trastuzumab-DM1 (T-DM1) retains all the mechanisms of action of trastuzumab and efficiently inhibits growth of lapatinib insensitive breast cancer**. *Breast Cancer Res Treat* 2011, **128**:347–356.

74. Barok M, Tanner M, Köninki K, Isola J: **Trastuzumab-DM1 causes tumour growth inhibition by mitotic catastrophe in trastuzumab-resistant breast cancer cells in vivo**. *Breast Cancer Res* 2011, **13**:R46.

75. Barok M, Tanner M, Köninki K, Isola J: **Trastuzumab-DM1 causes tumour growth inhibition by mitotic catastrophe in trastuzumab-resistant breast cancer cells in vivo**. *Breast Cancer Res* 2011, **13**:R46.

76. Krop IE, Beeram M, Modi S, Jones SF, Holden SN, Yu W, Girish S, Tibbitts J, Yi

J-H, Sliwkowski MX, Jacobson F, Lutzker SG, Burris HA: **Phase I study of trastuzumab-DM1, an HER2 antibody-drug conjugate, given every 3 weeks to patients with HER2-positive metastatic breast cancer.** *J Clin Oncol* 2010, **28**:2698–704.

77. Beeram M, Krop IE, Burris HA, Girish SR, Yu W, Lu MW, Holden SN, Modi S: **A phase 1 study of weekly dosing of trastuzumab emtansine (T-DM1) in patients with advanced human epidermal growth factor 2-positive breast cancer**. *Cancer* 2012, **118**:5733–5740.

78. Peddi PF, Hurvitz SA: **Ado-trastuzumab emtansine (T-DM1) in human epidermal growth factor receptor 2 (HER2)-positive metastatic breast cancer: latest evidence and clinical potential.** *Ther Adv Med Oncol* 2014, **6**:202–9.

79. Diéras V, Miles D, Verma S, Pegram M, Welslau M, Baselga J, Krop IE, Blackwell K, Hoersch S, Xu J, Green M, Gianni L: **Trastuzumab emtansine versus capecitabine plus lapatinib in patients with previously treated HER2-positive advanced breast cancer (EMILIA): a descriptive analysis of final overall survival results from a randomised, open-label, phase 3 trial**. *Lancet Oncol* 2017, **18**:732–742.

80. Guerin M, Sabatier R, Gonçalves A: **Autorisation de mise sur le marché du trastuzumab emtansine (Kadcyla®) dans les cancers du sein métastatiques HER2-positifs**. *Bull Cancer* 2015, **102**:390–397.

81. Miller KD, Diéras V, Harbeck N, Andre F, Mahtani RL, Gianni L, Albain KS, Crivellari D, Fang L, Michelson G, de Haas SL, Burris HA: **Phase IIa Trial of Trastuzumab Emtansine With Pertuzumab for Patients With Human Epidermal Growth Factor Receptor 2-Positive, Locally Advanced, or Metastatic Breast Cancer.** *J Clin Oncol* 2014.

82. Cameron D, Casey M, Press M, Lindquist D, Pienkowski T, Romieu CG, Chan S, Jagiello-Gruszfeld A, Kaufman B, Crown J, Chan A, Campone M, Viens P, Davidson N, Gorbounova V, Raats JI, Skarlos D, Newstat B, Roychowdhury D, Paoletti P, Oliva C, Rubin S, Stein S, Geyer CE: **A phase III randomized comparison of lapatinib plus capecitabine versus capecitabine alone in women with advanced breast cancer that has progressed on trastuzumab: updated efficacy and biomarker analyses.** *Breast Cancer Res Treat* 2008, **112**:533–43.

83. Villanueva C, Romieu G, Salvat J, Chaigneau L, Merrouche Y, N'guyen T, Vuillemin AT, Demarchi M, Dobi E, Pivot X: **Phase II study assessing lapatinib added to letrozole in patients with progressive disease under aromatase inhibitor in metastatic breast cancer-Study BES 06.** *Target Oncol* 2013, **8**:137–43.

84. **PubChem Compound Database**

85. Nahta R, Yuan LXH, Du Y, Esteva FJ: **Lapatinib induces apoptosis in trastuzumab-resistant breast cancer cells: effects on insulin-like growth factor I signaling.** *Mol Cancer Ther* 2007, **6**:667–74.

86. Wainberg ZA, Anghel A, Desai AJ, Ayala R, Luo T, Safran B, Fejzo MS, Hecht JR, Slamon DJ, Finn RS: **Lapatinib, a dual EGFR and HER2 kinase inhibitor, selectively inhibits HER2-amplified human gastric cancer cells and is synergistic with trastuzumab in vitro and in vivo.** *Clin Cancer Res* 2010, **16**:1509–19.

87. Zhu X, Wu L, Qiao H, Han T, Chen S, Liu X, Jiang R, Wei Y, Feng D, Zhang Y, Ma Y, Zhang S, Zhang J: **Autophagy stimulates apoptosis in HER2-overexpressing breast cancers treated by lapatinib.** *J Cell Biochem* 2013, **114**:2643–53.

88. Konecny GE, Pegram MD, Venkatesan N, Finn R, Yang G, Rahmeh M, Untch M, Rusnak DW, Spehar G, Mullin RJ, Keith BR, Gilmer TM, Berger M, Podratz KC, Slamon DJ: **Activity of the dual kinase inhibitor lapatinib (GW572016) against HER-2-overexpressing and trastuzumab-treated breast cancer cells.** *Cancer Res* 2006, **66**:1630–9.

89. Rusnak DW, Lackey K, Affleck K, Wood ER, Alligood KJ, Rhodes N, Keith BR, Murray DM, Knight WB, Mullin RJ, Gilmer TM: **The effects of the novel, reversible epidermal growth factor receptor/ErbB-2 tyrosine kinase inhibitor, GW2016, on the growth of human normal and tumor-derived cell lines in vitro and in vivo.** *Mol Cancer Ther* 2001, **1**:85–94.

90. Burris HA, Hurwitz HI, Dees EC, Dowlati A, Blackwell KL, O'Neil B, Marcom PK, Ellis MJ, Overmoyer B, Jones SF, Harris JL, Smith DA, Koch KM, Stead A, Mangum S, Spector NL: **Phase I safety, pharmacokinetics, and clinical activity study of lapatinib (GW572016), a reversible dual inhibitor of epidermal growth factor receptor tyrosine kinases, in heavily pretreated patients with metastatic carcinomas.** *J Clin Oncol* 2005, **23**:5305–13.

91. Tanizaki J, Okamoto I, Fumita S, Okamoto W, Nishio K, Nakagawa K: **Roles of BIM induction and survivin downregulation in lapatinib-induced apoptosis in breast cancer cells with HER2 amplification.** *Oncogene* 2011, **30**:4097–106.

92. Xia W, Bisi J, Strum J, Liu L, Carrick K, Graham KM, Treece AL, Hardwicke MA, Dush M, Liao Q, Westlund RE, Zhao S, Bacus S, Spector NL: **Regulation of survivin by ErbB2 signaling: therapeutic implications for ErbB2-overexpressing breast cancers.** *Cancer Res* 2006, **66**:1640–7.

93. Martin AP, Mitchell C, Rahmani M, Nephew KP, Grant S, Dent P: **Inhibition of MCL-1 enhances lapatinib toxicity and overcomes lapatinib resistance via BAK-dependent autophagy.** *Cancer Biol Ther* 2009, **8**:2084–96.

94. Mitchell C, Yacoub A, Hossein H, Martin AP, Bareford MD, Eulitt P, Yang C, Nephew KP, Dent P: **Inhibition of MCL-1 in breast cancer cells promotes cell death in vitro and in vivo.** *Cancer Biol Ther* 2010, **10**:903–17.

95. Tural D, Akar E, Mutlu H, Kilickap S: **P95 HER2 fragments and breast cancer outcome.** *Expert Rev Anticancer Ther* 2014, **14**:1089–96.

96. Scaltriti M, Verma C, Guzman M, Jimenez J, Parra JL, Pedersen K, Smith DJ, Landolfi S, Ramon y Cajal S, Arribas J, Baselga J: **Lapatinib, a HER2 tyrosine kinase inhibitor, induces stabilization and accumulation of HER2 and potentiates trastuzumab-dependent cell cytotoxicity.** *Oncogene* 2009, **28**:803–14.

97. Gelmon KA, Boyle FM, Kaufman B, Huntsman DG, Manikhas A, Di Leo A, Martin M, Schwartzberg LS, Lemieux J, Aparicio S, Shepherd LE, Dent S, Ellard SL, Tonkin K, Pritchard KI, Whelan TJ, Nomikos D, Nusch A, Coleman RE, Mukai H, Tjulandin S, Khasanov R, Rizel S, Connor AP, Santillana SL, Chapman J-AW, Parulekar WR: **Lapatinib or Trastuzumab Plus Taxane Therapy for Human Epidermal Growth Factor Receptor 2-Positive Advanced Breast Cancer: Final Results of NCIC CTG MA.31.** *J Clin Oncol* 2015, **33**:1574–83.

98. Geyer CE, Forster J, Lindquist D, Chan S, Romieu CG, Pienkowski T, Jagiello-Gruszfeld A, Crown J, Chan A, Kaufman B, Skarlos D, Campone M, Davidson N, Berger M, Oliva C, Rubin SD, Stein S, Cameron D: **Lapatinib plus capecitabine for HER2-positive advanced breast cancer.** *N Engl J Med* 2006, **355**:2733–43.

99. Bian L, Wang T, Zhang S, Jiang Z: **Trastuzumab plus capecitabine vs. lapatinib plus capecitabine in patients with trastuzumab resistance and taxane-pretreated metastatic breast cancer.** *Tumour Biol* 2013, **34**:3153–8.

100. Blackwell KL, Burstein HJ, Storniolo AM, Rugo HS, Sledge G, Aktan G, Ellis C, Florance A, Vukelja S, Bischoff J, Baselga J, O'Shaughnessy J: **Overall survival benefit with lapatinib in combination with trastuzumab for patients with human epidermal growth factor receptor 2-positive metastatic breast cancer: final results from the EGF104900 Study.** *J Clin Oncol* 2012, **30**:2585–92.

101. Piccart-Gebhart M, Holmes E, Baselga J, de Azambuja E, Dueck AC, Viale G, Zujewski JA, Goldhirsch A, Armour A, Pritchard KI, McCullough AE, Dolci S, McFadden E, Holmes AP, Tonghua L, Eidtmann H, Dinh P, Di Cosimo S, Harbeck N, Tjulandin S, Im Y-H, Huang C-S, Diéras V, Hillman DW, Wolff AC, Jackisch C, Lang I, Untch M, Smith I, Boyle F, et al.: **Adjuvant Lapatinib and Trastuzumab**

for Early Human Epidermal Growth Factor Receptor 2-Positive Breast Cancer: Results From the Randomized Phase III Adjuvant Lapatinib and/or Trastuzumab Treatment Optimization Trial. *J Clin Oncol* 2016, **34**:1034–42.

102. Baselga J, Bradbury I, Eidtmann H, Di Cosimo S, de Azambuja E, Aura C, Gómez H, Dinh P, Fauria K, Van Dooren V, Aktan G, Goldhirsch A, Chang T-W, Horváth Z, Coccia-Portugal M, Domont J, Tseng L-M, Kunz G, Sohn JH, Semiglazov V, Lerzo G, Palacova M, Probachai V, Pusztai L, Untch M, Gelber RD, Piccart-Gebhart M: **Lapatinib with trastuzumab for HER2-positive early breast cancer (NeoALTTO): a randomised, open-label, multicentre, phase 3 trial.** *Lancet* 2012, **379**:633–40.

103. **The association between event-free survival and pathological complete response to neoadjuvant lapatinib, trastuzumab or their combination in HER2-positive breast cancer. Survival follow-up analysis of the NeoALTTO study (BIG 1-06)** [http://www.abstracts2view.com/sabcs13/view.php?nu=SABCS13L_877&terms=]

104. Blackwell KL, Burstein HJ, Storniolo AM, Rugo H, Sledge G, Koehler M, Ellis C, Casey M, Vukelja S, Bischoff J, Baselga J, O'Shaughnessy J: **Randomized study of Lapatinib alone or in combination with trastuzumab in women with ErbB2-positive, trastuzumab-refractory metastatic breast cancer.** *J Clin Oncol* 2010, **28**:1124–30.

105. Bundred N, Cameron D, Armstrong D, Brunt A, Dodwell D, Evans A, Hanby A, Hartup S, Hong A, Horgan K, Khattak I, Morden J, Naik J, Narajan S, Ooi J, Shaaban A, Smith R, Webster-Smith M, Bliss J: **Effects of perioperative lapatinib and trastuzumab, alone and in combination, in early HER2+ breast cancer - the UK EPHOS-B trial (CRUK/08/002).** In *European Breast Cancer Conference 10*; 2016.

106. Llombart-Cussac A, Cortés J, Paré L, Galván P, Bermejo B, Martínez N, Vidal M, Pernas S, López R, Muñoz M, Nuciforo P, Morales S, Oliveira M, de la Peña L, Peláez A, Prat A: **HER2-enriched subtype as a predictor of pathological complete response following trastuzumab and lapatinib without chemotherapy in early-stage HER2-positive breast cancer (PAMELA): an open-label, single-group, multicentre, phase 2 trial.** *Lancet Oncol* 2017, **18**:545–554.

107. Rabindran SK, Discafani CM, Rosfjord EC, Baxter M, Floyd MB, Golas J, Hallett WA, Johnson BD, Nilakantan R, Overbeek E, Reich MF, Shen R, Shi X, Tsou H-R, Wang Y-F, Wissner A: **Antitumor activity of HKI-272, an orally active, irreversible inhibitor of the HER-2 tyrosine kinase.** *Cancer Res* 2004, **64**:3958–65.

108. Canonici A, Gijsen M, Mullooly M, Bennett R, Bouguern N, Pedersen K, O'Brien NA, Roxanis I, Li J-L, Bridge E, Finn R, Siamon D, McGowan P, Duffy MJ, O'Donovan N, Crown J, Kong A: **Neratinib overcomes trastuzumab resistance in**

HER2 amplified breast cancer. *Oncotarget* 2013, **4**:1592–605.

109. Mohd Nafi SN, Generali D, Kramer-Marek G, Gijsen M, Strina C, Cappelletti M, Andreis D, Haider S, Li J-L, Bridges E, Capala J, Ioannis R, Harris AL, Kong A: **Nuclear HER4 mediates acquired resistance to trastuzumab and is associated with poor outcome in HER2 positive breast cancer.** *Oncotarget* 2014, **5**:5934–49.

110. Wong K-K, Fracasso PM, Bukowski RM, Lynch TJ, Munster PN, Shapiro GI, Jänne PA, Eder JP, Naughton MJ, Ellis MJ, Jones SF, Mekhail T, Zacharchuk C, Vermette J, Abbas R, Quinn S, Powell C, Burris HA: **A phase I study with neratinib (HKI-272), an irreversible pan ErbB receptor tyrosine kinase inhibitor, in patients with solid tumors.** *Clin Cancer Res* 2009, **15**:2552–8.

111. Ben-Baruch NE, Bose R, Kavuri SM, Ma CX, Ellis MJ: **HER2-Mutated Breast Cancer Responds to Treatment With Single-Agent Neratinib, a Second-Generation HER2/EGFR Tyrosine Kinase Inhibitor.** *J Natl Compr Canc Netw* 2015, **13**:1061–4.

112. Sequist L V., Besse B, Lynch TJ, Miller VA, Wong KK, Gitlitz B, Eaton K, Zacharchuk C, Freyman A, Powell C, Ananthakrishnan R, Quinn S, Soria J-C: **Neratinib, an Irreversible Pan-ErbB Receptor Tyrosine Kinase Inhibitor: Results of a Phase II Trial in Patients With Advanced Non–Small-Cell Lung Cancer.** *J Clin Oncol* 2010, **28**:3076–3083.

113. Burstein HJ, Sun Y, Dirix LY, Jiang Z, Paridaens R, Tan AR, Awada A, Ranade A, Jiao S, Schwartz G, Abbas R, Powell C, Turnbull K, Vermette J, Zacharchuk C, Badwe R: **Neratinib, an irreversible ErbB receptor tyrosine kinase inhibitor, in patients with advanced ErbB2-positive breast cancer.** *J Clin Oncol* 2010, **28**:1301–7.

114. Saura C, Garcia-Saenz JA, Xu B, Harb W, Moroose R, Pluard T, Cortes J, Kiger C, Germa C, Wang K, Martin M, Baselga J, Kim S-B: **Safety and Efficacy of Neratinib in Combination With Capecitabine in Patients With Metastatic Human Epidermal Growth Factor Receptor 2-Positive Breast Cancer.** *J Clin Oncol* 2014.

115. Martin M, Bonneterre J, Geyer CE, Ito Y, Ro J, Lang I, Kim S-B, Germa C, Vermette J, Wang K, Wang K, Awada A: **A phase two randomised trial of neratinib monotherapy versus lapatinib plus capecitabine combination therapy in patients with HER2+ advanced breast cancer.** *Eur J Cancer* 2013, **49**:3763–72.

116. **A Study of Neratinib Plus Capecitabine Versus Lapatinib Plus Capecitabine in Patients With HER2+ Metastatic Breast Cancer Who Have Received Two or More Prior HER2 Directed Regimens in the Metastatic Setting - Full Text View -**

ClinicalTrials.gov [https://clinicaltrials.gov/ct2/show/NCT01808573]

117. Jankowitz RC, Abraham J, Tan AR, Limentani S a, Tierno MB, Adamson LM, Buyse M, Wolmark N, Jacobs S a: **Safety and efficacy of neratinib in combination with weekly paclitaxel and trastuzumab in women with metastatic HER2‑positive breast cancer: an NSABP Foundation Research Program phase I study.** *Cancer Chemother Pharmacol* 2013, **72**:1205–12.

118. Li D, Ambrogio L, Shimamura T, Kubo S, Takahashi M, Chirieac LR, Padera RF, Shapiro GI, Baum A, Himmelsbach F, Rettig WJ, Meyerson M, Solca F, Greulich H, Wong K-K: **BIBW2992, an irreversible EGFR/HER2 inhibitor highly effective in preclinical lung cancer models.** *Oncogene* 2008, **27**:4702–11.

119. Sequist L V, Yang JC-H, Yamamoto N, O'Byrne K, Hirsh V, Mok T, Geater SL, Orlov S, Tsai C-M, Boyer M, Su W-C, Bennouna J, Kato T, Gorbunova V, Lee KH, Shah R, Massey D, Zazulina V, Shahidi M, Schuler M: **Phase III study of afatinib or cisplatin plus pemetrexed in patients with metastatic lung adenocarcinoma with EGFR mutations.** *J Clin Oncol* 2013, **31**:3327–34.

120. Solca F, Dahl G, Zoephel A, Bader G, Sanderson M, Klein C, Kraemer O, Himmelsbach F, Haaksma E, Adolf GR: **Target binding properties and cellular activity of afatinib (BIBW 2992), an irreversible ErbB family blocker.** *J Pharmacol Exp Ther* 2012, **343**:342–50.

121. Solca F, Dahl G, Zoephel A, Bader G, Sanderson M, Klein C, Kraemer O, Himmelsbach F, Haaksma E, Adolf GR: **Target binding properties and cellular activity of afatinib (BIBW 2992), an irreversible ErbB family blocker.** *J Pharmacol Exp Ther* 2012, **343**:342–50.

122. Ioannou N, Dalgleish AG, Seddon AM, Mackintosh D, Guertler U, Solca F, Modjtahedi H: **Anti-tumour activity of afatinib, an irreversible ErbB family blocker, in human pancreatic tumour cells.** *Br J Cancer* 2011, **105**:1554–62.

123. **Effect of afatinib alone and in combination with trastuzumab in HER2-positive breast cancer cell lines. | 2013 ASCO Annual Meeting | Virtual Meeting | Meeting Library** [http://meetinglibrary.asco.org/content/85383?media=vm&poster=1]

124. Gordon MS, Mendelson DS, Gross M, Uttenreuther-Fischer M, Ould-Kaci M, Zhao Y, Stopfer P, Agus DB: **A Phase I, open-label, dose-escalation study of continuous once-daily oral treatment with afatinib in patients with advanced solid tumors.** *Invest New Drugs* 2013, **31**:409–16.

125. Yap TA, Vidal L, Adam J, Stephens P, Spicer J, Shaw H, Ang J, Temple G, Bell S, Shahidi M, Uttenreuther-Fischer M, Stopfer P, Futreal A, Calvert H, de Bono JS, Plummer R: **Phase I trial of the irreversible EGFR and HER2 kinase inhibitor BIBW 2992 in patients with advanced solid tumors.** *J Clin Oncol* 2010, **28**:3965–72.

126. Eskens FALM, Mom CH, Planting AST, Gietema JA, Amelsberg A, Huisman H, van Doorn L, Burger H, Stopfer P, Verweij J, de Vries EGE: **A phase I dose escalation study of BIBW 2992, an irreversible dual inhibitor of epidermal growth factor receptor 1 (EGFR) and 2 (HER2) tyrosine kinase in a 2-week on, 2-week off schedule in patients with advanced solid tumours.** *Br J Cancer* 2008, **98**:80–5.

127. Marshall J, Hwang J, Eskens FALM, Burger H, Malik S, Uttenreuther-Fischer M, Stopfer P, Ould-Kaci M, Cohen RB, Lewis NL: **A Phase I, open-label, dose escalation study of afatinib, in a 3-week-on/1-week-off schedule in patients with advanced solid tumors.** *Invest New Drugs* 2013, **31**:399–408.

128. Lin NU, Winer EP, Wheatley D, Carey L a, Houston S, Mendelson D, Munster P, Frakes L, Kelly S, Garcia A a, Cleator S, Uttenreuther-Fischer M, Jones H, Wind S, Vinisko R, Hickish T: **A phase II study of afatinib (BIBW 2992), an irreversible ErbB family blocker, in patients with HER2-positive metastatic breast cancer progressing after trastuzumab.** *Breast Cancer Res Treat* 2012, **133**:1057–65.

129. Harbeck N, Huang C-S, Hurvitz S, Yeh D-C, Shao Z, Im S-A, Jung KH, Shen K, Ro J, Jassem J, Zhang Q, Im Y-H, Wojtukiewicz M, Sun Q, Chen S-C, Goeldner R-G, Uttenreuther-Fischer M, Xu B, Piccart-Gebhart M, Senkus E, Kyriakides S, Penault-Llorca F, al. et, Network NCC, Narayan M, Wilken J, Harris L, Baron A, Kimbler K, Maihle N, et al.: **Afatinib plus vinorelbine versus trastuzumab plus vinorelbine in patients with HER2-overexpressing metastatic breast cancer who had progressed on one previous trastuzumab treatment (LUX-Breast 1): an open-label, randomised, phase 3 trial**. *Lancet Oncol* 2016, **17**:357–366.

130. Cortés J, Dieras V, Ro J, Barriere J, Bachelot T, Hurvitz S, Le Rhun E, Espié M, Kim S-B, Schneeweiss A, Sohn JH, Nabholtz J-M, Kellokumpu-Lehtinen P-L, Taguchi J, Piacentini F, Ciruelos E, Bono P, Ould-Kaci M, Roux F, Joensuu H: **Afatinib alone or afatinib plus vinorelbine versus investigator's choice of treatment for HER2-positive breast cancer with progressive brain metastases after trastuzumab, lapatinib, or both (LUX-Breast 3): a randomised, open-label, multicentre, phase 2 tr**. *Lancet Oncol* 2015, **16**:1700–10.

131. Hickish T, Tseng L-M, Jay M, Tsang J, Kovalenko N, Udovitsa D, Pelling K, Ullenreuther-Fischer M, Huang C-S: **LUX-breast 2: Phase II, open-label study of oral afatinib in HER2-overexpressing metastatic breast cancer (MBC) patients (pts) who progressed on prior trastuzumab (T) and/or lapatanib (L).** *J Clin Oncol* 2012, **30**.

132. Rimawi MF, Aleixo SB, Rozas AA, Nunes de Matos Neto J, Caleffi M, Figueira AC, Souza SC, Reiriz AB, Gutierrez C, Arantes H, Uttenreuther-Fischer MM, Solca F, Osborne CK: **A Neoadjuvant, Randomized, Open-Label Phase II Trial of Afatinib Versus Trastuzumab Versus Lapatinib in Patients With Locally Advanced HER2-Positive Breast Cancer**. *Clin Breast Cancer* 2015, **15**:101–109.

133. Hanusch C, Schneeweiss A, Loibl S, Untch M, Paepke S, Kummel S, Jackisch C, Huober J, Hilfrich J, Gerber B, Eidtmann H, Denkert C, Costa S, Blohmer JU, Engels K, Burchardi N, von Minckwitz G: **Dual Blockade with AFatinib and Trastuzumab as NEoadjuvant Treatment for Patients with Locally Advanced or Operable Breast Cancer Receiving Taxane-Anthracycline Containing Chemotherapy--DAFNE (GBG-70)**. *Clin Cancer Res* 2015, **21**:2924–2931.

134. Wistuba II, Behrens C, Milchgrub S, Wistuba I, Cunningham H, Minna D: **Comparison of features of human breast cancer cell lines and their corresponding tumors . of Features of Human and**. 1998:2931–2938.

135. Lacroix M, Leclercq G: **Relevance of breast cancer cell lines as models for breast tumours: an update.** *Breast Cancer Res Treat* 2004, **83**:249–89.

136. Vu T, Claret FX: **Trastuzumab: updated mechanisms of action and resistance in breast cancer.** *Front Oncol* 2012, **2**:62.

137. Vu T, Sliwkowski MX, Claret FX: **Personalized drug combinations to overcome trastuzumab resistance in HER2-positive breast cancer.** *Biochim Biophys Acta* 2014, **1846**:353–65.

138. Lavaud P, Andre F: **Strategies to overcome trastuzumab resistance in HER2-overexpressing breast cancers: focus on new data from clinical trials.** *BMC Med* 2014, **12**:132.

139. Luque-Cabal M, García-Teijido P, Fernández-Pérez Y, Sánchez-Lorenzo L, Palacio-Vázquez I: **Mechanisms Behind the Resistance to Trastuzumab in HER2-Amplified Breast Cancer and Strategies to Overcome It.** *Clin Med Insights Oncol* 2016, **10**(Suppl 1):21–30.

140. Narayan M, Wilken JA, Harris LN, Baron AT, Kimbler KD, Maihle NJ: **Trastuzumab-induced HER reprogramming in "resistant" breast carcinoma cells.** *Cancer Res* 2009, **69**:2191–4.

141. Shattuck DL, Miller JK, Carraway KL, Sweeney C: **Met Receptor Contributes to Trastuzumab Resistance of Her2-Overexpressing Breast Cancer Cells**. *Cancer Res* 2008, **68**:1471–1477.

142. Minuti G, Cappuzzo F, Duchnowska R, Jassem J, Fabi A, O'Brien T, Mendoza AD, Landi L, Biernat W, Czartoryska-Arłukowicz B, Jankowski T, Zuziak D, Zok J, Szostakiewicz B, Foszczyńska-Kłoda M, Tempińska-Szałach A, Rossi E, Varella-Garcia M: **Increased MET and HGF gene copy numbers are associated with trastuzumab failure in HER2-positive metastatic breast cancer.** *Br J Cancer* 2012, **107**:793–9.

143. Browne BC, Crown J, Venkatesan N, Duffy MJ, Clynes M, Slamon D, O'Donovan N: **Inhibition of IGF1R activity enhances response to trastuzumab in HER-2-positive breast cancer cells**. *Ann Oncol* 2011, **22**:68–73.

144. Price-Schiavi SA, Jepson S, Li P, Arango M, Rudland PS, Yee L, Carraway KL: **Rat Muc4 (sialomucin complex) reduces binding of anti-ErbB2 antibodies to tumor cell surfaces, a potential mechanism for herceptin resistance**. *Int J Cancer* 2002, **99**:783–791.

145. Li G, Zhao L, Li W, Fan K, Qian W, Hou S, Wang H, Dai J, Wei H, Guo Y: **Feedback activation of STAT3 mediates trastuzumab resistance via upregulation of MUC1 and MUC4 expression**. *Oncotarget* 2014, **5**:8317–8329.

146. Chen AC, Migliaccio I, Rimawi M, Lopez-Tarruella S, Creighton CJ, Massarweh S, Huang C, Wang Y-C, Batra SK, Gutierrez MC, Osborne CK, Schiff R: **Upregulation of mucin4 in ER-positive/HER2-overexpressing breast cancer xenografts with acquired resistance to endocrine and HER2-targeted therapies.** *Breast Cancer Res Treat* 2012, **134**:583–93.

147. Tsé C, Gauchez A-S, Jacot W, Lamy P-J: **HER2 shedding and serum HER2 extracellular domain: Biology and clinical utility in breast cancer**. *Cancer Treat Rev* 2012, **38**:133–142.

148. McDermott M, Eustace AJ, Busschots S, Breen L, Crown J, Clynes M, O'Donovan N, Stordal B: **In vitro Development of Chemotherapy and Targeted Therapy Drug-Resistant Cancer Cell Lines: A Practical Guide with Case Studies.** *Front Oncol* 2014, **4**(March):40.

149. Xia W, Petricoin EF, Zhao S, Liu L, Osada T, Cheng Q, Wulfkuhle JD, Gwin WR, Yang X, Gallagher RI, Bacus S, Lyerly HK, Spector NL: **An heregulin-EGFR-HER3 autocrine signaling axis can mediate acquired lapatinib resistance in HER2+ breast cancer models.** *Breast Cancer Res* 2013, **15**:R85.

150. Liu L, Greger J, Shi H, Liu Y, Greshock J, Annan R, Halsey W, Sathe GM, Martin A-M, Gilmer TM: **Novel mechanism of lapatinib resistance in HER2-positive breast tumor cells: activation of AXL.** *Cancer Res* 2009, **69**:6871–8.

151. Corcoran C, Rani S, Breslin S, Gogarty M, Ghobrial IM, Crown J, O'Driscoll L: **miR-630 targets IGF1R to regulate response to HER-targeting drugs and overall cancer cell progression in HER2 over-expressing breast cancer.** *Mol Cancer* 2014, **13**:71.

152. Ma C, Niu X, Luo J, Shao Z, Shen K: **Combined effects of lapatinib and bortezomib in human epidermal receptor 2 (HER2)-overexpressing breast cancer cells and activity of bortezomib against lapatinib-resistant breast cancer cells.** *Cancer Sci* 2010, **101**:2220–2226.

153. Jegg A-M, Ward TM, Iorns E, Hoe N, Zhou J, Liu X, Singh S, Landgraf R, Pegram MD: **PI3K independent activation of mTORC1 as a target in lapatinib-resistant ERBB2+ breast cancer cells.** *Breast Cancer Res Treat* 2012, **136**:683–92.

154. McDermott MS, Browne BC, Conlon NT, O'Brien NA, Slamon DJ, Henry M, Meleady P, Clynes M, Dowling P, Crown J, O'Donovan N: **PP2A inhibition overcomes acquired resistance to HER2 targeted therapy.** *Mol Cancer* 2014, **13**:157.

155. Azuma K, Tsurutani J, Sakai K, Kaneda H, Fujisaka Y, Takeda M, Watatani M, Arao T, Satoh T, Okamoto I, Kurata T, Nishio K, Nakagawa K: **Switching addictions between HER2 and FGFR2 in HER2-positive breast tumor cells: FGFR2 as a potential target for salvage after lapatinib failure.** *Biochem Biophys Res Commun* 2011, **407**:219–24.

156. Bi X, Rexer B, Arteaga CL, Guo M, Mahadevan-Jansen A: **Evaluating HER2 amplification status and acquired drug resistance in breast cancer cells using Raman spectroscopy.** *J Biomed Opt* 2014, **19**:25001.

157. Rexer BN, Ham A-JL, Rinehart C, Hill S, Granja-Ingram N de M, González-Angulo AM, Mills GB, Dave B, Chang JC, Liebler DC, Arteaga CL: **Phosphoproteomic mass spectrometry profiling links Src family kinases to escape from HER2 tyrosine kinase inhibition.** *Oncogene* 2011, **30**:4163–74.

158. Brady SW, Zhang J, Seok D, Wang H, Yu D: **Enhanced PI3K p110α signaling confers acquired lapatinib resistance that can be effectively reversed by a p110α-selective PI3K inhibitor.** *Mol Cancer Ther* 2014, **13**:60–70.

159. Chen S, Zhu X, Qiao H, Ye M, Lai X, Yu S, Ding L, Wen A, Zhang J: **Protective autophagy promotes the resistance of HER2-positive breast cancer cells to lapatinib**. *Tumor Biol* 2016, **37**:2321–2331.

160. Formisano L, Nappi L, Rosa R, Marciano R, D Amato C, D Amato V, Damiano

V, Raimondo L, Iommelli F, Scorziello A, Troncone G, Veneziani BM, Parsons SJ, De Placido S, Bianco R: **Epidermal growth factor receptor activation modulates Src-dependent resistance to lapatinib in breast cancer models.** *Breast Cancer Res* 2014, **16**:R45.

161. Huang C, Park CC, Hilsenbeck SG, Ward R, Rimawi MF, Wang Y-C, Shou J, Bissell MJ, Osborne CK, Schiff R: **β1 integrin mediates an alternative survival pathway in breast cancer cells resistant to lapatinib.** *Breast Cancer Res* 2011, **13**:R84.

162. Komurov K, Tseng J-T, Muller M, Seviour EG, Moss TJ, Yang L, Nagrath D, Ram PT: **The glucose-deprivation network counteracts lapatinib-induced toxicity in resistant ErbB2-positive breast cancer cells.** *Mol Syst Biol* 2012, **8**:596.

163. Lesniak D, Sabri S, Xu Y, Graham K, Bhatnagar P, Suresh M, Abdulkarim B: **Spontaneous epithelial-mesenchymal transition and resistance to HER-2-targeted therapies in HER-2-positive luminal breast cancer.** *PLoS One* 2013, **8**:e71987.

164. Puig T, Aguilar H, Cufí S, Oliveras G, Turrado C, Ortega-Gutiérrez S, Benhamú B, López-Rodríguez ML, Urruticoechea A, Colomer R: **A novel inhibitor of fatty acid synthase shows activity against HER2+ breast cancer xenografts and is active in anti-HER2 drug-resistant cell lines.** *Breast Cancer Res* 2011, **13**:R131.

165. Rani S, Corcoran C, Shiels L, Germano S, Breslin S, Madden S, McDermott MS, Browne BC, O'Donovan N, Crown J, Gogarty M, Byrne AT, O'Driscoll L: **Neuromedin U: A Candidate Biomarker and Therapeutic Target to Predict and Overcome Resistance to HER-Tyrosine Kinase Inhibitors.** *Cancer Res* 2014.

166. Wang Y-C, Morrison G, Gillihan R, Guo J, Ward RM, Fu X, Botero MF, Healy NA, Hilsenbeck SG, Phillips GL, Chamness GC, Rimawi MF, Osborne CK, Schiff R: **Different mechanisms for resistance to trastuzumab versus lapatinib in HER2-positive breast cancers--role of estrogen receptor and HER2 reactivation.** *Breast Cancer Res* 2011, **13**:R121.

167. Wang Q, Quan H, Zhao J, Xie C, Wang L, Lou L: **RON confers lapatinib resistance in HER2-positive breast cancer cells.** *Cancer Lett* 2013, **340**:43–50.

168. Xia W, Bacus S, Hegde P, Husain I, Strum J, Liu L, Paulazzo G, Lyass L, Trusk P, Hill J, Harris J, Spector NL: **A model of acquired autoresistance to a potent ErbB2 tyrosine kinase inhibitor and a therapeutic strategy to prevent its onset in breast cancer.** *Proc Natl Acad Sci U S A* 2006, **103**:7795–800.

169. Xia W, Petricoin EF, Zhao S, Liu L, Osada T, Cheng Q, Wulfkuhle JD, Gwin WR, Yang X, Gallagher RI, Bacus S, Lyerly HK, Spector NL: **An heregulin-EGFR-HER3 autocrine signaling axis can mediate acquired lapatinib resistance in HER2+ breast cancer models.** *Breast Cancer Res* 2013, **15**:R85.

170. Xu X, De Angelis C, Burke KA, Nardone A, Hu H, Qin L, Veeraraghavan J, Sethunath V, Heiser LM, Wang N, Ng CKY, Chen ES, Renwick A, Wang T, Nanda S, Shea M, Mitchell T, Rajendran M, Waters I, Zabransky DJ, Scott KL, Gutierrez C, Nagi C, Geyer FC, Chamness GC, Park BH, Shaw CA, Hilsenbeck SG, Rimawi MF, Gray JW, et al.: **HER2 Reactivation through Acquisition of the HER2 L755S Mutation as a Mechanism of Acquired Resistance to HER2-targeted Therapy in HER2 ⁺ Breast Cancer**. *Clin Cancer Res* 2017, **23**:5123–5134.

171. Trowe T, Boukouvala S, Calkins K, Cutler RE, Fong R, Funke R, Gendreau SB, Kim YD, Miller N, Woolfrey JR, Vysotskaia V, Yang JP, Gerritsen ME, Matthews DJ, Lamb P, Heuer TS: **EXEL-7647 inhibits mutant forms of ErbB2 associated with lapatinib resistance and neoplastic transformation.** *Clin Cancer Res* 2008, **14**:2465–75.

172. De Leon DD, Wilson DM, Powers M, Rosenfeld RG: **Effects of insulin-like growth factors (IGFs) and IGF receptor antibodies on the proliferation of human breast cancer cells.** *Growth Factors* 1992, **6**:327–36.

173. Grimberg A, Cohen P: **Role of insulin-like growth factors and their binding proteins in growth control and carcinogenesis.** *J Cell Physiol* 2000, **183**:1–9.

174. Farhana L, Dawson MI, Murshed F, Das JK, Rishi AK, Fontana JA: **Upregulation of miR-150* and miR-630 induces apoptosis in pancreatic cancer cells by targeting IGF-1R.** *PLoS One* 2013, **8**:e61015.

175. O'Bryan JP, Frye RA, Cogswell PC, Neubauer A, Kitch B, Prokop C, Espinosa R, Le Beau MM, Earp HS, Liu ET: **axl, a transforming gene isolated from primary human myeloid leukemia cells, encodes a novel receptor tyrosine kinase.** *Mol Cell Biol* 1991, **11**:5016–31.

176. Chia SK, Ellard SL, Mates M, Welch S, Mihalcioiu C, Miller WH, Gelmon K, Lohrisch C, Kumar V, Taylor S, Hagerman L, Goodwin R, Wang T, Sakashita S, Tsao MS, Eisenhauer E, Bradbury P: **A phase-I study of lapatinib in combination with foretinib, a c-MET, AXL and vascular endothelial growth factor receptor inhibitor, in human epidermal growth factor receptor 2 (HER-2)-positive metastatic breast cancer**. *Breast Cancer Res* 2017, **19**:54.

177. Eswarakumar VP, Lax I, Schlessinger J: **Cellular signaling by fibroblast growth factor receptors.** *Cytokine Growth Factor Rev* 2005, **16**:139–49.

178. Hanker AB, Garrett JT, Estrada MV, Moore PD, Ericsson PG, Koch JP, Langley E, Singh S, Kim PS, Frampton GM, Sanford E, Owens P, Becker J, Groseclose MR, Castellino S, Joensuu H, Huober J, Brase JC, Majjaj S, Brohée S, Venet D, Brown D, Baselga J, Piccart M, Sotiriou C, Arteaga CL: **HER2-Overexpressing Breast Cancers Amplify FGFR Signaling upon Acquisition of Resistance to Dual Therapeutic Blockade of HER2**. *Clin Cancer Res* 2017, **23**:4323–4334.

179. Bachman KE, Argani P, Samuels Y, Silliman N, Ptak J, Szabo S, Konishi H, Karakas B, Blair BG, Lin C, Peters BA, Velculescu VE, Park BH: **The PIK3CA gene is mutated with high frequency in human breast cancers.** *Cancer Biol Ther* 2004, **3**:772–5.

180. Li J, Yen C, Liaw D, Podsypanina K, Bose S, Wang SI, Puc J, Miliaresis C, Rodgers L, McCombie R, Bigner SH, Giovanella BC, Ittmann M, Tycko B, Hibshoosh H, Wigler MH, Parsons R: **PTEN, a putative protein tyrosine phosphatase gene mutated in human brain, breast, and prostate cancer.** *Science* 1997, **275**:1943–7.

181. Carpten JD, Faber AL, Horn C, Donoho GP, Briggs SL, Robbins CM, Hostetter G, Boguslawski S, Moses TY, Savage S, Uhlik M, Lin A, Du J, Qian Y-W, Zeckner DJ, Tucker-Kellogg G, Touchman J, Patel K, Mousses S, Bittner M, Schevitz R, Lai M-HT, Blanchard KL, Thomas JE: **A transforming mutation in the pleckstrin homology domain of AKT1 in cancer.** *Nature* 2007, **448**:439–44.

182. Bellacosa A, de Feo D, Godwin AK, Bell DW, Cheng JQ, Altomare DA, Wan M, Dubeau L, Scambia G, Masciullo V, Ferrandina G, Benedetti Panici P, Mancuso S, Neri G, Testa JR: **Molecular alterations of the AKT2 oncogene in ovarian and breast carcinomas.** *Int J Cancer* 1995, **64**:280–5.

183. Wang L, Zhang Q, Zhang J, Sun S, Guo H, Jia Z, Wang B, Shao Z, Wang Z, Hu X: **PI3K pathway activation results in low efficacy of both trastuzumab and lapatinib.** *BMC Cancer* 2011, **11**:248.

184. O'Brien N a, Browne BC, Chow L, Wang Y, Ginther C, Arboleda J, Duffy MJ, Crown J, O'Donovan N, Slamon DJ: **Activated phosphoinositide 3-kinase/AKT signaling confers resistance to trastuzumab but not lapatinib.** *Mol Cancer Ther* 2010, **9**:1489–502.

185. Elster N, Cremona M, Morgan C, Toomey S, Carr A, O'Grady A, Hennessy BT, Eustace AJ: **A preclinical evaluation of the PI3K alpha/delta dominant inhibitor BAY 80-6946 in HER2-positive breast cancer models with acquired resistance to the HER2-targeted therapies trastuzumab and lapatinib**. *Breast Cancer Res Treat* 2015, **149**:373–383.

186. Ikink GJ, Hilkens J: **Insulin receptor substrate 4 (IRS4) is a constitutive active oncogenic driver collaborating with HER2 and causing therapeutic resistance**. *Mol Cell Oncol* 2017, **4**:e1279722.

187. Gahlaut R, Bennett A, Fatayer H, Dall BJ, Sharma N, Velikova G, Perren T, Dodwell D, Lansdown M, Shaaban AM: **Effect of neoadjuvant chemotherapy on breast cancer phenotype, ER/PR and HER2 expression – Implications for the practising oncologist**. *Eur J Cancer* 2016, **60**:40–48.

188. Shibue T, Weinberg RA: **EMT, CSCs, and drug resistance: the mechanistic link and clinical implications**. *Nat Rev Clin Oncol* 2017, **14**:611–629.

189. Oliveras-Ferraros C, Corominas-Faja B, Cufí S, Vazquez-Martin A, Martin-Castillo B, Iglesias JM, López-Bonet E, Martin ÁG, Menendez JA: **Epithelial-to-mesenchymal transition (EMT) confers primary resistance to trastuzumab (Herceptin)**. *Cell Cycle* 2012, **11**:4020–32.

190. Seshacharyulu P, Pandey P, Datta K, Batra SK: **Phosphatase: PP2A structural importance, regulation and its aberrant expression in cancer.** *Cancer Lett* 2013, **335**:9–18.

191. Yang J, Wu J, Tan C, Klein PS: **PP2A:B56epsilon is required for Wnt/beta-catenin signaling during embryonic development.** *Development* 2003, **130**:5569–78.

192. Westermarck J, Hahn WC: **Multiple pathways regulated by the tumor suppressor PP2A in transformation.** *Trends Mol Med* 2008, **14**:152–60.

193. Wong LL, Chang CF, Koay ESC, Zhang D: **Tyrosine phosphorylation of PP2A is regulated by HER-2 signalling and correlates with breast cancer progression**. *Int J Oncol* 2009, **34**:1291–1301.

194. Martiniova L, Lu J, Chiang J, Bernardo M, Lonser R, Zhuang Z, Pacak K: **Pharmacologic modulation of serine/threonine phosphorylation highly sensitizes PHEO in a MPC cell and mouse model to conventional chemotherapy.** *PLoS One* 2011, **6**:e14678.

195. Lu J, Zhuang Z, Song DK, Mehta GU, Ikejiri B, Mushlin H, Park DM, Lonser RR: **The effect of a PP2A inhibitor on the nuclear receptor corepressor pathway in glioma.** *J Neurosurg* 2010, **113**:225–33.

196. Wei D, Parsels L a, Karnak D, Davis M a, Parsels JD, Marsh AC, Zhao L, Maybaum J, Lawrence TS, Sun Y, Morgan M a: **Inhibition of protein phosphatase**

2A radiosensitizes pancreatic cancers by modulating CDC25C/CDK1 and homologous recombination repair. *Clin Cancer Res* 2013, **19**:4422–32.

197. Zhao M, Howard EW, Parris AB, Guo Z, Zhao Q, Ma Z, Xing Y, Liu B, Edgerton SM, Thor AD, Yang X: **Activation of cancerous inhibitor of PP2A (CIP2A) contributes to lapatinib resistance through induction of CIP2A-Akt feedback loop in ErbB2-positive breast cancer cells**. *Oncotarget* 2017, **8**:58847–58864.

198. Yamaoka T, Ohmori T, Ohba M, Arata S, Murata Y, Kusumoto S, Ando K, Ishida H, Ohnishi T, Sasaki Y: **Distinct Afatinib Resistance Mechanisms Identified in Lung Adenocarcinoma Harboring an EGFR Mutation.** *Mol Cancer Res* 2017, **15**:915–928.

199. Wu S-G, Liu Y-N, Tsai M-F, Chang Y-L, Yu C-J, Yang P-C, Yang JC-H, Wen Y-F, Shih J-Y: **The mechanism of acquired resistance to irreversible EGFR tyrosine kinase inhibitor-afatinib in lung adenocarcinoma patients**. *Oncotarget* 2016, **7**:12404–13.

200. van der Wekken AJ, Kuiper JL, Saber A, Terpstra MM, Wei J, Hiltermann TJN, Thunnissen E, Heideman DAM, Timens W, Schuuring E, Kok K, Smit EF, van den Berg A, Groen HJM: **Overall survival in EGFR mutated non-small-cell lung cancer patients treated with afatinib after EGFR TKI and resistant mechanisms upon disease progression**. *PLoS One* 2017, **12**:e0182885.

201. **V843I, a Lung Cancer Predisposing EGFR Mutation, Is Responsible for Resistance to EGFR Tyrosine Kinase Inhibitors**. *J Thorac Oncol* 2014, **9**:1377–1384.

202. O'Brien NA, McDonald K, Tong L, von Euw E, Kalous O, Conklin D, Hurvitz SA, di Tomaso E, Schnell C, Linnartz R, Finn RS, Hirawat S, Slamon DJ: **Targeting PI3K/mTOR overcomes resistance to HER2-targeted therapy independent of feedback activation of AKT.** *Clin Cancer Res* 2014, **20**:3507–20.

203. Pirazzoli V, Nebhan C, Song X, Wurtz A, Walther Z, Cai G, Zhao Z, Jia P, de Stanchina E, Shapiro EM, Gale M, Yin R, Horn L, Carbone DP, Stephens PJ, Miller V, Gettinger S, Pao W, Politi K: **Acquired Resistance of EGFR-Mutant Lung Adenocarcinomas to Afatinib plus Cetuximab Is Associated with Activation of mTORC1**. *Cell Rep* 2014, **7**:999–1008.

204. Booth L, Roberts JL, Tavallai M, Webb T, Leon D, Chen J, McGuire WP, Poklepovic A, Dent P: **The afatinib resistance of <i>in vivo</i> generated H1975 lung cancer cell clones is mediated by SRC/ERBB3/c-KIT/c-MET compensatory survival signaling**. *Oncotarget* 2016, **7**:19620–19630.

205. Creelan B, Gray J, Lima D, Antonia S, Chiappori A, Tanvetyanon T, DeVane R, Williams C, Haura E: **Abstract CT060: Efficacy, safety and tolerability of dasatinib combined with afatinib: a phase I trial in patients with epidermal growth factor receptor mutant (EGFRm) advanced non-small-cell lung cancer (NSCLC) after acquired tyrosine kinase inhibitor (TKI) resistance**. *Cancer Res* 2016, **76**(14 Supplement):CT060-CT060.

206. Breslin S, Lowry MC, O'Driscoll L: **Neratinib resistance and cross-resistance to other HER2-targeted drugs due to increased activity of metabolism enzyme cytochrome P4503A4**. *Br J Cancer* 2017, **116**:620–625.

207. Bose R, Kavuri SM, Searleman AC, Shen W, Shen D, Koboldt DC, Monsey J, Goel N, Aronson AB, Li S, Ma CX, Ding L, Mardis ER, Ellis MJ: **Activating HER2 mutations in HER2 gene amplification negative breast cancer.** *Cancer Discov* 2013, **3**:224–37.

208. Hanker AB, Red Brewer M, Sheehan JH, Koch JP, Nagy R, Lanman R, Berger MF, Hyman DM, Solit DB, He J, Miller V, Cutler RE, Lalani AS, Cross D, Meiler J, Arteaga CL: **An acquired HER2 T798I gatekeeper mutation induces resistance to neratinib in a patient with HER2 mutant-driven breast cancer**. .

209. Nam S, Kim D, Cheng JQ, Zhang S, Lee J-H, Buettner R, Mirosevich J, Lee FY, Jove R: **Action of the Src Family Kinase Inhibitor, Dasatinib (BMS-354825), on Human Prostate Cancer Cells**. *Cancer Res* 2005, **65**:9185–9189.

210. Finn RS, Dering J, Ginther C, Wilson CA, Glaspy P, Tchekmedyian N, Slamon DJ: **Dasatinib, an orally active small molecule inhibitor of both the src and abl kinases, selectively inhibits growth of basal-type/?triple-negative? breast cancer cell lines growing in vitro**. *Breast Cancer Res Treat* 2007, **105**:319–326.

211. Lombardo LJ, Lee FY, Chen P, Norris D, Barrish JC, Behnia K, Castaneda S, Cornelius LAM, Das J, Doweyko AM, Fairchild C, Hunt JT, Inigo I, Johnston K, Kamath A, Kan D, Klei H, Marathe P, Pang S, Peterson R, Pitt S, Schieven GL, Schmidt RJ, Tokarski J, Wen M-L, Wityak J, Borzilleri RM: **Discovery of *N* -(2-Chloro-6-methyl- phenyl)-2-(6-(4-(2-hydroxyethyl)- piperazin-1-yl)-2-methylpyrimidin-4- ylamino)thiazole-5-carboxamide (BMS-354825), a Dual Src/Abl Kinase Inhibitor with Potent Antitumor Activity in Preclinical Assays**. *J Med Chem* 2004, **47**:6658–6661.

212. Roskoski R: **Src protein–tyrosine kinase structure and regulation**. *Biochem Biophys Res Commun* 2004, **324**:1155–1164.

213. Finn RS, Dering J, Ginther C, Wilson CA, Glaspy P, Tchekmedyian N, Slamon DJ: **Dasatinib, an orally active small molecule inhibitor of both the src and abl**

kinases, selectively inhibits growth of basal-type/"triple-negative" breast cancer cell lines growing in vitro. *Breast Cancer Res Treat* 2007, **105**:319–326.

214. Tai Y-L, Chu P-Y, Lai I-R, Wang M-Y, Tseng H-Y, Guan J-L, Liou J-Y, Shen T-L: **An EGFR/Src-dependent β4 integrin/FAK complex contributes to malignancy of breast cancer.** *Sci Rep* 2015, **5**:16408.

215. Larsen SL, Laenkholm A-V, Duun-Henriksen AK, Bak M, Lykkesfeldt AE, Kirkegaard T: **Src Drives Growth of Antiestrogen Resistant Breast Cancer Cell Lines and Is a Marker for Reduced Benefit of Tamoxifen Treatment**. *PLoS One* 2015, **10**:e0118346.

216. Jain S, Wang X, Chang C-C, Ibarra-Drendall C, Wang H, Zhang Q, Brady SW, Li P, Zhao H, Dobbs J, Kyrish M, Tkaczyk TS, Ambrose A, Sistrunk C, Arun BK, Richards-Kortum R, Jia W, Seewaldt VL, Yu D: **Src Inhibition Blocks c-Myc Translation and Glucose Metabolism to Prevent the Development of Breast Cancer**. *Cancer Res* 2015, **75**:4863–4875.

217. Zhang S, Huang W-C, Zhang L, Zhang C, Lowery FJ, Ding Z, Guo H, Wang H, Huang S, Sahin AA, Aldape KD, Steeg PS, Yu D: **Src Family Kinases as Novel Therapeutic Targets to Treat Breast Cancer Brain Metastases**. *Cancer Res* 2013, **73**:5764–5774.

218. De Luca A, D'Alessio A, Gallo M, Maiello MR, Bode AM, Normanno N: **Src and CXCR4 are involved in the invasiveness of breast cancer cells with acquired resistance to lapatinib.** *Cell Cycle* 2014, **13**:148–56.

219. Nam S, Kim D, Cheng JQ, Zhang S, Lee J-H, Buettner R, Mirosevich J, Lee FY, Jove R: **Action of the Src Family Kinase Inhibitor, Dasatinib (BMS-354825), on Human Prostate Cancer Cells**. *Cancer Res* 2005, **65**:9185–9.

220. **FDA Approval for Dasatinib - National Cancer Institute** [https://www.cancer.gov/about-cancer/treatment/drugs/fda-dasatinib]

221. Brooks HD, Glisson BS, Bekele BN, Ginsberg LE, El-Naggar A, Culotta KS, Takebe N, Wright J, Tran HT, Papadimitrakopoulou VA, Papadimitrakopoulou VA: **Phase 2 study of dasatinib in the treatment of head and neck squamous cell carcinoma**. *Cancer* 2011, **117**:2112–2119.

222. Kluger HM, Dudek AZ, McCann C, Ritacco J, Southard N, Jilaveanu LB, Molinaro A, Sznol M: **A phase 2 trial of dasatinib in advanced melanoma**. *Cancer* 2011, **117**:2202–2208.

223. Kelley MJ, Jha G, Shoemaker D, Herndon JE, Gu L, Barry WT, Crawford J, Ready N: **Phase II Study of Dasatinib in Previously Treated Patients with Advanced Non-Small Cell Lung Cancer.** *Cancer Invest* 2017, **35**:32–35.

224. Haesen D, Sents W, Lemaire K, Hoorne Y, Janssens V: **The Basic Biology of PP2A in Hematologic Cells and Malignancies**. *Front Oncol* 2014, **4**:347.

225. Gu P, Qi X, Zhou Y, Wang Y, Gao X: **Generation of Ppp2Ca and Ppp2Cb conditional null alleles in mouse**. *genesis* 2012, **50**:429–436.

226. Ross JA, Cheng H, Nagy ZS, Frost JA, Kirken RA: **Protein phosphatase 2A regulates interleukin-2 receptor complex formation and JAK3/STAT5 activation.** *J Biol Chem* 2010, **285**:3582–91.

227. Buchert M, Burns CJ, Ernst M: **Targeting JAK kinase in solid tumors: emerging opportunities and challenges**. *Oncogene* 2016, **35**:939–951.

228. Fukukawa C, Tanuma N, Okada T, Kikuchi K, Shima H: **pp32/ I-1PP2A negatively regulates the Raf-1/MEK/ERK pathway**. *Cancer Lett* 2005, **226**:155–160.

229. Arroyo JD, Hahn WC: **Involvement of PP2A in viral and cellular transformation.** *Oncogene* 2005, **24**:7746–55.

230. Junttila MR, Puustinen P, Niemelä M, Ahola R, Arnold H, Böttzauw T, Ala-aho R, Nielsen C, Ivaska J, Taya Y, Lu S-L, Lin S, Chan EKL, Wang X-J, Grènman R, Kast J, Kallunki T, Sears R, Kähäri V-M, Westermarck J: **CIP2A inhibits PP2A in human malignancies.** *Cell* 2007, **130**:51–62.

231. Rincón R, Cristóbal I, Zazo S, Arpí O, Menéndez S, Manso R, Lluch A, Eroles P, Rovira A, Albanell J, García-Foncillas J, Madoz-Gúrpide J, Rojo F: **PP2A inhibition determines poor outcome and doxorubicin resistance in early breast cancer and its activation shows promising therapeutic effects.** *Oncotarget* 2015, **6**:4299–314.

232. Cristóbal I, Garcia-Orti L, Cirauqui C, Alonso MM, Calasanz MJ, Odero MD: **PP2A impaired activity is a common event in acute myeloid leukemia and its activation by forskolin has a potent anti-leukemic effect**. *Leukemia* 2011, **25**:606–614.

233. Bos CL, Kodach LL, van den Brink GR, Diks SH, van Santen MM, Richel DJ, Peppelenbosch MP, Hardwick JCH: **Effect of aspirin on the Wnt/beta-catenin pathway is mediated via protein phosphatase 2A.** *Oncogene* 2006, **25**:6447–56.

234. Duong FHT, Dill MT, Matter MS, Makowska Z, Calabrese D, Dietsche T, Ketterer S, Terracciano L, Heim MH: **Protein phosphatase 2A promotes hepatocellular carcinogenesis in the diethylnitrosamine mouse model through inhibition of p53**. *Carcinogenesis* 2014, **35**:114–122.

235. Ruvolo PP, Deng X, May WS: **Phosphorylation of Bcl2 and regulation of apoptosis.** *Leukemia* 2001, **15**:515–22.

236. Shouse GP, Cai X, Liu X: **Serine 15 phosphorylation of p53 directs its interaction with B56gamma and the tumor suppressor activity of B56gamma-specific protein phosphatase 2A.** *Mol Cell Biol* 2008, **28**:448–56.

237. Tachibana K, Scheuer PJ, Tsukitani Y, Kikuchi H, Van Engen D, Clardy J, Gopichand Y, Schmitz FJ: **Okadaic acid, a cytotoxic polyether from two marine sponges of the genus Halichondria**. *J Am Chem Soc* 1981, **103**:2469–2471.

238. Valdiglesias V, Laffon B, Pásaro E, Méndez J: **Okadaic acid induces morphological changes, apoptosis and cell cycle alterations in different human cell types**. *J Environ Monit* 2011, **13**:1831.

239. Yang H, Chen X, Wang X, Li Y, Chen S, Qian X, Wang R, Chen L, Han W, Ruan A, Du Q, Olumi AF, Zhang X: **Inhibition of PP2A Activity Confers a TRAIL-sensitive Phenotype During Malignant Transformation.** *Mol Cancer Res* 2013.

240. Walsh AH, Cheng A, Honkanen RE: **Fostriecin, an antitumor antibiotic with inhibitory activity against serine/threonine protein phosphatases types 1 (PP1) and 2A (PP2A), is highly selective for PP2A.** *FEBS Lett* 1997, **416**:230–4.

241. Lewy DS, Gauss C-M, Soenen DR, Boger DL: **Fostriecin: chemistry and biology.** *Curr Med Chem* 2002, **9**:2005–32.

242. Boritzki TJ, Wolfard TS, Besserer JA, Jackson RC, Fry DW: **Inhibition of type II topoisomerase by fostriecin.** *Biochem Pharmacol* 1988, **37**:4063–8.

243. Takeuchi T, Takahashi N, Ishi K, Kusayanagi T, Kuramochi K, Sugawara F: **Antitumor antibiotic fostriecin covalently binds to cysteine-269 residue of protein phosphatase 2A catalytic subunit in mammalian cells**. *Bioorg Med Chem* 2009, **17**:8113–8122.

244. Scheithauer W, Von Hoff DD, Clark GM, Shillis JL, Elslager EF: **In vitro activity of the novel antitumor antibiotic fostriecin (CI-920) in a human tumor cloning assay.** *Eur J Cancer Clin Oncol* 1986, **22**:921–6.

245. Leopold WR, Shillis JL, Mertus AE, Nelson JM, Roberts BJ, Jackson RC: **Anticancer activity of the structurally novel antibiotic Cl-920 and its analogues.** *Cancer Res* 1984, **44**:1928–32.

246. Lê LH, Erlichman C, Pillon L, Thiessen JJ, Day A, Wainman N, Eisenhauer EA, Moore MJ: **Phase I and pharmacokinetic study of fostriecin given as an intravenous bolus daily for five consecutive days.** *Invest New Drugs* 2004, **22**:159–67.

247. Gao D, O'Doherty GA: **Total Synthesis of Fostriecin: Via a Regio- and Stereoselective Polyene Hydration, Oxidation, and Hydroboration Sequence**. *Org Lett* 2010, **12**:3752–3755.

248. Reddy YK, Falck J: **Asymmetric Total Synthesis of (+)-Fostriecin†**. *Org Lett* 2002, **21**:961–71.

249. Kadioglu O, Kermani NS, Kelter G, Schumacher U, Fiebig HH, Greten HJ ET: **Pharmacogenomics of Cantharidin in Tumor Cells.** *Biochem Pharmacol* 2012, **doi:pii: S**.

250. Efferth T, Rauh R, Kahl S, Tomicic M, Böchzelt H, Tome ME, Briehl MM, Bauer R, Kaina B: **Molecular modes of action of cantharidin in tumor cells**. *Biochem Pharmacol* 2005, **69**:811–818.

251. Rauh R, Kahl S, Boechzelt H, Bauer R, Kaina B, Efferth T: **Molecular biology of cantharidin in cancer cells.** *Chin Med* 2007, **2**:8.

252. Chen Y-N, Chen J-C, Yin S-C, Wang G-S, Tsauer W, Hsu S-F, Hsu S-L: **Effector mechanisms of norcantharidin-induced mitotic arrest and apoptosis in human hepatoma cells**. *Int J Cancer* 2002, **100**:158–165.

253. Gu X-D, Xu L-L, Zhao H, Gu J-Z, Xie X-H: **Cantharidin suppressed breast cancer MDA-MB-231 cell growth and migration by inhibiting MAPK signaling pathway.** *Brazilian J Med Biol Res = Rev Bras Pesqui medicas e Biol* 2017, **50**:e5920.

254. Su C-C, Lee K-I, Chen M-K, Kuo C-Y, Tang C-H, Liu SH: **Cantharidin Induced Oral Squamous Cell Carcinoma Cell Apoptosis via the JNK-Regulated Mitochondria and Endoplasmic Reticulum Stress-Related Signaling Pathways**. *PLoS One* 2016, **11**:e0168095.

255. Shen M, Wu M-Y, Chen L-P, Zhi Q, Gong F-R, Chen K, Li D-M, Wu Y, Tao M, Li W: **Cantharidin represses invasion of pancreatic cancer cells through**

accelerated degradation of MMP2 mRNA. *Sci Rep* 2015, **5**:11836.

256. Xie X, Wu M-Y, Shou L-M, Chen L-P, Gong F-R, Chen K, Li D-M, Duan W-M, Xie Y-F, Mao Y-X, Li W, Tao M: **Tamoxifen enhances the anticancer effect of cantharidin and norcantharidin in pancreatic cancer cell lines through inhibition of the protein kinase C signaling pathway.** *Oncol Lett* 2015, **9**:837–844.

257. Coloe Dosal J, Stewart PW, Lin J-A, Williams CS, Morrell DS: **Cantharidin for the Treatment of Molluscum Contagiosum: A Prospective, Double-Blinded, Placebo-Controlled Trial**. *Pediatr Dermatol* 2014, **31**:440–449.

258. Ho WS, Feldman MJ, Maric D, Amable L, Hall MD, Feldman GM, Ray-Chaudhury A, Lizak MJ, Vera J-C, Robison RA, Zhuang Z, Heiss JD: **PP2A inhibition with LB100 enhances cisplatin cytotoxicity and overcomes cisplatin resistance in medulloblastoma cells.** *Oncotarget* 2016.

259. Hong CS, Ho W, Zhang C, Yang C, Elder JB, Zhuang Z: **LB100, a small molecule inhibitor of PP2A with potent chemo- and radio-sensitizing potential**. *Cancer Biol Ther* 2015.

260. Chang K-E, Wei B-R, Madigan JP, Hall MD, Simpson RM, Zhuang Z, Gottesman MM: **The protein phosphatase 2A inhibitor LB100 sensitizes ovarian carcinoma cells to cisplatin-mediated cytotoxicity.** *Mol Cancer Ther* 2015, **14**:90–100.

261. Zhang C, Hong CS, Hu X, Yang C, Wang H, Zhu D, Moon S, Dmitriev P, Lu J, Chiang J, Zhuang Z, Zhou Y: **Inhibition of protein phosphatase 2A with the small molecule LB100 overcomes cell cycle arrest in osteosarcoma after cisplatin treatment.** *Cell Cycle* 2015, **14**:2100–8.

262. Lv P, Wang Y, Ma J, Wang Z, Li J-L, Hong CS, Zhuang Z, Zeng Y-X: **Inhibition of protein phosphatase 2A with a small molecule LB100 radiosensitizes nasopharyngeal carcinoma xenografts by inducing mitotic catastrophe and blocking DNA damage repair.** *Oncotarget* 2014, **5**:7512–24.

263. Wei D, Parsels LA, Karnak D, Davis MA, Parsels JD, Marsh AC, Zhao L, Maybaum J, Lawrence TS, Sun Y, Morgan MA: **Inhibition of protein phosphatase 2A radiosensitizes pancreatic cancers by modulating CDC25C/CDK1 and homologous recombination repair.** *Clin Cancer Res* 2013, **19**:4422–32.

264. Gordon IK, Lu J, Graves CA, Huntoon K, Frerich JM, Hanson RH, Wang X, Hong CS, Ho W, Feldman MJ, Ikejiri B, Bisht K, Chen XS, Tandle A, Yang C, Arscott WT, Ye D, Heiss JD, Lonser RR, Camphausen K, Zhuang Z: **Protein**

Phosphatase 2A Inhibition with LB100 Enhances Radiation-Induced Mitotic Catastrophe and Tumor Growth Delay in Glioblastoma. *Mol Cancer Ther* 2015, **14**:1540–7.

265. Bai X, Zhi X, Zhang Q, Liang F, Chen W, Liang C, Hu Q, Sun X, Zhuang Z, Liang T: **Inhibition of protein phosphatase 2A sensitizes pancreatic cancer to chemotherapy by increasing drug perfusion via HIF-1α-VEGF mediated angiogenesis.** *Cancer Lett* 2014, **355**:281–7.

266. Fu Q-H, Zhang Q, Zhang J-Y, Sun X, Lou Y, Li G-G, Chen Z-L, Bai X-L, Liang T-B: **LB-100 sensitizes hepatocellular carcinoma cells to the effects of sorafenib during hypoxia by activation of Smad3 phosphorylation.** *Tumour Biol* 2015.

267. Shan S, Wang YD, Ren T: **[LB100 reverses the acquired resistance to gefitinib in lung adenocarcinoma cells with EGFR mutation].** *Zhonghua Yi Xue Za Zhi* 2016, **96**:3398–3402.

268. Chung V, Mansfield AS, Braiteh F, Richards D, Durivage H, Ungerleider RS, Johnson F, Kovach JS: **Safety, Tolerability, and Preliminary Activity of LB-100, an Inhibitor of Protein Phosphatase 2A, in Patients with Relapsed Solid Tumors: An Open-Label, Dose Escalation, First-in-Human, Phase I Trial**. *Clin Cancer Res* 2017, **23**:3277–3284.

269. Browne B: **The role of receptor tyrosine kinase signalling in HER-2-positive cells and Trastuzumab (Herceptin) Resistance in Breast Cancer . A Thesis submitted for the degree of Ph . D . by Brigid Browne , BSc The work in this thesis was carried out under the supe**. 2008(October).

270. Hennessy BT, Lu Y, Gonzalez-Angulo AM, Carey MS, Myhre S, Ju Z, Davies MA, Liu W, Coombes K, Meric-Bernstam F, Bedrosian I, McGahren M, Agarwal R, Zhang F, Overgaard J, Alsner J, Neve RM, Kuo W-L, Gray JW, Borresen-Dale A-L, Mills GB: **A Technical Assessment of the Utility of Reverse Phase Protein Arrays for the Study of the Functional Proteome in Non-microdissected Human Breast Cancers**. *Clin Proteomics* 2010, **6**:129–151.

271. Chen R, Im H, Snyder M: **Whole-Exome Enrichment with the Agilent SureSelect Human All Exon Platform.** *Cold Spring Harb Protoc* 2015, **2015**:626–33.

272. Mukaka MM: **Statistics corner: A guide to appropriate use of correlation coefficient in medical research.** *Malawi Med J* 2012, **24**:69–71.

273. Chou T-C: **Drug Combination Studies and Their Synergy Quantification**

Using the Chou-Talalay Method. *Cancer Res* 2010, **70**:440–446.

274. Burris HA, Taylor CW, Jones SF, Koch KM, Versola MJ, Arya N, Fleming RA, Smith DA, Pandite L, Spector N, Wilding G, Wilding G: **A phase I and pharmacokinetic study of oral lapatinib administered once or twice daily in patients with solid malignancies.** *Clin Cancer Res* 2009, **15**:6702–8.

275. Von Minckwitz G, Loibl S, Untch M: **What is the current standard of care for anti-HER2 neoadjuvant therapy in breast cancer?** *Oncology (Williston Park)* 2012, **26**:20–6.

276. Araki K, Fukada I, Horii R, Takahashi S, Akiyama F, Iwase T, Ito Y: **Trastuzumab Rechallenge After Lapatinib- and Trastuzumab-Resistant Disease Progression in HER2-Positive Breast Cancer**. *Clin Breast Cancer* 2015, **15**:432–439.

277. Eichhorn PJ a, Creyghton MP, Bernards R: **Protein phosphatase 2A regulatory subunits and cancer.** *Biochim Biophys Acta* 2009, **1795**:1–15.

278. Matsuoka Y, Nagahara Y, Ikekita M, Shinomiya T: **A novel immunosuppressive agent FTY720 induced Akt dephosphorylation in leukemia cells**. *Br J Pharmacol* 2003, **138**:1303–1312.

279. Seshacharyulu P, Pandey P, Datta K, Batra SK: **Phosphatase: PP2A structural importance, regulation and its aberrant expression in cancer**. *Cancer Lett* 2013, **335**:9–18.

280. Organ SL, Tsao M-S: **An overview of the c-MET signaling pathway.** *Ther Adv Med Oncol* 2011, **3**(1 Suppl):S7–S19.

281. Oda K, Matsuoka Y, Funahashi A, Kitano H: **A comprehensive pathway map of epidermal growth factor receptor signaling.** *Mol Syst Biol* 2005, **1**:2005.0010.

282. Valdiglesias V, Prego-Faraldo M, Pásaro E, Méndez J, Laffon B: **Okadaic Acid: More than a Diarrheic Toxin**. *Mar Drugs* 2013, **11**:4328–4349.

283. Clinchy B, Gazdar A, Rabinovsky R, Yefenof E, Gordon B, Vitetta ES: **The growth and metastasis of human, HER-2/neu-overexpressing tumor cell lines in male SCID mice.** *Breast Cancer Res Treat* 2000, **61**:217–28.

284. Workman P, Aboagye EO, Balkwill F, Balmain A, Bruder G, Chaplin DJ, Double JA, Everitt J, Farningham DAH, Glennie MJ, Kelland LR, Robinson V,

Stratford IJ, Tozer GM, Watson S, Wedge SR, Eccles SA, Navaratnam V, Ryder S: **Guidelines for the welfare and use of animals in cancer research**. *Br J Cancer* 2010, **102**:1555–1577.

285. Kocatürk B, Versteeg HH: **Orthotopic injection of breast cancer cells into the mammary fat pad of mice to study tumor growth.** *J Vis Exp* 2015.

286. Azim HA, Agbor-Tarh D, Bradbury I, Dinh P, Baselga J, Di Cosimo S, Greger JG, Smith I, Jackisch C, Kim S-B, Aktas B, Huang C-S, Vuylsteke P, Hsieh RK, Dreosti L, Eidtmann H, Piccart M, de Azambuja E: **Pattern of rash, diarrhea, and hepatic toxicities secondary to lapatinib and their association with age and response to neoadjuvant therapy: analysis from the NeoALTTO trial.** *J Clin Oncol* 2013, **31**:4504–11.

287. Moy B, Goss PE: **Lapatinib-associated toxicity and practical management recommendations.** *Oncologist* 2007, **12**:756–65.

288. Turner P V, Brabb T, Pekow C, Vasbinder MA: **Administration of substances to laboratory animals: routes of administration and factors to consider.** *J Am Assoc Lab Anim Sci* 2011, **50**:600–13.

289. Swingle M, Ni L, Honkanen RE: **Small-molecule inhibitors of ser/thr protein phosphatases: specificity, use and common forms of abuse.** *Methods Mol Biol* 2007, **365**:23–38.

290. Baldacchino S, Saliba C, Petroni V, Fenech AG, Borg N, Grech G: **Deregulation of the phosphatase, PP2A is a common event in breast cancer, predicting sensitivity to FTY720.** *EPMA J* 2014, **5**:3.

291. Wang SS, Esplin ED, Li JL, Huang L, Gazdar A, Minna J, Evans GA: **Alterations of the PPP2R1B gene in human lung and colon cancer.** *Science* 1998, **282**:284–7.

292. Madden SF, Clarke C, Gaule P, Aherne ST, O'Donovan N, Clynes M, Crown J, Gallagher WM: **BreastMark: an integrated approach to mining publicly available transcriptomic datasets relating to breast cancer outcome.** *Breast Cancer Res* 2013, **15**:R52.

293. Come C, Laine A, Chanrion M, Edgren H, Mattila E, Liu X, Jonkers J, Ivaska J, Isola J, Darbon J-M, Kallioniemi O, Thezenas S, Westermarck J: **CIP2A Is Associated with Human Breast Cancer Aggressivity**. *Clin Cancer Res* 2009, **15**:5092–5100.

294. Chan A, Delaloge S, Holmes FA, Moy B, Iwata H, Harvey VJ, Robert NJ, Silovski T, Gokmen E, von Minckwitz G, Ejlertsen B, Chia SKL, Mansi J, Barrios CH, Gnant M, Buyse M, Gore I, Smith J, Harker G, Masuda N, Petrakova K, Zotano AG, Iannotti N, Rodriguez G, Tassone P, Wong A, Bryce R, Ye Y, Yao B, Martin M: **Neratinib after trastuzumab-based adjuvant therapy in patients with HER2-positive breast cancer (ExteNET): a multicentre, randomised, double-blind, placebo-controlled, phase 3 trial**. *Lancet Oncol* 2016, **17**:367–377.

295. Wind S, Schnell D, Ebner T, Freiwald M, Stopfer P: **Clinical Pharmacokinetics and Pharmacodynamics of Afatinib.** *Clin Pharmacokinet* 2017, **56**:235–250.

296. De P, Hasmann M, Leyland-Jones B: **Molecular determinants of trastuzumab efficacy: What is their clinical relevance?** *Cancer Treat Rev* 2013, **39**:925–934.

297. Kolosionek E, Savai R, Ghofrani HA, Weissmann N, Guenther A, Grimminger F, Seeger W, Banat GA, Schermuly RT, Pullamsetti SS: **Expression and Activity of Phosphodiesterase Isoforms during Epithelial Mesenchymal Transition: The Role of Phosphodiesterase 4**. *Mol Biol Cell* 2009, **20**:4751–4765.

298. Masugi Y, Yamazaki K, Emoto K, Effendi K, Tsujikawa H, Kitago M, Itano O, Kitagawa Y, Sakamoto M: **Upregulation of integrin β4 promotes epithelial–mesenchymal transition and is a novel prognostic marker in pancreatic ductal adenocarcinoma**. *Lab Investig* 2015, **95**:308–319.

299. Ni M, Shi X-L, Qu Z-G, Jiang H, Chen Z-Q, Hu J: **Epithelial mesenchymal transition of non–small–cell lung cancer cells A549 induced by SPHK1**. *Asian Pac J Trop Med* 2015, **8**:142–146.

300. Cormier K, Harquail J, Ouellette RJ, Tessier PA, Guerrette R, Robichaud GA: **Intracellular expression of inflammatory proteins S100A8 and S100A9 leads to epithelial-mesenchymal transition and attenuated aggressivity of breast cancer cells.** *Anticancer Agents Med Chem* 2014, **14**:35–45.

301. Zhou F, Drabsch Y, Dekker TJA, de Vinuesa AG, Li Y, Hawinkels LJAC, Sheppard K-A, Goumans M-J, Luwor RB, de Vries CJ, Mesker WE, Tollenaar RAEM, Devilee P, Lu CX, Zhu H, Zhang L, Dijke P ten: **Nuclear receptor NR4A1 promotes breast cancer invasion and metastasis by activating TGF-β signalling**. *Nat Commun* 2014, **5**:3388.

302. Yu D-H, Zhang X, Wang H, Zhang L, Chen H, Hu M, Dong Z, Zhu G, Qian Z, Fan J, Su X, Xu Y, Zheng L, Dong H, Yin X, Ji Q, Ji J: **The essential role of TNIK gene amplification in gastric cancer growth**. *Oncogenesis* 2014, **2**:e89.

303. Lee T-G, Jeong E-H, Kim SY, Kim H-R, Kim CH: **The combination of irreversible EGFR TKIs and SAHA induces apoptosis and autophagy-mediated cell death to overcome acquired resistance in EGFRT790M-mutated lung cancer**. *Int J Cancer* 2015, **136**:2717–2729.

304. Hedrick E, Lee S-O, Doddapaneni R, Singh M, Safe S: **Nuclear receptor 4A1 as a drug target for breast cancer chemotherapy**. *Endocr Relat Cancer* 2015, **22**:831–840.

305. Peiró G, Ortiz-Martínez F, Gallardo A, Pérez-Balaguer A, Sánchez-Payá J, Ponce JJ, Tibau A, López-Vilaro L, Escuin D, Adrover E, Barnadas A, Lerma E: **Src, a potential target for overcoming trastuzumab resistance in HER2-positive breast carcinoma.** *Br J Cancer* 2014, **111**:689–95.

306. Eustace AJ, Crown J, Clynes M, O'Donovan N: **Preclinical evaluation of dasatinib, a potent Src kinase inhibitor, in melanoma cell lines**. *J Transl Med* 2008, **6**:53.

307. Konecny GE, Glas R, Dering J, Manivong K, Qi J, Finn RS, Yang GR, Hong K-L, Ginther C, Winterhoff B, Gao G, Brugge J, Slamon DJ: **Activity of the multikinase inhibitor dasatinib against ovarian cancer cells**. *Br J Cancer* 2009, **101**:1699–1708.

308. Le X-F, Mao W, Lu Z, Carter BZ, Bast RC: **Dasatinib induces autophagic cell death in human ovarian cancer**. *Cancer* 2010, **116**:4980–4990.

309. Chao T-T, Wang C-Y, Chen Y-L, Lai C-C, Chang F-Y, Tsai Y-T, Chao C-HH, Shiau C-W, Huang Y-CT, Yu C-J, Chen K-F: **Afatinib induces apoptosis in NSCLC without EGFR mutation through Elk-1-mediated suppression of CIP2A**. *Oncotarget* 2015, **6**:2164–2179.

310. Scaffidi P, Misteli T, Bianchi ME: **Release of chromatin protein HMGB1 by necrotic cells triggers inflammation**. *Nature* 2002, **418**:191–195.

311. Bell CW, Jiang W, Reich CF, Pisetsky DS: **The extracellular release of HMGB1 during apoptotic cell death**. *AJP Cell Physiol* 2006, **291**:C1318–C1325.

312. Finn RS, Bengala C, Ibrahim N, Roche H, Sparano J, Strauss LC, Fairchild J, Sy O, Goldstein LJ: **Dasatinib as a Single Agent in Triple-Negative Breast Cancer: Results of an Open-Label Phase 2 Study**. *Clin Cancer Res* 2011, **17**:6905–6913.

313. Amiri-Kordestani L, Blumenthal GM, Xu QC, Zhang L, Tang SW, Ha L, Weinberg WC, Chi B, Candau-Chacon R, Hughes P, Russell AM, Miksinski SP,

Chen XH, McGuinn WD, Palmby T, Schrieber SJ, Liu Q, Wang J, Song P, Mehrotra N, Skarupa L, Clouse K, Al-Hakim A, Sridhara R, Ibrahim A, Justice R, Pazdur R, Cortazar P: **FDA Approval: Ado-Trastuzumab Emtansine for the Treatment of Patients with HER2-Positive Metastatic Breast Cancer**. *Clin Cancer Res* 2014, **20**:4436–4441.

314. von Minckwitz G, Procter M, de Azambuja E, Zardavas D, Benyunes M, Viale G, Suter T, Arahmani A, Rouchet N, Clark E, Knott A, Lang I, Levy C, Yardley DA, Bines J, Gelber RD, Piccart M, Baselga J, APHINITY Steering Committee and Investigators: **Adjuvant Pertuzumab and Trastuzumab in Early HER2-Positive Breast Cancer.** *N Engl J Med* 2017, **377**:122–131.

315. Kalous O, Conklin D, Desai AJ, O'Brien NA, Ginther C, Anderson L, Cohen DJ, Britten CD, Taylor I, Christensen JG, Slamon DJ, Finn RS: **Dacomitinib (PF-00299804), an irreversible Pan-HER inhibitor, inhibits proliferation of HER2-amplified breast cancer cell lines resistant to trastuzumab and lapatinib.** *Mol Cancer Ther* 2012, **11**:1978–87.

316. Diaby V, Adunlin G, Ali AA, Zeichner SB, de Lima Lopes G, Kohn CG, Montero AJ: **Cost-effectiveness analysis of 1st through 3rd line sequential targeted therapy in HER2-positive metastatic breast cancer in the United States.** *Breast Cancer Res Treat* 2016.

317. Tóth G, Szöőr Á, Simon L, Yarden Y, Szöllősi J, Vereb G: **The combination of trastuzumab and pertuzumab administered at approved doses may delay development of trastuzumab resistance by additively enhancing antibody-dependent cell-mediated cytotoxicity.** *MAbs* 2016, **8**:1361–1370.

318. Harbeck N, Huang C-S, Hurvitz S, Yeh D-C, Shao Z, Im S-A, Jung KH, Shen K, Ro J, Jassem J, Zhang Q, Im Y-H, Wojtukiewicz M, Sun Q, Chen S-C, Goeldner R-G, Uttenreuther-Fischer M, Xu B, Piccart-Gebhart M: **Afatinib plus vinorelbine versus trastuzumab plus vinorelbine in patients with HER2-overexpressing metastatic breast cancer who had progressed on one previous trastuzumab treatment (LUX-Breast 1): an open-label, randomised, phase 3 trial.** *Lancet Oncol* 2016.

319. Campo M, Gerber D, Gainor JF, Heist RS, Temel JS, Shaw AT, Fidias P, Muzikansky A, Engelman JA, Sequist L V.: **Acquired Resistance to First-Line Afatinib and the Challenges of Prearranged Progression Biopsies**. *J Thorac Oncol* 2016, **11**:2022–2026.

320. Kazandjian D, Blumenthal GM, Yuan W, He K, Keegan P, Pazdur R: **FDA Approval of Gefitinib for the Treatment of Patients with Metastatic EGFR Mutation-Positive Non-Small Cell Lung Cancer**. *Clin Cancer Res* 2016, **22**:1307–1312.

321. Khozin S, Blumenthal GM, Jiang X, He K, Boyd K, Murgo A, Justice R, Keegan P, Pazdur R: **U.S. Food and Drug Administration Approval Summary: Erlotinib for the First-Line Treatment of Metastatic Non-Small Cell Lung Cancer With Epidermal Growth Factor Receptor Exon 19 Deletions or Exon 21 (L858R) Substitution Mutations**. *Oncologist* 2014, **19**:774–779.

322. Miller VA, Hirsh V, Cadranel J, Chen Y-M, Park K, Kim S-W, Zhou C, Su W-C, Wang M, Sun Y, Heo DS, Crino L, Tan E-H, Chao T-Y, Shahidi M, Cong XJ, Lorence RM, Yang JC-H: **Afatinib versus placebo for patients with advanced, metastatic non-small-cell lung cancer after failure of erlotinib, gefitinib, or both, and one or two lines of chemotherapy (LUX-Lung 1): a phase 2b/3 randomised trial.** *Lancet Oncol* 2012, **13**:528–38.

323. Everett AD, Stoops TD, Nairn AC, Brautigan D: **Angiotensin II regulates phosphorylation of translation elongation factor-2 in cardiac myocytes**. *Am J Physiol Hear Circ Physiol* 2001, **281**:H161-167.

324. Gergs U, Boknik P, Buchwalow I, Fabritz L, Matus M, Justus I, Hanske G, Schmitz W, Neumann J: **Overexpression of the catalytic subunit of protein phosphatase 2A impairs cardiac function.** *J Biol Chem* 2004, **279**:40827–34.

325. Wong LL, Zhang D, Chang CF, Koay ESC: **Silencing of the PP2A catalytic subunit causes HER-2/neu positive breast cancer cells to undergo apoptosis.** *Exp Cell Res* 2010, **316**:3387–96.

326. Boudreau RTM, Conrad DM, Hoskin DW: **Apoptosis induced by protein phosphatase 2A (PP2A) inhibition in T leukemia cells is negatively regulated by PP2A-associated p38 mitogen-activated protein kinase.** *Cell Signal* 2007, **19**:139–51.

327. Li W, Chen Z, Gong F-R, Zong Y, Chen K, Li D-M, Yin H, Duan W-M, Miao Y, Tao M, Han X, Xu Z-K: **Growth of the pancreatic cancer cell line PANC-1 is inhibited by protein phosphatase 2A inhibitors through overactivation of the c-Jun N-terminal kinase pathway.** *Eur J Cancer* 2011, **47**:2654–64.

328. Kiely M, Kiely PA: **PP2A: The Wolf in Sheep's Clothing?** *Cancers (Basel)* 2015, **7**:648–669.

329. Sharma S, Mathur AG, Pradhan S, Singh DB, Gupta S: **Fingolimod (FTY720): First approved oral therapy for multiple sclerosis.** *J Pharmacol Pharmacother* 2011, **2**:49–51.

330. Saddoughi SA, Gencer S, Peterson YK, Ward KE, Mukhopadhyay A, Oaks J,

Bielawski J, Szulc ZM, Thomas RJ, Selvam SP, Senkal CE, Garrett-Mayer E, De Palma RM, Fedarovich D, Liu A, Habib AA, Stahelin R V., Perrotti D, Ogretmen B: **Sphingosine analogue drug FTY720 targets I2PP2A/SET and mediates lung tumour suppression via activation of PP2A-RIPK1-dependent necroptosis**. *EMBO Mol Med* 2013, **5**:105–121.

331. Cristóbal I, González-Alonso P, Daoud L, Solano E, Torrejón B, Manso R, Madoz-Gúrpide J, Rojo F, García-Foncillas J: **Activation of the Tumor Suppressor PP2A Emerges as a Potential Therapeutic Strategy for Treating Prostate Cancer**. *Mar Drugs* 2015, **13**:3276–3286.

332. Oaks JJ, Santhanam R, Walker CJ, Roof S, Harb JG, Ferenchak G, Eisfeld A-K, Van Brocklyn JR, Briesewitz R, Saddoughi SA, Nagata K, Bittman R, Caligiuri MA, Abdel-Wahab O, Levine R, Arlinghaus RB, Quintas-Cardama A, Goldman JM, Apperley J, Reid A, Milojkovic D, Ziolo MT, Marcucci G, Ogretmen B, Neviani P, Perrotti D: **Antagonistic activities of the immunomodulator and PP2A-activating drug FTY720 (Fingolimod, Gilenya) in Jak2-driven hematologic malignancies.** *Blood* 2013, **122**:1923–34.

333. Zonta F, Pagano MA, Trentin L, Tibaldi E, Frezzato F, Trimarco V, Facco M, Zagotto G, Pavan V, Ribaudo G, Bordin L, Semenzato G, Brunati AM: **Lyn sustains oncogenic signaling in chronic lymphocytic leukemia by strengthening SET-mediated inhibition of PP2A**. *Blood* 2015, **125**:3747–3755.

334. Pai P, Velmurugan BK, Kuo C-H, Yen C-Y, Ho T-J, Lin Y-M, Chen Y-F, Lai C-H, Day CH, Huang C-Y: **17β-Estradiol and/or estrogen receptor alpha blocks isoproterenol-induced calcium accumulation and hypertrophy via GSK3β/PP2A/NFAT3/ANP pathway**. *Mol Cell Biochem* 2017, **434**:181–195.

335. Oaks J, Ogretmen B: **Regulation of PP2A by Sphingolipid Metabolism and Signaling.** *Front Oncol* 2014, **4**:388.

336. Yokoyama N, Miller WT: **Inhibition of Src by direct interaction with protein phosphatase 2A.** *FEBS Lett* 2001, **505**:460–4.

337. Lee T, Kim SJ, Sumpio BE: **Role of PP2A in the regulation of p38 MAPK activation in bovine aortic endothelial cells exposed to cyclic strain**. *J Cell Physiol* 2003, **194**:349–355.

338. Oji Y, Tatsumi N, Fukuda M, Nakatsuka S-I, Aoyagi S, Hirata E, Nanchi I, Fujiki F, Nakajima H, Yamamoto Y, Shibata S, Nakamura M, Hasegawa K, Takagi S, Fukuda I, Hoshikawa T, Murakami Y, Mori M, Inoue M, Naka T, Tomonaga T, Shimizu Y, Nakagawa M, Hasegawa J, Nezu R, Inohara H, Izumoto S, Nonomura N, Yoshimine T, Okumura M, et al.: **The translation elongation factor eEF2 is a novel**

tumor‑associated antigen overexpressed in various types of cancers. *Int J Oncol* 2014, **44**:1461–1469.

339. Nakamura J, Aoyagi S, Nanchi I, Nakatsuka S-I, Hirata E, Shibata S, Fukuda M, Yamamoto Y, Fukuda I, Tatsumi N, Ueda T, Fujiki F, Nomura M, Nishida S, Shirakata T, Hosen N, Tsuboi A, Oka Y, Nezu R, Mori M, Doki Y, Aozasa K, Sugiyama H, Oji Y: **Overexpression of eukaryotic elongation factor eEF2 in gastrointestinal cancers and its involvement in G2/M progression in the cell cycle**. *Int J Oncol* 2009, **34**:1181–1189.

340. Xia W, Mullin RJ, Keith BR, Liu L-H, Ma H, Rusnak DW, Owens G, Alligood KJ, Spector NL: **Anti-tumor activity of GW572016: a dual tyrosine kinase inhibitor blocks EGF activation of EGFR/erbB2 and downstream Erk1/2 and AKT pathways**. *Oncogene* 2002, **21**:6255–6263.

341. Chen Y-J, Yeh M-H, Yu M-C, Wei Y-L, Chen W-S, Chen J-Y, Shih C-Y, Tu C-Y, Chen C-H, Hsia T-C, Chien P-H, Liu S-H, Yu Y-L, Huang W-C: **Lapatinib– induced NF-kappaB activation sensitizes triple-negative breast cancer cells to proteasome inhibitors**. *Breast Cancer Res* 2013, **15**:R108.

342. Bailey ST, Miron PL, Choi YJ, Kochupurakkal B, Maulik G, Rodig SJ, Tian R, Foley KM, Bowman T, Miron A, Brown M, Iglehart JD, Biswas DK: **NF-κB activation-induced anti-apoptosis renders HER2-positive cells drug resistant and accelerates tumor growth.** *Mol Cancer Res* 2014, **12**:408–20.

343. Chen C-T, Kim H, Liska D, Gao S, Christensen JG, Weiser MR: **MET activation mediates resistance to lapatinib inhibition of HER2-amplified gastric cancer cells.** *Mol Cancer Ther* 2012, **11**:660–9.

344. Letourneux C, Rocher G, Porteu F: **B56-containing PP2A dephosphorylate ERK and their activity is controlled by the early gene IEX-1 and ERK**. *EMBO J* 2006, **25**:727–738.

345. Roberts PJ, Der CJ: **Targeting the Raf-MEK-ERK mitogen-activated protein kinase cascade for the treatment of cancer**. *Oncogene* 2007, **26**:3291–3310.

346. McDermott M: **Mechanisms of resistance to lapatinib in HER2-positive breast cancer A thesis submitted for the degree of PhD The work in this thesis was carried out under the supervision of**. Dublin City University; 2012.

347. Zhang L, Shao L, Creighton CJ, Zhang Y, Xin L, Ittmann M, Wang J: **Function of phosphorylation of NF-kB p65 ser536 in prostate cancer oncogenesis**. *Oncotarget* 2015, **6**:6281–6294.

348. Li W, Chen Z, Zong Y, Gong F, Zhu Y, Zhu Y, Lv J, Zhang J, Xie L, Sun Y, Miao Y, Tao M, Han X, Xu Z: **PP2A inhibitors induce apoptosis in pancreatic cancer cell line PANC-1 through persistent phosphorylation of IKKα and sustained activation of the NF-κB pathway**. *Cancer Lett* 2011, **304**:117–127.

349. Wee P, Wang Z: **Epidermal Growth Factor Receptor Cell Proliferation Signaling Pathways.** *Cancers (Basel)* 2017, **9**.

350. Calin GA, di Iasio MG, Caprini E, Vorechovsky I, Natali PG, Sozzi G, Croce CM, Barbanti-Brodano G, Russo G, Negrini M: **Low frequency of alterations of the alpha (PPP2R1A) and beta (PPP2R1B) isoforms of the subunit A of the serine-threonine phosphatase 2A in human neoplasms.** *Oncogene* 2000, **19**:1191–5.

351. Chen J, Martin BL, Brautigan DL: **Regulation of protein serine-threonine phosphatase type-2A by tyrosine phosphorylation.** *Science* 1992, **257**:1261–4.

352. Longin S, Zwaenepoel K, Louis J V, Dilworth S, Goris J, Janssens V: **Selection of protein phosphatase 2A regulatory subunits is mediated by the C terminus of the catalytic Subunit.** *J Biol Chem* 2007, **282**:26971–80.

353. Takai A, Murata M, Torigoe K, Isobe M, Mieskes G, Yasumoto T: **Inhibitory effect of okadaic acid derivatives on protein phosphatases. A study on structure-affinity relationship.** *Biochem J* 1992, **1**:539–44.

354. Walsh AH, Cheng A, Honkanen RE: **Fostriecin, an antitumor antibiotic with inhibitory activity against serine/threonine protein phosphatases types 1 (PP1) and 2A (PP2A), is highly selective for PP2A.** *FEBS Lett* 1997, **416**:230–4.

355. Kadioglu O, Kermani NS, Kelter G, Schumacher U, Fiebig H-H, Greten HJ, Efferth T: **Pharmacogenomics of cantharidin in tumor cells**. *Biochem Pharmacol* 2014, **87**:399–409.

356. Lu J, Kovach JS, Johnson F, Chiang J, Hodes R, Lonser R, Zhuang Z: **Inhibition of serine/threonine phosphatase PP2A enhances cancer chemotherapy by blocking DNA damage induced defense mechanisms.** *Proc Natl Acad Sci U S A* 2009, **106**:11697–702.

357. Lanthaler K, Bilsland E, Dobson PD, Moss HJ, Pir P, Kell DB, Oliver SG: **Genome-wide assessment of the carriers involved in the cellular uptake of drugs: a model system in yeast.** *BMC Biol* 2011, **9**:70.

358. Citrin DE: **Short-Term Screening Assays for the Identification of Therapeutics for Cancer.** *Cancer Res* 2016, **76**:3443–5.

359. Keller PJ, Lin A, Arendt LM, Klebba I, Jones AD, Rudnick JA, DiMeo TA, Gilmore H, Jefferson DM, Graham RA, Naber SP, Schnitt S, Kuperwasser C: **Mapping the cellular and molecular heterogeneity of normal and malignant breast tissues and cultured cell lines**. *Breast Cancer Res* 2010, **12**:R87.

360. Zhang C, Peng Y, Wang F, Tan X, Liu N, Fan S, Wang D, Zhang L, Liu D, Wang T, Wang S, Zhou Y, Su Y, Cheng T, Zhuang Z, Shi C: **A synthetic cantharidin analog for the enhancement of doxorubicin suppression of stem cell-derived aggressive sarcoma**. *Biomaterials* 2010, **31**:9535–9543.

361. Bence AK, Anderson EB, Halepota MA, Doukas MA, DeSimone PA, Davis GA, Smith DA, Koch KM, Stead AG, Mangum S, Bowen CJ, Spector NL, Hsieh S, Adams VR: **Phase I pharmacokinetic studies evaluating single and multiple doses of oral GW572016, a dual EGFR-ErbB2 inhibitor, in healthy subjects.** *Invest New Drugs* 2005, **23**:39–49.

362. Moy B, Goss PE: **Lapatinib-associated toxicity and practical management recommendations.** *Oncologist* 2007, **12**:756–65.

363. Wallace J: **Humane Endpoints and Cancer Research**. *ILAR J* 2000, **41**:87–93.

364. Fantozzi A, Christofori G: **Mouse models of breast cancer metastasis**. *Breast Cancer Res* 2006, **8**:212.

365. Werbeck JL, Thudi NK, Martin CK, Premanandan C, Yu L, Ostrowksi MC, Rosol TJ: **Tumor microenvironment regulates metastasis and metastasis genes of mouse MMTV-PymT mammary cancer cells in vivo.** *Vet Pathol* 2014, **51**:868–81.

366. Beyer I, van Rensburg R, Strauss R, Li Z, Wang H, Persson J, Yumul R, Feng Q, Song H, Bartek J, Fender P, Lieber A: **Epithelial junction opener JO-1 improves monoclonal antibody therapy of cancer.** *Cancer Res* 2011, **71**:7080–90.

367. De Goeij BECG, Satijn D, Freitag CM, Wubbolts R, Bleeker WK, Khasanov A, Zhu T, Chen G, Miao D, van Berkel PHC, Parren PWHI: **High turnover of tissue factor enables efficient intracellular delivery of antibody-drug conjugates.** *Mol Cancer Ther* 2015, **14**:1130–40.

368. Kiguchi K, Glesne D, Chubb CH, Fujiki H, Huberman E: **Differential induction of apoptosis in human breast tumor cells by okadaic acid and related inhibitors of protein phosphatases 1 and 2A.** *Cell Growth Differ* 1994, **5**:995–1004.

369. Morimoto H, Morimoto Y, Ohba T, Kido H, Kobayashi S, Haneji T: **Inhibitors of protein synthesis and RNA synthesis protect against okadaic acid-induced**

apoptosis in human osteosarcoma cell line MG63 cells but not in Saos-2 cells. *J Bone Miner Metab* 1999, **17**:266–73.

370. Kiguchi K, Giometti C, Chubb CH, Fujiki H, Huberman E: **Differentiation induction in human breast tumor cells by okadaic acid and related inhibitors of protein phosphatases 1 and 2A.** *Biochem Biophys Res Commun* 1992, **189**:1261–7.

371. Fujita M, Goto K, Yoshida K, Okamura H, Morimoto H, Kito S, Fukuda J, Haneji T: **Okadaic acid stimulates expression of Fas receptor and Fas ligand by activation of nuclear factor kappa-B in human oral squamous carcinoma cells.** *Oral Oncol* 2004, **40**:199–206.

372. Hirai A, Bold RJ, Ishizuka J, Hirai M, Townsend CM, Thompson JC: **Hyperphosphorylation of retinoblastoma protein and stimulation of growth by okadaic acid in human pancreatic cancer.** *Dig Dis Sci* 1996, **41**:1975–80.

373. Ehlers A, These A, Hessel S, Preiss-Weigert A, Lampen A: **Active elimination of the marine biotoxin okadaic acid by P-glycoprotein through an in vitro gastrointestinal barrier**. *Toxicol Lett* 2014, **225**:311–317.

374. Ikema S, Takumi S, Maeda Y, Kurimoto T, Bohda S, Chigwechokha PK, Sugiyama Y, Shiozaki K, Furukawa T, Komatsu M: **Okadaic acid is taken-up into the cells mediated by human hepatocytes transporter OATP1B3**. *Food Chem Toxicol* 2015, **83**:229–236.

375. Ruediger R, Pham HT, Walter G: **Alterations in protein phosphatase 2A subunit interaction in human carcinomas of the lung and colon with mutations in the Aβ subunit gene**. *Oncogene* 2001, **20**:1892–1899.

376. Hashida S, Yamamoto H, Shien K, Miyoshi Y, Ohtsuka T, Suzawa K, Watanabe M, Maki Y, Soh J, Asano H, Tsukuda K, Miyoshi S, Toyooka S: **Acquisition of cancer stem cell-like properties in non-small cell lung cancer with acquired resistance to afatinib**. *Cancer Sci* 2015, **106**:1377–1384.

377. Coco S, Truini A, Alama A, Dal Bello MG, Venè R, Garuti A, Carminati E, Rijavec E, Genova C, Barletta G, Sini C, Ballestrero A, Boccardo F, Grossi F: **Afatinib resistance in non-small cell lung cancer involves the PI3K/AKT and MAPK/ERK signalling pathways and epithelial-to-mesenchymal transition**. *Target Oncol* 2015, **10**:393–404.

378. Lee Y, Wang Y, James M, Jeong JH, You M: **Inhibition of IGF1R signaling abrogates resistance to afatinib (BIBW2992) in EGFR T790M mutant lung cancer cells.** *Mol Carcinog* 2015.

379. Kobayashi Y, Togashi Y, Yatabe Y, Mizuuchi H, Jangchul P, Kondo C, Shimoji M, Sato K, Suda K, Tomizawa K, Takemoto T, Hida T, Nishio K, Mitsudomi T: **EGFR Exon 18 Mutations in Lung Cancer: Molecular Predictors of Augmented Sensitivity to Afatinib or Neratinib as Compared with First- or Third-Generation TKIs**. *Clin Cancer Res* 2015, **21**:5305–5313.

380. Hashida S, Yamamoto H, Shien K, Miyoshi Y, Ohtsuka T, Suzawa K, Watanabe M, Maki Y, Soh J, Asano H, Tsukuda K, Miyoshi S, Toyooka S: **Acquisition of cancer stem cell-like properties in non-small cell lung cancer with acquired resistance to afatinib.** *Cancer Sci* 2015.

381. Dong J, Ramachandiran S, Tikoo K, Jia Z, Lau SS, Monks TJ: **EGFR-independent activation of p38 MAPK and EGFR-dependent activation of ERK1/2 are required for ROS-induced renal cell death.** *Am J Physiol Renal Physiol* 2004, **287**:F1049-58.

382. Mueller K, Powell K, Madden J, Eblen S, Boerner J: **EGFR Tyrosine 845 Phosphorylation-Dependent Proliferation and Transformation of Breast Cancer Cells Require Activation of p38 MAPK**. *Transl Oncol* 2012, **5**:327–IN1.

383. Khabele D, Kabir SM, Dong Y, Lee E, Rice VM, Son D-S: **Preferential Effect of Akt2-Dependent Signaling on the Cellular Viability of Ovarian Cancer Cells in Response to EGF**. *J Cancer* 2014, **5**:670–678.

384. Formisano L, Nappi L, Rosa R, Marciano R, D'Amato C, D'Amato V, Damiano V, Raimondo L, Iommelli F, Scorziello A, Troncone G, Veneziani B, Parsons SJ, De Placido S, Bianco R: **Epidermal growth factor-receptor activation modulates Src-dependent resistance to lapatinib in breast cancer models.** *Breast Cancer Res* 2014, **16**:R45.

385. Wang H-Y, Hsu M-K, Wang K-H, Tseng C-P, Chen F-C, Hsu JT-A: **Non-small-cell lung cancer cells combat epidermal growth factor receptor tyrosine kinase inhibition through immediate adhesion-related responses.** *Onco Targets Ther* 2016, **9**:2961–73.

386. Sato K-I: **Cellular functions regulated by phosphorylation of EGFR on Tyr845.** *Int J Mol Sci* 2013, **14**:10761–90.

387. Hedrick E, Lee S-O, Kim G, Abdelrahim M, Jin U-H, Safe S, Abudayyeh A: **Nuclear Receptor 4A1 (NR4A1) as a Drug Target for Renal Cell Adenocarcinoma**. *PLoS One* 2015, **10**:e0128308.

388. Lee S-O, Li X, Hedrick E, Jin U-H, Tjalkens RB, Backos DS, Li L, Zhang Y,

Wu Q, Safe S: **Diindolylmethane Analogs Bind NR4A1 and Are NR4A1 Antagonists in Colon Cancer Cells**. *Mol Endocrinol* 2014, **28**:1729–1739.

389. Lee S-O, Jin U-H, Kang JH, Kim SB, Guthrie AS, Sreevalsan S, Lee J-S, Safe S: **The Orphan Nuclear Receptor NR4A1 (Nur77) Regulates Oxidative and Endoplasmic Reticulum Stress in Pancreatic Cancer Cells**. *Mol Cancer Res* 2014, **12**:527–538.

390. Kim H-P, Han S-W, Song S-H, Jeong E-G, Lee M-Y, Hwang D, Im S-A, Bang Y-J, Kim T-Y: **Testican-1-mediated epithelial-mesenchymal transition signaling confers acquired resistance to lapatinib in HER2-positive gastric cancer.** *Oncogene* 2014, **33**:3334–41.

391. Shaw FL, Harrison H, Spence K, Ablett MP, Simões BM, Farnie G, Clarke RB: **A Detailed Mammosphere Assay Protocol for the Quantification of Breast Stem Cell Activity**. *J Mammary Gland Biol Neoplasia* 2012, **17**:111–117.

392. Lombardo Y, de Giorgio A, Coombes CR, Stebbing J, Castellano L: **Mammosphere formation assay from human breast cancer tissues and cell lines.** *J Vis Exp* 2015.

393. Desgrosellier JS, Cheresh DA: **Integrins in cancer: biological implications and therapeutic opportunities.** *Nat Rev Cancer* 2010, **10**:9–22.

394. Pastuszak-Lewandoska D, Kordiak J, Antczak A, Migdalska-Sęk M, Czarnecka KH, Górski P, Nawrot E, Kiszałkiewicz JM, Domańska-Senderowska D, Brzeziańska-Lasota E: **Expression level and methylation status of three tumor suppressor genes, DLEC1, ITGA9 and MLH1, in non-small cell lung cancer**. *Med Oncol* 2016, **33**:75.

395. Mostovich LA, Prudnikova TY, Kondratov AG, Loginova D, Vavilov P V., Rykova VI, Sidorov S V., Pavlova T V., Kashuba VI, Zabarovsky ER, Grigorieva E V.: **Integrin alpha9 (ITGA9) expression and epigenetic silencing in human breast tumors**. *Cell Adh Migr* 2011, **5**:395–401.

396. Nawaz I, Hu L-F, Du Z-M, Moumad K, Ignatyev I, Pavlova T V., Kashuba V, Almgren M, Zabarovsky ER, Ernberg I: **Integrin &alpha;9 gene promoter is hypermethylated and downregulated in nasopharyngeal carcinoma**. *Oncotarget* 2015, **6**:31493–31507.

397. Leng C, Zhang Z, Chen W, Luo H, Song J, Dong W, Zhu X, Chen X, Liang H, Zhang B: **An integrin beta4-EGFR unit promotes hepatocellular carcinoma lung metastases by enhancing anchorage independence through activation of FAK–**

AKT pathway. *Cancer Lett* 2016, **376**:188–196.

398. Kawakami K, Fujita Y, Kato T, Mizutani K, Kameyama K, Tsumoto H, Miura Y, Deguchi T, Ito M: **Integrin β4 and vinculin contained in exosomes are potential markers for progression of prostate cancer associated with taxane-resistance**. *Int J Oncol* 2015, **47**:384–90.

399. Liu S, Ge D, Chen L, Zhao J, Su L, Zhang S, Miao J, Zhao B: **A small molecule induces integrin &beta;4 nuclear translocation and apoptosis selectively in cancer cells with high expression of integrin &beta;4**. *Oncotarget* 2016, **7**:16282–16296.

400. Martin AP, Miller A, Emad L, Rahmani M, Walker T, Mitchell C, Hagan MP, Park MA, Yacoub A, Fisher PB, Grant S, Dent P: **Lapatinib resistance in HCT116 cells is mediated by elevated MCL-1 expression and decreased BAK activation and not by ERBB receptor kinase mutation.** *Mol Pharmacol* 2008, **74**:807–22.

401. Eustace A, Browne B, Madden S, O'Driscoll L, McDermott M, O'Brien N, Watson W, Crown J, Walsh N, O'Donovan N: **Effect of acquired resistance to lapatinib in HER2-positive breast cancer cells on the Bcl-2 family members MCL-1 and BAX.** In *ASCO*; 2012.

402. Li H, Kolluri SK, Gu J, Dawson MI, Cao X, Hobbs PD, Lin B, Chen G, Lu J, Lin F, Xie Z, Fontana JA, Reed JC, Zhang X: **Cytochrome c release and apoptosis induced by mitochondrial targeting of nuclear orphan receptor TR3.** *Science* 2000, **289**:1159–64.

403. Pawlak A, Strzadala L, Kalas W: **Non-genomic effects of the NR4A1/Nur77/TR3/NGFIB orphan nuclear receptor**. *Steroids* 2015, **95**:1–6.

404. Inamoto T, Papineni S, Chintharlapalli S, Cho S-D, Safe S, Kamat AM: **1,1-Bis(3'-indolyl)-1-(p-chlorophenyl)methane activates the orphan nuclear receptor Nurr1 and inhibits bladder cancer growth**. *Mol Cancer Ther* 2008, **7**:3825–3833.

405. Cho SD, Lei P, Abdelrahim M, Yoon K, Liu S, Guo J, Papineni S, Chintharlapalli S, Safe S: **1,1-bis(3′-indolyl)-1-(p-methoxyphenyl)methane activates Nur77-independent proapoptotic responses in colon cancer cells**. *Mol Carcinog* 2008, **47**:252–263.

406. Canonici A, Ibrahim M, Fanning K, Cremona M, Morgan C, Hennesy B, Solca F, Crown J, O'Donovan N: **Biomarkers for afatinib and dasatinib treatment in triple negative breast cancer | OncologyPRO**. In *ESMO*; 2016.

407. Pichot CS, Hartig SM, Xia L, Arvanitis C, Monisvais D, Lee FY, Frost JA, Corey SJ: **Dasatinib synergizes with doxorubicin to block growth, migration, and invasion of breast cancer cells.** *Br J Cancer* 2009, **101**:38–47.

408. Ocana A, Gil-Martin M, Martín M, Rojo F, Antolín S, Guerrero Á, Trigo JM, Muñoz M, Carrasco E, Urruticoechea A: **A phase I study of the SRC kinase inhibitor dasatinib with trastuzumab and paclitaxel as first line therapy for patients with HER2-overexpressing advanced breast cancer. GEICAM/2010-04 study**. *Oncotarget* 2017.

409. Stanley A, Ashrafi GH, Seddon AM, Modjtahedi H: **Synergistic effects of various Her inhibitors in combination with IGF-1R, C-MET and Src targeting agents in breast cancer cell lines**. *Sci Rep* 2017, **7**:3964.

410. Du G-J, Lin H-H, Xu Q-T, Wang M-W: **Bcl-2 switches the type of demise from apoptosis to necrosis via cyclooxygenase-2 upregulation in HeLa cell induced by hydrogen peroxide**. *Cancer Lett* 2006, **232**:179–188.

411. Zhan W, Zhu J, Wang L: **Inhibition of proliferation and induction of apoptosis in RB116 retinoblastoma cells by afatinib treatment**. *Tumor Biol* 2016, **37**:9249–9254.

412. Wang S, Liu S, Zhao B, Yang F, Wang Y, Liang Q-Y, Sun Y, Liu Y, Song Z, Cai Y, Li G: **Afatinib reverses multidrug resistance in ovarian cancer via dually inhibiting ATP binding cassette subfamily B member 1.** *Oncotarget* 2015, **6**:26142–60.

413. Bianchi ME, Manfredi A: **Chromatin and cell death**. *Biochim Biophys Acta - Gene Struct Expr* 2004, **1677**:181–186.

414. Holliday DL, Speirs V: **Choosing the right cell line for breast cancer research**. *Breast Cancer Res* 2011, **13**:215.

415. Zhou S-F: **Drugs behave as substrates, inhibitors and inducers of human cytochrome P450 3A4.** *Curr Drug Metab* 2008, **9**:310–22.

416. Abbas R, Hug BA, Leister C, Burns J, Sonnichsen D: **Pharmacokinetics of oral neratinib during co-administration of ketoconazole in healthy subjects.** *Br J Clin Pharmacol* 2011, **71**:522–7.

417. Johnson FM, Agrawal S, Burris H, Rosen L, Dhillon N, Hong D, Blackwood-Chirchir A, Feng ;, Luo R, Sy O, Kaul S, Chiappori AA: **Phase 1 Pharmacokinetic and Drug-Interaction Study of Dasatinib in Patients With Advanced Solid**

Tumors. *Cancer* 2010.

9 Appendix

Table 9-1: All significant copy number variations in SKBR3-A compared to SKBR3-Par cells. Copy number ratio is given as a relative number of gene copies in SKBR3-A cells to SKBR3-Par cells. A cut of > 1.4 and < 0.35 copy ratio was used.

Gene	Gene description	Copy ratio
LSM5	LSM5 Homolog, U6 Small Nuclear RNA And MRNA Degradation Associated	0.350
STS	Steroid Sulfatase	0.394
STAC	SH3 And Cysteine Rich Domain	0.527
ITGA9	Integrin Subunit Alpha 9	0.581
MUC16	Mucin 16	1.401
TRAF4	TNF Receptor Associated Factor 4	1.401
ENPP2	Ectonucleotide Pyrophosphatase/Phosphodiesterase 2	1.403
BPTF	Bromodomain PHD Finger Transcription Factor	1.404
C17orf58	Chromosome 17 Open Reading Frame 58	1.404
LINC00674	Long Intergenic Non-Protein Coding RNA 674	1.404
AMZ2	Archaelysin Family Metallopeptidase 2	1.404
CCNL1	Cyclin L1	1.406
KRT8	Keratin 8	1.406
JPH1	Junctophilin 1	1.406
MUC16	Mucin 16	1.408
MRPL13	Mitochondrial Ribosomal Protein L13	1.411
ENPP2	Ectonucleotide Pyrophosphatase/Phosphodiesterase 2	1.411
DCLK3	Doublecortin Like Kinase 3	1.412
NFE2L3	Nuclear Factor, Erythroid 2 Like 3	1.412
HNRNPA2B1	Heterogeneous Nuclear Ribonucleoprotein A2/B1	1.412
CBX3	Chromobox 3	1.412
RGAG1	Retrotransposon GAG Domain-Containing Protein 1	1.412
MUC16	Mucin 16	1.412
ZNFX1	Zinc Finger NFX1-Type Containing 1	1.413

ZNF217	Zinc Finger Protein 217	1.414
FRMPD3	FERM And PDZ Domain Containing 3	1.414
CX3CR1	C-X3-C Motif Chemokine Receptor 1	1.415
MRPS28	Mitochondrial Ribosomal Protein S28	1.415
ANKMY1	Ankyrin Repeat And MYND Domain Containing 1	1.417
SCN5A	Sodium Voltage-Gated Channel Alpha Subunit 5	1.417
SCN10A	Sodium Voltage-Gated Channel Alpha Subunit 10	1.418
TRAM1	Translocation Associated Membrane Protein 1	1.420
NUDT8	Nudix Hydrolase 8	1.423
RBM39	RNA Binding Motif Protein 39	1.425
ZNF799	Zinc Finger Protein 799	1.426
GPRASP1	G Protein-Coupled Receptor Associated Sorting Protein 1	1.426
SPATA7	Spermatogenesis Associated 7	1.427
CTDNEP1	CTD Nuclear Envelope Phosphatase 1	1.428
KPNA2	Karyopherin Subunit Alpha 2	1.430
ID3	Inhibitor Of DNA Binding 3, HLH Protein	1.433
ANKRD11	Ankyrin Repeat Domain 11	1.433
TRPS1	Transcriptional Repressor GATA Binding 1	1.434
SCN11A	Sodium Voltage-Gated Channel Alpha Subunit 11	1.435
TRPS1	Transcriptional Repressor GATA Binding 1	1.435
TPD52	Tumor Protein D52	1.437
COL14A1	Collagen Type XIV Alpha 1 Chain	1.438
LOC286190	LACTB2 antisense RNA 1	1.438
SLITRK4	SLIT And NTRK Like Family Member 4	1.438
ZCCHC14	Zinc Finger CCHC-Type Containing 14	1.443
SNAI3-AS1	SNAI3 Antisense RNA 1	1.443
APRT	Adenine Phosphoribosyltransferase	1.443
DEF8	Differentially Expressed In FDCP 8 Homolog	1.443
MAGEC1	MAGE Family Member C1	1.444

THOP1	Thimet Oligopeptidase 1	1.446
PTPRS	Protein Tyrosine Phosphatase, Receptor Type S	1.446
MUC16	Mucin 16	1.446
EIF3G	Eukaryotic Translation Initiation Factor 3 Subunit G	1.446
PDE4A	Phosphodiesterase 4A	1.446
ZNF799	Zinc Finger Protein 799	1.446
RTBDN	Retbindin	1.446
HIST1H3J	Histone Cluster 1 H3 Family Member J	1.446
TRPM8	Transient Receptor Potential Cation Channel Subfamily M Member 8	1.447
BCORL1	BCL6 Corepressor Like 1	1.447
BPTF	Bromodomain PHD Finger Transcription Factor	1.448
ACTB	Actin Beta	1.450
IRS4	Insulin Receptor Substrate 4	1.452
ITPR1	Inositol 1,4,5-Trisphosphate Receptor Type 1	1.456
PTPN21	Protein Tyrosine Phosphatase, Non-Receptor Type 21	1.458
LRRC27	Leucine Rich Repeat Containing 27	1.464
NRDE2	NRDE-2, Necessary For RNA Interference, Domain Containing	1.465
STMN2	Stathmin 2	1.466
RNF213	Ring Finger Protein 213	1.466
NUDT4P2	Nudix Hydrolase 4 Pseudogene 2	1.468
BRWD3	Bromodomain And WD Repeat Domain Containing 3	1.469
CENPI	Centromere Protein I	1.469
TCP11X2	T-Complex 11 Family, X-Linked 2	1.469
LINC00630	Long Intergenic Non-Protein Coding RNA 630	1.469
CLDN2	Claudin 2	1.469
COL4A6	Collagen Type IV Alpha 6 Chain	1.469
ACSL4	Acyl-CoA Synthetase Long-Chain Family	1.469

	Member 4	
LRCH2	Leucine Rich Repeats And Calponin Homology Domain Containing 2	1.469
PLS3	Lipoprotein Lipase	1.469
SEPT6	Septin 6	1.469
CT47A4	Cancer/Testis Antigen Family 47, Member A4	1.469
IGSF1	Immunoglobulin Superfamily Member 1	1.469
CT45A5	Cancer/Testis Antigen Family 45 Member A5	1.469
MCF2	MCF.2 Cell Line Derived Transforming Sequence	1.469
MAGEC3	MAGE Family Member C3	1.469
SPANXN4	SPANX Family Member N4	1.469
SPANXN2	SPANX Family Member N2	1.469
NSDHL	NAD(P) Dependent Steroid Dehydrogenase-Like	1.469
DNASE1L1	Deoxyribonuclease 1 Like 1	1.469
DKC1	Dyskerin Pseudouridine Synthase 1	1.469
MIR1184-1	MicroRNA 1184-1	1.469
PLCL2	Phospholipase C Like 2	1.470
TRANK1	Tetratricopeptide Repeat And Ankyrin Repeat Containing 1	1.470
TPD52	Tumor Protein D52	1.471
XIRP1	Xin Actin Binding Repeat Containing 1	1.473
PKM	Pyruvate Kinase, Muscle	1.474
MTBP	MDM2 Binding Protein	1.475
FLRT2	Fibronectin Leucine Rich Transmembrane Protein 2	1.478
GALC	Galactosylceramidase	1.478
SPATA7	Spermatogenesis Associated 7	1.478
PTPN21	Protein Tyrosine Phosphatase, Non-Receptor Type 21	1.478
ZC3H14	Zinc Finger CCCH-Type Containing 14	1.478
TTC7B	Tetratricopeptide Repeat Domain 7B	1.478
GPR68	Protein-Coupled Receptor 68	1.478

TC2N	Tandem C2 Domains, Nuclear	1.478
TRIP11	Thyroid Hormone Receptor Interactor 11	1.478
CSNK1A1	Casein Kinase 1 Alpha 1	1.480
CTU2	Cytosolic Thiouridylase Subunit 2	1.481
LOC100132891	MSC antisense RNA 1	1.481
PLXNA3	Plexin A3	1.483
MYO15B	Myosin XVB	1.485
TRIP11	Thyroid Hormone Receptor Interactor 11	1.487
CCR8	C-C Motif Chemokine Receptor 8	1.488
MYO15B	Myosin XVB	1.489
NID2	Nidogen 2	1.494
TXNDC16	Thioredoxin Domain Containing 16	1.494
DDX27	DEAD-Box Helicase 27	1.495
ZNFX1	Zinc Finger NFX1-Type Containing 1	1.495
SNORD12B	Small Nucleolar RNA, C/D Box 12B	1.495
PLCL2	Phospholipase C Like 2	1.499
TRPS1	Transcriptional Repressor GATA Binding 1	1.501
TFAP2C	Transcription Factor AP-2 Gamma	1.501
ZBTB33	Zinc Finger And BTB Domain Containing 33	1.502
COL14A1	Collagen Type XIV Alpha 1 Chain	1.506
QRICH2	Glutamine Rich 2	1.511
ZNFX1	Zinc Finger NFX1-Type Containing 1	1.514
EIF4G2	Eukaryotic Translation Initiation Factor 4 Gamma 2	1.520
TPD52L2	Tumor Protein D52 Like 2	1.524
F8	Coagulation Factor VIII	1.524
USP26	Ubiquitin Specific Peptidase 26	1.528
EPM2AIP1	EPM2A Interacting Protein 1	1.530
CASKIN2	CASK Interacting Protein 2	1.531
DCLK3	Doublecortin Like Kinase 3	1.531
TRANK1	Tetratricopeptide Repeat And Ankyrin Repeat Containing 1	1.531
MLH1	MutL Homolog 1	1.531
COL14A1	Collagen Type XIV Alpha 1 Chain	1.538
ATP6V0D2	ATPase H+ Transporting V0 Subunit D2	1.539

CNGB3	yclic Nucleotide Gated Channel Beta 3	1.539
ITPR1	Inositol 1,4,5-Trisphosphate Receptor Type 1	1.541
GRM7	Glutamate Metabotropic Receptor 7	1.541
DSCC1	DNA Replication And Sister Chromatid Cohesion 1	1.542
MSC	Musculin	1.542
TRPA1	Transient Receptor Potential Cation Channel Subfamily A Member 1	1.542
TERF1	Telomeric Repeat Binding Factor 1	1.542
STAU2	Staufen Double-Stranded RNA Binding Protein 2	1.542
TCEB1	Transcription elongation factor B polypeptide 1	1.542
JPH1	Junctophilin 1	1.542
PEX2	Peroxisomal Biogenesis Factor 2	1.542
STMN2	Stathmin 2	1.542
MRPS28	Mitochondrial Ribosomal Protein S28	1.542
TPD52	Tumor Protein D52	1.542
KCNB2	Potassium Voltage-Gated Channel Subfamily B Member 2	1.543
KCNB2	Potassium Voltage-Gated Channel Subfamily B Member 2	1.551
S100A9	S100 Calcium Binding Protein A9	1.551
BHLHE40	Basic Helix-Loop-Helix Family Member E40	1.553
RHBDF2	Rhomboid 5 Homolog 2	1.554
RDH10	Retinol Dehydrogenase 10	1.556
KIAA1210	KIAA1210	1.559
FLNA	Filamin A	1.560
STAU2	Staufen Double-Stranded RNA Binding Protein 2	1.565
HERPUD1	Homocysteine Inducible ER Protein With Ubiquitin Like Domain 1	1.565
COL14A1	Collagen Type XIV Alpha 1 Chain	1.567
MRPL13	Mitochondrial Ribosomal Protein L13	1.567

MTBP	MDM2 Binding Protein	1.567
ZACN	Zinc Activated Ion Channel	1.569
C17orf80	Chromosome 17 Open Reading Frame 80	1.570
MYO15B	Myosin XVB	1.574
MTBP	MDM2 Binding Protein	1.577
SEC16B	SEC16 Homolog B, Endoplasmic Reticulum Export Factor	1.579
PDE4D	Phosphodiesterase 4D	1.584
GPR112	G protein-coupled receptor 112	1.590
FOXK2	Forkhead Box K2	1.598
JPH1	Junctophilin 1	1.617
DLEC1	Deleted In Lung And Esophageal Cancer 1	1.628
SCN5A	Sodium Voltage-Gated Channel Alpha Subunit 5	1.628
SCN10A	Sodium Voltage-Gated Channel Alpha Subunit 10	1.628
CSRNP1	Cysteine And Serine Rich Nuclear Protein 1	1.628
CX3CR1	C-X3-C Motif Chemokine Receptor 1	1.628
RPSA	Ribosomal Protein SA	1.628
FAM104A	Family With Sequence Similarity 104 Member A	1.631
GPRC5C	G Protein-Coupled Receptor Class C Group 5 Member C	1.631
MYO15B	Myosin XVB	1.631
ITGB4	Integrin Subunit Beta 4	1.631
EXOC7	Exocyst Complex Component 7	1.631
SPHK1	Sphingosine Kinase 1	1.631
CYTH1	Cytohesin 1	1.631
RPTOR	Regulatory Associated Protein Of MTOR Complex 1	1.631
NPB	Neuropeptide B	1.631
TUFT1	Tuftelin 1	1.649
SCYL1	SCY1 Like Pseudokinase 1	1.670
TAF2	TATA-Box Binding Protein Associated Factor 2	1.682

DEPTOR	DEP Domain Containing MTOR Interacting Protein	1.682
PRKDC	Protein Kinase, DNA-Activated, Catalytic Polypeptide	1.712
NR4A1	Nuclear Receptor Subfamily 4 Group A Member 1	1.751
REEP2	Receptor Accessory Protein 2	1.834
HIST1H2BD	Histone Cluster 1 H2B Family Member D	1.866
TNIK	TRAF2 And NCK Interacting Kinase	1.892
KRT7	Keratin 7	1.921
HIST2H3A	Histone Cluster 2 H3 Family Member A	1.950
FLJ42969	Uncharacterized LOC441374	1.966
TXNRD1	Thioredoxin Reductase 1	2.055
CCDC57	Coiled-Coil Domain Containing 57	2.160
AADACL2	Arylacetamide Deacetylase Like 2	2.217